KAPOSI'S SARCOMA-ASSOCIATED HERPESVIRUS MODULATES THE UNFOLDED PROTEIN RESPONSE DURING LYTIC REPLICATION

by

Benjamin P. Johnston

Submitted in partial fulfilment of the requirements
for the degree of Doctor of Philosophy

at

Dalhousie University
Halifax, Nova Scotia
March 2019

DEDICATION

I dedicate this thesis to my wife and best friend, Hannah. Her unwavering support and motivation made it possible to keep trekking on this wild seven-year adventure.

TABLE OF CONTENTS

TABLE OF CONTENTS ..... **iii**
LIST OF TABLES ..... **viii**
LIST OF FIGURES ..... **ix**
ABSTRACT… ..... **xi**
LIST OF ABBREVIATIONS USED ..... **xii**
ACKNOWLEDGEMENTS ..... **xviii**
CHAPTER 1 INTRODUCTION **1**
1.1 Overview 1
1.2 ER stress and the Unfolded Protein Response (UPR) 3
1.2.1 Inositol-Requiring Enzyme 1 (IRE1) 4
1.2.1.1 IRE1 Sensing of ER Stress 5
1.2.1.2 Activation of the IRE1 RNase Domain. 6
1.2.1.3 XBP1/Hac1 mRNA Splicing Causes a Translational Frameshift 7
1.2.1.4 Regulation of XBP1/Hac1 mRNA Splicing 7
1.2.1.5 XBP1 is a bZIP Transcription Factor 8
1.2.1.6 XBP1s Target Genes 9
1.2.1.7 Regulation of XBP1 Expression 11
1.2.1.8 Other Roles of XBP1u 11
1.2.1.9 Regulated IRE1-Dependent Decay (RIDD) 12
1.2.2 PKR-like Endoplasmic Reticulum Kinase (PERK) and the Integrated Stress Response (ISR) 14
1.2.2.1 Eukaryotic Initiation Factor 2α (eIF2α) Kinases 14
1.2.2.2 PERK is Activated by ER Stress 16
1.2.2.3 uORF-Mediated Translational Control during the ISR 17
1.2.2.4 Activating Transcription Factor 4 (ATF4) 19
1.2.2.5 C/EBP Homologous Protein (CHOP) 20
1.2.3 Activating Transcription Factor 6 (ATF6) 21
1.2.4 UPR Activation by ER Lipid Bilayer Stress 24
1.2.5 The UPR Induces Apoptosis in Response to Persistent or Acute ER stress. 25
1.2.5.1 An Overview of Apoptotic Pathways 25
1.2.5.2 ER Stress may Activate Different Apoptotic Pathways 26
1.2.5.3 PERK Signaling Promotes Apoptosis 27

1.2.5.4 IRE1 Signaling can Initiate Apoptosis 28
1.2.6 Crosstalk among Branches of the UPR 30
1.2.7 The UPR and Disease 31
1.2.7.1 The UPR in Inflammation and Immunity 31
1.2.7.2 The UPR in Tumorigenesis 34
1.2.7.3 The UPR in Type II diabetes 36
1.2.7.4 The UPR in Neurodegenerative Diseases 39
1.2.8 UPR Modulation during Pathogen Infection 41
1.2.8.1 Bacteria can Activate the UPR 43
1.2.8.2 Flaviviruses Modulate the UPR to Control Autophagy and ERAD ... 44
1.2.8.3 The Chaperone BiP can Promote Virus Infection 45
1.2.8.4 Regulated IRE1-Dependent Decay (RIDD) and Viruses 46
1.2.8.5 Herpesviruses Control UPR Signaling to Promote Replication 46
1.2.8.6 Gamma-Herpesviruses use the UPR to Reactivate in Response to Stress 48
1.3 Kaposi's Sarcoma-Associated Herpesvirus 50
1.3.1. Herpesviridae 50
1.3.2 KSHV Genome and its ORFs 52
1.3.3 Viral Entry 53
1.3.4 Latency and the Latency Locus 54
1.3.4.1 Latency-Associated Nuclear Antigen (LANA) 55
1.3.4.2 vCyclin and vFLIP 55
1.3.4.3 The Kaposins 56
1.3.4.4 KSHV microRNAs 57
1.3.5 Lytic Replication 58
1.3.5.1 RTA is the Latent-Lytic Switch 58
1.3.5.2 Maintenance of Latency 59
1.3.5.3 RTA Expression is Induced in Response to Environmental Factors or Stress. 60
1.3.5.4 PAN lncRNA is Important in Regulating Lytic Gene Expression 63
1.3.5.5 SOX Protein Induces Host Shutoff 63
1.3.5.6 Lytic Genome Replication and Late Gene Expression 64
1.3.5.7 Virus Assembly and Release 65
1.3.6 KSHV and its Diseases 67

1.3.6.1 Kaposi's Sarcoma 67
1.3.6.2 Plasmablastic Multicentric Castleman's Disease (MCD) 69
1.3.6.3 Primary Effusion Lymphoma (PEL) 70
1.4 Rationale and Overview 71
CHAPTER 2 MATERIALS AND METHODS 76
2.1 Cell Culture and Chemicals 76
2.2 Poly(I:C) (Polyinosinic-Polycytidylic Acid) dsRNA Transfection 77
2.3 Plasmid Generation 77
2.4 Lentivirus Generation and Transduction 78
2.5 Luciferase Plasmid Generation and Dual Luciferase Assay 79
2.6 shRNA Lentivirus Cloning and Knockdown 80
2.7 Fluorescent Imaging 81
2.8 Immunoblotting 81
2.9 XBP1 RT-PCR Splicing Assay 82
2.10 Quantitative Reverse-Transcription PCR (RT-qPCR) 83
2.11 Viral Genome Amplification 83
2.12 DNAse I-Protected Virus Titer 83
2.13 rKSHV.219 Infection and Quantification of Virus Titer 83
2.14 KSHV ORF Lentiviral Vector Library Generation and Flow Cytometry Analysis with the UPR Reporter Cell Line 84
2.15 Graphing and Statistical Analysis 86
CHAPTER 3 KSHV LYTIC REPLICATION ACTIVATES UPR SENSOR PROTEINS BUT THE DOWNSTREAM TRANSCRIPTIONAL RESPONSES ARE INHIBITED 90
3.1 Introduction 90
3.2 Results 95
3.2.1 KSHV Lytic Replication Activates IRE1, PERK, but the Downstream Transcription Factors XBP1s and ATF4 are Inhibited 95
3.2.2 KSHV Lytic Replication Triggers ATF6 Processing but ATF6 Transcriptional Activity is Inhibited 97
3.2.3 PERK Dependent Phosphorylation of eIF2α During Lytic Replication 98
3.2.4 Lytic Replication Inhibits ATF4 and XBP1s Regardless of the Type and Duration of ER Stress 99
3.2.5 XBP1s Target Genes are not Transactivated During Lytic Replication 100
3.2.6 UPR Sensors are Required for Robust Virus Production 101

3.3 Discussion 102
CHAPTER 4 SELECTIVE INHIBITION OF KSHV LYTIC REPLICATION BY XBP1S 122
4.1 Introduction 122
4.2 Results 128
4.2.1 Viral Gene Expression is Enhanced Early by XBP1s Overexpression 128
4.2.2 XBP1s Ectopic Expression Suppresses Virus Production in iSLK.219 Cells 130
4.2.3 XBP1s Inhibition of KSHV is not due to Enhanced RTA Expression . 131
4.2.4 KSHV Titer is not Enhanced in iSLK.219 with Increasing Levels of XBP1s 132
4.2.5 XBP1s Overexpression does not Inhibit Virus Production in TREx BCBL1-RTA Cells 133
4.2.6 The HDAC Inhibitor NaB Reverses XBP1s Suppression of KSHV Lytic Replication 134
4.3 Discussion 135
CHAPTER 5 IDENTIFICATION OF VIRAL PROTEINS THAT MODULATE THE UPR 148
5.1 Introduction 148
5.2 Results 150
5.2.1 Flow Cytometry-based Screen of a KSHV Lentiviral ORF Library using a Dual Fluorescent UPR Reporter 150
5.2.2 RTA is not an Inhibitor of IRE1α 153
5.2.3 Kaposin C Downregulates IRE1α 154
5.2.4 ORF45 Upregulates Components of the UPR 156
5.2.5 ATF6 Expression Constructs Impact ORF45 Expression 159
5.2.6 ORF45 does not Induce Conventional UPR Signaling 160
5.2.7 BiP is not Upregulated during Lytic Replication 163
5.3 Discussion 163
CHAPTER 6 CONCLUSIONS 183
6.1 Summary 183
6.2 KSHV Modulates UPR Signaling 185
6.3 XBP1s Promotes Lytic Reactivation but can Inhibit Replication at a Late Phase 187
6.4 Multiple KSHV Proteins Control the UPR Sensors 189
6.5 Future Investigations 191
BIBLIOGRAPHY 193

APPENDIX A THE ISR PROMOTES ACTIVATION OF THE IRE1-XBP1 PATHWAY 247

Introduction 247

Results 249

Discussion 253

APPENDIX B KSHV PROTEIN-CODING ORFS; EXPRESSION AND PRIMARY FUNCTIONS. 261

APPENDIX C RELATIVE CHANGES IN MFI OF UPR REPORTERS WITH KSHV ORF EXPRESSION 271

APPENDIX D PLASMID MAP AND MCS OF PLJM1 B* PURO 277

APPENDIX E SUMMARY OF THE IMPACT THAT XBP1 HAS ON KSHV REPLICATION 278

LIST OF TABLES

Table 2.1 pLKO.1-Blast and -Puro shRNA lentiviral vectors 87
Table 2.2 Antibodies and dilutions used for immunoblots 88
Table 2.3 Sequences of primer sets used for RT-qPCR..... 89

LIST OF FIGURES

Fig 1.1 ER stress activates the unfolded protein response 73
Fig 1.2 Translation initiation requires recycling of the eIF2/GTP/Met-tRNAi^{Met} ternary complex 74
Fig 1.3 The integrated stress response 75
Fig 3.1 XBP1s transactivates KSHV immediate early gene RTA 109
Fig 3.2 KSHV lytic replication activates IRE1 and PERK but their downstream transcription factors are inhibited 110
Fig 3.3 Caspase cleavage of eIF2α is not responsible for inhibition of ATF4 expression . 111
Fig 3.4 KSHV lytic replication activates ATF6α intra-membrane proteolytic cleavage but downstream gene targets are inhibited 112
Fig 3.5 PERK-dependent eIF2α phosphorylation during lytic replication 113
Fig. 3.6 Lytic replication inhibits ATF4 and XBP1s in response to different inducers of ER stress 114
Fig 3.7 Low levels of XBP1s protein are induced during lytic replication 115
Fig 3.8 XBP1s target genes are not upregulated during lytic replication 116
Fig 3.9 Tg-induced RTA but not Nab/TPA-induced RTA is dependent on XBP1 splicing 117
Fig 3.10 ATF6α activation supports robust KSHV replication 118
Fig 3.11 PERK activation supports robust KSHV replication 119
Fig 3.12 IRE1α activation supports robust KSHV replication 120
Fig 4.1 XBP1s overexpression enhances accelerates viral gene expression 140
Fig 4.2 XBP1s overexpression inhibits KSHV replication at a late stage 141
Fig 4.3 XBP1s ectopic expression inhibits KSHV production in iSLK.219 cells 142
Fig 4.4 Inhibition of KSHV replication in iSLK.219 cells by XBP1s is not due to increased RTA expression 144
Fig 4.5 KSHV replication does not increase with increasing levels of XBP1s in iSLK.219 cells 145
Fig 4.6 XBP1s over-expression does not inhibit KSHV replication in TREx BCBL1-RTA cells 146
Fig 4.7 XBP1s does not inhibit KSHV replication in iSLK.219 cells when co-treated with sodium butyrate 147

Fig 5.1 KSHV lentiviral ORF screen for modulators of the ISR and IRE1 using a dual fluorescence cell reporter 172
Fig 5.2 A discrepancy between IRE1 fluorescence reporter and endogenous IRE1 activity in RTA-expressing CHO-7.1 cells 173
Fig 5.3 Kaposin C decreases IRE1α expression 174
Fig 5.4 ORF45 upregulates IRE1 and XBP1 and activates the ISR 175
Fig 5.5 ORF45 upregulates components of the UPR in a time-dependent manner 176
Fig 5.6 ORF45 enhances HA-ATF6 expression to promote BiP accumulation 178
Fig 5.7 ORF45 does not induce canonical ER stress-induced UPR signaling 179
Fig 5.8 ORF45 upregulation of IRE1 and XBP1 may be dependent on the ISR 181
Fig 5.9 ATF6 is activated but BiP is not upregulated during lytic replication 182

ABSTRACT

Kaposi's sarcoma-associated herpesvirus (KSHV) is the infectious cause of the complex endothelial neoplasm Kaposi's sarcoma, and two B cell malignancies, primary effusion lymphoma and multicentric Castleman's disease. KSHV activates multiple cellular stress responses during infection but the impact of stress on viral replication and tumorigenesis remain obscure. One such stress management pathway is the unfolded protein response (UPR), which is activated by endoplasmic reticulum (ER) stress. Activation of the three host cell sensors of ER stress, IRE1, PERK, and ATF6, stimulates synthesis of transcription factors XBP1s, ATF4, and ATF6-N, respectively, which coordinate a transcriptional program to mitigate stress and restore protein homeostasis. Failure to restore homeostasis results causes the UPR to shift from an adaptive response to a pro-apoptotic response. In cells latently infected with KSHV, ER stress initiates lytic reactivation through XBP1s-mediated transcription of the KSHV lytic switch gene, RTA. Thus, it appears that KSHV has evolved a mechanism to respond to ER stress. I investigated the role of the UPR during lytic replication in this thesis. Here, I demonstrate that lytic replication activates all three sensors of the UPR, but the downstream transcription factors are inhibited. RNA silencing or chemical inhibition of any of the UPR sensors inhibits virion production, indicating that their activation is important for some aspect of productive viral replication. Surprisingly, ectopic expression of XBP1s can also inhibit viral production. Therefore, while XBP1s plays an important role in reactivation from latency, it inhibits later steps in lytic replication. This suggests that XBP1s downregulation by viral gene products may effectively remove an anti-viral host factor. To identify potential KSHV proteins that can modulate the UPR, I screened a KSHV lentiviral ORF library with a UPR fluorescent reporter cell line. I found multiple viral proteins that showed UPR-modulating ability. Of these hits, I found that ectopic expression of Kaposin C inhibits IRE1, and that ORF45 upregulates multiple UPR markers, but likely not through ER stress induction. Overall these findings suggest that KSHV modulates UPR signaling during lytic replication to promote virus production instead of resolving ER stress.

LIST OF ABBREVIATIONS USED

˚C	degree Celsius
~	approximate, or approximately
%	percent
•O2-	superoxide
α-syn	α-synuclein
ΔΔCt	delta-delta cycle threshold
µg	microgram
µM	micromolar
1x	one-times
2x	two-times
2-DG	2-deoxyglucose
3x	three-times
4x	four times
7x	seven-times
A	adenine
AARE	amino-acid response element
AD	Alzheimer's disease
ADP	adenosine diphosphate
AIDS	acquired immune deficiency syndrome
Ala	alanine
ANOVA	analysis of variance
AP-1	activator protein 1
APP	amyloid precursor protein
Ars	sodium arsenite
ASK1	apoptosis signal-regulating kinase 1
ATF6-FL	full length ATF6
ATP	adenosine triphosphate
BAC	bacterial artificial chromosome
BCBL	body cavity-based lymphoma
BCR	B cell receptor
BiP	binding immunoglobin protein
bp	base-pairs
bZIP	basic-leucine zipper
C	cytosine
C-terminal	carboxy terminal
CA	constitutively active
Ca2+	calcium
cDCs	conventional dendritic cells
cFLIP	cellular Fas-associated death domain-like interleukin-1β-converting enzyme-inhibitory protein
CHIKV	Chikungunya virus
CHO	Chinese hamster ovary
CHOP	C/EBP homologous protein
CHX	cycloheximide
CMV	cytomegalovirus
CREB	cAMP responsive element-binding

CRISPR	clustered regulatory interspaced short palindromic repeats
CTR	C-terminal region
d	day, or days
DCs	dendritic cells
DDIT3	DNA-damage-inducible transcript 3
DE	delayed early gene
DENV	Dengue Virus
DISC	death-inducing signaling complex
DMEM	Dulbecco's modified Eagle's medium
DMSO	dimethyl sulfoxide
DN	dominant negative
DNA	deoxyribonucleic acid
DNase I	deoxyribonuclease I
dox	doxycycline
DR	direct repeats
DR5	death receptor 5
DRR	DNA damage response
dsDNA	double-stranded deoxyribonucleic acid
dsRNA	double-stranded ribonucleic acid
DSS	dextran sodium disulfate
DTT	dithiothreitol
DUB	deubiquitinase
E	early gene
EBNA1	Epstein-Barr nuclear antigen 1
EBV	Epstein-Barr virus
EDEMs	enhancing Alpha-Mannosidase Like Proteins
eIF	eukaryotic initiation factor
EMSA	electrophoretic mobility shift assay
ER	endoplasmic reticulum
ERAD	ER-associated degradation
ERdj4	endoplasmic reticulum–localized DnaJ 4
ERSE	ER stress element
FADD	fas-associated death domain
FBS	fetal bovine serum
FFA	free fatty acid
Fig	figure
G	guanine
G3BP	Ras–GTPase-activating protein binding-protein 1
GADD153	growth and arrest DNA damage protein 153
GCN2	general control nonderepressible 2
GEF	guanine nucleotide exchange factor
gL	glycoprotein L
Gly	glycine
Grp	glucose-regulated protein
GTP	guanosine triphosphate
GTPase	guanosine triphosphate hydrolase
h	hour, or hours
H_2O_2	hydrogen peroxide

HA	hemagglutinin
HAC1	homologous to ATF/CREB 1
HCMV	human cytomegalovirus
HCV	hepatitis C virus
HD	Huntington's disease
HDAC	histone deacetylase
HERPUD1	homocysteine-responsive endoplasmic reticulum-resident ubiquitin-like domain member 1
HHV	human herpesvirus
HIF	hypoxia-inducible factor
HisD	L-histidinol
HO-1	heme oxygenase-1
HR	hydrophobic region
HREs	hypoxia response elements
HRI	heme-regulated inhibitor
HSP	heat shock protein
HSV-1	herpes simplex virus 1
HSV-2	herpes simplex virus 2
HTA	host-targeting anti-viral
Htt	Huntingtin
HVS	herpesvirus saimiri
IAPP	islet amyloid polypeptide
IAV	Influenza A virus
IBD	inflammatory bowel disease
IE	immediate early gene
IFN	interferon
Ig	immunoglobin
Ile	isoleucine
INSIG	insulin-induced gene protein
IP3	Inositol-1,4,5-triphosphate
IP3R	Inositol-1,4,5-triphosphate receptor
IRE1	inositol-requiring enzyme 1
IRES	internal ribosome entry site
IRS-1	insulin receptor substrate 1
ISG	interferon-stimulated genes
ISR	integrated stress response
ISRIB	ISR inhibitor
IU	infectious units
JEV	Japanese encephalitis virus
JNK	c-Jun N-terminal kinase
KapA	Kaposin A
KapB	Kaposin B
KapC	Kaposin C
Keap1	Kelch-like ECH-associated protein 1
KS	Kaposi's sarcoma
KSHV	Kaposi's sarcoma-associated herpesvirus
L	late gene
LCL	lymphoblastoid cell line

LD	luminal domain
LLO	Listeriolysin O
lncRNA	long non-coding ribonucleic acid
LV	lentivirus
m^6A	N^6-methyladenosine
mg	milligram
mL	milliliter
mM	millimolar
MCD	multicentric Castleman's disease
MCMV	murine cytomegalovirus
MCP	major capsid protein
MCS	multiple cloning site
mHtt	mutant Huntingtin
MHV68	murine herpesvirus 68
miRNA	micro-ribonucleic acid
MM	multiple myeloma
MOMP	mitochondrial outer membrane permeabilization
mRNA	messenger ribonucleic acid
MRSA	Methicillin-resistant *Staphylococcus aureus*
mTORC1	mechanistic target of rapamycin complex 1
MW	molecular weight
N-terminal	amino terminal
NaB	sodium butyrate
NaCl	sodium chloride
NDV	Newcastle disease virus
NEC	nuclear egress complex
NEF	nucleotide exchange factor
NFκB	nuclear factor kappa-light-chain-enhancer of activated B cells
NF-Y	nuclear transcription factor Y
ng	nanogram
nm	nanometer
Nrf2	nuclear factor erythroid 2-related factor 2
nt	nucleotide
OIS	oncogene-induced senescence
ORF	open reading frame
PAA	phosphonoacetic acid
PABP	poly(A)-binding protein
PAMP	pathogen-associated molecular pattern
PAN	polyadenylated nuclear
PBS	phosphate-buffered saline
Poly(I:C)	polyinosinic-polycytidylic Acid
PC	plasma cell
PCR	polymerase chain reaction
PD	Parkinson's disease
PEK	pancreatic eIF2α kinase
PEL	primary effusion lymphoma
PERK	PKR-like ER kinase
PERKi	GSK2606414

PI	proteasome inhibitor
PI3K	phosphoinositide 3-kinase
PIC	pre-initiation complex
PKR	Protein kinase R
PP1	protein phosphatase 1
PP1 α	protein phosphatase 1α
PP2A	protein phosphatase 2 A
PRRs	pattern recognition receptors
PTM	post-transcriptional modification
qPCR	quantitative polymerase chain reaction
RDA	representational difference analysis
RE	restriction enzyme
RIDD	regulated IRE1-dependent decay
RIP	regulated intramembrane proteolysis
RNA	ribonucleic acid
RNA-Seq	ribonucleic acid sequencing
RNAPII	RNA polymerase II
RNase	ribonuclease
RPMI	Roswell Park Memorial Institute
ROS	reactive oxygen species
RRE	RTA response element
RRL	rabbit reticulocyte lysate
rRNA	ribosomal ribonucleic acid
RSV	respiratory syncytial virus
RT-PCR	reverse-transcription polymerase chain reaction
RT-qPCR	quantitative reverse-transcription polymerase chain reaction
RTA	replication and transcription activator
RyR	ryanodine receptor
S1P	Site-1 protease
S2P	Site-2 protease
SCAP	SREBP cleavage activating protein
SD	standard deviation
SDS-PAGE	sodium dodecyl sulfate polyacrylamide gel electrophoresis
SEM	standard error of the mean
Ser	serine
SERCA	sarco/endoplasmic reticulum Ca2+-ATPase
SG	stress granule
shRNA	short-hairpin ribonucleic acid
SINV	Sindbis virus
SOX	shutoff and exonuclease
SREBP	sterol regulatory element-binding protein
SRP	signal recognition particle
STAT3	signal transducer and activator of transcription 3
STEC	Shiga toxin-producing Escherichia coli
STUbl	SUMO-targeted ubiquitin ligase
SubAB	subtilase cytotoxin
SUMO	small ubiquitin-related modifier
T	thymine

T2D	type II diabetes
tBID	truncated BID
TC	ternary complex
TEM	transmission electron microscopy
TetO	tetracycline operator
Tg	thapsigargin
TGN	*trans*-Golgi network
Thr	threonine
TIA-1	T-cell intracellular antigen 1
TLR	toll like receptor
Tm	tunicamycin
TNF	tumor necrosis factor
TPA	12-O-tetradecanoyl-phorbol-13-acetate
TRADD	tumor necrosis factor receptor type 1-associated DEATH domain
TRE	tetracycline response element
TREx	tetracycline-regulated expression system
tRNA	transfer ribonucleic acid
TSC	tuberous sclerosis complex
TXNIP	thioredoxin-interacting protein
U	uracil
uORF	upstream open reading frame
UPR	unfolded protein response
UPRE	unfolded protein response element
UTR	untranslated region
v	viral
vFLIP	viral Fas-associated death domain-like interleukin-1β-converting enzyme-inhibitory protein
vGPCR	viral G protein-coupled receptor
VPA	valproic acid
vPIC	viral pre-initiation complex
WNV	West Nile virus
WRS	Wolcatt-Rallison syndrome
XBP1	X box binding protein 1
XBP1s	spliced XBP1
XBP1u	unspliced XBP1

ACKNOWLEDGEMENTS

Foremost, I would like express my deepest gratitude to my supervisor, Dr. Craig McCormick, for helping me discover a passion for research and guiding and supporting me along the way. Thank you for giving me the freedom to explore the beauty and intricacies of life at the molecular level.

I would also like to thank the members of the McCormick Lab, past and present. Thank you for the fruitful discussions about viruses and stress responses and making it a fun place to work. I would also like to thank the members of the lab that helped clone the KSHV ORF library, especially Siobhan O'Brien for being one of the main drivers of this huge endeavor. Importantly, I would like to thank my friend and lab mate, Eric Pringle, who optimized many of the viral assays that were done in this thesis. Thank you for all your guidance and excellent ideas that were integral to the completion of this work.

To my dissertation committee members, Dr. John Rohde, Dr. Jim Fawcett, and Dr. Chris Richardson, thank you for all your helpful suggestions over the past seven years and your commitment to my success. I sincerely appreciate the time that you sacrificed, especially reviewing and editing my rather "dense" thesis.

I would like to extend a heartfelt thank you to Dr. David Ron and Dr. Heather Harding at the University of Cambridge, as well as the members of the Ron Lab. Thank you for hosting me for 2 months in your lab and helping me conduct the ORF screen. Thanks especially to Heather for her excellent mentorship and putting up with some of my less intelligent questions. The time spent with you and the rest of the lab was an invaluable learning experience.

I would like to thank my parents, Brian and Carol Johnston, for instilling in me characteristics like perseverance, patience, determination, and hard work, which have made it possible to complete a PhD. Thank you for your steadfast love and support, and for cheering me on! Also thank you to my in-laws, Callum and Lorraine Beck, for their love and support. Callum, thank you for copy-editing, especially considering you didn't understand a single sentence.

Finally, and most importantly, I would like to thank my wife, Hannah Beck, and our son Arlo. Arlo, thank you for making me the luckiest dad. Hannah, you are my rock that holds me up; my lighthouse that guides me when I am lost; and my anchor that keeps me grounded. I could not have done this without you. You are my champion.

CHAPTER 1 INTRODUCTION

1.1 Overview

Protein folding is necessary for cellular function. To ensure proteins are properly folded, the cell has evolved a highly regulated and interconnected system to control protein homeostasis, which is often referred to as the proteostasis (a portmanteau of protein and homeostasis) network (reviewed in Klaips, Jayaraj, & Hartl, 2018). Changes in energy levels or exposure to environmental or intrinsic stress can cause protein misfolding, which would be lethal if unresolved. The proteostasis network regulates multiple signaling pathways to restore protein folding in response to stress. This was first exemplified in the early 1960s when *Drosophila* cells exposed to increased temperatures rapidly upregulated the expression of heat shock proteins (HSPs) (Ritossa, 1962) . HSPs were subsequently identified as a family of chaperones and it was found that the heat shock response can be induced by wide array of stresses besides changes in temperature (Lindquist & Craig, 1988; Santoro, 2000).

Protein folding in the endoplasmic reticulum (ER) is tightly regulated (Araki & Nagata, 2011). All proteins destined for secretion are translated at the ER, which accounts for one-third of the entire translatome. The ER proteostasis network comprises protein folding and quality control machinery that function to establish an environment that can cope with an immense burden of protein translation. ER quality control machinery is required to tightly regulate disulfide bond formation, glycosylation, and membrane insertion for single- and multi-spanning membrane proteins to ensure proper folding and trafficking to their final destination. If the protein cannot be folded, then it is targeted for proteasomal degradation by a process call ER-associated degradation (ERAD) (reviewed in Ruggiano, Foresti, & Carvalho, 2014). The ER is also a major site of lipid synthesis and the major cellular reservoir of calcium (Ca^{2+}) ions; this stored Ca^{2+} is required for the function of calcium-dependent chaperones, and plays important roles in signal transduction (reviewed in Michalak, Robert Parker, & Opas, 2002). Disruption of ER proteostasis results in the accumulation of misfolded proteins, which is commonly referred to as ER stress (reviewed in Xu, Bailly-Maitre, & Reed, 2005). Misfolded proteins can aggregate and their aggregation can impair normal cellular functions (Bucciantini et al., 2002; Holmes, Klaips, & Serio, 2014).

To cope with ER stress, eukaryotic cells have developed an evolutionary conserved signaling response called the unfolded protein response (UPR) (reviewed in Walter & Ron, 2011). UPR activation reprograms gene expression to expand the protein folding and degradation capacity of the ER in an attempt to restore protein homeostasis. In the face of chronic or severe protein misfolding, the UPR switches from an adaptive response and induces apoptosis. There is increasing evidence that the UPR plays an important role in normal physiology, and dysregulated UPR signaling or chronic ER stress is implicated in multiple disease states (S. Wang & Kaufman, 2012).

Much of what we know about the molecular events surrounding UPR signaling is with the use of drugs that disrupt protein folding. These include the N-linked glycosylation inhibitor tunicamycin (Tm), sarco/endoplasmic reticulum Ca2+-ATPase (SERCA) pump inhibitor thapsigargin (Tg), and the reducing agent dithiothreitol (DTT). Other UPR studies use misfolding-prone mutant proteins to activate the UPR, such as the mutations in alpha-1 antitrypsin (Lawless et al., 2004). Different diseases have also implicated UPR signaling but their mechanism of inducing ER stress and/or UPR activation is not well understood (S. Wang & Kaufman, 2012). There is increasing evidence that certain viruses, especially enveloped viruses, can activate the UPR (reviewed in Chan, 2014). The UPR likely has both pro- and anti-viral properties and viruses may fine-tune UPR signaling to promote the pro-viral properties while simultaneously suppressing its anti-viral function. However, the mechanistic details of how the UPR is usurped by viruses and how the UPR impacts viral replication are lacking.

Kaposi's sarcoma-associated herpesvirus (KSHV) is a large enveloped oncogenic herpesvirus that hijacks multiple cellular stress responses to promote infection and tumorigenesis (Qiliang Cai, Verma, Lu, & Robertson, 2010). KSHV has been reported to use the UPR to promote viral reactivation from latency (Wilson et al., 2007; F. Yu et al., 2007), but precise role(s) of the UPR during lytic replication remain unknown. This was the motivation for my thesis.

The first part of this Introduction provides a comprehensive overview of some of the key processes involved in UPR signaling in response to ER stress, as well as roles for the UPR in different physiological responses. In addition, I provide examples of viral manipulation of the UPR that promote replication. The second part of the Introduction

summarizes KSHV and KSHV-initiated cancers and provides an overview of the viral replication cycle and some of the key viral gene products. The remainder of the Introduction lays out the foundation upon which the work for this thesis was undertaken. My work is an in-depth analysis of UPR signaling during KSHV replication and identifies ways in which the virus may modulate key UPR effectors to promote infection. The research presented here demonstrates an important role for this evolutionarily conserved cellular stress response in KSHV replication.

1.2 ER stress and the Unfolded Protein Response (UPR)

All eukaryotic cells have evolved a mechanism to sense ER stress and attempt to restore proteostasis by signaling from the ER to the nucleus to enhance expression of genes that regulate ER protein folding and degradation (reviewed in Walter & Ron, 2011). This ER stress response is called the UPR, which was first described in *Saccharomyces cerevisiae* (Cox, Shamu, & Walter, 1993; Mori, Ma, Gething, & Sambrook, 1993). Initial characterization of the UPR began in the 1970s with the identification of two mammalian proteins with molecular weights of 78 and 94 kDa that were upregulated by glucose depletion following Rous sarcoma virus-induced transformation of chick embryo fibroblasts. These proteins were named glucose regulated proteins Grp78 and Grp94 (Shiu, Pouyssegur, & Pastan, 1977). Pastan's group went on to show that Grp78 and Grp94 are also upregulated following treatment with the glucose analog 2-deoxyglucose (2-DG), or glucosamine, which inhibit glycosylation by blocking the addition of mannose to growing glycoproteins (Pouysségur, Shiu, & Pastan, 1977). Grp78 and Grp94 were also upregulated following treatment with Tm (Olden, Pratt, Jaworski, & Yamada, 1979), further indicating that glucose depletion is not the only mechanism of upregulation.

Another research group identified a protein from Pre-B lymphocytes that bound to free heavy chain immunoglobin (Ig), which they called BiP (binding immunoglobin protein) (Haas & Wabl, 1983). It eventually was revealed that Grp78 and BiP are the same protein and share sequence homology to members of the Hsp70 family of chaperones (Munro & Pelham, 1986). Therefore, it was concluded that BiP acts as a chaperone to bind ER proteins to promote folding. The laboratory of Joseph Sambrook showed that a mutant influenza A virus hemagglutinin (HA) protein that has the propensity to misfold is bound by BiP in the ER (Gething, McCammon, & Sambrook,

1986) and that both BiP and Grp94 were upregulated by this mutant HA protein, indicating that protein misfolding is responsible for their upregulation (Kozutsumi, Segal, Normington, Gething, & Sambrook, 1988). Promoter studies showed that BiP is transcriptionally upregulated suggesting that increases in protein misfolding in the ER triggers a signal to the nucleus to upregulate these chaperones to try to restore proper protein folding (S.C. Chang et al., 1987). A yeast homolog of BiP was subsequently identified and is encoded by the *KAR2* gene (Normington, Kohno, Kozutsumi, Gething, & Sambrook, 1989) and the signal transducer that upregulates Kar2p is a type I ER transmembrane protein with kinase and RNase activity named Ire1p (Cox et al., 1993; Mori et al., 1993).

The metazoan homolog of Ire1p was identified and called IRE1; the two mammalian IRE1 isoforms are known as IRE1α and IRE1β (Tirasophon, Welihinda, & Kaufman, 1998; X.-Z. Wang et al., 1998). Eventually it became clear that through evolution, metazoans have acquired two more sensors of ER stress, PERK (Harding, Zhang, & Ron, 1999) and ATF6 (Kyosuke Haze, Yoshida, Yanagi, Yura, & Mori, 1999; Yoshida, Haze, Yanagi, Yura, & Mori, 1998). Collectively, these sensors reprogram gene expression in an attempt to resolve ER stress (Fig 1.1). If the stress persists and becomes chronic or the stress is too robust for the sensors to resolve, then the UPR switches from an adaptive response to a pro-apoptotic response (Walter & Ron, 2011). The following sections will discuss the activation and signaling of the three UPR sensors.

1.2.1 Inositol-Requiring Enzyme 1 (IRE1)

The serine/threonine kinase and ribonuclease inositol-requiring enzyme 1 (IRE1, or Ire1p in yeast) was first identified in 1992 in *S. cerevisiae* by genetic complementation of a myo-inositol auxotroph, hence its name (Nikawa & Yamashita, 1992). Ire1p was shown to protect yeast from ER stress, which was dependent on its kinase activity (Cox et al., 1993; Mori et al., 1993). Ire1p is encoded by the *ERN1* gene, which is named based on its involvement in ER to nucleus signaling during ER stress. *S. cerevisiae* Ire1p is a large (1115 amino acids) transmembrane protein that contains an ER stress-sensing N-terminal luminal domain and a protein kinase domain and RNase domain in the cytoplasm (Credle, Finer-Moore, Papa, Stroud, & Walter, 2005). IRE1 was subsequently identified in metazoans (Tirasophon et al., 1998; X.-Z. Wang et al., 1998). More primitive animals such as Drosophila and nematodes have only one IRE1 gene, while mammals express

two isoforms: IRE1α and IRE1β. IRE1α is constitutively expressed and mice lacking IRE1α are embryonic lethal (Iwawaki, Akai, Yamanaka, & Kohno, 2009; K. Zhang et al., 2005). IRE1β expression is restricted to airway and intestinal epithelial cells and mice lacking IRE1β through homologous recombination technology are indistinguishable from their wild type and heterozygous littermates (Bertolotti et al., 2001). Although the exact reason for acquiring this tissue-specific isoform of IRE1 is not clear, it may be that the mRNA substrate specificity has diverged to some degree (D. Nakamura et al., 2011). For simplicity, throughout the thesis, IRE1 will always refer to IRE1α.

The mechanism of Ire1p signaling to the nucleus was eventually discovered following a UPR reporter screen of yeast mutants (Cox & Walter, 1996). A mutation in the HAC1 (homologous to ATF/CREB 1) gene blocked UPR activation following treatment with the N-linked glycosylation inhibitor Tm. HAC1 encodes a basic-leucine zipper (bZIP) transcription factor and was originally hypothesized to play a role in meiosis(Nojima et al., 1994). Following ER stress, Ire1p excises a 252-nt (nucleotide) intron of Hac1 mRNA and mRNA re-ligation results in a translational frameshift of Hac1(Cox & Walter, 1996; J. Nikawa, Akiyoshi, Hirata, & Fukuda, 1996; Sidrauski, Cox, & Walter, 1996). The translating ribosome bypasses the first stop codon and synthesizes a larger isoform that contains a transcriptional activation domain (Cox & Walter, 1996). Thus, splicing of Hac1 mRNA transforms Hac1p into a potent transcription factor that upregulates multiple genes, such as BiP, in an attempt to restore proteostasis.

Metazoans do not encode a Hac1p ortholog. Instead, in response to ER stress, IRE1 recognizes and excises a 26-nt intron from the mRNA that encodes the bZIP transcription factor, X Box binding protein 1 (XBP1) (Calfon et al., 2002; Yoshida, Matsui, Yamamoto, Okada, & Mori, 2001). Like Hac1p, XBP1 splicing triggers a translational frameshift generating a larger isoform spliced XBP1 (XBP1s), which contains a transactivation domain in the C-terminus. XBP1s upregulates chaperones, ERAD machinery, and lipid biosynthetic enzymes (A.-H Lee, Iwakoshi, & Glimcher, 2003a; Sriburi, Jackowski, Mori, & Brewer, 2004).

1.2.1.1 IRE1 Sensing of ER Stress

In the absence of ER stress, BiP binds the luminal domain of IRE1 to maintain it an inactive, monomeric form. Since BiP has higher affinity for misfolded proteins than

IRE1, the accumulation of unfolded proteins during ER stress releases IRE1 from BiP (Okamura, Kimata, Higashio, Tsuru, & Kohno, 2000). This allows IRE1 to homo-dimerize and subsequently oligomerize (Shamu & Walter, 1996; Welihinda & Kaufman, 1996).

Oligomerization is essential for IRE1 activity (Welihinda & Kaufman, 1996). The crystal structure of the yeast IRE1 luminal domain (LD), in its dimerized form, reveals a groove that resembles the peptide binding pocket of MHC (Credle et al., 2005). A subsequent study demonstrated that unfolded proteins can bind to this pocket, which promotes IRE1 oligomerization (B. M. Gardner & Walter, 2011). Conversely, crystal structure analysis of the human IRE1 LD dimers reveals a groove that was predicted to be too narrow for peptide binding (Jiahai Zhou et al., 2006). However, a recent study showed that, at least *in vitro*, peptides and unfolded proteins with a particular amino acid bias can bind to the human IRE1 luminal domain inducing allosteric changes that promote oligomerization (Karagöz et al., 2017). Thus, IRE1 can likely "sense" ER stress by a two-step mechanism: the release of BiP from the luminal domain, followed by dimerization and binding of unfolded proteins or peptides.

1.2.1.2 Activation of the IRE1 RNase Domain.

BiP release from monomeric IRE1, and dimerization of the luminal domains bring the cytoplasmic domains in close proximity in a face-to-face conformation (K. P. K. Lee et al., 2008). This proximity facilitates *trans*-autophosphorylation, where monomers phosphorylate one another at three serine residues in the kinase domain. In yeast these residues are Ser840, Ser841, and Ser850, which correspond to Ser724, Ser726, and Ser729 in human IRE1 (K. P. K. Lee et al., 2008; Shamu & Walter, 1996). Thr844 in yeast IRE1, which is not conserved in human IRE1, is also auto-phosphorylated and mutation of this residue greatly inhibits IRE1 activity (K. P. K. Lee et al., 2008). Interestingly, phosphorylation *per se* does not activate the RNase domain directly. In vitro experiments showed that both ADP and a non-hydrolysable mutant of ATP, AMPPNP, can activate its RNase activity, with ADP having the strongest activating effect (Sidrauski & Walter, 1997). Furthermore, in the presence of the non-hydrolysable ATP analog 1NM-PP1, the human IRE1 point mutant Ile642Gly can activate XBP1 splicing without the need for phosphorylation (Papa, Zhang, Shokat, & Walter, 2003). These findings support a mechanism of generating ADP from *trans*-autophosphorylation

that can be used to activate the RNase domain (Papa et al., 2003). The crystal structure of cytoplasmic IRE1 revealed that phosphorylation in the activation loop allowed for binding of ADP, which results in a transition to a back-to-back conformation to facilitate dimerization at the C-terminus (K. P. K. Lee et al., 2008). This dimerization of the ribonuclease domain generates the ribonuclease active site, which can recognize XBP1/Hac1 mRNA.

1.2.1.3 XBP1/Hac1 mRNA Splicing Causes a Translational Frameshift

Hac1/XBP1 mRNA contains two stem-loop structures that have a highly evolutionarily conserved 7-nucleotide (nt) loop with a consensus sequence of CNG/CNGN, which is recognized by IRE1 (Maurel, Chevet, Tavernier, & Gerlo, 2014; Oikawa, Tokuda, Hosoda, & Iwawaki, 2010; Sidrauski & Walter, 1997). IRE1 cleaves the mRNA between the conserved G-C (denoted by "/"), excising the 26-nt intron in mammalian XBP1 (252-nt in Hac1). Cleavage generates a 2',3'-cyclic phosphate at the 3'-end of the 5'-exon (T. N. Gonzalez, Sidrauski, Dö, & Walter, 1999), which is analogous to precursor tRNA cleavage. In fact, the yeast tRNA ligase Rlg1 (also known as Trl1) is also the Hac1 mRNA ligase (Sidrauski & Walter, 1997). In mammals, the catalytic subunit of the tRNA-splicing ligase complex, RtcB, along with its co-factor archease, ligate the 5' and 3' ends of XBP1 mRNA (Jurkin et al., 2014; Kosmaczewski et al., 2014; Y. Lu, Liang, & Wang, 2014).

Translation of the newly ligated XBP1 mRNA results in a frameshift in the reading frame causing ribosomes to bypass the stop codon that would generate 29 kDa XBP1u (XBP1-unspliced) resulting in the translation of the 56 kDa isoform, XBP1s (XBP1-spliced). The extended C-terminal region of this isoform contains a transactivation domain that is necessary and sufficient to upregulate genes involved in resolving ER stress (A.-H. Lee et al., 2003a; Yoshida et al., 2001).

1.2.1.4 Regulation of XBP1/Hac1 mRNA Splicing

The mechanisms involved in targeting XBP1 mRNA to the endoplasmic reticulum so that it can be cleaved by IRE1 have been fairly well characterized and are much different than the mechanisms that control Hac1 targeting to IRE1. In yeast, Hac1 mRNA is translationally repressed by the IRE1-targeted intron through direct base pairing with the 5'UTR. Translational repression allows a bipartite segment in the 3'UTR of Hac1 mRNA to facilitate recruitment to the ER where Hac1 mRNA associates with IRE1 oligomers

and is cleaved (Aragón et al., 2008). Whereas yeast Hac1 splicing requires translation repression, a different model of XBP1 splicing in mammals has been identified and requires protein translation. At the C-terminal, half of unspliced XBP1 protein there are two hydrophobic regions (HR) HR1 and HR2 and a C-terminal region (CTR) downstream of HR2 (Yanagitani et al., 2009; Yanagitani, Kimata, Kadokura, & Kohno, 2011). The CTR is responsible for translational pausing and stabilization of the mRNA-ribosome-nascent peptide chain which exposes HR2. HR2 acts as a signal sequence for SRP-dependent trafficking to the ER where it forms a pseudo-transmembrane protein in the Sec61 translocon (Kanda, Yanagitani, Yokota, Esaki, & Kohno, 2016). IRE1 also interacts with the Sec61 translocon and therefore brings IRE1 and the XBP1 intron into close proximity for excision and re-ligation (Plumb, Zhang, Appathurai, & Mariappan, 2015).

1.2.1.5 XBP1 is a bZIP Transcription Factor

X box binding protein 1 (XBP1) was identified 15 years before its mRNA was identified as the substrate for IRE1. As its name indicates, it was first identified as a DNA binding protein that binds to a motif called the X box in the promoter of MHC class II HLA-DRA gene (Liou et al., 1990). The X box (5'-CCTAGCAACAGAT-3') is contained in a subset of MHC class II genes and thus XBP1 is likely important for their expression (Liou, Boothby, & Glimcher, 1988; Liou et al., 1990; Ono, Liou, Davidon, Strominger, & Glimcher, 1991; Reith et al., 1988). Unspliced XBP1 (XBP1u) is a 29 kDa protein that contains a basic-leucine zipper (bZIP) domain and is a member of the CREB (cAMP regulatory element-binding protein) family of transcription factors because of its preferential binding for CRE-like elements that contain a highly conserved core ACGT sequence (Clauss, Chu, Zhao, & Glimcher, 1996). Paradoxically, there is no ACGT sequence in the human MHC-DRA X bot motif.

XBP1, like all bZIP transcription factors, contains leucine heptad repeats (a leucine at every seventh interval) to form an amphipathic alpha helical domain, which facilitates homo- and heterodimerization through an intertwined coiled-coil interaction. The N-terminal basic region of the bZIP transcription factor binds the major groove of DNA in a sequence specific manner (Miller, 2009). Depending on the organism, XBP1 can heterodimerize with other bZIP transcription factors including c-fos and ATF6, which can affect DNA sequence recognition and therefore change the repertoire of genes

that they transactivate (Ono et al., 1991; Reinke, Baek, Ashenberg, & Keating, 2013; Keisuke Yamamoto et al., 2007).

1.2.1.6 XBP1s Target Genes

Before XBP1 was known to be involved in the UPR, a consensus sequence based on EMSA and mutations of oligonucleotides proposed an XBP1 consensus target sequence of GAT-GACGTG(T/G)NNN(A/T)T, where N is any nucleotide and "-" shows that there may or may not require an extra nucleotide (Clauss et al., 1996).

After XBP1 was shown to be involved in the UPR, EMSA was used to identify a consensus sequence TGACGTG(G/A) (Yoshida et al., 2001). The sequence is called UPR-dependent cis-acting element (UPRE) because the consensus targeting sequence for yeast Hac1p is also called UPRE, although there is no consensus between sequences. Before XBP1 was identified as the substrate of IRE1, the UPRE sequence was originally characterized as a consensus sequence for the UPR transcription factor ATF6-N and was called the ATF6 site (Y Wang et al., 2000). However, a later study showed that XBP1s bound much stronger to this sequence, whereas minimal ATF6 binding could be detected, indicating that this sequence is more specific to XBP1s binding (Yoshida et al., 2001).

In addition to the UPRE, two other conserved cis-acting elements have been identified in ER stress-dependent genes. ERSE (ER stress element) was the first motif identified through ATF6 binding analysis and has the consensus sequence CCAAT-N9-CCACG, with the two 5-nt motifs separated by nine unspecific nucleotides.
ATF6 binds CCACG, which is dependent on the heterotrimeric transcription factor NF-Y (nuclear transcription factor Y) binding to CCAAT (Roy & Lee, 1999; Yoshida et al., 2000; Yoshida et al., 1998).

Another motif with the consensus sequence ATTGG-N-CCACG was later identified and named ERSE-II based on some of the shared features with ERSE; the CCACG motif is conserved, and the ATTGG is the reverse complement of CCAAT found in ERSE (Kokame, Kato, & Miyata, 2001; K. Yamamoto, Yoshida, Kokame, Kaufman, & Mori, 2004). EMSA and luciferase reporter assays showed that XBP1 can bind to UPRE the strongest but can also bind to ERSE-II and only weakly bind to ERSE, which was also dependent on NF-Y binding to the CCAAT motif. Interestingly, the defined ERSE and ERSE-II consensus sequences appear to lack the core ACGT that was shown to be important for XBP1 binding (K. Yamamoto et al., 2004). An analysis of the

sequences used in the study revealed that there is a thymine (T) directly adjacent to the CCACG motif in ERSE-II generating the ACGT core; this was not the case for ERSE and therefore may explain why XBP1s transcriptional activity was low with an ERSE luciferase reporter.

Multiple groups have tried to identify XBP1s-specific target genes (Acosta-Alvear et al., 2007; A.-H. Lee et al., 2003a; Shoulders et al., 2013). Different experimental protocols, including treating XBP1 knockout MEFs with UPR-activating drugs or ectopic XBP1 expression experiments combined with DNA microarrays, RNA-seq, and proteome experiments have been conducted. Differences in cell types or stimuli often yielded distinct XBP1s-dependent gene expression profiles. Similarly, since XBP1s can heterodimerize with ATF6 during ER stress, this can also impact XBP1 target genes. Acosta-Alvear *et al.* (2007) conducted ChIP-on-chip experiments to determine XBP1s-dependent gene expression in five different cell populations experiencing physiological levels of ER stress. Unsurprisingly they found that XBP1s bound to a core set of genes that regulate ER physiology. They also identified other genes not directly linked to ER stress such as genes involved in the DNA damage response. Using computational analyses, they also confirmed XBP1 consensus sequences and proposed additional consensus sequences including a CCAAT box, CCACG box, and UPRE A and UPRE B motifs, which are highly similar to the previously characterized UPRE. CCAAT and CCACG are part of ERSE and/or ERSE-II, although the researchers did not detect these cis-acting elements in their analyses. The researchers also showed that the location of the these XBP1 binding sites occur within 500 bp of the transcription start site (both upstream and downstream), with significant enrichment within 200 bp (Acosta-Alvear et al., 2007).

A.-H. Lee, *et al.* (2003a) used DNA microarrays to compare gene expression profiles among XBP1s-overexpressing MEFs and Tm-treated wild type and XBP1 knockout MEFs. They identified ERdj4, EDEM1, and $p58^{IPK}$ as evident XBP1s-specific genes. Shoulders *et al.* (2013) conducted combined transcriptomic and proteomic analysis of HEK293 cells ectopically-expressing inducible XBP1s, ATF6, or both, to determine the stress independent gene expression programs of these transcription factors and how either alone or combined expression changes the genetic landscape. At the mRNA level they found that ectopic XBP1 expression induced 180 genes (based on a false discovery

rate of < 0.05). Like A.-H. Lee *et al.* (2003a), they found that XBP1 specifically upregulated ERdj4. They also found that XBP1 upregulated EDEM2 and EDEM3 but could only upregulate EDEM1 with the combined expression of ATF6 (Shoulders et al., 2013). These differences in regulation of different gene targets by XBP1 could be due to the differences between experimental models or may reflect species-specific gene regulation by XBP1s.

1.2.1.7 Regulation of XBP1 Expression

Since XBP1u translation is required for XBP1 mRNA trafficking to the ER, XBP1 translation must be on during ER stress. ER stress also causes a global attenuation of translation by PERK activation (discussed below), which may impact XBP1 translation. Conversely, in the absence of stress, high levels of XBP1 translation could cause unnecessary XBP1 splicing. This is most evident through the spontaneous splicing of XBP1 following ectopic expression (Calfon et al., 2002; Yoshida et al., 2001). This indicates that if XBP1 mRNA and or/protein levels accumulate above a certain threshold, IRE1 can induce XBP1 splicing. Therefore, XBP1 translation must be upregulated during ER stress but carefully controlled in the absence of ER stress.

One mechanism of control is that XBP1u protein contains a degradation domain at the C-terminus and is targeted for rapid proteasomal degradation (Calfon et al., 2002; Yoshida et al., 2001; Yoshida, Oku, Suzuki, & Mori, 2006). Its half-life is approximately 11 minutes and thus XBP1u protein likely does not accumulate to high enough levels in the absence of stress to cause spontaneous mRNA splicing (Calfon et al., 2002). XBP1 is also regulated at the transcriptional level and can be induced by ATF6 (Yoshida et al., 2000; Yoshida et al., 2001). The amount of mRNA also corresponds to the amount of splicing, and likely correlates with the levels of XBP1u translation. Therefore, regulating XBP1 mRNA and XBP1u translation levels may be important control mechanisms to ensure that XBP1 splicing only occurs when needed.

1.2.1.8 Other Roles of XBP1u

XBP1u has been shown to have other roles than regulating the UPR. However, it is unclear how XBP1u can facilitate these other roles, since it is expressed at low levels and is highly unstable and quickly degraded. These inconsistencies may be resolved due the cell/animal model used. I will provide a few examples of functions that have been ascribed to XBP1u.

Since XBP1u and XBP1s share the same N-terminus, there is evidence that XBP1u can bind XBP1s and act as a negative feedback regulator. Following activation of the UPR by pharmacological inducers of ER stress, IRE1 splicing of XBP1 mRNA is attenuated after 8 to 16 h (depending on the drug or cell used) and XBP1u accumulates. XBP1u has a nuclear export signal and can recruit XBP1s to the cytoplasm to induce proteasomal degradation of both XBP1 isoforms (Yoshida et al., 2006).

Most of the other functions ascribed to XBP1u have been in the context of overexpression. Since XBP1u is intimately linked to XBP1s biogenesis, it has been challenging to ascribe clear phenotypes to XBP1u without also considering the contribution of newly-synthesized XBP1s in the system. XBP1u protected endothelial cells from oxidative stress by activating Akt through an interaction with HDAC3 (D. Martin et al., 2014). Another study showed that XBP1u played a role in regulating autophagy following chronic glutamine starvation in the human colon cancer cell line HCT116. Autophagy is a conserved catabolic process that degrades cytoplasmic constituents and organelles and is regulated by the transcription factor FOXO1. Following chronic glutamine starvation, XBP1u was phosphorylated by the MAPK ERK1/2 to increase binding and subsequent proteasomal degradation of FOXO1, which suppressed autophagy (Zhao et al., 2013).

Another group showed that XBP1 deficiency protected against Huntington's disease in a mouse model that expresses the mutant Huntingtin (mHtt) protein. A conditional XBP1 knockout in the mouse nervous system promoted FOXO1-induced autophagy to facilitate clearance of mHtt protein (Vidal et al., 2012). In this model, the authors showed that XBP1s promoted FOXO1 proteasomal degradation. Therefore, it is possible that both XBP1u and XBP1s can inhibit FOXO1-dependent autophagy to some degree.

1.2.1.9 Regulated IRE1-Dependent Decay (RIDD)

XBP1 is the only substrate that undergoes IRE1-mediated splicing due to the cleavage of two stem-loops (Sidrauski & Walter, 1997), while other ER-targeted mRNAs can be targeted by IRE1 due to the presence of one XBP1-like stem-loop (Maurel et al., 2014). This cleavage event results in mRNA degradation through a process known as regulated IRE1-dependent decay (RIDD) (Hollien et al., 2009). RIDD was first identified in Drosophila cells and resulted in strong decreases in mRNA levels of a broad array of

genes (Hollien & Weissman, 2006). RIDD was subsequently identified in mammalian cells but occurs in a smaller set of genes that are down-regulated 2-fold or less compared to 5 – 10-fold in Drosophila (Hollien et al., 2009). RIDD is thought to act as a mechanism to reduce the burden on the ER folding machinery by degrading mRNAs of translating ER proteins during ER stress. However, it is unclear how much the subtle changes in mRNA levels in a small subset of genes in mammalian cells impacts the protein load to promote protein folding. Interestingly, IRE1β, the IRE1 isoform that is expressed solely in airway and intestinal epithelial cells has less RNase activity against XBP1 splicing compared to IRE1α but a broader range of RIDD substrates (D. Nakamura et al., 2011). IRE1β has also been shown to cleave 28S rRNA, which can decrease the protein burden in the ER through translation repression (Iwawaki et al., 2001). The reason for the evolutionary divergence in RIDD activity between the two mammalian IRE1 isoforms is currently not known. Interestingly, XBP1 splicing and RIDD functionality co-exists in metazoan IRE1, whereas it is separated in two different yeast species. IRE1 in the budding yeast, *S. cerevisiae,* solely induces Hac1 splicing (Weihan Li et al., 2018; Niwa, Patil, DeRisi, & Walter, 2005). Conversely, there is no Hac1 ortholog in the fission yeast, *Schizosaccharomyces pombe,* and its IRE1 exclusively engages RIDD (Kimmig et al., 2012).

Unlike XBP1 splicing, IRE1 kinase activity is required for RIDD (Hollien et al., 2009). Bypassing IRE1 kinase activity by exposing the IRE1 Ile642Gly point mutant to the ATP analog 1NM-PP1 prevents RIDD even though XBP1 is spliced. It is not known precisely how IRE1 coordinates RIDD and XBP1 splicing activity. *In vitro* study suggests that IRE1 levels or oligomerization status dictates function; low levels of IRE1 promote a dimeric conformation that has reduced mRNA specificity and initiates RIDD, whereas high levels of IRE1 undergo oligomerization that promotes XBP1 splicing (Tam, Koong, & Niwa, 2014).

IRE1 is more active in XBP1 deficient cells resulting in increased RIDD (Maurel et al., 2014). Therefore, some of the ascribed phenotypes of XBP1 deficiency may in fact be due to hyperactivated IRE1 through RIDD. This includes the observation that XBP1 deficiency resulted in hypolipidemia and is promoted by IRE1 cleavage of mRNAs involved in lipid biosynthesis (So et al., 2012). RIDD has also been shown to play a direct role in diabetes through the cleavage of insulin mRNA (D. Han et al., 2009; A.-H.

Lee, Heidtman, Hotamisligil, & Glimcher, 2011; Lipson et al., 2006). A role for RIDD was also seen in dendritic cell biology where XBP1 deficiency in CD8α+ conventional DCs (cDCs) resulted in a decrease in mRNAs that encode important integrins and MHC class I machinery (Tavernier et al., 2017). RIDD has also been shown to protect XBP1-deficient B cells from overloading the ER by degrading μS mRNA, resulting in decreased IgM (Benhamron et al., 2014; Tang et al., 2018). RIDD also may play a role in virus infection and apoptosis (Bhattacharyya, 2014) (discussed below).

1.2.2 PKR-like Endoplasmic Reticulum Kinase (PERK) and the Integrated Stress Response (ISR)

1.2.2.1 Eukaryotic Initiation Factor 2α (eIF2α) Kinases

Eukaryotic cells attenuate global translation of non-essential genes in response to different stresses. In the absence of stress, the translation cycle of mRNAs begins with the heterotrimeric eIF2 (eukaryotic initiation factor 2) GTPase, which binds to methionine-loaded $tRNAi^{Met}$ (Fig 1.2). eIF2 is a heterotrimer of eIF2α, β, and γ, where the γ subunit is responsible for direct binding of GTP and Met-$tRNAi^{Met}$ (reveiwed in Sonenberg & Hinnebusch, 2009). The α and β subunits stabilize the tRNA interaction, and as discussed below, the α subunit has regulatory activity (Kashiwagi et al., 2016). When bound to GTP, eIF2 binds Met-$tRNAi^{Met}$ to form the ternary complex (TC).

The TC is loaded onto the 40S small ribosomal subunit. Further recruitment of eIF1, eIF1A, eIF3, and eIF5 form the 43S pre-initiation complex (PIC). The 43S PIC indirectly binds to the 5'-cap of mRNAs by binding the eIF4F heterotrimeric complex (composed of eIF4E, eIF4G, and eIF4A). eIF4F links the 5'cap to the poly(A) tail by binding the poly(A)-binding protein (PABP) to circularize the mRNA. The 43S PIC initiates scanning of the 5'UTR in a 5'-3' direction to find the AUG start codon. Once Met-$tRNAi^{Met}$ engages with the start codon, with the help of GTPase activating protein eIF5, GTP is hydrolyzed to GDP releasing eIF2 from the ribosomal protein complex. Released eIF2 can participate in a new translation initiation cycle. However, successful recycling depends on exchange of GDP-bound eIF2 for GTP by the guanine nucleotide exchange factor (GEF) eIF2B (Sonenberg & Hinnebusch, 2009).

In response to different types of stress, the α subunit of eIF2 can be phosphorylated on Serine 51 by stress-specific eIF2α kinases. Mammals encode four different eIF2α kinases that are activated by different types of stress (discussed below).

eIF2α phosphorylation induces higher affinity binding to eIF2B, inhibiting its GEF activity and thus reducing translation (Krishnamoorthy, Pavitt, Zhang, Dever, & Hinnebusch, 2001; Pavitt, Ramaiah, Kimball, & Hinnebusch, 1998). This initiates a cellular stress response known as the integrated stress response (ISR) (Harding et al., 2003).

The ISR involves the phosphorylation of eIF2α in response to a variety of different stresses to attenuate bulk translation, while specifically upregulating a set of stress responsive genes (discussed below) (Fig 1.3). Recently, a small molecule called ISRIB (ISR inhibitor) was shown to bind eIF2B promoting its GEF activity, which attenuated translation inhibition following activation of an eIF2α kinase (Sekine et al., 2015; Sidrauski et al., 2013, 2015; Zyryanova et al., 2018). Bulk translation attenuation, both through phospho-eIF2α-dependent and -independent mechanisms can trigger stalled 48S pre-initiation complexes to aggregate into large macromolecular structures called stress granules (SGs). SG formation is mediated through the protein-protein interaction of RNA binding proteins with glutamine/asparagine-rich prion-like domains such as TIA-1 (T-cell intracellular antigen 1) and G3BP (Ras–GTPase-activating protein binding-protein 1). SGs are sites of mRNA triage that control the fate of these non-translating mRNAs, as well as other cellular functions (Anderson & Kedersha, 2008). ISRIB treatment potently reduces SG formation in response to eIF2α phosphorylation (Sidrauski, McGeachy, Ingolia, & Walter, 2015).

Mammals express four eIF2α kinases: GCN2 (general control nonderepressible 2), PERK (PKR-like ER kinase), PKR (Protein kinase R; "R" stands for RNA), and HRI (heme regulated inhibitor) (Pakos-Zebrucka et al., 2016; Taniuchi, Miyake, Tsugawa, Oyadomari, & Oyadomari, 2016) (Fig 1.3). The eIF2α kinase HRI was first identified as responsive to decreases in heme levels in rabbit reticulocyte lysate (RRL), which attenuated translation through eIF2α phosphorylation (Farrell, Balkow, Hunt, Jackson, & Trachsel, 1977). HRI is most highly expressed in erythroid cells and plays an essential role in responding to heme deficiency. Normally, heme binds the HRI kinase domain keeping HRI in an inactive state; decreased levels of heme promotes HRI phosphorylation of eIF2α. HRI has also been reported to be activated by oxidative stress, heat shock, and osmotic shock (A.-P. Han et al., 2001; McEwen et al., 2005).

dsRNA in the presence of the anti-viral molecule interferon (IFN) was also shown to inhibit translation in RRL through eIF2α phosphorylation by PKR (Lebleu, Sen, Shaila, Cabrer, & Lengyel, 1976; Levin, Petryshyn, & London, 1980). PKR is constitutively expressed at low levels but can be induced by IFN (Meurs et al., 1990).

GCN2 was discovered in yeast shortly after the discovery of HRI and PKR. GCN2 was identified as a protein kinase activated in response to amino acid starvation which bound to uncharged tRNAs and inhibited translation (Roussou, Thireos, & Hauge, 1988; Wek, Jackson, & Hinnebusch, 1989). However, its identity as an eIF2α kinase was not revealed until HRI was cloned, which showed sequence similarity to GCN2 (J. J. Chen et al., 1991; Dever et al., 1992). GCN2 is the only eIF2α kinase encoded by the yeast *S. cerevisiae*, whereas *S. pombe* also encodes two isoforms of HRI, as well as GCN2 (Zhan, Narasimhan, & Wek, 2004; Zhan et al., 2002). The human ortholog of GCN2 was identified based on sequence conservation with the yeast eIF2α kinase (Berlanga, Santoyo, & De Haro, 1999; Sood, Porter, Olsen, Cavener, & Wek, 2000). GCN2 can also be activated by DNA damage, oxidative stress, and osmotic stress (Anda, Zach, & Grallert, 2017). Interestingly, a study showed that osmotic stress induced from high NaCl concentrations activated all four mammalian eIF2α kinases, which corresponded to a robust increase in phospho-eIF2α (Taniuchi et al., 2016). Through these eIF2α kinases the cell has an ability to sense a wide variety of different types of stress and respond by attenuating global translation. Depending on the type stress there may also be redundancies, since some stresses have been shown to activate more than one of the eIF2α kinases at a time (Taniuchi et al., 2016).

1.2.2.2 PERK is Activated by ER Stress

ER stress, such as treatment with the reducing agent DTT or the N-linked glycosylation inhibitor Tm, was also shown to increase eIF2α phosphorylation (Prostko, Brostrom, & Brostrom, 1993). Around the same time that the human GCN2 was identified, Harding, Zhang, & Ron (1999) identified a gene from a *C. elegans* database that is a type I transmembrane ER protein with a cytoplasmic protein kinase domain that has striking similarity to HRI and PKR and an ER luminal domain that has regions that share similarities to IRE1; they called the kinase PERK (for PKR-like ER kinase). They demonstrated that PERK is localized in the ER and undergoes autophosphorylation for

activation and is a *bona fide* eIF2α kinase. Furthermore, they showed that PERK was activated in response to drugs that cause ER stress. When exposed to ER stress, mouse embryonic stem cells deficient in PERK failed to phosphorylate eIF2α and attenuate bulk translation (Harding 2000). This failure to phosphorylate eIF2α resulted in decreased cell survival following exposure to persistent ER stress. At around the same time as the discovery of PERK, Shi *et al.* (1998) also identified the same gene from rat pancreatic islet cells and called the protein PEK (pancreatic eIF2α kinase); despite this, the name PERK has gained widespread acceptance in the literature.

The similar luminal domain to IRE1 highlights a conserved mechanism of responding to ER stress (Harding et al., 1999). In the absence of stress, BiP binds both PERK and IRE1 to maintain them as inactive monomers. Upon ER stress, release of BiP leads to dimerization and autophosphorylation of these two ER stress sensors (Bertolotti, Zhang, Hendershot, Harding, & Ron, 2000; K. Ma, Vattem, & Wek, 2002). There is also evidence that PERK may form higher-order oligomers, including tetramers that may also bind misfolded proteins directly, which is analogous to the mode of activation for IRE1 (Bertolotti et al., 2000; Carrara, Prischi, Nowak, & Ali, 2015; P. Wang, Li, Tao, & Sha, 2018). Activated PERK forms a back-to-back dimeric conformation, which can bind and phosphorylate eIF2α to attenuate bulk translation (Cui, Li, Ron, & Sha, 2011).

1.2.2.3 uORF-Mediated Translational Control during the ISR

While eIF2α phosphorylation attenuates bulk translation, not all mRNAs are susceptible to this inhibition. In fact, some mRNAs are translated only in response to eIF2α phosphorylation. These mRNAs often encode stress-responsive genes. Their translational regulation is largely due to the presence of upstream ORFs (uORFs) in their 5'UTRs. Central to these uORF-containing genes is ATF4 in humans and GCN4 in yeast (Vattem & Wek, 2004).

Before the identification of the yeast eIF2α kinase GCN2, it was known that the transcription factor GCN4 was specifically translated in response to amino acid starvation, a nutritional stress that stimulates production amino acid biosynthetic enzymes (Hinnebusch, 1984). This mechanism of translational control is through the presence of short ORFs upstream of the AUG start codon that initiates translation of GCN4. These small ORFs are classically called uORFs (upstream ORFs) (Mueller & Hinnebusch,

1986; Tzamarias, Alexandraki, & Thireos, 1986). GCN4 has 4 uORFs in tandem and all contain an AUG start codon, an ORF, followed by a stop codon. In the absence of stress there are high levels of eIF2 in its GTP bound form. The 43S PIC scans the 5'UTR until it reaches the AUG codon of first uORF, uORF1. The ribosome will initiate translation of uORF1 and terminate at its stop codon. However, instead of releasing from the mRNA, the small ribosomal subunit continues to scan until it encounters the next AUG that is part of uORF2. This continuation of ribosomal scanning is likely due to the short length of uORFs. However, re-initiation of translation is not 100% efficient and as the number of ribosomes that re-initiate translation at uORF2, 3, and 4 diminishes preventing initiation of translation at the GCN4 AUG start codon. Every round of translational re-initiation requires an active eIF2-GTP bound to Met-tRNAi^{Met} to form the ternary complex (TC). In the presence of stress, eIF2α phosphorylation reduces the levels of eIF2-GTP by inhibiting the GEF, eIF2B. This delays TC binding to the scanning 40S ribosomal subunit and thus bypassing the uORFs. This allows the ribosome to preferentially initiate translation at the GCN4 AUG start codon (Hinnebusch, 1997).

Although there are no mammalian orthologs of GCN4, a protein analogous to GCN4 is the bZIP transcription factor ATF4, which is also preferentially upregulated by eIF2α phosphorylation (Harding et al., 2000). Mouse and human ATF4 mRNAs contain only two uORFs and the 3'-proximal uORF, uORF2, overlaps a short segment of the ATF4 ORF. In the absence of stress, low levels of eIF2α phosphorylation results in translation of uORF1 and re-initiation of translation of uORF2. Since the STOP codon is downstream of the ATF4 AUG start codon, this prevents translation of ATF4. Analogous to what is seen for GCN4, increased eIF2α phosphorylation increases the time required for re-initiation. Thus, following termination of uORF1 translation, the ribosome bypasses the uORF2 start codon and preferentially translates ATF4 (Vattem & Wek, 2004).

The full coverage of genes with uORF-containing mRNAs that control translation in response to eIF2α phosphorylation is not fully known. Multiple large-scale studies have been conducted and uORF databases have been generated in an attempt to identify these genes (Chew, Pauli, & Schier, 2016; McGillivray et al., 2018). However, simply identifying mRNAs with uORFs may not be sufficient because these uORFs may be functionally inert. Furthermore, many of the predicted uORFs have been based on

translation initiation from an AUG codon, but there is increasing evidence that non-AUG (or near-cognate) start codons such as GUG, CUG and UUG, can control uORF translation. Therefore, the number of genes with uORF regulatory elements is much larger than previously appreciated (Ingolia, Lareau, & Weissman, 2011; Young & Wek, 2016).

Another intriguing example of the role of uORFs in translational control is that the peptide encoded by the uORF rather than the ORF itself may be important for ribosome termination or re-initiation to control expression of uORF-containing mRNAs (Morris & Geballe, 2000). For example, ATF4 transactivates a transcription factor CHOP, which also contains uORFs in its mRNA. A 31 amino acid peptide expressed from one of the uORFs is important for inhibiting translation of the CHOP ORF in the absence of stress (Jousse et al., 2001). Alternatively, these uORF-derived peptides may also have translation-independent functions (Oyama et al., 2007; Slavoff et al., 2013).

1.2.2.4 Activating Transcription Factor 4 (ATF4)

ATF4 is a bZIP transcription factor and belongs to the CREB (cAMP responsive element-binding)/ATF family. ATF4 is a master regulator of the integrated stress response (ISR) that upregulates transcription of many stress-response genes (Harding et al., 2003). To promote gene expression, ATF4 can bind to the ATF/CRE consensus sequence 5'-TGACGTCA-3' as well as the amino-acid response element (AARE), which contains the core sequence 5'-ATTGCATCA-3' (Hai & Hartman, 2001). Some of these pro-survival genes that ATF4 targets are involved in amino acid import and metabolism, the anti-oxidant response, and catabolic processes such as autophagy (B'chir et al., 2013; Harding et al., 2003; Rzymski et al., 2010).

In response to ER stress, PERK upregulates ATF4 by inducing eIF2α phosphorylation through the previously described uORF-dependent mechanism (Harding et al., 2000). PERK has also been shown to directly activate the bZIP transcription factor Nrf2 (nuclear factor erythroid 2 [NFE2]-related factor 2) (Cullinan et al., 2003). Nrf2 is classically associated with oxidative stress. In the absence of stress Nrf2 is retained in the cytoplasm by binding to Keap1 (Kelch-like ECH-associated protein 1). Keap1 is an adaptor protein for Cullin 3 and Ring-Box 1-dependent E3 ubiquitin ligase complex and together can promote proteasomal degradation of Nrf2. Increases in ROS causes oxidation of Keap1 leading to conformational changes that prevent Nrf2 binding; free

Nrf2 can translocate to the nucleus and upregulate genes to facilitate an anti-oxidant response (Q. Ma, 2013). In response to ER stress, PERK phosphorylates Nrf2, which also stimulates Keap1 release. ATF4 and Nrf2 can interact to upregulate anti-oxidant response genes such as heme oxygenase-1 (HO-1). Interestingly, Nrf2-deficient cells are more sensitive to ER stress than wild-type cells and display increased cell death, indicating an important coordination between the UPR and the anti-oxidant response (Cullinan et al., 2003). ATF4 also transcriptionally upregulates other transcription factors, including ATF3 and CHOP (Harding et al., 2000; H.-Y. Jiang et al., 2004). ATF4 can heterodimerize with CHOP and change the repertoire of transactivated genes (Gachon et al., 2001; J. Han et al., 2013; Pakos-Zebrucka et al., 2016).

1.2.2.5 C/EBP Homologous Protein (CHOP)

CHOP (C/EBP homologous protein), originally identified as part of the DNA damage response, is a 29 kDa bZIP transcription factor that belongs to the subfamily C/EBP (CCAAT-enhancer-binding-protein), which consists of 6 members: C/EBPα, β, γ, δ, ε, and CHOP (also called C/EBPζ) (Ramji & Foka, 2002). Because it was first identified as upregulated in response to DNA damaging agents like UV light, CHOP is also called DDIT3 (DNA-damage-inducible transcript 3) or GADD153 (growth and arrest DNA damage protein 153) (Oyadomari & Mori, 2004).

ATF4 transcriptionally upregulates CHOP due to the presence of AAREs and ATF/CRE motif in the CHOP promoter (Averous et al., 2004; Y. Ma, Brewer, Alan Diehl, & Hendershot, 2002). The CHOP promoter also contains ERSE and ERSE-II sequences and can be transcriptionally upregulated by ATF6 (Ubeda & Habener, 2000; Yoshida et al., 2000). However, upregulation of CHOP mRNA was almost completely abolished in PERK knockout cells indicating that ISR/ATF4 branch of the UPR plays a dominant role (Harding et al., 2000). Furthermore, CHOP mRNA also contains uORFs that permit translation of CHOP following increases in eIF2α phosphorylation (Jousse et al., 2001; Palam, Baird, & Wek, 2011). As mentioned previously, CHOP forms homodimers and can heterodimerize with ATF4 (Gachon et al., 2001). Both CHOP homodimers and CHOP/ATF4 heterodimers can upregulate stress-responsive genes (Pakos-Zebrucka et al., 2016). CHOP can also heterodimerize with other members of the C/EBP family, such as C/EBPα, and act as a dominant negative inhibitor (Ron & Habener, 1992).

CHOP is widely-known as a pro-apoptosis transcription factor. One of the transcriptional gene targets of CHOP is GADD34 (Marciniak et al., 2004). GADD34 bridges phospho-eIF2α to protein phosphatase 1α (PP1α) to facilitate eIF2α dephosphorylation to restore translation (Novoa, Zeng, Harding, & Ron, 2001). This occurs regardless of ER stress resolution, which can have an important impact on cell fate (discussed below). GADD34 also contains uORFs, and like ATF4 and CHOP, these uORFs are required for maximal translation of GADD34 during the UPR (Y.-Y. Lee, Cevallos, & Jan, 2009). Interestingly, the human herpesvirus herpes simplex virus type 1 (HSV-1) expresses an ortholog of GADD34, $\gamma_1$34.5, which dephosphorylates eIF2α to prevent stress-induced translation arrest in HSV-1 infected cells (He, Gross, & Roizman, 1997, 1998).

1.2.3 Activating Transcription Factor 6 (ATF6)

The third sensor of ER stress is ATF6. ATF6 is a 90 kDa type-II transmembrane glycoprotein with a bZIP transcription factor domain in its N-terminal cytosolic domain and is normally localized to the ER (Kyosuke Haze et al., 1999; Yoshida et al., 1998). It has two isoforms, ATF6α and ATF6β (originally named CREBP-RP or G13) that are both constitutively expressed and share multiple cytoplasmic and luminal domains with high amino acid sequence similarity (K Haze et al., 2001; C. Zhu, Johansen, & Prywes, 1997). Similar to IRE1 and PERK, ATF6 is bound to BiP in the absence of ER stress to prevent activation (Shen, Snapp, Lippincott-Schwartz, & Prywes, 2005). There are likely other modes of maintaining ATF6 in an inactive state, including the formation of intramolecular disulfide bonds and intermolecular disulfide bonds with other ATF6 proteins, creating ATF6 monomers, dimers, and oligomers (Nadanaka, Okada, Yoshida, & Mori, 2007).

The precise mechanism of ATF6 activation in response to ER stress is not clear. Upon induction of ER stress, ATF6 translocates to the Golgi in a CopII-dependent manner where it is cleaved at the luminal side of the ER by Site-1 protease (S1P) and the cytoplasmic side of the ER by S2P in a process referred to as regulated intramembrane proteolysis (RIP) (Schindler & Schekman, 2009; J. Ye et al., 2000). These cleavage events release a cytosolic fragment that is an active bZIP transcription factor ATF6-N. As an aside, I will often omit the "N" in "ATF6-N" when referring to the proteolytically cleaved ATF6 isoform. ATF6 translocates to the nucleus to transactivate genes involved

in protein folding, including the abundant chaperone BiP, and other chaperones and foldases. ATF6 also upregulates genes involved in degrading misfolded proteins through ERAD. ATF6 can also heterodimerize with XBP1s to upregulate a different set of UPR genes and can likely also synergistically activate ATF6 or XBP1s-dependent genes (Shoulders et al., 2013; Keisuke Yamamoto et al., 2007).

Although the precise mechanism of sensing misfolded proteins is unclear, there is evidence that the reduction of inter- and intra-molecular disulfide bonds promotes monomeric ATF6, which is the correct conformation for trafficking (Nadanaka et al., 2007). Under-glycosylation has also been reported to be important for trafficking to the Golgi (Hong et al., 2004). Only the luminal domain is involved in ER stress sensing and trafficking to the Golgi; swapping the C-terminal luminal domain of ATF6 onto a constitutively transported protein Sec22 resulted in its ER retention and trafficking to the Golgi upon ER stress (Sato, Nadanaka, Okada, Okawa, & Mori, 2011). CopII is located on the cytoplasmic side of the ER and therefore it is not known how the luminal domain of ATF6 signals to COPII for trafficking (Gallagher & Walter, 2016; Schindler & Schekman, 2009).

This mechanism of controlling ATF6 activation through ER-to-Golgi trafficking to undergo proteolytic cleavage is not unique to ATF6. SREBP1 and SREBP2 are ER membrane bound transcription factors that undergo RIP by S1P and S2P in response to low cholesterol and the released cytosolic transcription factors upregulate genes involved in cholesterol biosynthesis (Reimold et al., 2000). The SREBPs interact with SCAP (SREBP cleavage activating protein) which is the protein that actually senses sterol levels. SREBP and SCAP are retained in the ER by INSIG (insulin-induced gene) binding of SCAP. Low levels of sterols releases INSIG from SCAP allowing SCAP and SREBP to translocate to the Golgi in COPII vesicles (T. Yang et al., 2002). ATF6 processing does not require SCAP, and there may be an ACAP (ATF6 cleavage activating protein) and or INSIG-like protein that regulates trafficking of ATF6 that remains to be discovered (Gallagher et al., 2016).

With the use of high-throughput small molecule screens and ATF6-luciferase reporters, a class of small molecule ATF6 inhibitors called Ceapins (after the Irish verb ‘ceap,’ which means ‘to trap’) were identified and were found to inhibit ATF6 trafficking to the Golgi and promote oligomerization (Gallagher et al., 2016a; Gallagher & Walter,

2016b). Another HTS identified a group of small molecule ATF6 activators (Plate et al., 2016). In another study, the luminal domain was fused to tandem affinity purification tag that behaved like full length ATF6 and mass spectrometry revealed unique binding factors such as PDI and calnexin as well as the previously identified binding partner BiP (Sato et al., 2011). With the use of ATF6 inhibitors, activators, and protein interaction studies, it is likely only a matter of time before the molecular details of ATF6 activation are fully elucidated.

There are also other ER transmembrane proteins that share similar domain structure to ATF6 and belong to the OASIS subfamily of bZIP transcription factors (reviewed in Asada, Kanemoto, Kondo, Saito, & Imaizumi, 2011). These include Luman/LZIP/CREB3, OASIS/CREB3L1, BBF2H7/CREB3L2, CREBH/CREB3L3, and CREB4/AIbZIP/Tisp40/CREB3L4. Like ATF6, these proteins are also processed by RIP to release their N-terminal bZIP transcription factor. Other than Luman, these proteins have cell or tissue-specific expression indicating that they have different physiological roles. Interestingly, some of these ATF6-like proteins can also be activated by ER stress, indicating that the UPR in different tissues may have a different gene expression profile depending on the presence of other ATF6-like transcription factors (Asada et al., 2011).

ATF6-N recognizes and binds to conserved consensus sequence ERSE (consensus sequence CCAAT-N9-CCACG) and ERSE-II (ATTGG-N-CCACG), which are found in a variety of UPR dependent genes (Kokame et al., 2001; Shoulders et al., 2013; Yoshida et al., 2001). Furthermore, ATF6 binding is dependent on the heterotrimeric transcription factor NF-Y (composed of NF-YA, NF-YB, and NF-YC) (Yoshida, et al., 2001). ATF6-N binds to CCACG while NF-Y occupies CCAAT (Yoshida et al., 2000).

Genetic knockout and overexpression studies in the presence or absence of ER stress have identified ATF6-dependent genes (Adachi et al., 2008; A.-H. Lee et al., 2003a; Okada, Yoshida, Akazawa, Negishi, & Mori, 2002; Shoulders et al., 2013; Keisuke Yamamoto et al., 2007). ATF6-N forms a homodimer to upregulate chaperone genes, genes involved in protein quality control and protein degradation through ERAD, as well as components of the redox pathway. Two of the best-characterized genes that ATF6-N upregulates are BiP and Grp94 (M. Li et al., 2000; Shoulders et al., 2013; J. Wu et al., 2007), the abundant ER chaperones that were first characterized as ER stress-responsive genes (Shiu et al., 1977). ATF6-N can also upregulate the ISR gene CHOP

due to the presence of an ERSE in the CHOP promoter (Y. Ma et al., 2002; Yoshida et al., 2000). ATF6 has also been shown to upregulate XBP1 expression, which is thought to be important for robust XBP1 splicing in response to ER stress (Yoshida et al., 2001).

The two ATF6 isoforms, α and β, can also heterodimerize, which likely impacts target gene expression (Thuerauf, Morrison, & Glembotski, 2004; Yoshida et al., 2001). The two different isoforms also likely have redundant roles since there are no obvious defects in ATF6α or β single knockout mice, but a double knockout is embryonic lethal (Yamamoto et al., 2007). Interestingly, following treatment with Tm, ATF6α knockout MEFs were severely defective in their ability to upregulate UPR genes, such as BiP and components of ERAD, and as a result were highly susceptible to cell death. Conversely, ATF6β knockout MEFs only showed a slight decrease in BiP expression compared to wild-type MEFs and as a result were less susceptible to ER stress-induced cell death. This indicates that in response to high levels of stress, ATF6α plays a more prominent role in resolving ER stress than the β isoform (Wu et al., 2007; Yamamoto et al., 2007). These studies also indicate that ATF6β is sufficient to promote survival in response to more physiological levels of ER stress that are encountered during development.

Other than α/β ATF6 heterodimers, ATF6-N can also heterodimerize with XBP1 to bind ERSE-II and UPRE sequences (Yoshida et al., 2001). ATF6-N has also been reported to heterodimerize with the liver-specific RIP-dependent transcription factor CREBH which changes its gene expression profile to synergistically promote a CREBH-driven inflammatory response (K. Zhang et al., 2006). Future studies of ATF6 heterodimers with other bZIP transcription factors will likely reveal unique gene expression profiles that are different than the classical ATF6-dependent UPR gene expression profile.

1.2.4 UPR Activation by ER Lipid Bilayer Stress

The ER is a major site of lipid synthesis and plays a central role to sensing and regulating lipid dynamics (reviewed in Fagone & Jackowski, 2009). Membrane protein folding is also impacted by the ER lipid composition. Generally, the ER membrane consists of loosely-packed lipids and low amounts of bulky sterol groups to allow for protein insertion. Changes in lipid dynamics can cause aberrant lipid composition that can impede protein insertion and folding, which can cause ER stress. Furthermore, there is accumulating evidence that disruption in lipid homeostasis can cause lipid bilayer stress,

which can directly activate the UPR (reviewed in Covino, Hummer, & Ernst, 2018). Depletion of inositol, changes in phosphatidylethanolamine : phosphatidylcholine ratios, increases in fatty acid saturation, or increases in sterol levels can activate the UPR sensors (Pineau et al., 2009; Promlek et al., 2011; Surma et al., 2013; Thibault et al., 2012; Volmer, van der Ploeg, & Ron, 2013). Interestingly, IRE1 and PERK activation from lipid bilayer stress is independent of their luminal domains (LDs), since a mutant protein with a deleted LD is resistant to activation by protein misfolding but can be still activated by lipid dysregulation (Promlek et al., 2011; Volmer et al., 2013). The activation of IRE1 and PERK is likely due the changes in the conformation of their transmembrane domains, which promotes clustering and subsequent activation (Halbleib et al., 2017).

In response to lipid bilayer stress, activation of the UPR facilitates the upregulation of lipid biosynthetic genes by ATF6 and XBP1s to expand the ER membranes to help restore membrane homeostasis (Bommiasamy et al., 2009; Sriburi et al., 2004). ATF6 and XBP1s also upregulate genes involved in protein folding and ERAD. Interestingly, a recent study showed that activation ATF6 by lipid bilayer stress induced a gene expression profile different than in response to proteotoxic stress and preferentially upregulated lipid metabolism genes compared to protein folding genes (Tam et al., 2018). Based on these studies there is strong evidence that indicates that the UPR not only responds to increases in protein misfolding in the ER but also to perturbations in the ER membrane. Multiple diseases are heavily linked to dysregulation of lipid metabolism, including obesity and type II diabetes, and thus UPR sensing of lipid composition likely plays an integral role in the pathophysiology of many of these diseases (see Section 1.2.6).

1.2.5 The UPR Induces Apoptosis in Response to Persistent or Acute ER stress.

1.2.5.1 An Overview of Apoptotic Pathways

There are two major types of apoptotic pathways: extrinsic and intrinsic (reviewed in Elmore, 2007). Ultimately the apoptosis pathways signal through cleavage-dependent activation of initiator caspases that go on to cleave effector caspases. The effector caspases facilitate cell death by cleaving a wide variety of cellular proteins. The extrinsic (or death receptor-mediated) pathway induces apoptosis from signals outside the cell through the binding and activation of death receptors, which belong to the TNF

superfamily and include Fas, TNF receptor 1, TRAIL-R1 (DR4), and TRAIL-R2 (DR5). Upon ligand binding, the cytoplasmic domains associate with FADD directly or with the help of TRADD. FADD interacts with pro-caspase-8 to form the death-inducing signaling complex (DISC), which initiates cleavage and activation of caspase-8. Activated caspase-8 can cleave and activate caspase-3, which then goes on to cleave many different cellular proteins, ultimately triggering cell death.

The intrinsic (or mitochondrial mediated) pathway uses a subclass of BCL2 family of proteins called BH3-only proteins, such as tBID (truncated BID), BIM, and PUMA, to promote mitochondrial dysfunction (Kim et al., 2009). Normally, these BH3-only proteins are inhibited by other BCL2 family members, including Bcl-2. However, in the presence of apoptosis-inducing stimuli, the anti-apoptotic BCL2 proteins are inhibited allowing the BH3-only proteins to activate two mitochondrial proteins Bax and Bak, which cause mitochondrial outer membrane permeabilization (MOMP) (reviewed in Dewson & Kluck, 2009). Cytochrome c is localized between the inner and outer mitochondrial membranes, and MOMP facilitates the release of cytochrome c (Kim et al., 2009). In the cytoplasm, cytochrome c recruits Apaf-1 and promotes the heptamerization and activation of caspase-9, which collectively is referred to as the apoptosome. Once activated, caspase-9 cleaves and activates effector caspases (reviewed in Bratton & Salvesen, 2010).

1.2.5.2 ER Stress may Activate Different Apoptotic Pathways

ER stress has been shown to activate both extrinsic and intrinsic apoptosis pathways (Puthalakath et al., 2007; Yamaguchi & Wang, 2004). Depending on the stimuli, activation of death receptors can also activate the mitochondrial mediated pathway. This is primarily through caspase-8 cleavage of BID to generate the active tBID, which initiates mitochondrial dysfunction (H Li, Zhu, Xu, & Yuan, 1998). There are other less well-defined caspases that are thought to be able to induce apoptosis, and some groups suggest that ER stress can activate these pathways. Caspase-12 is located on the cytoplasmic face of the ER and has been reported to activate apoptosis in response to ER stress (Nakagawa et al., 2000). Caspase-12 likely cleaves and activates caspase-9, which then activates caspase-3 (Morishima, Nakanishi, Takenouchi, Shibata, & Yasuhiko, 2002). Therefore, in caspase-12 mediated apoptosis, activation of caspase-3 is independent of mitochondrial dysfunction and cytochrome c release. ER stress has also

been shown to activate caspase-2, which through the cleavage of BID to tBID, can activate Bax/Bak-dependent MOMP (J.-P. Upton et al., 2008). Thus, it appears that ER stress may activate multiple different apoptotic pathways involving different initiator caspases. These differences may be the result of cell-specific mechanisms of apoptosis or the type of ER stress that was applied. Alternatively, it is possible that multiple apoptotic pathways may be activated in response to stress or there may be compensatory mechanisms between different pathways when they are disrupted.

The UPR is involved in regulating apoptosis signaling (Walter & Ron, 2011). This switch from adaptation to pro-apoptosis depends on the strength, type, and duration of the stimuli. The precise mechanism that control this switch is not known. Furthermore, some of the pro-apoptotic factors induced by the UPR, such as CHOP, are induced during the adaptive phase and it is not clear how these pro-apoptotic factors are regulated to ensure that their apoptotic functions are implemented only after the cell has acknowledged that the stress cannot be resolved (Rutkowski et al., 2006). Nonetheless, there has been some considerable effort in trying to identify how the UPR promotes apoptosis and how the switch from adaptive signaling to apoptosis occurs. Generally, ATF6 is only thought to play a role in promoting protein homeostasis, whereas IRE1 and PERK are important for controlling cell fate (Hetz & Papa, 2018). The following subsections will highlight some of the main findings that demonstrate that PERK and IRE1 can control the activation of different apoptotic caspases.

1.2.5.3 PERK Signaling Promotes Apoptosis

PERK phosphorylates eIF2α which arrests bulk translation, whereas stress responsive proteins are specifically upregulated due to the presence of uORFs in the 5'UTRs of their mRNAs. These include the transcription factors ATF4 and CHOP. CHOP is considered a pro-apoptotic transcription factor and is upregulated by ATF4 and ATF6 during ER stress. CHOP has been reported to transactivate Death receptor 5 (DR5) to promote apoptosis by activating caspase-8 (Yamaguchi & Wang, 2004). CHOP has also been shown to upregulate Bim transcription through heterodimerization with C/EBPα (Puthalakath et al., 2007). Increased Bim promotes activation of Bax to trigger mitochondrial dysfunction. Normally the anti-apoptotic protein Bcl-2 can antagonize Bim activity, and CHOP has also been reported to repress Bcl-2 expression (McCullough, Martindale, Klotz, Aw, & Holbrook, 2001).

CHOP has also been shown to be important for inducing apoptosis following prolonged exposure to ER stress through the upregulation of Ero1α, which leads to increased ROS and hyperoxidation of ER resident proteins that causes additional protein misfolding (Marciniak et al., 2004). Increased Ero1α also activates the Inositol-1,4,5-triphosphate (IP3) receptor (IP3R) leading to calcium release from the ER (G. Li et al., 2009). Large increases in cytoplasmic calcium can be taken up by the mitochondria, which has been shown to induce mitochondrial permeabilization and cytochrome c release (Hajnóczky, Davies, & Madesh, 2003). ER calcium is required for protein folding and therefore secretion of calcium through the IP3R may also potentiate ER stress leading to further toxicity (Michalak et al., 2002).

As previously mentioned, CHOP transcriptionally upregulates GADD34, which directs dephosphorylation of eIF2α by PP1α, thereby restoring translation (Marciniak et al., 2004; Novoa et al., 2001). This is an important step during the adaptive phase of the UPR if the stress has been resolved. However, apoptosis can likely be promoted by restoration of translation and translocation of nascent proteins into the ER when it is already burdened by misfolded proteins (Marciniak et al., 2004). GADD34 expression likely also facilitates translation of pro-apoptotic proteins (Szegezdi, Logue, Gorman, & Samali, 2006). J. Han *et al.* (2013) also showed that the combined action of ATF4 and CHOP, through both homo- and hetero-dimerization, transcriptionally upregulates genes that promote protein synthesis, including GADD34, and it is a combination of this increase in protein synthesis and oxidative stress that drives apoptosis. Blocking the restoration of translation by inhibiting GADD34 can protect cells from chronic ER stress (Tsaytler, Harding, Ron, & Bertolotti, 2011). ATF4 and CHOP are upregulated during the adaptive phase of the UPR and therefore it is not entirely clear why early induction of these transcription factors does not pre-destine the cell to apoptosis. ATF4 and CHOP mRNAs and proteins are quite labile. Therefore, one theory is that if the stress was resolved then ATF4 and CHOP signaling would be rapidly quenched; but chronic activation of PERK allows these proteins to promote apoptosis (Rutkowski 2006).

1.2.5.4 IRE1 Signaling can Initiate Apoptosis

During ER stress, IRE1 dimerizes and is *trans*-autophosphorylated which flips it into an active conformation (K. P. K. Lee et al., 2008). IRE1 activation has been associated with increased apoptosis through multiple potential mechanisms. During ER stress, IRE1 has

been shown to control different signaling pathways through protein-protein interactions. IRE1 can bind TRAF2 and recruit and activate the MAP3K apoptosis signal-regulating kinase 1 (ASK1) (Nishitoh et al., 2002; Urano et al., 2000). Activated ASK1 phosphorylates the MAPK JNK, which then phosphorylates and activates the transcription factor c-Jun. IRE1-dependent activation of JNK signaling is believed to be important in promoting apoptosis through the phosphorylation and inhibition of the anti-apoptotic BCL2 family member Bcl-2, and the phosphorylation of Bim to enhance its pro-apoptotic potential (McCullough et al., 2001; Puthalakath et al., 2007). IRE1-TRAF2 can also promote pro-caspase-12 activation in response to ER stress (Yoneda et al., 2001). Caspase-12, which is localized to the cytosolic face of the ER membrane, activates caspase-9, which activates caspase-3 (Morishima et al., 2002).

RIDD has also been shown to play a role in promoting apoptosis. IRE1 has been shown to upregulate pro-caspase-2 expression, by cleaving anti-caspase-2 miRNAs such as miR-17, -34a, -96, and -125 (Upton et al., 2012). Activation of caspase-2 can cleave BID into active tBID, which activates Bax (Upton et al., 2008). Surprisingly, treating cells expressing the IRE1 phospho-transfer-null Ile642Gly point mutant with the small molecule 1NM-PP1, which has been reported to activate XBP1 splicing but not RIDD, still upregulated caspase-2 (Upton et al., 2012). These cells did however fail to activate caspase-2 through proteolytic cleavage, while wild type IRE1 expressing cells both upregulated and cleaved caspase-2 to activate apoptosis. These inconsistencies between models of IRE1 activity have been called into question and a subsequent study found that caspase-2 was not upregulated during ER stress and did not play a role in ER stress-induced cell death (Sandow et al., 2014).

RIDD has also been shown to attenuate apoptosis. Activation of DR5 can induce the extrinsic apoptosis pathway and has been shown to be induced by prolonged ER stress (M. Lu et al., 2014). This was partly mediated through transcriptional upregulation by CHOP, but during earlier stages of ER stress, DR5 expression was silenced by RIDD. These findings suggest that there is a coordination between PERK and IRE1 signaling to regulate apoptosis. However, recently the role of DR5 and caspase-8 activation in ER stress-induced apoptosis has also been disputed (Glab et al., 2017). Therefore, further work is needed to elucidate precise mechanisms that regulate IRE1-dependent cell death mechanisms in response to chronic ER stress.

1.2.6 Crosstalk among Branches of the UPR

Although activation of the three UPR sensors during ER stress have different outcomes, it is clear that there is coordination and co-regulation between the different branches. Furthermore, the type and duration of stress seems to impact the activation status of each of the branches. Exposure to lethal doses of either Tm or Tg results in stable PERK activity, whereas IRE1 signaling does not persist and is attenuated 8 to 16 h after treatment. ATF6 activity diminished shortly after IRE1 inhibition (J. H. Lin, Li, Zhang, Ron, & Walter, 2009).

The inhibition of IRE1 is not fully understood but a recent study has shown that the phosphatase RPAP2 is activated in a PERK-dependent manner and dephosphorylates IRE1 (T.-K. Chang et al., 2018). PERK has also been shown to silence XBP1 expression through the upregulation of miR30c-2-3p, which may be another mechanism of attenuating IRE1 signaling after prolonged ER stress (Byrd, Aragon, & Brewer, 2012). Alternatively, IRE1 has also been shown to bind the XBP1 target gene hsp40 co-chaperone ERdj4 to facilitate BiP recruitment and stabilize IRE1 monomers (Amin-Wetzel et al., 2017). This may indicate that the IRE1-XBP1 pathway may institute a negative feedback loop through XBP1 upregulation of ERdj4 to control IRE1 signaling. Along these lines, the lack of XBP1 results in hyperactivation of IRE1 signaling leading to increased JNK phosphorylation (Akiyama et al., 2013; Olivares & Henkel, 2015) and RIDD (Maurel et al., 2014), which may be due to the lack of ERdj4-dependent monomerization of IRE1.

Another potential mechanism of crosstalk between the PERK and IRE1 branch is that XBP1s can transcriptionally upregulate another hsp40 family member $p58^{IPK}$, which was reported to repress PERK activity (Yan et al., 2002). $p58^{IPK}$ was originally identified as an inhibitor of PKR (Polyak, Tang, Wambach, Barber, & Katze, 1996) but since the two eIF2α kinases share sequence similarity in the cytoplasmic domain, it is not surprising that $p58^{IPK}$ can also repress PERK. $p58^{IPK}$ has also been shown to act as a co-chaperone for BiP and thus $p58^{IPK}$ may indirectly control PERK activity through BiP binding to PERK (Rutkowski et al., 2007). A potential model would be that prolonged XBP1s expression could promote inactivation of PERK through $p58^{IPK}$ upregulation, although this has not been confirmed experimentally.

There is evidence that the PERK activation can suppress IRE1 signaling, but there has also been a report that demonstrated that PERK signaling can promote IRE1 activity through ATF4 transactivation of IRE1 (Tsuru, Imai, Saito, & Kohno, 2016). These conflicting observations may be due to cell-type differences. Further research is required to understand how PERK coordinates IRE1 activity.

As previously mentioned, ATF6 transactivates XBP1 and CHOP, and therefore impacts both IRE1 and PERK pathways, respectively (Yoshida et al., 2000; Yoshida et al., 2001). ATF6 and XBP1s can form heterodimers which can either enhance gene expression or broaden the transcriptional landscape compared to XBP1 and ATF6 homodimers. ATF6 primarily upregulates BiP, but ATF4, with the help of ATF1 and CREB1 has also been reported to promote BiP transcription (Luo, Baumeister, Yang, Abcouwer, & Lee, 2003). The ISR has also been shown to be important for regulating BiP through the presence of uORFs in the 5'UTR of BiP mRNA (Starck et al., 2016). However, this uORF-dependent translation of BiP is dependent on eIF2A rather than eIF2α, which does not rely on eIF2B for GTP cycling (Komar et al., 2005). These examples, and likely others, are evidence that crosstalk among the branches of the UPR is important for coordinating a robust and tightly regulated response to ER stress and as a result contribute to the fate of the cell. Disruption of a coordinated UPR may have harsh consequences and promote disease onset.

1.2.7 The UPR and Disease

There is accumulating evidence that the UPR is important for regulating multiple different biological processes, such as inflammation and immunity. Chronic ER stress or dysregulated UPR signaling is implicated in multiple diseases. Some of the different physiological and disease models prioritize activation of different ER stress sensors and may occur independent of ER stress. The UPR has been shown to be activated during bacterial and viral infection and in many of these instances, UPR signaling is also dysregulated by the pathogen. This subsection provides multiple examples of the role of the UPR in health and disease to highlight its importance and to show that the signaling response can vary from the classical model of ER stress-induced UPR activation.

1.2.7.1 The UPR in Inflammation and Immunity

There is mounting evidence that the UPR plays a central role in controlling inflammation and the immune response, with a crucial role ascribed to XBP1 (Grootjans, Kaser,

Kaufman, & Blumberg, 2016). The IRE1-XBP1 pathway is important for the development and survival of many different immune cells, including dendritic cells (Tavernier et al., 2017). Depending on the location or type of dendritic cell, XBP1 can be essential for survival or impact DC function, such as MHC-I surface expression. Constitutive expression of XBP1s can promote lipid accumulation in DCs, which can inhibit antigen presentation (Cubillos-Ruiz et al., 2015; Herber et al., 2010). IRE1-XBP1 signaling was also reported to be activated in CD8+ T cells in response to infection and loss of XBP1 abrogated effector T cell differentiation (Kamimura & Bevan, 2008).

Many dedicated immune cells have a prominent secretory phenotype that is central to their function. These cells require an augmented ER to handle this increased secretory load. XBP1 is essential for the differentiation of granulocytic eosinophils, which are associated with a type II immune response and involved in allergic reactions or parasitic infections (Bettigole et al., 2015). In the intestinal epithelial layer, Paneth cells and goblet cells are important for protecting against infection. Paneth cells secrete anti-microbial peptides and goblet cells secrete large amounts of mucins to block pathogens from infiltrating past the intestinal barrier. Mice with an XBP1-specific knockout in the intestine had decreased levels of goblet cells and were completely devoid of Paneth cells (Kaser et al., 2008). As a result, XBP1-deficient mice were susceptible to spontaneous enteritis and significantly more susceptible to *Listeria monocytogenes* infection.

Paneth cell dysfunction can also lead to inflammatory bowel disease (IBD), such as Crohn's disease or ulcerative colitis (reviewed in Elphick & Mahida, 2005). XBP1 deletion in Paneth cells leads to increased ER stress, which can be mitigated by increased autophagy (Adolph et al., 2013). One of the autophagy related genes, ATG16L1, contains an autophagy-inhibiting polymorphism (T300A) and is a major risk factor for Crohn's disease (Lassen et al., 2014). Mice with this polymorphism activate the UPR in Paneth cells as a protective measure, but ATG16L1 mutant mice that are also deficient in XBP1 develop a Crohn's-like disease through IRE1 hyperactivation. Autophagy protected against IRE1 hyperactivation by targeting IRE1 for degradation, which mitigate disease onset (Tschurtschenthaler et al., 2017). The intestinal and bronchial epithelial cell specific IRE1β has also been implicated in IBD. Using the dextran sodium disulfate (DSS)-induced colitis mouse model, IRE1β knockout mice developed IBD-like symptoms significantly quicker than wild type mice (Bertolotti et al., 2001).

The UPR is also essential for plasma cell (PC) differentiation specifically the transcription factor XBP1s (Iwakoshi et al., 2003; Reimold et al., 2001; Shaffer et al., 2004). In response to antigen binding to the B cell receptor (BCR), naïve mature B cells undergo transcriptional reprogramming through the use of multiple activating and repressing transcription factors to terminally differentiate into antibody-secreting PCs. Activated BCR signaling inhibits the transcriptional repressor BCL-6, which de-represses transcription of Blimp-1 to initiate PC differentiation (Shaffer et al., 2002, 2000). Blimp-1 inhibits c-myc and PAX-5, which is a repressor of XBP1 (Reimold et al., 1996; Shaffer et al., 2002). IRF4 is also required for the upregulation of XBP1 and is likely activated downstream of Blimp-1 (Klein et al., 2006). IRF4 promotes the expression of the classical PC marker CD138 (or Syndecan-1). XBP1 is essential for PC differentiation since reconstitution of T and B cells in Rag2 knockout mice with XBP1 deficient embryonic stem cells failed to generate PCs (Reimold et al., 2001). Furthermore, XBP1 deficiency promotes IRE1 hyperactivation, which was shown to cleave and degrade mRNAs encoding Ig μ heavy chain (Benhamron et al., 2014; Tang et al., 2018). PC differentiation activates IRE1 and ATF6 but inhibits PERK; the net result is ER expansion and increased folding capacity to prepare the cell for the increase in Ig production and secretion (Y. Ma, Shimizu, Mann, Jin, & Hendershot, 2010). XBP1 regulates a late phase event in PC differentiation since XBP1-deficient pre-plasma cells (or plasmablasts) express Syndecan-1 but have not undergone the morphological changes that are indicative of Ig-secreting PCs (Todd et al., 2009).

The IRE1-XBP1 pathway also likely plays an important role in regulating inflammation in response to infection. Toll like receptors (TLRs) are pattern recognition receptors (PRRs) that are activated in response to infection by binding pathogen-associated molecular patterns (PAMPs) associated with the infecting pathogen (reviewed in Mogensen, 2009). Activation of TLR2 or TLR4 in macrophages specifically engaged the IRE1-XBP1 pathway and XBP1 was required to augment expression of IL-6, TNFα, and IFN-β (Martinon, Chen, Lee, & Glimcher, 2010). Engagement of TLR2 and TLR4 was reported to promote IRE1 polyubiquitination by TRAF6, which blocked IRE1 dephosphorylation by PP2A to prolong signaling (Qiu et al., 2013). TLR signaling was specific to IRE1 activation and inhibited ATF6 and the ISR (Martinon et al., 2010). The ISR was also inhibited by TLR signaling following treatment with Tm (Woo et al., 2009).

TLR signaling was reported to inhibit the ISR by de-phosphorylating the epsilon subunit of eIF2B GEF at Ser539 by the phosphatase PP2A (Woo, Kutzler, Kimball, & Tabas, 2012).

NFκB signaling in response to ER stress has also been demonstrated, which involved IRE1 and PERK signaling (Tam, Mercado, Hoffmann, & Niwa, 2012). IRE1 recruited TRAF2 to activate IKK, which activated NFκB through phosphorylation and subsequent proteasomal degradation of the NFκB inhibitor IκBα (P. Hu, Han, Couvillon, Kaufman, & Exton, 2006). The half-life of IκBα is much shorter than NFκB, and inhibition of translation by PERK phosphorylation of eIF2α increased the ratio of NFκB to IκBα, further promoting an inflammatory response (Deng et al., 2004). Currently the precise role of the NFκB pathway in response to ER stress is not clear but likely plays a role in many of the aforementioned inflammatory diseases. Our understanding of the role for the UPR in immunity and inflammation is only in its infancy and further studies will hopefully lead to potential new treatments.

1.2.7.2 The UPR in Tumorigenesis

In response to ER stress the UPR initiates an adaptive response to mitigate the stress but switches to a pro-apoptotic response if the stress cannot be resolved. Since the UPR has both pro- and anti-apoptotic signaling it is not surprising that the UPR has been reported to both promote and inhibit tumorigenesis.

Cancer cells require a robust secretory system to continue to grow in and adapt to unfavorable environments. This is likely to adjust the ER proteostasis network and therefore impact UPR signaling (Dejeans et al., 2014). As such, histological samples of multiple different cancer types displayed markers of an activated UPR (Avril, Vauléon, & Chevet, 2017; Yadav, Chae, Kim, & Chae, 2014). The plasma cell neoplasm, multiple myeloma (MM), is characterized by the secretion of large amounts of defective Ig proteins, which contributes to persistent ER and activation of the UPR (Obeng et al., 2006). XBP1s signaling has been reported to be important for MM pathogenesis (Carrasco et al., 2007). Current therapies for MM include combinatorial treatment with proteasome inhibitors (PIs), such as bortezomib, which likely exasperates UPR signaling due to the inability to degrade misfolded proteins in the ER. Therefore, PIs likely shift the UPR to induce apoptosis in MM cells (A.-H. Lee, Iwakoshi, Anderson, & Glimcher, 2003b). IRE1 is thought to play a central role in controlling MM cell death following PI

treatment and depending on the cell model used IRE1 inhibition has been shown to both promote and suppress MM apoptosis (Leung-Hagesteijn et al., 2013; Mimura et al., 2012).

Tumor formation is associated with an increase in hypoxia (decrease in O_2 levels) that inhibits oxygen-dependent post-translational protein folding and isomerization of ER proteins, resulting in ER stress (Koritzinsky et al., 2013). UPR activation in response to hypoxia likely plays an important role in tumor growth in a variety of ways including upregulation of angiogenesis. Classically, angiogenesis is induced by the transcription factor HIF (hypoxia-inducible factor)-1, which is a heterodimer of HIF-1α and β. In response to hypoxia, HIF-1α protein is stabilized and heterodimerizes with the constitutively active HIF-1β to upregulate genes that contain hypoxia response elements (HREs) in their promoters, such as angiogenic growth factors like VEGF (reviewed in Krock, Skuli, & Simon, 2011).

Increases in neo-angiogenesis genes vascularizes the tumor to restore oxygen levels. XBP1 has also been reported to be important for promoting angiogenesis. Angiogenesis in an XBP1 knock out mouse model for triple-negative breast cancer (estrogen receptor, progesterone receptor, and HER2-negative) was markedly reduced compared to wild type tumors. Mechanistically, XBP1 bound HIF-1α to regulate expression of HIF-1 target genes (X. Chen et al., 2014). PERK activation was also shown to promote angiogenesis through increased translation of VEGF, FGF-2, IL-6 and downregulation of anti-angiogenic factors CXCL10 and CXCL14. PERK also promoted VEGF expression through ATF4-dependent transactivation (Yugang Wang et al., 2012). Reciprocally, VEGF has been shown to activate PERK, and ATF6, in an ER stress-independent mechanism to promote endothelial cell survival to further enforce angiogenesis (Karali et al., 2014).

Cells deficient in PERK have increased apoptosis in response to hypoxia and as a result, the tumors are smaller and less angiogenic (Bi et al., 2005; Blais et al., 2006). PERK activation can also promote apoptosis through the upregulation of the pro-apoptotic transcription factor CHOP. During chronic ER stress, CHOP is thought to promote apoptosis through increased protein translation by transactivating GADD34 to further exasperate protein misfolding, thus intensifying cell toxicity (Marciniak et al.,

2004). Reduction of CHOP has been associated with increased tumorigenesis (Huber et al., 2013).

The anti-tumor immune response is also impacted by UPR signaling. M. Song *et al.* (2018) showed that T cells from patients with ovarian cancer had increased levels of XBP1 splicing and were associated with a decrease in tumor infiltration. Through an unknown secreted factor, the tumor induced IRE1 activation in T cells and XBP1s reduced IFNγ production and mitochondrial respiration. Ovarian tumors in mice with XBP1-deficient T cells showed a significantly stronger anti-tumor response, which corresponded with reduced tumor growth and increased survival (M. Song et al., 2018). XBP1 splicing was also activated in ovarian cancer-associated dendritic cells (DCs) (Cubillos-Ruiz et al., 2015). Chronic XBP1s signaling led to an accumulation of intracellular lipids that disrupted tumor antigen processing. XBP1 deletion in DCs enabled antigen presentation to T cells to promote anti-tumor immunity (Cubillos-Ruiz et al., 2015; Herber et al., 2010). Thus, XBP1 can promote both intrinsic and extrinsic tumor growth.

1.2.7.3 The UPR in Type II diabetes

Obesity is a major problem in the modernized western world and is linked to multiple disorders including type II diabetes (T2D). Insulin resistance - the lack of metabolic changes in response to regular levels of insulin - is considered a predisposing factor to the development of T2D. Although the mechanisms underlying insulin resistance and T2D are not fully understood, it is apparent that they are multifactorial. Accumulating evidence indicates that ER stress and the UPR are major regulators of T2D (Cnop, Foufelle, & Velloso, 2012).

Insulin is produced by pancreatic β cells and secreted in response to the intake of carbohydrates to lower blood glucose levels. Insulin stimulates the liver to take up glucose and store it in glycogen polymers. However, beyond a certain level of glycogen, increased glucose is converted to triglycerides which are secreted from hepatocytes through the association of lipoproteins. Circulating triglycerides are delivered to adipose tissue for storage. Insulin also stimulates adipocytes to uptake glucose through the GLUT4 transporter and convert glucose to glycerol (Abel et al., 2001). Insulin resistance results in a decreased sensitivity to insulin and therefore increased blood glucose levels.

Insulin resistance is thought to occur through activation of the JNK pathway (Hirosumi et al., 2002) but the precise mechanistic details are unclear. One model suggests that JNK promotes phosphorylation and inhibition of the insulin receptor substrate 1 (IRS-1), which blocks signaling in response to insulin binding (Aguirre, Uchida, Yenush, Davis, & White, 2000). XBP1 deficient mice also displayed increased ER stress in the livers, which was associated with increased JNK-mediated IRS-1 phosphorylation and glucose tolerance indicating that XBP1 plays a protective role against T2D (Ozcan et al., 2004). A follow-up study showed that inflammatory signaling induced S-nitrosylation of the RNase domain of IRE1, which inhibited XBP1 splicing and the loss of XBP1s, while enhancing its kinase activity to promote JNK-mediated IRS-1 phosphorylation (L. Yang et al., 2015).

Insulin resistance results in hyperglycemia and requires an enhanced synthesis of insulin to mitigate this effect. As a result, this increase in insulin expression increases the demands on the protein folding machinery, which can activate the UPR (R. B. Sharma et al., 2015; Szabat et al., 2016). Chronic hyperglycemia results in prolonged and hyperactivation of IRE1 (Lipson et al., 2006). Through RIDD, IRE1 can cleave insulin mRNA and other ER targeted proteins, eventually leading to β cell apoptosis (D. Han et al., 2009).

While hyperactivated IRE1 may promote T2D, XBP1 has been shown to be have a protective role. XBP1 was shown to be constitutively spliced in pancreatic β cells and the deletion of XBP1 in pancreatic β cells also led to a decrease in insulin secretion resulting in hyperglycemia and glucose intolerance. XBP1 deficiency corresponded to hyperactivation of IRE1, which cleaved mRNAs encoding insulin and pro-insulin processing enzymes (A.-H. Lee et al., 2011). Through the upregulation of enzymes including protein disulfide isomerases, activation of the IRE1-XBP1 pathway was recently shown to be essential for the oxidative folding of pro-insulin, which is required for its secretion (Tsuchiya et al., 2018).

Wolcatt-Rallison syndrome (WRS) is a rare recessive genetic disorder that results in neonatal or early infancy T2D and loss-of-function mutations in PERK have been identified in these patients (Delépine et al., 2000). PERK knockout mice recapitulated the symptoms of WRS and became hyperglycemic and showed defects in serum insulin levels due to increased apoptosis of β cells (Harding et al., 2001). Pre-diabetic PERK

knockout mice displayed increased insulin translation and elevated ER stress in the pancreas indicating that the inability to attenuate translation likely leads to increased insulin production, which could likely saturate the ER protein folding machinery and trigger ER stress. This unresolved ER stress could initiate apoptosis of β cells leading to T2D (Harding et al., 2001).

The way in which ER stress and the UPR promotes β cell death is not completely known. However, there is increased survival of β cells in CHOP knockout mice in many disease models of T2D, indicating that pro-apoptotic transcription factor CHOP likely plays a central role in controlling β cell death (B. Song, Scheuner, Ron, Pennathur, & Kaufman, 2008). As discussed previously, CHOP may induce apoptosis in ER stressed β cells through multiple mechanisms including increasing ROS through transactivating ERO1α (Marciniak et al., 2004). ROS and ER stress has also been linked to the activation of the NLRP3 inflammasome to mediate β cell death (Bronner et al., 2015; Oslowski et al., 2012). Notably, IRE1 activation was shown to upregulate TXNIP (thioredoxin-interacting protein) through the cleavage of TXNIP-silencing miR-17, resulting in TXNIP activation of the NLRP3 inflammasome. Deletion of TXNIP rescued ER stress induced apoptosis in β cells leading to reduced diabetes in a mouse model (Lerner et al., 2012).

Although there are clear links between dysregulated UPR signaling and T2D onset, there is also some evidence that chronic ER stress can promote T2D. There is a strong connection between high fat diets, obesity, and T2D; and free fatty acids (FFAs) are an important link (Bergman & Ader, 2000). Long-chain saturated FFAs, such as palmitate, can also cause ER stress (Volmer et al., 2013). ER stress and increased FFAs have been shown to activate FoxO1 in β cells and inhibition of FoxO1 increased β cell survival (Martinez et al., 2008). Interestingly, XBP1s can bind to FoxO1 and promote proteasomal degradation, suggesting another potential role for XBP1s in mitigating T2D (Y. Zhou et al., 2011).

Another study showed that increased ER stress in the livers of obese mice was linked to T2D. Mechanistically, they showed that increased PC:PE lipid ratios impaired SERCA activity, which resulted in decreased ER calcium levels, causing ER stress and

activation of the UPR. Impaired SERCA activity led to dysregulated glucose homeostasis and overexpressing SERCA2b ameliorated this effect (Fu et al., 2011).

The saturated FFA palmitate has also been shown to decrease ER calcium concentration in β cells, promoting ER stress (reviewed in Ly et al., 2017). Increases in FFA can also cause bilayer stress in the ER and activate the UPR in the absence of protein misfolding (Volmer et al., 2013). These studies indicate that UPR activation in obesity may come from multiple sources, and together can promote insulin resistance and T2D.

Amyloids of aggregated islet amyloid polypeptide (IAPP) are found in 90% of T2D patients and are believed to play a role in disease progression (reviewed in Mukherjee, Morales-Scheihing, Butler, & Soto, 2015). IAPP is secreted along with insulin from β cells. *In vitro* studies suggested that the amyloids are toxic and can induce ER stress in β cells (Huang et al., 2007). Silencing CHOP expression reduced cell death in these amyloid-expressing cells (Gurlo et al., 2016). These findings remain controversial because another group was unable to detect ER stress in cells expressing IAPP oligomers (Hull et al., 2009). Further studies are warranted to determine the role of the UPR and IAPP oligomers in the progression of T2D.

1.2.7.4 The UPR in Neurodegenerative Diseases

Amyloids or amyloid fibrils are also associated with the onset of multiple neurological disorders, including Huntington's disease (HD), Parkinson's disease (PD), and Alzheimer's disease (AD) (Koo, Lansbury, & Kelly, 1999). These diseases are often classified as protein misfolding diseases or proteopathies, as they all involve the misfolding and aggregation of disease-specific proteins: Huntingtin (Htt) in HD, α-synuclein (α-syn) in PD, and amyloid-β and tau in AD. There is increasing evidence that ER dysfunction and the UPR plays a role in disease progression of these neurodegenerative diseases (reviewed in Roussel et al., 2013). Histology has shown activation of many UPR markers like BiP, phospho-IRE1, phospho-PERK, phospho-eIF2α and CHOP in the brains of patients with these diseases (reviewed in Hughes & Mallucci, 2019).

Increased levels of phosphorylated eIF2α has been observed in the brains of patients with AD (R. C. C. Chang, Wong, Ng, & Hugon, 2002). eIF2α phosphorylation

was also reported to promote BACE1 expression, which is the enzyme responsible for cleaving amyloid precursor protein (APP) to form amyloid-β (Devi & Ohno, 2014) Genetic deletion of PERK in a mouse model of AD prevented attenuation of protein synthesis and improved memory deficits associated with AD (T. Ma et al., 2013). Additionally, CHOP silencing after amyloid-β treatment also promoted survival (Prasanthi, Larson, Schommer, & Ghribi, 2011; Schapansky, Olson, Van Der Ploeg, & Glazner, 2007), indicating that PERK activation may promote AD.

XBP1 splicing was observed in Drosophila exposed to amyloid-β and XBP1 silencing increased toxicity (Casas-Tinto et al., 2011; Marcora, Belfiori-Carrasco, Bocai, Morelli, & Castaño, 2017). XBP1s can upregulate genes in the ERAD machinery that are important for the ubiquitination and clearance of APP to reduce the levels of amyloid-β (Kaneko et al., 2010). Interestingly, an intronic polymorphism of one of the ERAD components, SEL1L, is associated with Alzheimer's disease (Saltini et al., 2006).

Parkinson's disease is also associated with ER stress and the UPR. Overexpression of α-syn has been reported to induce ER stress and contribute to cell death (W. W. Smith et al., 2005). A PD mouse model that expresses a mutant form of α-syn also showed UPR activation; however, in this model eIF2α phosphorylation was largely unaffected. Treatment with the GADD34 inhibitor, salubrinal, enhanced eIF2α phosphorylation, which corresponded to decrease in α-syn in the ER and delayed disease progression (Colla et al., 2012). Other *in vivo* models of PD that rely on the use of toxins to induce disease symptoms, such as 6-hydroxydopamine, have been shown to cause ER stress. Importantly, CHOP is induced by 6-hydroxydopamine and CHOP knockout mice show decreased sensitivity to the toxin (Silva et al., 2005). ATF6 activation was also disrupted in a PD mouse model leading to impaired ERAD, which would normally promote clearance of misfolded α-syn (Credle et al., 2015).

Huntington's disease is another protein misfolding disease that is caused by the expansion of CAG trinucleotides in the Htt gene resulting in increased polyglutamine repeats that promote aggregation. Although Htt aggregation largely occurs in the cytosol, polyglutamine-expanded Htt expression in a HD mouse model was shown to impair ERAD (Duennwald & Lindquist, 2008). The exact outcome of this disruption of ERAD is not clear, but it likely sensitizes the cells to protein misfolding and increases

susceptibility to ER stress. In agreement with this, expression of these polyglutamine repeats in neurons activated ER stress and triggered activation of the IRE1-TRAF2-ASK1 pathway to induce JNK phosphorylation, thereby promoting apoptosis (Nishitoh et al., 2002). Collectively, these studies indicate a potential role for the UPR in neurodegeneration in HD and other polyglutamine-related diseases. The role of ER stress and UPR signaling in neurological diseases expands beyond PD, AD, and HD, and future studies will be important to determine if modulating the UPR with small molecules may be a potential therapy to mitigate disease progression (Roussel et al., 2013).

1.2.8 UPR Modulation during Pathogen Infection

Some of the initial studies that led to the eventual characterization of the UPR were dependent on viruses. The UPR was first characterized for its ability to upregulate two highly abundant ER chaperones, BiP (Grp78) and Grp94, and one of the first studies showed that mutated HA protein from Influenza A virus could upregulate these chaperones (Gething et al., 1986). In 1978, a study showed that the paramyxovirus Simian virus 5 could also upregulate BiP and Grp94 (Peluso, Lamb, & Choppin, 1978).

Since the discovery of IRE1, PERK, and ATF6 as the three sensors of the UPR, there have been many studies investigating if certain viruses can trigger ER stress and/or activate the UPR. Many of the viruses studied are enveloped viruses, since the synthesis of envelope glycoproteins in the ER may presumably tax the folding machinery and cause ER stress. Multiple different viruses have been shown to activate all three of the ER stress sensors, while other viruses may selectively activate or inhibit one of the sensors. The UPR presents many features that may be advantageous to viruses, such as promoting cell survival through increased synthesis of chaperone proteins and expansion of the ER. However, there are other aspects of the UPR that may be unfavorable to an infecting virus, including attenuation of translation through eIF2α phosphorylation, and the increase in protein degradation through ERAD. The UPR can also induce apoptosis, which is usually considered anti-viral but some viruses induce apoptosis to facilitate viral transmission (Roulston, Marcellus, & Branton, 1999). There are also links that the UPR can regulate autophagy and pro-inflammatory responses that can impact virus replication (reviewed in Senft & Ronai, 2015). Since the UPR may have both pro- and anti-viral effects on virus replication, it is not surprising that many viruses appear to fine-tune UPR

signaling by blocking the activation of one or multiple branches of the UPR to promote virus replication.

UPR activation is the most telling way to determine if a cell is experiencing ER stress. Therefore, if activation of one or two (but not all three) branches of the UPR is observed during infection, it is unclear if there is selective engagement of certain branches of the UPR in an ER stress-independent mechanism or if the virus is causing ER stress but one or two of the sensors are inhibited. Depending on the virus in question, this selective activation of the ER stressors may impact the nature of the type of signaling response that is elicited. In addition, during infection some UPR signaling branches may be engaged while the downstream effectors are inhibited which would also impact signaling. Therefore, we cannot generalize that the UPR is either pro- or anti-viral for a particular virus, nor can we assign broad anti-viral or pro-viral labels to the different branches.

To clearly determine UPR activation status and its role in infection, a careful analysis of each of the branches needs to be conducted by determining the expression of the downstream transcription factors of the sensors, namely ATF4, ATF6-N, and XBP1s, and their target genes. Genetic and pharmacological activation or inhibition of the sensors would also need to be done to determine their impact on virus replication.

Many of the studies to date have failed in their attempt to convincingly show the impact that the UPR has during infection. Nonetheless, there are a few examples of viruses where this is not the case and these viruses likely fine-tune the UPR to promote virus replication through the direct activation or inhibition of certain UPR sensors, often by a viral protein. However, in most scenarios the mechanistic details of the role of the UPR in regulating infection are still unclear.

Bacteria have also been shown to activate or fine-tune UPR signaling. In the following subsections I will provide a few examples that highlight some of the potential pro- and anti-bacterial/viral roles of the UPR that have been ascribed to a short list of pathogens and some of the viral or bacterial proteins that modulate UPR signaling. Based on the evidence, there is clearly much work needed to be done to better understand the role of the UPR during infection.

1.2.8.1 Bacteria can Activate the UPR

Legionella pneumophila and *Brucella spp*. are intracellular bacteria that hijack ER-derived vesicles to promote intracellular survival and replication (C. R. Roy, 2005). An RNAi screen revealed that IRE1 but not ATF6 or PERK was required for *Brucella melitensis* replication (Q.-M. Qin et al., 2008). A subsequent study showed that the microtubule modulating bacterial protein TcpB can activate the UPR, which may facilitate IRE1-dependent bacterial replication (J. A. Smith et al., 2013). However, the mechanism of how IRE1 promotes replication has not yet been characterized. *Brucella abortus* was also shown to activate IRE1 to promote bacterial replication through the direct interaction with the bacterial protein Yip1a (Taguchi et al., 2015). Yip1a facilitates IRE1 oligomerization and subsequent activation.

Legionella pneumophila can inhibit translation of UPR markers BiP, CHOP, and XBP1s through the Type IV dependent secretion of Lgt2 and Lgt3 (Hempstead & Isberg, 2015; Treacy-Abarca & Mukherjee, 2015). These bacterial effectors glucosylate the host's eEF1α to inhibit translation elongation, which results in UPR suppression. Since the XBP1 is activated by TLR signaling (Martinon et al., 2010), *Legionella* may block XBP1s signaling through Lgt2 and Lgt3. IRE1 of the UPR inhibits MRSA (Methicillin-resistant *Staphylococcus aureus*) through the sustained production of ROS that mediates bacterial killing, further demonstrating cooperativity between the IRE1-XBP1 pathway and TLR signaling (Abuaita, Burkholder, Boles, & O'Riordan, 2015).

Different bacterial toxins have been shown to activate the UPR. Both Listeriolysin O (LLO) from *Listeria monocytogenes* and the subtilase cytotoxin (SubAB) from Shiga toxin-producing *Escherichia coli* (STEC) activate the UPR (Pillich, Loose, Zimmer, & Chakraborty, 2012; Wolfson et al., 2008). The mechanism by which LLO activates the UPR is not known; but SubAB toxin activates the UPR through direct cleavage of the chaperone BiP (Paton et al., 2006).

Pseudomonas aeruginosa is an important respiratory pathogen that secretes many virulence factors. Two secreted factors, pyocyanin and alkaline protease were shown to induce the UPR, which was dependent on p38-MAPK activation (van 't Wout et al., 2015). Interestingly, treatment with the p38 inhibitor SB203580 suppressed UPR signaling by the virulence factors, except for phospho-eIF2α-mediated GADD34 upregulation. The researchers found that the virulence factors activated the eIF2α kinase

HRI and not PERK, which increased GADD34. This intriguing finding raises the point that differences in UPR and ISR activation may be observed in different scenarios and that one cannot assume that co-activation of XBP1s and eIF2α phosphorylation is indicative of a global ER stress response. Based on these examples it appears that the UPR can promote or inhibit bacterial replication through different mechanisms and that bacteria can express effectors that directly dysregulate UPR signaling.

1.2.8.2 Flaviviruses Modulate the UPR to Control Autophagy and ERAD

Flaviviruses are enveloped, positive-sense RNA viruses that express a single, multi-pass ER membrane polypeptide that is proteolytically cleaved into functional structural and non-structural proteins. Flaviviruses also remodel the ER to generate a viral replication compartment (Gillespie, Hoenen, Morgan, & Mackenzie, 2010). Hepatitis C virus belongs to the *Hepacivirus* genus and selectively replicates in the liver and is a major cause of hepatocellular carcinoma.

HCV activates all three UPR sensors, however, XBP1s protein has been reported to be inhibited by the virus (Ke & Chen, 2011). Multiple studies have shown that multiple HCV proteins can activate the UPR, including E1 and E2 glycoproteins, the core protein, NS2, and NS4B (S.-W. Chan & Egan, 2005; M.-Q. Du et al., 2002; S. Li et al., 2009; von dem Bussche et al., 2010). E2 has also been reported to bind and inhibit PERK signaling (Pavio, Romano, Graczyk, Feinstone, & Taylor, 2003). In response to ER stress, XBP1s (and ATF6) upregulate genes involved in ERAD, including the family of ER Degradation Enhancing Alpha-Mannosidase Like Proteins (EDEMs), EDEM1, EDEM2, and EDEM3. EDEM1 can promote the degradation of HCV E1 and E2 glycoproteins (Saeed et al., 2011); therefore, blocking XBP1s activation may help the glycoproteins to evade ERAD. ERAD may have pan-anti-viral functions since Influenza A virus (IAV) HA protein was also susceptible to ERAD and knockdown of EDEMs enhanced IAV production (Frabutt, Wang, Riaz, Schwartz, & Zheng, 2018).

Like ERAD, autophagy is also a catabolic cellular process used to degrade proteins and it has strong links to virus infection, with known pro-viral and anti-viral roles (Choi, Bowman, & Jung, 2018). One of the pro-viral roles of autophagy is through inhibition of the IFN response. ATG12-ATG5 heterodimer was reported to bind and block MAVS and RIG-I, which normally regulate the IFN response (Jounai et al., 2007).

Autophagy is also induced during HCV infection, but this pathway is aborted at a late phase, preventing autophagosome fusion with lysosomes (Sir et al., 2008). HCV activation of the ISR and ATF6 can induce autophagy, which has been reported to inhibit IFN activation during HCV infection (Ke & Chen, 2011). PERK activation has also been reported to promote phosphorylation and subsequent ubiquitination-dependent degradation of the Type I IFN receptor subunit IFNAR1, further supporting an IFN inhibiting mechanism by the UPR (J. Liu et al., 2009). Thus, PERK activation by HCV may highlight another mechanism of controlling the IFN response.

Other flavivirus infections, including Japanese encephalitis virus (JEV) and Dengue Virus (DENV), have also been shown to induce autophagy in a UPR-dependent manner; however, in the case of JEV, there are conflicting reports as to whether autophagy activation promotes virus replication similarly to HCV (Datan et al., 2016; Y.-R. Lee et al., 2018; M. Sharma et al., 2017). The togaviruses Chikungunya virus (CHIKV) and Sindbis virus (SINV), and the paramyxovirus Newcastle disease virus (NDV), also activate autophagy through different UPR branches (J.-H. Cheng et al., 2016; Joubert et al., 2012). Thus, it appears that some virus infections may activate the UPR or branches of the UPR to activate autophagy and, depending on the virus, may impact replication by modulating the IFN response.

1.2.8.3 The Chaperone BiP can Promote Virus Infection

BiP is an abundant hsp70 ER chaperone that participates in folding of ER proteins, as well as maintaining the UPR sensors in a dormant state in the absence of ER stress. BiP expression during the UPR is regulated at the transcriptional level through ATF6 transactivation (J. Ye et al., 2000; Yoshida et al., 1998). BiP mRNA also contains an IRES (internal ribosome entry site) in the 5'UTR that can regulate expression in a UPR-independent manner (Fernandez, Yaman, Sarnow, Snider, & Hatzoglou, 2002; Q. Yang & Sarnow, 1997). Multiple viruses have been shown to upregulate BiP independent of a transcriptional response, including enterovirus 71 (Jheng, Lau, Tang, Wu, & Horng, 2010), respiratory syncytial virus (RSV) (I. Hassan et al., 2014), and human cytomegalovirus (HCMV) (Isler, Skalet, & Alwine, 2005). HCMV upregulation of BiP was shown to be IRES-dependent (N. J. Buchkovich, Yu, Pierciey, & Alwine, 2010). During HCMV infection, BiP was also shown to colocalize with HCMV replication compartments and decreasing BiP through siRNAs or treatment with the SubAB Shiga

toxin disrupts formation of the replication complex leading to a block in trafficking of viral nucleocapsids (N. J. Buchkovich, Maguire, Paton, Paton, & Alwine, 2009). BiP was also shown to colocalize with West Nile virus (WNV) replication compartments (Ambrose & Mackenzie, 2013).

BiP is mainly found in the ER but in some cell types BiP can translocate to the cell surface and may also be secreted (Casas, 2017; Y. Zhang, Liu, Ni, Gill, & Lee, 2010). BiP was found associated with extracellular JEV and cell surface-associated BiP was shown to be important for JEV entry (Nain et al., 2017; Y.-P. Wu et al., 2011). BiP inhibition also disrupted JEV replication at a post-entry step, indicating a crucial role for BiP during multiple phases of the JEV replication cycle, which may be conserved in other flaviviruses.

1.2.8.4 Regulated IRE1-Dependent Decay (RIDD) and Viruses

IRE1 activation results in XBP1 splicing but can also cleave and degrade ER-targeted mRNAs that contain XBP1-like cleavage sites through a process called RIDD (Hollien et al., 2009). This is believed to reduce translation to help the ER folding machinery restore proteostasis. There are a few examples of virus infections, including HCMV, HCV, and Rotavirus, in which IRE1 is active but XBP1 or its target genes are not upregulated (Isler et al., 2005; Tardif, Mori, Kaufman, & Siddiqui, 2004; Trujillo-Alonso, Maruri-Avidal, Arias, & Lopez, 2011). The reason for activating IRE1 while simultaneously blocking XBP1 activity during infection is not known. Activated IRE1 in XBP1 deficient cells can activate RIDD and may be activated in these virus infection models.

The role of RIDD during virus infection has not yet been thoroughly investigated. One report shows that JEV infection can induce RIDD of canonical gene targets and that treatment with IRE1 inhibitor decreased JEV production, indicating that RIDD may promote JEV replication (Bhattacharyya, Sen, & Vrati, 2014). However, this study failed to distinguish if this inhibition of virus was due to a lack of XBP1s. An appealing hypothesis is that some viruses may activate RIDD as a host shutoff mechanism to prioritize translation of viral mRNAs in the ER. Based on this hypothesis, the infecting virus must ensure that its own viral messages are devoid of XBP1-like cleavage motifs.

1.2.8.5 Herpesviruses Control UPR Signaling to Promote Replication

Herpesviruses have large DNA genomes, which allow for the expression of many accessory proteins to fine-tune host-viral interactions for maximum virus replication and

suppression of innate cellular defenses. MCMV (murine CMV) and HCMV both activate PERK signaling and upregulate ATF4, although interestingly, in HCMV infection this corresponds with minimal translation attenuation (Isler et al., 2005; Qian, Xuan, Chapa, Gualberto, & Yu, 2012). CHOP is not upregulated in MCMV infection, whereas CHOP levels have not been investigated in HCMV infection models. HCMV UL38 was shown to upregulate ATF4 through PERK phosphorylation to promote cell survival (Xuan, Qian, Torigoi, & Yu, 2009). ATF4 upregulation during MCMV infection was also important for promoting virus production (Qian et al., 2012). Interestingly, MCMV was also shown to inhibit Tm-induced ATF4 expression through an unidentified mechanism. HCMV activation of PERK has also been reported to promote virus replication through the activation and cleavage of SREBP1 which transactivates genes involved in lipid biosynthesis pathway (Yongjun Yu, Pierciey, Maguire, & Alwine, 2013). HCMV UL148 was shown to activate PERK, as well as IRE1, and a UL148 knockout virus had delayed activation of ATF4 and attenuated XBPl splicing (Siddiquey, Zhang, Nguyen, Domma, & Kamil, 2018). ATF6 signaling was not investigated in this study.

Interestingly, MCMV and the lab-adapted HCMV strain AD169 do not induce XBP1 splicing and can block pharmacological induction of ER stress through the downregulation of IRE1 by MCMV M50 and the HCMV homolog UL50 (Stahl et al., 2013). The mechanism of IRE1 downregulation by these viral proteins is not fully understood but does not appear to be through proteasomal degradation. It is also not known how IRE1 inhibition might provide an advantage for HCMV or MCMV. Interestingly, XBP1-deficient cells display reduced titers of MCMV (Drori, Messerle, Brune, & Tirosh, 2014) indicating that IRE1 inhibition by M50/UL50 may promote XBP1u expression, which could promote virus production.

Even though PERK and IRE1 were activated during HCMV infection, ATF6 was not activated by regulated intramembrane cleavage (RIP) (Isler et al., 2005). Interestingly, BiP was upregulated at the protein level, and as previously mentioned this is likely through IRES-dependent translation (N. J. Buchkovich et al., 2010). Collectively, these CMV studies indicate that PERK signaling is likely pro-viral through multiple mechanisms but the role of IRE1 and ATF6 are unclear and may depend on the strain of virus involved.

HSV-1 is an alpha-herpesvirus and it too has been shown to modulate the UPR (Burnett, Audas, Liang, & Lu, 2012; G. Cheng, Feng, & He, 2005). Probably the best-known example of control over the UPR is that HSV-1 expresses an ortholog of GADD34, $\gamma_1$34.5. $\gamma_1$34.5 promotes dephosphorylation of eIF2α in response to PERK or PKR activation to prevent translation inhibition (G. Cheng et al., 2005; He et al., 1997). Us11 is another HSV-1 protein that can bind and block PKR activation (Poppers, Mulvey, Khoo, & Mohr, 2000). Interestingly, a Us11 and γ34.5 double-knockout virus was still resistant to PERK activation in response to Tg treatment, indicating that there may be other viral inhibitors of the ISR that act directly on PERK (Mulvey, Arias, & Mohr, 2006). Mulvey, Arias, & Mohr (2007) showed that the viral glycoprotein gB bound to PERK and this binding was important for blocking eIF2α phosphorylation in response to stress, likely to enable viral protein translation to occur. Thus, in contrast to CMV, PERK and activation of the ISR is likely inhibitory to HSV-1.

HSV-1 has been shown to cleave ATF6 but there is no impact on the ATF6 target gene BiP suggesting that HSV-1 also blocks the ATF6 branch of the UPR (Burnett et al., 2012). IRE1 has also been reported to be activated during HSV-1 infection but its RNase activity is blocked through an unknown mechanism (Su et al., 2017). Alternatively, IRE1 kinase activity and the IRE1-dependent phosphorylation of JNK was reported to promote virus replication, whereas XBP1s overexpression inhibits virus production. This suggests that HSV-1 directly fine-tunes IRE1's output signaling to suppress XBP1s activation while promoting activation of the JNK pathway in order to promote HSV-1 replication. Since XBP1s inhibits HSV-1, restoring IRE1 RNase activity may promote HSV-1 inhibition. Understanding how HSV-1 regulates IRE1 activity is also likely of interest to the broader UPR research community to help tease out the bifunctional roles of IRE1 activity in controlling UPR signaling.

1.2.8.6 Gamma-Herpesviruses use the UPR to Reactivate in Response to Stress

All herpesviruses have a biphasic replication cycle and can undergo a dormant phase known as latency. During the latency there is minimal viral gene expression and the viral genome is maintained as an episome tethered to host chromatin. Latency is the default replication program for gamma-herpesviruses, which include the human herpesviruses Epstein-Barr virus (EBV) and Kaposi's sarcoma-associated herpesvirus (KSHV) (Speck & Ganem, 2010). Herpesviruses can reactivate to undergo lytic replication, which is the

culmination of expression of all the viral genes in a temporally-regulated cascade, replication and packaging of the genome, and the production of infectious viral progeny. Details of KSHV latency and lytic replication will be explored in more detail in Section 1.3.

The signals that control the switch from latency to lytic replication are unclear, but in cell culture viral reactivation has often been linked to exposure of stressful stimuli. In fact, ER stress can trigger reactivation of EBV, KSHV, and the close relative of KSHV, murine herpesvirus 68 (MHV68) (Bhende, Dickerson, Sun, Feng, & Kenney, 2007; Matar, Rangaswamy, Wakeman, Iwakoshi, & Speck, 2014; Wilson et al., 2007; F. Yu et al., 2007). Presumably, this is a way for the virus to respond to potentially lethal levels of ER stress allowing the virus to "sense" and escape this potentially terminal situation. Reactivation in response to ER stress is primarily due to XBP1s. The mechanism of sensing involves the presence of XBP1s target sequences in the promoters of immediate early viral genes. KSHV and MHV68 express the immediate early protein RTA, which is essential and sufficient to induce lytic replication (Lukac, Renne, Kirshner, & Ganem, 1998; Ren Sun et al., 1998). The RTA promoter in KSHV contains at least one XBP1s response element, which contains an ACGT core (Dalton-Griffin, Wilson, & Kellam, 2009). The RTA promoter also contains hypoxia-inducible factor 1 (HIF-1) response elements, which also contain an ACGT core sequence and thus KSHV can reactivate in response to hypoxia (Q. Cai et al., 2006) . Hypoxia was also shown to induce XBP1 splicing, and robust RTA expression was dependent on both HIF1α and XBP1s (Dalton-Griffin et al., 2009).

EBV lytic replication requires immediate early proteins BRLF1 and BZLF1. It has been reported that reactivation is minimal with XBP1s alone and requires the combination of Protein kinase D for robust expression of BRLF1 and BZLF1 (Bhende et al., 2007). ER stress has also been shown to induce EBV Lmp1 protein through the direct transactivation by XBP1s and possibly ATF4 (Hsiao et al., 2009). Lmp1 is an important transforming protein and can be expressed in latency (Kaye, Izumi, & Kieff, 1993). Lmp1 has also been reported to induce the UPR, possibly acting as a positive feedback mechanism for expression (D. Y. Lee & Sugden, 2008).

Gamma-herpesviruses primarily infect and differentiate B cells and XBP1s is essential for terminal differentiation of B cells into plasma cells (Reimold et al., 2001)

which may be disadvantageous to the virus. Activation of the BCR to promote plasma cell differentiation can also induce lytic replication. BCR activation by IgM crosslinking in one KSHV latency model can induce lytic replication in an XBP1s-dependent manner (Kati et al., 2013). Collectively, these studies demonstrate a link between the UPR and herpesvirus reactivation, but the role of the UPR during lytic replication is relatively unknown.

The ER localized M1 protein of MHV68 can induce low levels of XBP1 splicing and trigger an increase in ATF6-dependent genes such as BiP and Grp94 (Feng et al., 2015). However, M1 expression had no impact on eIF2α phosphorylation suggesting that M1 may only activate the IRE1 and ATF6 branch of the UPR. There is no M1 ortholog in other gamma-herpesviruses.

There are a few studies that show that drugs that cause ER stress and induce the UPR, such as 2-DG or proteasome inhibitors, can inhibit KSHV replication and promote apoptosis (Leung et al., 2012; Saji et al., 2011). This indicates that high levels of ER stress are likely inhibitory to KSHV replication. However, the activation status of the UPR during KSHV lytic infection that originates from a non-ER stress induced mechanism has not been explored. In the following sections of the Introduction, I will examine some of the details of KSHV latency and lytic replication, and the connection between stress and virus reactivation.

1.3 Kaposi's Sarcoma-Associated Herpesvirus

1.3.1. Herpesviridae

The *Herpesviridae* family is a large family of viruses, with over 100 members, and are primarily classified based on virion morphology (Davison et al., 2009). This includes a large (125-240 kb) linear dsDNA genome packaged into an icosahedral capsid that is surrounded by a glycoprotein-containing envelope. Between the capsid and envelope is an electron-dense proteinaceous component called the tegument, which is unique to herpesviruses.

Another unique feature of *Herpesviridae* is that they exhibit a life-long persistent infection that is biphasic (Speck & Ganem, 2010). These two replication cycles are known as latent and lytic replication. In latency, viral gene expression is typically limited to a handful of genes and the viral genome is usually maintained as a circular episome in

the nucleus that is tethered to the host chromosome. During mitosis, the episome is replicated by the cellular DNA polymerase and segregated to the daughter cells. During lytic replication the majority of viral genes are expressed, and the viral genome is replicated by a viral DNA polymerase into linear DNA that is packaged into capsids to generate infectious virions. These newly replicated virions can spread to infect new cells. The name *Herpes* originates from the Greek word "herpein", which means "to creep" because of the recurring nature of infection. The default replication program depends on the herpesvirus and the type of infected cell.

Herpesviridae is divided into 3 subfamilies that are further divided into multiple genera: *Alphaherpesvirinae* (includes the genera *Iltovirus, Mardivirus, Scutavirus, Simplexvirus, and Varicellovirus*)*, Betaherpesvirinae* (includes *Cytomegalovirus, Muromegalovirus, Proboscivirus, and Roseolavirus*) *and Gammaherpesvirinae* (includes *Lymphocryptovirus*, *Macavirus*, *Percavirus*, *Rhadinovirus*).

There are eight human herpesviruses (HHV), HHV-1-8 that are named according to the order of discovery. Most of the human herpesviruses also have a common name, usually based on a distinguishing feature of the infection or disease. HHV-1 and HHV-2 (*Alphaherpesvirinae* subfamily) are the commonly known herpes simplex viruses (HSV) type 1 and 2, which cause blisters around the mouth or genitals, respectively. HHV-3 (*Alphaherpesvirinae*) is varicella zoster virus, which causes chicken pox in young children or can resurface as shingles in adulthood. HHV-5 (*Betaherpesvirinae*) is also known as cytomegalovirus (CMV), which means "large cell" in Greek due to the characteristic large granules that are a defining feature in histological samples. CMV can cause a wide array of symptoms and diseases. HHV-6 and -7 are beta-herpesviruses belonging to the *Roseolovirus* genus. These viruses can cause roseola, a relatively mild febrile illness that normally affects infants and is accompanied with a distinctive rash. HHV-4 and HHV-8 are from the *Gammaherpesvirinae* subfamily and are often referred to as lymphotropic gamma-herpesviruses based on their propensity to infect B lymphocytes. They are also oncogenic viruses (Jha, Banerjee, & Robertson, 2016).

HHV-4 is commonly known as Epstein-Barr virus (EBV), a gamma-herpesvirus that belongs to the genus *Lymphocryptovirus*. EBV was named after the scientists that first identified the virus, Anthony Epstein and Yvonne Barr, and was the first human tumor virus identified. EBV is commonly associated with Burkitt's lymphoma,

Hodgkin's lymphoma, diffuse large B cell lymphoma, and other non-lymphoid tumors, such as gastric carcinomas (Ko, 2015). *In vitro*, EBV infection activates B cells, transforming them into proliferating lymphoblastoid cell lines (LCLs) (Frisan, Levitsky, & Masucci, 2001). B cell transformation is largely mediated through expression of the latency protein LMP1 (Kaye et al., 1993). EBV can also infect epithelial cells in the oral cavity and is the causative agent of infectious mononucleosis, popularly referred to as the "kissing disease" in teenagers because of viral transmission through saliva (Shannon-Lowe, Neuhierl, Baldwin, Rickinson, & Delecluse, 2006).

HHV-8, or Kaposi's sarcoma-associated herpesvirus (KSHV) is the infectious cause of Kaposi's sarcoma (KS). KSHV was first identified by Y. Chang *et al.* (1994) through the use of representational difference analysis (RDA) of a tumor biopsy from a patient with KS. RDA identifies unique DNA sequences that are found in the tumor sample but not in the healthy tissue. DNA sequence alignment showed similar homology to the squirrel monkey virus, herpesvirus saimiri (HVS), a gamma-herpesvirus that belongs to the genus *Rhadinovirus*. Soon after KSHV was discovered, the virus was found associated with two rare B cell lymphomas, multicentric Castleman's disease (MCD) (Soulier et al., 1995) and primary effusion lymphoma (PEL; originally called body cavity-based lymphoma [BCBL]) (Cesarman, Chang, Moore, Said, & Knowles, 1995). PEL has a poor prognosis with a median survival rate of approximately 6 months (Simonelli et al., 2003). These KSHV-infected B cell tumors present with a pre-plasma cell (or plasmablast) phenotype (Chadburn et al., 2008; Hassman, Ellison, & Kedes, 2011; Jenner et al., 2003). Both EBV and KSHV-based tumors are often associated with HIV infection and immunosuppression through AIDS and thus rarely cause cancer in healthy individuals. EBV and KSHV co-infection is also found in some PEL samples and co-infection correlates with the occurrence of AIDS (Chadburn et al., 2017). KSHV is considered a lymphotropic virus but *in vitro* and *in vivo* evidence demonstrates that KSHV has evolved to infect a wide variety of immune and non-immune cell types, including endothelial cells, which are likely the cells involved in promoting KS (Bechtel, Liang, Hvidding, & Ganem, 2003).

1.3.2 KSHV Genome and its ORFs

Sequencing of the KSHV genome in 1996 revealed that it is a linear dsDNA genome of approximately 165-170kb that contains a 140-kb unique coding region flanked by

repetitive GC-rich 801-bp sequences, which collectively are called long terminal repeats (LTRs) (Russo et al., 1996). The number of ORFs originally classified was approximately 90, which was based on two criteria: (1) ORFs were initiated with an AUG start codon, and (2) the ORFs encode proteins of > 100 amino acids. 66 of the viral gene sequences showed significant similarity to the closely related gamma-herpesvirus, HVS. Some of the ORFs identified are unique to KSHV and are designated K1 to K15. The virus has also pirated multiple human genes that may or may not be unique to KSHV. Many of these viral homologs and KSHV-specific ORFs are potent oncogenes and likely play a key role in KSHV tumorigenesis (Giffin & Damania, 2014). These include the cyclin D homolog vCyclin (viral Cyclin; ORF72), and the constitutively active vGPCR (ORF74), a homolog of human CXCR1/CXCR2. KSHV also encodes multiple immune-modulatory proteins, such as E3 ubiquitin ligases K3 and K5. These viral E3 ligases polyubiquitinate and downregulate immune signaling molecules such as MHC-I, ICAM-1, and B7-2 (Brulois et al., 2014).

Further studies identified that the virus encodes 12 pre-microRNAs (pre-miRNAs) that can be processed to up to 25 mature microRNAs (miRNAs) that also are involved in tumorigenesis, immune modulation, and viral replication (reviewed in J. Qin, Li, Gao, & Lu, 2017). lncRNAs (long non-coding RNAs), and ORFs with CUG translation start codons have also been identified (S. Chandriani, Xu, & Ganem, 2010; Sadler et al., 1999). See Appendix B for the list of the protein coding ORFs, their primary functions, and timing of expression during the replication cycle.

Advances in deep sequencing and ribosomal footprinting methodology revealed that the coding potential of the KSHV genome is much more complex than previously appreciated, with many new candidate ORFs or ORFs with multiple isoforms based on ribosomal occupancy (Arias et al., 2014). Furthermore, the earlier labeling of the genome was based on *in silico* genome analysis and some of these potential ORFs may not be translated during infection or expression may be cell-type-specific. This highlights the need for further investigation of the viral genome to fully document the coding potential of this virus.

1.3.3 Viral Entry

The KSHV virion is large (~220 nm) and comprises a glycoprotein-studded envelope that surrounds a genome-containing icosahedral capsid (F. Liu & Zhou, 2007). The space

between the capsid and the viral envelope is an electron dense proteinaceous layer called the tegument that is unique to herpesviruses. The tegument contains viral proteins and possibly viral and cellular microRNAs (X. Lin, Li, Liang, & Lan, 2012). The different factors in the tegument are important during entry to facilitate cell reprogramming, immune evasion, and delivery of the genome to the nucleus (reviewed in Sathish, Wang, & Yuan, 2012).

Depending on the cell type, KSHV glycoproteins bind to various cellular receptors on the plasma membrane including heparan sulfate, DC-sign, integrins, and the glutamate/cysteine exchange transporter protein xCT (reviewed in Chakraborty, Veettil, & Chandran, 2012). Binding of the receptors triggers a signaling cascade that results in activation of multiple kinases, including focal adhesion kinases, Src, and PI3K to facilitate internalization. KSHV has been reported to enter the cell by macropinocytosis, or clathrin- or caveolin-mediated endocytosis, which is dependent on cell type and the cellular receptors involved. Upon fusion of the viral envelope with the endocytic vesicle, the nucleocapsid is released into the cytoplasm and traffics to the nucleus through dynein-dependent transport on microtubules. The capsid associates with the nuclear core complex to deliver the linear genome into the nucleus. Inside the nucleus, the genome undergoes circularization and becomes tightly packed as nucleosomes with the help of cellular factors.

1.3.4 Latency and the Latency Locus

KSHV's default replication program is latency, which is a quiescent replication cycle that the virus uses primarily to avoid immune detection. A subset of viral genes are expressed during KSHV latency to facilitate the maintenance of the viral genome as a circular episome and promote cell growth and survival. The pro-growth environment is largely facilitated through the expression of oncogenes and virally encoded cytokines, which as a result can promote tumorigenesis (Mesri, Cesarman, & Boshoff, 2010).

The core of the viral genes that are expressed during latency include LANA, vCyclin, vFLIP, the Kaposins, and the miRNAs. In MCD, gene expression during latency is "leaky", and traditional lytic genes have also been detected, including vIL-6, K1, and ORF59. These viral genes may also be expressed during latency in non-MCD cases, although at reduced levels compared to lytic. vIL-6 and K1 have pro-inflammatory and

transforming properties and vIL-6 is strongly associated with MCD and PEL pathogenesis (Polizzotto, Uldrick, Hu, & Yarchoan, 2012; Polizzotto et al., 2013).

1.3.4.1 Latency-Associated Nuclear Antigen (LANA)

LANA is a large (1162 amino acids) protein expressed immediately following circularization. LANA is analogous to EBV's EBNA1 (Epstein-Barr nuclear antigen 1) and their main function during latency is to ensure that the viral episome is partitioned into the daughter cell nuclei following cell division by tethering the chromatinized viral genome to the host chromosome (Uppal, Banerjee, Sun, Verma, & Robertson, 2014). LANA forms a dimer that further oligomerizes into higher-order structures such as pentameric rings or right-handed, continuous spirals (Domsic, Chen, Lu, Marmorstein, & Lieberman, 2013; Hellert et al., 2015). Through multimerization, the C-terminal domain of LANA binds to a 78-bp region in the LTRs of the viral genome. The N-terminal domain binds mitotic chromosomes through the interaction with multiple cellular proteins, including histone H1, and H2A and B in nucleosomes (Barbera et al., 2006). The importance of LANA to bridge the viral episome to the host chromosomes was demonstrated through genetic silencing of LANA, which caused the rapid loss of viral episomes (Ballestas, Chatis, & Kaye, 1999; F.-C. Ye et al., 2004).

LANA is expressed on a tricistronic mRNA upstream of vCyclin and vFLIP, which is regulated by a promoter that is constitutively transactivated by cellular factors, and therefore, does not rely on any viral genes for expression (Bieleski & Talbot, 2001; D. Dittmer et al., 1998). LANA has also been reported to regulate its own mRNA expression likely by a DNA binding-independent mechanism (Jeong, Papin, & Dittmer, 2001). *In vitro* experiments have also revealed that LANA can repress or activate multiple inflammatory cytokines such as human IL-6 (An, Sun, & Rettig, 2004), and has been reported to antagonize DNA sensing by the innate immune DNA sensor cGAS (G. Zhang et al., 2016). LANA has also been reported to regulate multiple different signaling pathways to promote inflammation, angiogenesis, and to establish latency (Verma, Lan, & Robertson, 2007).

1.3.4.2 vCyclin and vFLIP

vCyclin is a cyclin D homolog that is constitutively signaling (Cannell & Mittnacht, 1999). vCyclin promotes cell-cycle progression though CDK6 heterodimerization, and together phosphorylate an expanded repertoire of substrates that control the cell cycle,

including Rb, p53, and CDC6 (M. Li et al., 1997). The vCyclin/CDK6 heterodimer is also refractory to inhibition by cell cycle-dependent kinases, such as p21/Sip1, or p27/Kip1 (Swanton et al., 1997). Ectopic vCyclin expression activates a DNA damage response that can cause apoptosis, or irreversible cell cycle arrest in primary cells known as oncogene-induced senescence (OIS) (Koopal et al., 2007).

vCyclin and vFLIP (viral Fas-associated death domain-like interleukin-1β-converting enzyme-inhibitory protein; or K13) are expressed from a tricistronic mRNA along with LANA, but through alternative splicing, the LANA ORF is excised resulting in a bicistronic mRNA. vFLIP is translated from these mRNAs by an IRES found downstream of vCyclin (Bieleski & Talbot, 2001). vFLIP shares limited sequence homology with cellular FLIP (cFLIP) but both contain two death effector domains that prevent apoptosis. This is primarily accomplished by activating NFκB signaling through interacting with IKK and promoting phosphorylation and inhibition of IκB (Guasparri, Keller, & Cesarman, 2004). In addition, cFLIP and vFLIP can also inhibit the autophagy pathway by direct binding and inhibition of ATG3, which is required for autophagosome biogenesis (J.-S. Lee et al., 2009).

A key component of OIS is an increase in cytokine secretion, which has been shown to be dependent on the autophagy machinery (Narita et al., 2011). Autophagy also drives vCyclin-mediated OIS (Leidal, Cyr, Hill, Lee, & McCormick, 2012). Therefore, by inhibiting ATG3, vFLIP blocks vCyclin-driven OIS. vFLIP expression can cause B cell tumors in mice and knockdown of vFLIP in PEL cells significantly increased apoptosis demonstrating an important role for vFLIP in KSHV tumorigenesis (Ballon, Chen, Perez, Tam, & Cesarman, 2011; Guasparri et al., 2004).

1.3.4.3 The Kaposins

The K12 ORF (also called Kaposin A or KapA) was first identified as a single ORF-containing mRNA and is the most abundant transcript detected in latently infected cells (Hong Li, Komatsu, Dezube, & Kaye, 2002). KapA encodes a short (60 amino acid) type II transmembrane protein and was reported to have transforming potential by activating ARF GTPase through cytohesin-1 (Kliche et al., 2001). Further analysis of the K12 transcript revealed that there are two other predominant ORFs that contain CUG start codons upstream of the K12 ORF (Muralidhar et al., 1998; Sadler et al., 1999). The coding sequences are composed of 23 nucleotide repeats that when translated, regardless

of reading frame, generate 2 different motifs of the same 23-amino acid direct repeats (DR), termed DR1 and DR2. Screening monoclonal antibodies from hybridomas that were generated by immunizing mice with TPA-induced BCBL1 whole cell lysates confirmed that these DR-containing ORFs are translated (Sadler et al., 1999).

Depending on the reading frame, translation of the DR-containing ORFs will result in expression of KapB or KapC (Sadler et al., 1999). KapB translation terminates upstream of the K12 ORF and generates a cytoplasmic/nuclear protein that activates the MAPK p38-MK2 pathway to stabilize mRNAs that contain AU-rich elements in the 3'UTR (McCormick & Ganem, 2005). These mRNAs are normally labile and encode pro-inflammatory, angiogenic, and oncogenic signaling molecules such as cytokines and growth factors. Thus, KapB also likely plays an important role in tumorigenesis through stabilization of these mRNAs. KapC translation encompasses the KapA ORF, and therefore contains the transmembrane domain, which localizes KapC to the ER and Golgi apparatus (Muralidhar et al., 1998). Currently, nothing is known about the function of KapC. The Kaposin transcripts are also upregulated during lytic replication (P.-J. Chang et al., 2002).

1.3.4.4 KSHV microRNAs

Many large DNA viruses, including KSHV, express lncRNAs and microRNAs (miRNAs) that are important for replication (Z. Wang, Zhao, & Zhang, 2017). KSHV encodes 12 pre-miRNAs that are located within the Kaposin locus and transcribed from the K12 promoter. At last count, the 12 pre-miRNAs are further processed into 25 mature miRNAs (J. Qin et al., 2017). Like cellular miRNAs, KSHV pre-miRNAs are processed by the cellular machinery Drosha and Dicer to generate mature miRNAs. By binding the complementary target sequence typically in the 3'UTR, the miRNAs can silence translation of these mRNAs. All the KSHV miRNAs are expressed during latency, although their levels of expression are variable (Giffin & Damania, 2014). Two of these pre-miRNAs, miR-K10 and mir-K12, are also upregulated during lytic replication. Furthermore, miR-K10 is located in the K12 ORF and thus the transforming function of KapA may be actually due to miR-K10 and not KapA protein (Forte et al., 2015). Through high-throughput sequencing of miRNA-bound targets through HITS-CLIP and PAR-CLIP, bioinformatics, and target validation, it is becoming increasingly clear that KSHV miRNAs play essential roles in controlling latency, virus replication, immune

evasion, cell survival, and tumorigenesis. This may largely be facilitated by targeting a signaling network that converges on the transcription factor STAT3 (signal transducer and activator of transcription 3) (Ramalingam & Ziegelbauer, 2017). Some of these miRNAs have also been reported to be incorporated into mature virus particles and thus may also play a role during entry (X. Lin et al., 2012). For a recent review of KSHV miRNAs please see (J. Qin et al., 2017).

1.3.5 Lytic Replication

1.3.5.1 RTA is the Latent-Lytic Switch

Serial-passaging of explanted KSHV-infected cells from KS lesions leads to rapid loss of viral episomes, and therefore it is likely that KSHV undergoes lytic replication to maintain the pool of latently infected cells (Grundhoff & Ganem, 2004). Since the default replication program is latency it was originally thought that the genes expressed during latency were the sole drivers of inflammation and tumorigenesis. However, it has become increasingly clear that both replication programs are essential for pathogenesis (Aneja & Yuan, 2017). This first evidence of this occurred when KS patients treated with ganciclovir or foscarnet, which inhibit herpesvirus lytic replication, caused KS regression (Casper, Nichols, Huang, Corey, & Wald, 2004; D. F. Martin et al., 1999).

Lytic replication is driven by the viral protein RTA (replication and transcription activator). RTA is an immediate early protein that is essential and sufficient to reactivate the virus from latency (Lukac et al., 1998; Ren Sun et al., 1998). This observation has spurred the use of RTA expression vectors to induce lytic reactivation in order to study lytic replication. Analogous to EBV studies, drugs such as the phorbol ester TPA and HDAC class I and II inhibitors, such as sodium butyrate (NaB) and valproic acid (VPA), can also induce KSHV lytic reactivation (Hausen, O'neill, Freese, & Hecker, 1978; Luka, Kallin, & Klein, 1979). TPA is thought to activate PKCδ, which signals through the ERK pathway to form an active AP-1 transcription complex that transactivates RTA (Cohen, Brodie, & Sarid, 2006). NaB and VPA treatment results in hyperacetylation of histones in the RTA promoter, which recruits further epigenetic remodeling and transactivating factors to promote RTA expression (H. Nakamura et al., 2003; Shin, DeCotiis, Giron, Palmeri, & Lukac, 2014). RTA-dependent viral gene expression can be divided into two classes: (1) direct DNA binding to RTA response elements (RREs), and (2) binding and activation of cellular transcription factors, such as RBP-J-κ and C/EBPα. Through these

two mechanisms, RTA can upregulate multiple viral genes including PAN, K1, K2, K5, K6, K8, K9, K12, K14, ORF6, ORF21, ORF57, ORF59, and ORF74. RTA can also promote its own gene expression as a positive feed-forward mechanism (reviewed in Staudt & Dittmer, 2007).

Lytic replication occurs through a transcriptional gene expression cascade of immediate early (IE) genes, followed by early (E) or delayed early (DE) genes. After genome replication, late (L) gene expression occurs (R Sun et al., 1999). Viral genes are categorized into these three phases based on their sensitivity of expression to the translation inhibitor cycloheximide (CHX) and the viral polymerase inhibitor phosphonoacetic acid (PAA). IE genes, which include RTA, are not dependent on any viral gene expression and thus are expressed in the presence of CHX treatment following treatment with TPA or NaB. Along with RTA, ORF45 and K8 expression are also resistant to CHX treatment and are classified as immediate early, although their expression can be further upregulated by RTA (F X Zhu, Cusano, & Yuan, 1999). E genes are dependent on the IE genes but not dependent on genome replication and so these genes are CHX-sensitive but insensitive to PAA treatment. The L genes are dependent on genome replication and therefore grouped based on their sensitivity to PAA treatment. The majority of L genes encode structural proteins that get incorporated into the virus particle (R Sun et al., 1999).

1.3.5.2 Maintenance of Latency

The LANA promoter also contains an RRE (Lan, Kuppers, Verma, et al., 2005). It has been reported that immediately following infection, there is a burst of lytic gene expression, which may promote RTA-dependent expression of LANA to facilitate episome binding to host chromosomes. Furthermore, LANA can directly bind to RTA protein to inhibit activity. LANA has also been reported to repress RTA expression, likely through inhibition of RBP-J-κ activation of the RTA promoter (Lan, Kuppers, & Robertson, 2005). Therefore, this balance between LANA and RTA expression likely plays a key role in dictating the replication program. Tentatively, gradual viral shedding of episomes would likely lead to a decrease in LANA, or *vice versa*, which would free RTA to induce the lytic cycle to ensure that the virus is not eliminated.

RTA may also regulate its own activity to prevent lytic replication. RTA has E3 ubiquitin ligase activity and may undergo auto-ubiquitylation and subsequent

proteasomal degradation (Aneja & Yuan, 2017; Yanxing Yu, Wang, & Hayward, 2005). KSHV miRNAs can also repress RTA expression, both directly and indirectly. In particular, miR-K9 binds to the 3'UTR of RTA mRNA to repress lytic replication (Bellare & Ganem, 2009). Some cellular proteins have also been reported to inhibit RTA expression, namely hKFC, OCT-2, KAP-1, PARP-1, and Hey-1, which may all play a role in promoting latency (Aneja & Yuan, 2017). The RTA promoter also undergoes chromatin remodeling during latency and is hypoacetylated by HDACs to repress expression. Histone 3 is also trimethylated at the RTA promoter and H3K27me3 chromatin marks are indicative of repressed transcription (Günther & Grundhoff, 2010). Interestingly, epigenetic analysis also revealed that the RTA promoter also contains H3K4me3 marks, which are activating chromatin marks (Toth et al., 2010). The presence of both active and repressive epigenetic modifications suggests that the RTA promoter may be poised for efficient upregulation in response to cues to facilitate rapid reactivation.

1.3.5.3 RTA Expression is Induced in Response to Environmental Factors or Stress.
In vitro, reactivation can be induced artificially with the treatment of NaB or TPA, or through ectopic expression of RTA. However, the real physiological cues that induce reactivation are not entirely clear. It is likely that environmental or cellular stresses can promote reactivation through RTA transactivation (Aneja & Yuan, 2017). This includes co-infection with other viruses, hypoxia, oxidative stress, and ER stress.

Multiple different viruses, including HIV, HSV-1, HCMV, HHV-6, and HHV-7, have been shown to induce KSHV reactivation, whereas co-infection with EBV represses reactivation (reviewed in Thakker & Verma, 2016). Many of the soluble factors secreted during co-infection, such as pro-inflammatory cytokines, are thought to play a prominent role in KSHV reactivation. During HIV co-infection, the secreted signaling molecule Tat-1 can penetrate KSHV-infected cells and trigger reactivation, as well as contribute to tumor progression by acting as a growth factor. Reciprocally, multiple KSHV proteins have also been reported to promote HIV replication by modulating the activity of the LTRs in the HIV genome. With respect to EBV co-infection, both EBV BZLF1 and LMP1 have been reported to repress RTA expression (Y. Jiang, Xu, Zhao, & Zhang, 2008).

Various forms of stress also promote reactivation. Reactive oxygen species (ROS) such as hydrogen peroxide (H_2O_2) and superoxide ($\bullet O_2^-$) are molecules that consist of a radical and non-radical oxygen from the partial reduction of oxygen (Ray, Huang, & Tsuji, 2012). ROS is generated from normal cellular processes, such as mitochondrial electron transport, the NADH oxidase complex, and oxidative protein folding in the ER. While low levels of ROS can promote cell growth, increasing levels of ROS can induce oxidative stress and apoptosis. The accumulation of H_2O_2 in KSHV-infected cells can induce reactivation mediated through activation of MAPKs, p38, ERK1/2, and JNK (F. Ye et al., 2011). Furthermore, inhibition of NFκB increased ROS-dependent viral reactivation (X. Li, Feng, & Sun, 2011), indicating that vFLIP may play an important role in regulating the latent-lytic switch by regulating ROS levels through activation of NFκB.

Hypoxia, which means a deficiency in oxygen, can also induce KSHV reactivation. In response to low O_2 levels, hypoxia inducible factors (HIF)-1 and -2 transcription factors reprogram gene expression to promote adaptation to a low O_2 environment (Kaelin & Ratcliffe, 2008). HIF-1 and -2 are heterodimers that contain an α and β subunit. The β subunit is constitutively expressed but during normal levels of O_2 (normoxia), the α subunit undergoes poly-ubiquitination by the tumor suppressor VHL (von Hippel-Lindau), and subsequent proteasomal degradation. Hypoxia increases stability of the α subunit by inhibiting VHL binding. HIF-1/2-dependent genes contain hypoxia response elements (HREs) in their promoter to facilitate transcription factor binding. The HIF-1/2 HRE consensus sequence contain a core binding motif 5'-RCGTG-3', where R is A or G (Mole et al., 2009). Seven putative HREs are present in the promoter of RTA, however only three were responsive to HIF-1 (Q. Cai et al., 2006; Muzammel Haque, Davis, Wang, Widmer, & Yarchoan, 2003). Therefore, in response to hypoxia, HIFs can induce lytic reactivation. This upregulation is thought to be dependent on LANA, as LANA has been reported to both promote and inhibit HIF-1 transactivation of RTA (Qiliang Cai, Murakami, Si, & Robertson, 2007). Six putative HREs were also identified in the promoter region of ORF34-ORF35-ORF36-ORF37, which induces a tricistronic mRNA encoding ORF35-36-37 and a longer transcript that encompasses ORF34 as well (Muzammel Haque, Wang, Davis, Zheng, & Yarchoan, 2006). One of the HREs in the promoter was critical for expression of both transcripts in response to hypoxia. ORF34 is part of the vPIC that drives late gene expression but has also been

reported to bind HIF-1α and promote proteasomal degradation (M. Haque & Kousoulas, 2013). ORF34-dependent regulation of HIF-1 may act as a negative feedback mechanism to minimize the potential negative effects of HIF-1 signaling, such as apoptosis.

HREs are markedly similar to XBP1s consensus binding sites, which also contain an ACGT core (Clauss et al., 1996). In fact, one of the putative HREs in the RTA promoter was more responsive to XBP1s than HIF-1 and thus ER stress was also shown to induce RTA expression by XBP1s (Dalton-Griffin, Wilson, & Kellam, 2009). XBP1s is also upregulated during hypoxia and has been shown to interact with HIF-1. Therefore, this dual action of XBP1s and HIF-1 likely facilitates robust transactivation of RTA in response to hypoxia (Dalton-Griffin et al., 2009). ER stress in PEL cells has also been reported to induce KSHV reactivation through caspase-dependent cleavage of RAD21 (De Leo, Chen, Hu, & Lieberman, 2017). RAD21 is a component of the cohesin complex that partners with CTCF to silence viral gene expression and maintain latency (H.-S. Chen et al., 2017).

As well as resolving ER stress, XBP1s in mature B cells controls a late phase in terminal differentiation of antibody-secreting plasma cells (PCs) (Reimold et al., 2001; Todd et al., 2009). Following recognition of a foreign antigen by the B cell receptor, B cells undergoes transcriptional reprogramming to differentiate into PCs. This transcriptional reprogramming requires XBP1s as well as a variety of other transcription factors (Shaffer et al., 2004). BCR activation by IgM crosslinking in a KSHV-infected, EBV-negative Burkitt's lymphoma cell line was shown to induce lytic reactivation in part through XBP1s (Kati et al., 2013). Since MCD and PEL cells have a plasmablast phenotype (Chadburn et al., 2017), further differentiation into PCs may allow KSHV to escape from cell cycle arrest through XBP1s transactivation of RTA. Alternatively, KSHV may actively repress XBP1 activity in order to maintain tight control of latency, which may contribute to the plasmablast phenotype.

XBP1s has also been reported to also induce expression of EBV master regulators of lytic replication, BZLF1 and BRLF1, however this may be cell type dependent and/or require additional cellular factors such as protein kinase D (Bhende et al., 2007). MHV68 RTA expression is also responsive to XBP1s expression *in vitro*. However, *in vivo* it appears that IRF4, another plasma cell differentiation transcription factor, but not XBP1s is required for robust MHV68 reactivation (Matar et al., 2014). These studies suggest that

activation of XBP1s may be an evolutionary conserved mechanism for reactivation among gamma-herpesviruses, but further studies are required to understand its full potential, especially *in vivo*. There are likely other stress-responsive transcription factors that regulate KSHV replication and further studies will be required to elucidate their roles.

1.3.5.4 PAN lncRNA is Important in Regulating Lytic Gene Expression

During lytic replication, RTA upregulates a 1.1 kb lncRNA called PAN (polyadenylated nuclear) RNA by binding to an RRE in the PAN promoter (Rossetto, Tarrant-Elorza, Verma, Purushothaman, & Pari, 2013). PAN RNA expression can also occur independent of RTA and is the most abundantly expressed viral transcript during lytic replication. PAN is essential for viral gene expression and is stabilized through a direct interaction with ORF57 (Massimelli, Majerciak, Kruhlak, & Zheng, 2013). PAN RNA binds to chromatin modifying complexes, including the histone demethylases UTX and JMJD3, which are recruited to the viral genome to promote gene expression by demethylating H3K27me3 marks (Rossetto & Pari, 2012). PAN RNA can also bind to epigenetic repressive factors to repress cellular genes involved in immune modulation (Rossetto & Pari, 2014). Recently, PAN was shown to regulate mRNA nuclear export of late viral transcripts thus impacting viral translation (Withers, Li, Vallery, Yario, & Steitz, 2018). PAN can be packaged into virus particles and thus may facilitate establishment of latency through epigenetic remodeling of the genome during *de novo* infection (Rossetto et al., 2013). Ribosomal footprinting has revealed that PAN RNA may also express small peptides that may further regulate viral or cellular gene expression or have other unrelated functions during lytic replication (Arias et al., 2014).

1.3.5.5 SOX Protein Induces Host Shutoff

Multiple diverse virus families encode nucleases that degrade host mRNAs, primarily as a means to gain access to translating ribosomes. KSHV also executes host shutoff through the expression of ORF37, which encodes the nuclease protein SOX (for shutoff and exonuclease) (Glaunsinger & Ganem, 2004b). Sox has both endo and exonuclease activity. It shares homology with other herpesvirus exonucleases that are DNases and are likely important for processing and packaging viral DNA into capsids. However, unlike other herpesviruses, Sox can also facilitate host shutoff through its endonuclease activity (Glaunsinger, Chavez, & Ganem, 2005). Sox activity results in widespread Xrn1-

dependent degradation of cellular mRNAs, which is likely based on sequence- and conformation-specific binding (Covarrubias et al., 2011; Mendez, Vogt, Bohne, & Glaunsinger, 2018). A subset of privileged mRNAs escape host shutoff (Sanjay Chandriani & Ganem, 2007; Glaunsinger & Ganem, 2004a). Central to these escapees is IL-6 mRNA, which contains protective RNA elements in the 3'UTR (Muller & Glaunsinger, 2017). IL-6 is important in KSHV tumorigenesis (Sakakibara & Tosato, 2011).

1.3.5.6 Lytic Genome Replication and Late Gene Expression

The viral genome contains two copies of lytic DNA replication origins and based on their locations in the genome are called *ori*-Lyt L (for left) and *ori*-Lyt R (for right) (Aneja & Yuan, 2017). The reason that KSHV has two *ori*-Lyts is not clear. Mutating *ori*-Lyt L but not *ori*-Lyt R inhibited genome replication in Vero cells, suggesting that one of the *ori*-Lyts may not be functional (Y. Xu, Rodriguez-Huete, & Pari, 2006). Alternatively, the multiple *ori*-Lyts may allow for cell type specific replication, which was recently demonstrated for MHV68 (Sattler, Steer, & Adler, 2016).

A 1.4kb (T1.4) or 0.7kb (T0.7) lncRNA is transcribed from *ori*-Lyt (L) or *ori*-Lyt (R), respectively, which are essential for genome replication (Aneja & Yuan, 2017). K8 and RTA bind to the *ori*-Lyt to facilitate genome replication (Yan Wang, Tang, Maul, & Yuan, 2006). Recently, K8 was shown to bind to the T1.4 RNA to recruit cellular and viral factors to the *ori*-Lyt to replicate the genome (D. Liu, Wang, & Yuan, 2018). The viral DNA polymerase (ORF9), along with viral replication accessory factors, including ORF6, ORF40, ORF41, ORF44, ORF56, and ORF59, synthesize head-to-tail concatemers of linear viral DNA by rolling circle replication (F. Y. Wu et al., 2001).

The cessation of genome replication initiates late gene expression, which includes the production of structural proteins, such as capsid proteins, glycoproteins, and tegument proteins. Treatment with the viral DNA polymerase inhibitor PAA can almost completely block late gene expression, but precisely how genome replication controls late gene expression is not known (D. Li, Fu, & Swaminathan, 2018). The majority of late genes are transcribed by the late gene transcription viral pre-initiation complex (vPIC), which is composed of the early proteins ORFs 18, 24, 30, 31, 34, and 66 (Davis, Hesser, Park, & Glaunsinger, 2016). ORF24 is a TATA box binding protein that recruits RNA polymerase II (RNAPII) and ORF18 promotes RNAPII elongation. Currently the roles of

the other viral proteins in the vPIC remain largely unknown. However, through mutational analysis it is becoming obvious that specific contacts between the different subunits of the vPIC are critical for late gene expression (Castañeda & Glaunsinger, 2018).

1.3.5.7 Virus Assembly and Release

KSHV icosahedral capsids self-assemble in the nucleus (Perkins et al., 2008). The major capsid protein (MCP; ORF25) forms 150 hexons and 11 pentons. Pentons are located at 11 of the 12 vertices and the remaining vertex is occupied by the portal protein, a dodecameric ring structure composed of ORF43, that facilitates DNA entry (Dünn-Kittenplon, Kalt, Lellouche, & Sarid, 2019). The scaffold protein (ORF17) and protease (ORF17.5) occupy the internal space of the capsid. The hexons are connected by heterotrimers of the triplex protein 1 (Tri-1; ORF62) and Tri-2 (ORF26) in a 1:2 ratio. The small capsid protein (SCP; ORF65) crosslinks neighboring MCPs in the same hexamer to stabilize the overall capsid structure. Interestingly, unlike HSV-1, EBV and KSHV SCPs are important but not essential for capsid assembly (Dai et al., 2015; Perkins et al., 2008).

Analogous to alpha- and beta-herpesviruses, KSHV encodes multiple factors that are involved in packaging the genome into capsids and cleaving the concatemeric DNA (M. R. Gardner & Glaunsinger, 2018). Inside the capsid, the protease cleaves the scaffold protein and becomes displaced as the DNA is fed into the capsid. Different types of capsids can be identified by transmission electron microscopy (TEM) and are called A-, B-, and C-capsids (Nealon et al., 2001). C-capsids are DNA packaged capsids and are characterized based on their electron dense core. A-capsids are empty, and B-capsids still contain the scaffold protein. It is not completely clear if A and B capsids are assembly intermediates, or are defective, and therefore unable to become infectious particles (Tandon, Mocarski, & Conway, 2015).

The DNA-containing capsids are ~ 120 nm in diameter and are thus too large to exit through the nuclear pores. All herpesviruses escape by budding at the inner nuclear membrane (reviewed in Mettenleiter, 2002). To facilitate budding, KSHV encodes two proteins, ORF67 and ORF69, that interact to form the nuclear egress complex (NEC) (Desai, Pryce, Henson, Luitweiler, & Cothran, 2012; Luitweiler et al., 2013). ORF67 is inserted into the inner nuclear membrane and together with ORF69, facilitates the

disassembly of the nuclear lamina through the hyperphosphorylation of emerin (Farina et al., 2013). This provides access for the nucleocapsids to bud out of the inner nuclear membrane and into the perinuclear space, which is contiguous with the ER lumen; this phase is referred to as primary envelopment. KSHV becomes de-enveloped through fusion with the outer nuclear membrane as the nucleocapsid is released into the cytoplasm (Mettenleiter, 2002).

Details regarding trafficking of herpesvirus nucleocapsids are lacking but it is clear that components of the tegument play a role. Tegumentation, the process of acquiring tegument proteins, occurs primarily in the cytoplasm and was originally thought to be a stochastic process. However, it is now appreciated that tegumentation occurs through an ordered addition of proteins through protein-protein interactions with other tegument proteins, capsid proteins, and glycoproteins (Dai, Gong, Wu, Sun, & Zhou, 2014). ORF64 is a large (290 kDa) tegument protein that can interact with capsid proteins, multiple different tegument proteins, as well as some glycoproteins (Rozen et al., 2008). Therefore, ORF64 may act as a scaffold in which to spatially organize the tegument, as well as link the capsid to the glycoproteins. The tegument protein ORF32 was also shown to bridge ORF19 to the capsid by binding the capsid triplex proteins and may also interact with other tegument proteins (Dai et al., 2014). In addition, ORF33, ORF38, and ORF52 tegument proteins are also likely important in the tegumentation process since their deletion prevents the acquiring of other tegument proteins, like ORF45 (Wenwei Li et al., 2016; J.-J. Wu et al., 2016). Tegumented capsids associate with viral glycoproteins found on the *trans*-Golgi network (TGN) or vesicles derived from the TGN. ORF45 tegument protein was reported to be important for capsid recruitment to the TGN by trafficking viral capsids on microtubules through an interaction with kinsesin-2 (Sathish, Zhu, & Yuan, 2009). Furthermore, ORF45 can interact with lipid rafts at the TGN (TGN). This interaction with lipid rafts is dependent on ORF45 mono-ubiquitination at Lys297 (X. Wang et al., 2015). The virus undergoes secondary and final envelopment through intra-luminal budding of TGN-derived vesicles. ORF64 tegument protein is also likely involved in budding at the TGN due to its ability to bind envelope glycoproteins that are situated on these vesicles (Aneja & Yuan, 2017). The virus-containing vesicles eventually fuse with the plasma membrane releasing the

infectious virus particles into the extracellular space to allow for spread and infection of neighboring cells.

1.3.6 KSHV and its Diseases

KSHV is the infectious cause of Kaposi's sarcoma (KS) and the B cell lymphoma PEL; it can also cause multicentric Castleman's disease (Ganem, 2007). All three of these KSHV-related diseases are directly linked to immunosuppression, primarily occurring with the onset of AIDS. KSHV infection results in the establishment of latency, which is the default replication program. Through the expression of latent viral proteins and miRNAs, KSHV can trigger paracrine and autocrine signaling through the secretion of growth factors, and pro-inflammatory cytokines. In a tumor sample, while the majority of infected cells are latent, lytic replication is found in a subset of infected cells and is also important for inflammation and oncogenesis (Giffin & Damania, 2014). The mechanism of KSHV-induced tumorigenesis is unclear, which is largely due to the lack of effective cell systems and animal models (D. P. Dittmer, Damania, & Sin, 2015). KSHV encodes multiple latent and lytic proteins that demonstrate tumorigenic potential *in vitro* and are likely important for inducing tumorigenesis *in vivo.* This includes, Kaposin A, vFLIP, vGPCR, K1, and vIL-6. Latent and lytic proteins also modulate cellular immunity and metabolism, which further promotes cell growth and survival (Giffin & Damania, 2014).

1.3.6.1 Kaposi's Sarcoma

In 1872, the Hungarian physician Moritz Kaposi first characterized the KS tumor as an idiopathic, multi-pigmented sarcoma of the skin (Kaposi, 1872). Later it was identified that the tumor arises from the proliferation of spindle cells, which are thought to be of endothelial origin and are named based on their narrow, elongated shape (Boshoff et al., 1995). Over a century after the characterization of KS, the tumor-derived spindle cells were shown to be infected by KSHV (Y. Chang et al., 1994). Unlike most tumors, the histology of KS tumors shows that they are polyclonal nature and histologically complex (Ganem, 2007). The spindle cells are the primary infected cell type in the tumor. The KS tumor also contains infiltrating immune cells, such as monocytes, T-cells and plasma cells. Through aberrant angiogenesis, the tumor has an influx of leaky blood vessels that results in hemorrhaging, which gives the tumors a purplish or bruise-like appearance.

Based on clinical circumstances and epidemiology, KS is classified into four types: classical, endemic, iatrogenic, and AIDS-associated (reviewed in Mesri et al., 2010). Classical KS, which was what Moritz Kaposi first characterized, is an indolent tumor generally associated with elderly men in Eastern European and Mediterranean areas. Around the 1940s in sub-Saharan Africa, KS showed a chronic, nodular condition in HIV-negative individuals that predominantly affected the feet and legs and is associated with chronic lymphoedema; this type of KS is classified as endemic KS. With the advent of organ transplantation and immunosuppressive drugs in the 1970s, patients were developing KS, which was a significant cause of morbidity and mortality and is called iatrogenic KS. The onset of the AIDS epidemic brought on a highly aggressive form of KS in homosexual men, which is called AIDS-associated (or epidemic) KS.

In all clinical settings, the KS lesion begins as an early *patch* stage, in which the spindle cells are a minor component. As the spindle cells continue to proliferate the lesions develops into plaques (*plague* stage) and eventually into large nodules (*tumor* or *nodular* stage). Generally, these tumors are found on the skin, near the extremities. In more aggressive cases of KS, they can spread to the oral cavity and visceral organs. Aggressive forms of KS due to immunosuppression are often fatal (Ganem, 2007).

Unlike typical cancers, KS tumors are often polyclonal. While it is not completely clear, many histological and molecular features of the KS tumor suggest that the tumor cells are not truly transformed but rather promotes tumor cell growth that is driven through paracrine signaling and inflammation, which is dependent on the presence of the virus (Mesri et al., 2010). In support of this, transfection of KSHV bacterial artificial chromosome (BAC) into mouse primary cells of endothelial lineage generates tumors that are KS-like (Mutlu et al., 2007). These tumor cells were not transformed and the loss of KSHV blocked tumorigenicity. Therefore, a model of KSHV-induced tumorigenesis is through the elaboration of pro-inflammatory and neo-angiogenic cytokines such as IL-6, IL-8, and Cox2, VEGF, and GM-CSF (Mesri et al., 2010).

In a KS lesion, the majority of infected spindle cells are in the latent form. However, both latent and lytic replication are important for tumorigenesis and are likely driven by viral genes such as vGPCR, vCyclin, vFLIP, Kaposins A and B, vIL-6, K1, and K15 (Purushothaman, Uppal, Sarkar, & Verma, 2016).

1.3.6.2 Plasmablastic Multicentric Castleman's Disease (MCD)

Castleman's disease is a rare lymphoproliferative disorder first identified by Dr. Benjamin Castleman in 1956 (Castleman, Iverson, & Menendez, 1956). Later, different histological types where defined, namely plasmablastic/plasma cell, hyaline vascular, and mixed (reviewed in Chadburn et al., 2017). The plasmablastic type is characterized by a rapid proliferation of a pre-plasma cell, whereas the hyaline vascular type displays aberrant angiogenesis and abnormal germinal centers. In addition, two different forms of Castleman's disease were classified: unicentric and multicentric. KSHV is not associated with unicentric Castleman's disease, which involves a solitary lymph node and can usually be treated with local excision of the affected tissue. Multicentric Castleman's disease (MCD) is a more aggressive form affecting multiple lymph nodes and is associated with systemic symptoms such as fever, fatigue, weight loss, and splenomegaly. MCD is more prevalent in AIDS patients and virtually all of these cases are associated with the presence of KSHV. Conversely, KSHV is associated with approximately 40% of HIV-negative MCD cases (Chadburn et al., 2017). The prognosis for people with HIV-positive MCD has greatly improved since the introduction of rituximab, and one particular study had over an 80% 5-year relapse-free survival rate (Pria et al., 2017).

KSHV-infected B cells are characterized as monotypic IgM-λ-restricted plasmablasts in the intrafollicular area of the affected lymph node (M. Q. Du et al., 2001; Polizzotto et al., 2012; Totonchy et al., 2018). Plasmablasts are pre-plasma cells that have retained their ability to divide, whereas plasma cells are long-lived terminally-differentiated cells and thus have lost their proliferative capacity. KSHV-infected B cells in MCD demonstrate an early plasmablast phenotype since they express OCT-2, IRF4 (or MUM1), and Blimp-1, but lack PAX-5 and BCL-6. These cells also lack the plasma cell marker CD138 (Syndecan-1) and are usually EBV-negative (Chadburn et al., 2008).

The polyclonal nature and systemic symptoms of MCD implies that there is a robust production of signaling molecules such as growth factors and cytokines. In particular, there is a strong correlation between IL-6 and disease severity (Aoki, Tosato, Fonville, & Pittaluga, 2001). IL-10, and possibly IL-1β and TNFα, are also to linked disease severity in MCD (Polizzotto et al., 2013). While the default replication program for KSHV is latency, lytic genes are often detected in MCD tissue samples suggesting that lytic replication may be more prevalent in MCD or that there is "relaxed latency"

(Katano, Sato, Kurata, Mori, & Sata, 2000; Parravicini et al., 2000). vIL-6 is classically considered a lytic gene but its expression is prevalent in MCD tumors. Importantly, vIL-6 has been shown to play an important role in MCD pathogenesis. Unlike human IL-6 that requires both IL-6Rα and gp130 to signal, vIL-6 activity only requires binding to gp130 (Molden, Chang, You, Moore, & Goldsmith, 1997; Wan, Wang, & Nicholas, 1999). Human IL-6 and vIL-6 overexpression in mice phenocopied MCD pathogenesis and patients treated with monoclonal IL-6 antibody alleviated many of the symptoms associated with MCD (Matsuyama et al., 2007; Suthaus et al., 2012). Many other KSHV proteins can promote inflammation and the production of IL-6, including vFLIP, vGPCR, LANA, and Kaposin B, and thus also likely play an important role in MCD pathogenesis.

1.3.6.3 Primary Effusion Lymphoma (PEL)

Soon after the discovery of KSHV in KS samples, Cesarman *et al.* (1995) identified KSHV sequences in primary effusion lymphoma (PEL) samples, a rare non-Hodgkin's lymphoma most often associated with immunosuppressed HIV-positive individuals. Initially referred to as body cavity-based lymphomas, PEL is found in the pleural, pericardial, and abdominal cavities and lack a solid tumor mass. Extracavity (EC)-PEL is a subtype of PEL that presents as a solid tumor and lacks effusion (Chadburn et al., 2017). PEL is an aggressive malignancy that has a poor prognosis with a median survival rate of approximately 6 months (Boulanger et al., 2005). Currently, no specific treatment against PEL exists.

Unlike KS, PEL cells are monoclonal based on VDJ recombination (Ganem, 2007). PEL cells are also fully immortalized, allowing for easy growth in cell culture. Based on the B-cell markers, and somatic hypermutations of the Ig locus, PEL cells are likely derived from post-germinal center B cells, and like MCD have a plasmablast gene expression profile (Chadburn et al., 2017; Matolcsy, Nádor, Cesarman, & Knowles, 1998). PEL cells express similar B cell markers as in MCD, which include the presence of Blimp-1 and the lack of PAX-5 and BCL6. However, unlike plasmablasts from MCD, PEL cells are more differentiated and lack OCT-2 but express the plasma cell marker Syndecan-1. PEL cells also lack markers of an activated unfolded protein response (UPR), which is classically found in plasma cells (Jenner et al., 2003).

PEL cells also harbor more latent viral episomes than MCD cells; depending on the sample, > 50 viral episomes per PEL cell may be present, whereas MCD samples

typically contain less than 6 episomes per cell (Adang, Parsons, & Kedes, 2006; Asahi-Ozaki, Sato, Kanno, Sata, & Katano, 2006). PEL plasmablasts are often co-infected with EBV, especially in patients with late stages of HIV infection (Chadburn et al., 2017). Unlike in MCD, latency is more tightly maintained in PEL and thus the majority of infected cells carry the virus in the latent form (Ganem, 2007).

Several latency genes are important for promoting PEL proliferation and survival. The latent protein vFLIP induces NFκB and inhibition of vFLIP or NFκB induces apoptosis in PEL cells indicating the importance of this latent gene product (Guasparri et al., 2004). vIRF3 (LANA-2) is also expressed during latency in PEL and silencing its expression also promoted apoptosis (Wies et al., 2009). vIL-6 can be present in low amounts during latency but is upregulated in lytic and is likely important in disease progression (Moore, Boshoff, Weiss, & Chang, 1996).

Many PEL cell lines (both EBV-negative and -positive) have been recovered and because of their mainly latent phenotype, have been critical for understanding the molecular events of KSHV replication. Furthermore, unlike explanted KSHV-infected spindle cells and other *de novo* infected tumor cell lines, which rapidly lose the viral episome during cell passaging, KSHV is stably maintained in PEL cells (Grundhoff & Ganem, 2004), further validating their utility for study.

1.4 Rationale and Overview

KSHV is a large enveloped virus that encodes multiple ER-translated proteins, including glycoproteins and signaling molecules, and induces the secretion of pro-inflammatory cytokines and growth factors. Protein folding in the ER is a highly regulated process and this burst in protein synthesis could saturate the ER folding machinery leading to protein misfolding. A disruption in protein homeostasis could be detrimental to the cell, and ultimately the organism. Eukaryotic cells have evolved an intricate ER-to-nucleus signaling response called the UPR in order to protect the cell from potentially lethal forms of ER stress (Walter & Ron, 2011) (Fig 1.1). Through IRE1, PERK, and ATF6, the UPR reprograms gene expression in an attempt to restore protein homeostasis; however, in response to irremediable stress the UPR can induce apoptosis.

The UPR attenuates global translation through PERK-dependent eIF2α phosphorylation, which could theoretically inhibit viral protein synthesis, while

expansion of the ER and increase in protein folding machinery through ATF6 and XBP1s may promote virus production. Therefore, it is likely that activation of the UPR can have both pro-and anti-viral consequences.

Multiple viruses have been shown to co-opt different signaling arms of the UPR during infection, although in most cases, the reason for this modulation is unclear. ER stress can activate KSHV lytic reactivation through transactivation of RTA by IRE1-dependent activation of XBP1s (Wilson et al., 2007; F. Yu et al., 2007). However, UPR activation during KSHV lytic replication is not known.

In this thesis, I examine the activation status and importance of each of the branches of the UPR during lytic replication. I show that IRE1, PERK, and ATF6 are activated during lytic replication but their downstream transcription factors are stymied. Interestingly, even though the transcriptional responses are blocked, activation of the sensors are likely important for robust virus production. Furthermore, inhibition of the transcription factor XBP1s may be important for robust KSHV virion production, since I demonstrate that ectopic expression can potently inhibit production of KSHV virions. Thus, the virus is likely altering the UPR to promote robust lytic replication instead of resolving ER stress. To identify potential KSHV proteins that modulate the UPR, I conducted a lentiviral ORF screen using a dual fluorescent UPR reporter cell line. The screen revealed multiple viral proteins that may be important in controlling UPR signaling during infection.

There is crosstalk between the three branches of the UPR to ensure a coordinated response to ER stress, and I provide further evidence that the ISR can promote activation of the IRE1-XBP1 pathway. This coordination between the different UPR arms for maximum signaling may contribute to the reduction in UPR transcriptional responses observed during lytic replication. The findings in this thesis ultimately demonstrate that KSHV usurps the UPR to promote virus replication. This thesis will hopefully promote further investigation into the mechanistic details of (1) how the UPR sensors are activated while the downstream transcriptional responses are stymied; and (2) how KSHV re-purposes the UPR sensors to support virus replication.

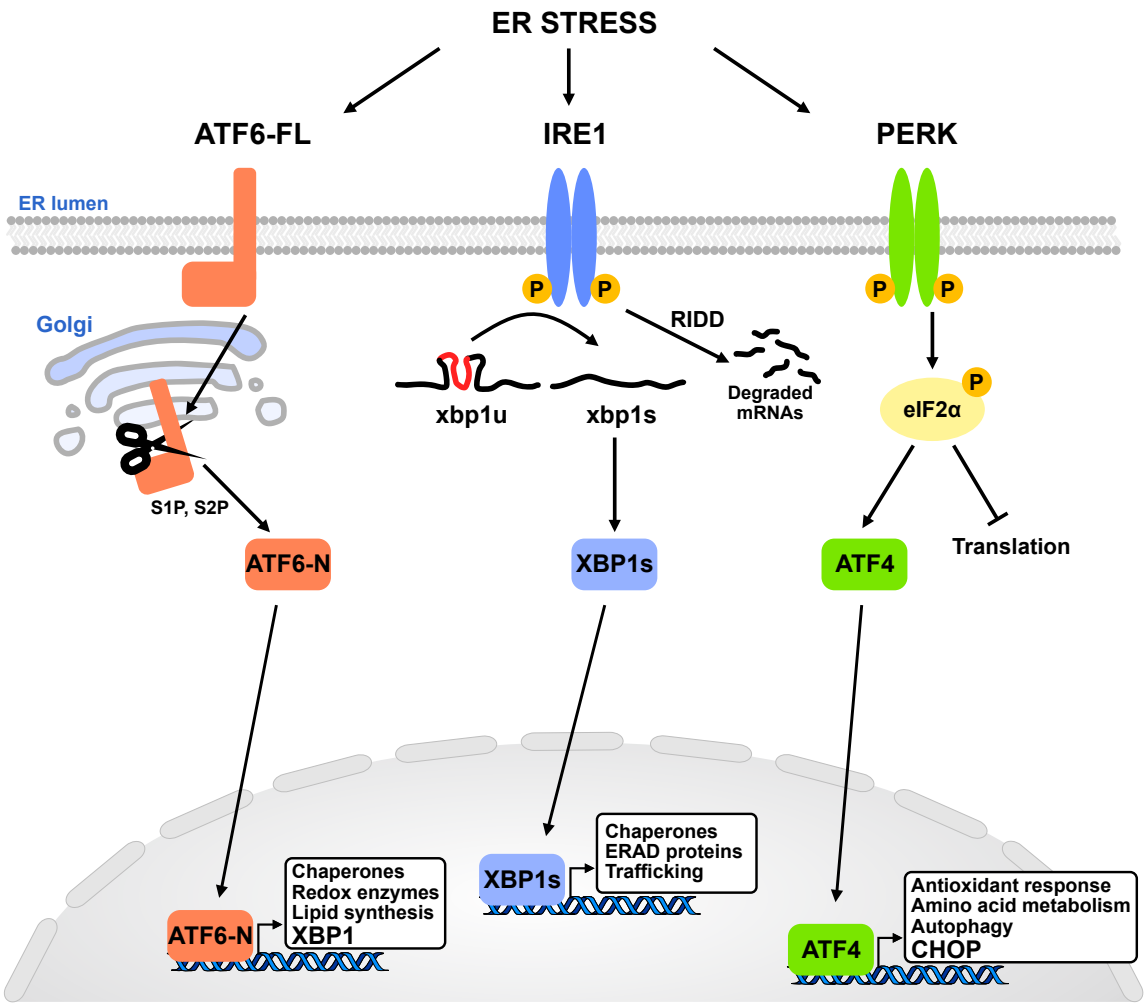

Fig 1.1 ER stress activates the unfolded protein response
The accumulation of misfolded proteins in the ER triggers ER stress, which activates the unfolded protein response (UPR). The UPR is carried out by ATF6, IRE1, and PERK, which induce a transcriptional response through the activation of the transcription factors ATF6-N, XBP1s, and ATF4, respectively, to upregulate genes to restore protein folding. In response to ER stress, ATF6 translocates to the Golgi and is proteolytically cleaved by S1P and S2P releasing the N-terminal cytoplasmic transcription factor ATF6-N. IRE1 is a kinase and endoribonuclease that splices out a 26-nucleotide intron for XBP1 mRNA, which causes a translational frameshift to generate the transcription factor XBP1s. PERK phosphorylates eIF2α, which attenuates bulk translation to reduce the protein load in the ER. Increased eIF2α phosphorylation also causes the selective translation of the transcription factor ATF4.

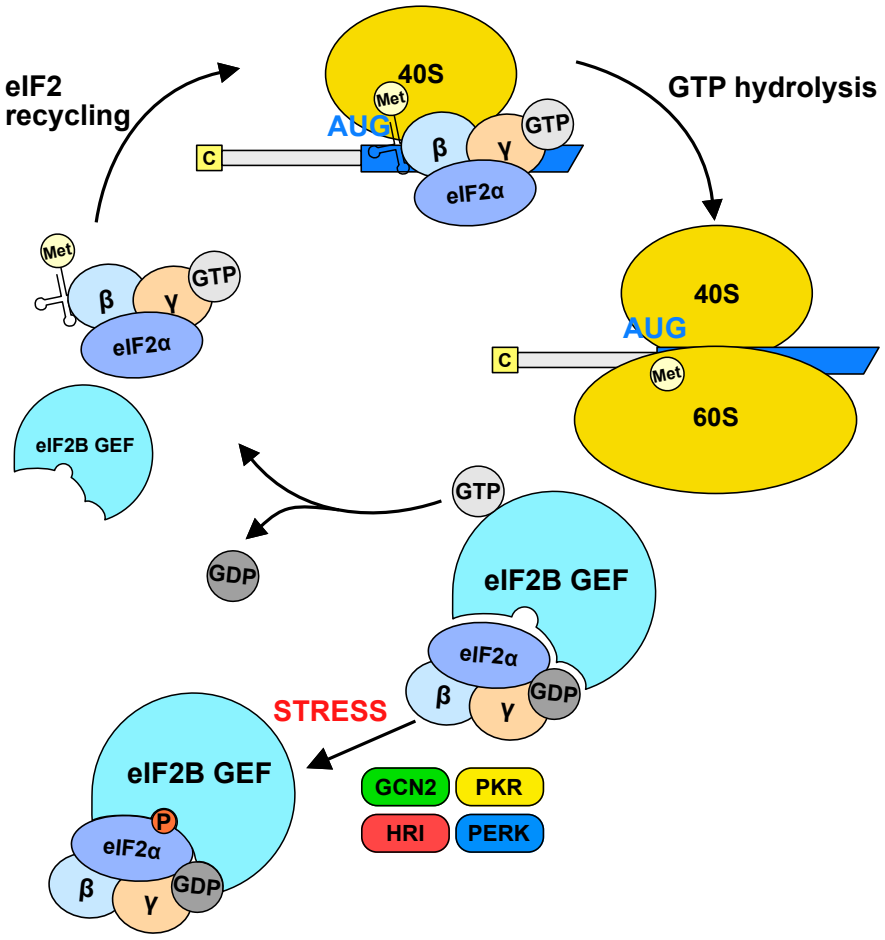

Fig 1.2 Translation initiation requires recycling of the eIF2/GTP/Met-tRNAi^{Met} ternary complex

The translation initiation factor eIF2 is a heterotrimer of the α, β, and γ subunit and binds Met-tRNAi^{Met} when bound to GTP generating the ternary complex (TC). The TC binds the 40S ribosomal subunit and other translation initiation factors (not shown) to form the 43S pre-initiation complex (PIC). The 43S PIC scans the 5'UTR of the mRNA until it recognizes the AUG start codon. GTP hydrolysis releases eIF2-GDP and allows the 60S ribosomal subunit to bind, which is followed by translation elongation. In order for eIF2 to participate in another round of translation initiation, the eIF2B guanine nucleotide exchange factor (GEF) swaps out GDP for GTP. In response to different types of stress, eIF2α kinases (GCN2, PKR, HRI, or PERK) phosphorylate the α subunit of eIF2, which inhibits eIF2B through high affinity binding. Inhibition of eIF2B decreases the pool of active TCs, thereby attenuating bulk translation.

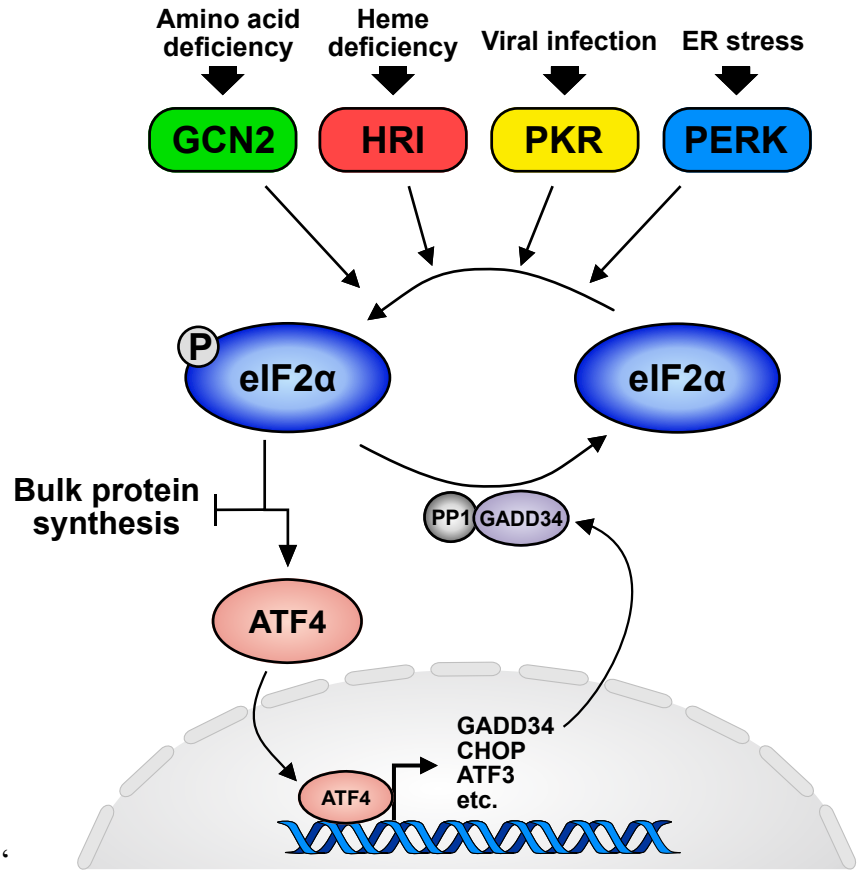

Fig 1.3 The integrated stress response
Different types of stimuli or stresses such as amino acid deficiency, heme deficiency, viral infection that generates double stranded RNA, and ER stress activate different eIF2α kinases (GCN2, HRI, PKR, or PERK) in mammalian cells depending on the type of stress. The activated eIF2α kinase phosphorylates the α subunit of the heterotrimeric translation initiation factor eIF2, which results in attenuation of bulk protein synthesis. eIF2α phosphorylation also results in the selective translation of stress-responsive genes due to the presence of upstream ORFs in the 5'UTR. Central to these genes is the transcription factor ATF4, which upregulates a set of genes in attempt to resolve the stress. ATF4 also upregulates the transcription factors ATF3 and CHOP. CHOP can upregulate the co-factor GADD34, which facilitates eIF2α dephosphorylation by recruiting protein phosphatase 1 (PP1). Restoration of translation by eIF2α dephosphorylation likely plays a role in determining cell fate following stress exposure.

CHAPTER 2 MATERIALS AND METHODS

2.1 Cell Culture and Chemicals

293A (ThermoFisher), HEK293T (ATCC), A549 (ATCC), HeLa Tet-Off (Clontech), HeLa eIF2α Ser51Ala CRISPR knock-in mutant cells and their matched HeLa wild type control (a kind gift from Jim Smiley; unpublished CRISPR cell line), and iSLK.219 cells (a kind gift from Don Ganem) (Myoung & Ganem, 2011b) were cultured in DMEM supplemented with 10% heat-inactivated fetal bovine serum (FBS), 100 Units/mL penicillin, 100 μg/mL streptomycin, and 2mM L-Glutamine (media and supplementation from ThermoFisher). iSLK.219 cells were also passaged in the presence of 10 μg/mL of puromycin (ThermoFisher) to maintain the rKSHV.219 episomal DNA. CHO-7.1 UPR reporter cells (a kind gift from David Ron; unpublished cell line that is a derivative of CHO-S21 cell line) (Sekine et al., 2015) were cultured in Ham's F12 (Sigma and ThermoFisher) media supplemented with 10% heat-inactivated FetalClone II serum (Fisher Scientific), and the same concentrations of penicillin, streptomycin, and L-Glutamine used in DMEM. Wild type BCBL1 cells (a kind gift from Don Ganem) and TREx BCBL1-RTA cells (a kind gift from Jae Jung) (H. Nakamura et al., 2003) were cultured in RPMI-1640 supplemented with 10% heat-inactivated FBS, 500 μM β-mercaptoethanol and the same concentrations of penicillin, streptomycin, and L-Glutamine as the adherent cell lines. All cells were maintained at 37˚C in 5% atmospheric CO_2.

To induce lytic replication via expression of the RTA transgene in TREx BCBL1-RTA and iSLK.219 cells, 1 μg/mL of doxycycline (dox; Sigma) was added to the cells. iSLK.219 cells were seeded at $2x10^5$ cells/well of a 6-well plate one day prior to lytic induction and TREx BCBL1-RTA cells were seeded at a concentration of $2.5x10^5$ cells/mL immediately prior to lytic induction. To induce lytic replication in wild type BCBL1 cells, 1 mM Sodium Butyrate (NaB; Sigma) and 20 ng/mL 12-O-tetradecanoyl-phorbol 13-acetate (TPA; Sigma) were added to $2.5x10^5$ cells/mL immediately prior to seeding.

4μ8c (Axon Medchem and Sigma), GSK2606414 (PERKi; Tocris), ISRIB (Sigma), thapsigargin (Tg; Sigma), tunicamycin (Sigma), etoposide (Sigma), and Z-VAD-DMK (Caspase inhibitor VI; Calbiochem) were dissolved in DMSO (Sigma) and L-histidinol (HisD; Sigma), and sodium arsenite (Sigma) were dissolved in nuclease-free

water (ThermoFisher) to stock concentrations and diluted to the indicated concentrations in cell media.

2.2 Poly(I:C) (Polyinosinic-Polycytidylic Acid) dsRNA Transfection

HeLa cells were seeded in a 6-well plate in antibiotic-free, full serum media to approximately 50 % confluency the following day and transfected with increasing concentrations of poly(I:C) (Invivogen) combined with cloning vector pUC19 for a total of 500 ng of nucleic acid per well using 1.5 μL FuGENE HD transfection reagent (Promega) according to manufacturer's instructions. The control sample was transfected with 500 ng of pUC19. Eight hours post-poly(I:C) transfection, HeLa cells were lysed for immunoblot analysis.

2.3 Plasmid Generation

To construct the plasmids pLJM1 B* Puro and pLJM1 B* BSD (derivatives of pLJM1 plasmid that was originally generated by the Sabatini Lab [MIT]), the genes encoding puromycin N-acetyltransferase and blasticidin S deaminase were amplified from pBMN-IRES-Puro and pBMN-IRES-Blast, respectively (previously generated in the McCormick Lab by switching GFP with PuroR or BlastR from pBMN-I-GFP that was a kind gift from the Nolan Lab [Stanford]), with forward and reverse primers containing BglII and KpnI RE sites. The antibiotic selection cassettes were ligated into pLJM1.D (previously generated in the McCormick Lab by modifying the MCS [multiple cloning site] of the original pLJM1 plasmid), deleting the BamHI RE site. A new MCS was generated by annealing overlapping oligos containing NheI and MfeI forward and reverse RE sites and inserted into the plasmid digested with NheI and EcoRI (MfeI and EcoRI have compatible sticky ends) to replace the existing MCS with common unique RE sites in the following order: NheI, AgeI, BamHI, EcoRI, PstI, XbaI, MluI, SalI, EcoRV. See Appendix D for a plasmid map of pLJM1 B* Puro and the MCS. 1x TetO (tetracycline operator) and 7x TetO promoters were generated by annealing overlapping oligos containing one and seven copies of the tetracycline operator (5'-TCCCTATCAGTGATAGAGA-3'), respectively, and a minimal CMV promoter and using PCR extension to amplify a blunt oligo containing NdeI and NheI RE sites. The

amplicon was digested with NdeI and NheI and pasted into the pLJM1 B* BSD replacing the CMV promoter to generate pLJM1 B* BSD 1x TetO and pLJM1 B* BSD 7x TetO.

To generate pLJM1 B* Puro HA-ATF6 WT, HA-ATF6 (1-373), and HA-ATF6 (1-373)m1, HA-ATF6 was PCR amplified from pCGN-ATF6, pCGN-ATF6 (1-373), and pCGN-ATF6 (1-373)m1, respectively (gifts from Ron Prywes, Addgene plasmids # 11974, 27173, and 27174), digested with NheI and AgeI, and ligated into pLJM1 B* Puro.

pCMV2B-XBP1s was generated by PCR amplifying XBP1 from cDNA reverse transcribed from total RNA isolated from Tg-treated TREx BCBL1-RTA cells. After PCR, cDNA was digested with PstI-HF (cleaves unspliced XBP1 cDNA only) to enrich for the spliced isoform of XBP1 (XBP1s). XBP1s cDNA was restriction digested with BamHI and XhoI and ligated into pCMV2B so that XBP1s is in-frame of the N-terminal FLAG-tag. pCMV2B-XBP1u and pCMV2B-XBP1*uG519A*, which were used as templates for cloning into lentivirus, were also generated similarly to pCMV2B-XBP1s, however the TREx BCBL1-RTA cells were left untreated and cDNA was not incubated with PstI-HF. The unspliceable XBP1 point mutant vector pCMV2B-XBP1uG519A, which has a guanine to adenine mutation corresponding to nucleotide position 519 of the XBP1 ORF, was generated by site-directed mutagenesis using inverse PCR. pLJM1 BSD, 1x TetO, and/or 7x TetO myc-XBP1u, myc-XBP1s, and myc-XBP1u*G519A* were generated by including myc-tag nucleotide sequence (5'-GAACAAAAACTCATCTCAGAAGAGGATCTG-3') in the forward primer and amplifying the XBP1 isoforms from the pCMV2B plasmids. Cloned myc-XBP1 isoforms were subsequently digested with BamHI and SalI and ligated into their corresponding lentiviral plasmids. FLAG-RTA was restriction digested from pcDNA3-FLAG-RTA (previously generated in the McCormick Lab) with EcoRI and XhoI and ligated into pLJM1 B* BSD and 7x TO (via compatible sticky ends between XhoI and SalI).

2.4 Lentivirus Generation and Transduction

HEK293T cells were seeded on 100mm plates to establish 60-70% cell density the following day. Cells were transfected with polyethylenimine (PEI; Sigma) diluted in Opti-MEM (ThermoFisher) and containing the following plasmids for lentiviral generation: lentiviral vector plasmid (pLJM1 B* for gene expression or pLKO.1 for

shRNA silencing), pMD2.G, and psPAX2. pMD2.G and psPAX2 are gifts from Didier Trono (Addgene plasmids # 12259 and # 12260). 48 h post-transfection, lentivirus containing supernatants were passed through a 0.45μM PES (polyethersulfone) filter and frozen at -80˚C.

For transducing iSLK.219, iSLK.219 cells were seeded at $5x10^4$ cells/well of a 6-well plate and the following day were resuspended in media containing 4 μg/mL polybrene (Sigma). Lentivirus was serially diluted dropwise onto cells and incubated at 37˚C for 24 h. Following infection, the media was refreshed containing 10 μg/mL blasticidin (ThermoFisher). For transducing TREx BCBL1-RTA cells, cells were seeded at a concentration of $2.5x10^5$ cells/mL in media containing the same concentration of polybrene and lentivirus was serially diluted onto cells. 24 h post-infection, the media was replaced with media containing 1 μg/mL puromycin. The first lentivirus dilution that resulted in minimal cell death following antibiotic selection was used for subsequent experiments.

To transduce cells with pLJM1 B* BSD CMV-driven myc-XBP1s or FLAG-RTA, iSLK.219 cells were seeded at $5x10^4$ cells/well of a 6 well plate and transduced the following day with increasing concentrations of lentiviral vectors in the presence of polybrene. The growth media was changed 24 h post-transduction and the transduced cells incubated for another 5 d prior to harvesting. Conversely, TREx BCBL1-RTA cells were seeded at $2.5x10^5$ cells/mL in polybrene and transduced with increasing concentrations of CMV-driven myc-XBP1s or FLAG-RTA for 3 d prior to analysis. 24 h post-transduction cells were pelleted by centrifugation and cells were resuspended in the same original volume of fresh growth media.

To transduce 293A or HeLa cells with pLJM1 B* Puro KSHV ORFs, $5x10^4$ cells/well of 6-well plate were seeded and either (1) transduced the following day with serial diluted lentivirus and 24 h (for 293A) or 48 h (for HeLa) post-transduction selected with puromycin to determine the most dilute lentivirus concentration that resulted in minimal cell death for subsequent experiments or (2) use increasing concentrations of lentivirus that results in an MOI of greater than one in order to increase expression of the vector.

2.5 Luciferase Plasmid Generation and Dual Luciferase Assay

4x pORF50$_{XRE}$-FLuc plasmid was generated by annealing oligos that have the XBP1 response element sequence 5'-ATGACACGTCCC-3' (ACGT core underlined) found in ORF50 promoter (Dalton-Griffin et al., 2009), and is repeated 4 times flanked by 10bp repeats. The oligo was digested with KpnI and XhoI and ligated into the firefly luciferase plasmid pGL4.26[*luc2*/minP/Hygro] (Promega). HeLa Tet-Off cells were seeded at $3.2x10^4$ cells/well of a 12-well plate and transfected the following day with FuGENE HD transfection reagent and the following plasmids per well: either 400 ng pCR3.1 vector (Invitrogen) or pCMV2B-XBP1s, 80ng 4x pORF50XRE-FLuc, and 20ng *Renilla* luciferase plasmid pRL-TK for normalization. 24 h post-transfection, cells transfected with pCR3.1 were untreated or treated with 150 nM Tg for 16h. Following treatment, the Glomax 20/20 Luminometer (Promega) was used to measure firefly and *Renilla* luciferase activity with the Dual-Luciferase Reporter™ Assay System (Promega), according to the manufacturer's instructions. Briefly, cells were washed once with PBS and lysed in 100 µL 1x passive lysis buffer. 5 µL of luciferase-containing lysate was combined with 25 µL Luciferase Assay Reagent II to measure firefly luciferase activity, followed by the addition of 25 µL Stop & Glo® Reagent to simultaneously quench the firefly luciferase reaction and measure *Renilla* luciferase activity. Firefly luciferase relative lights units (RLUs) were normalized to *Renilla* luciferase RLUs and expressed as fold change in ORF50$_{XRE}$ promoter activity relative to untreated vector control.

2.6 shRNA Lentivirus Cloning and Knockdown

Third generation shRNA lentiviral vectors pLKO.1-TRC control plasmid (puromycin resistant) was a gift from David Root (Addgene plasmid # 10879) and pLKO.1-blast (blasticidin resistant) was a gift from Keith Mostov (Addgene plasmid #26655). These plasmids express shRNAs under the control of human U6 promoter. The RNAi Consortium (TRC; Broad Institute) Library Database (https://portals.broadinstitute.org/gpp/public/) was used to design oligos for generating shRNAs against the UPR sensors based on the general format for forward (5'-CCGGNNNNNNNNNNNNNNNNNNNCTCGAGATTTAACCTGAGAGACTCTGTTTTTTG) and reverse (5'-AATTCAAAAAACAGAGTCTCTCAGGTTAAATCTCGAGNNNNNNNNNNNNNNNNNNN-3') oligos, where the unique targeting sequence for each construct

corresponds to the series of "N". A non-targeting control plasmid pLKO.1-blast-scramble (or NS), which does not match any mammalian sequence was a gift from Keith Mostov (Addgene plasmid #26701). pLKO.1-Puro-NS was created by swapping the puromycin resistance cassette from pLKO.1-TRC using restriction enzymes BamHI and KpnI. The shRNA oligos were annealed creating sticky ends that were ligated into AgeI/EcoRI-digested pLKO.1-TRC or pLKO.1-Blast based on the cloning strategy on the Addgene website (http://www.addgene.org/tools/protocols/plko/). See Table 2.1 for the list of shRNA lentiviral vectors and their corresponding targeting sequences. Lentivirus generation and transduction of cells with shRNA lentiviral vectors was performed as previously described.

2.7 Fluorescent Imaging

For Fig 4-4, iSLK.219 cells were seeded at $2x10^5$ cells/well of a 6-well plate and 48 h post-addition of dox, brightfield and fluorescent images were captured with an Olympus CKX41 microscope fitted with a QImaging QICAM Fast 1394 digital camera and Lumencor Mira light engine using the 10x objective. For Fig 4-5, iSLK.219 cells were seeded at $5x10^4$ cells/well of a 6-well plate and transduced with the indicated lentiviral vectors. Fluorescent images were captured with an EVOS FL Cell Imaging System with 10x objective (ThermoFisher) following 5 d post-transduction or 48 h post-dox.

2.8 Immunoblotting

Cells were washed once with ice-cold PBS and lysed in 2x Laemmli Buffer (120mM Tris-HCl pH 6.8, 20% glycerol, 4% SDS). Lysates were passed through a 21-gauge needle 5-7 times to minimize viscosity and protein concentration was quantified with the DC protein assay (Bio-Rad). 150 mM DTT (dithiothreitol; Sigma) and 2.5% bromophenol blue (Bio-Rad) were added to samples, boiled, and 5-20 μg of protein per sample were loaded on 6-15% polyacrylamide gels and resolved by SDS-PAGE. Proteins were transferred to PVDF membranes using the Trans-Blot Turbo Transfer System (Bio-Rad) and blocked in 5% skim milk diluted in Tris-buffered-saline (TBS) supplemented with 0.1% Tween 20 (Fisher Bio) (TBS-T) for 1 h at room temperature followed by overnight incubation at 4˚C with primary antibody diluted in 5% bovine serum albumin (BSA) in TBS-T, except total eIF2α antibody and β-actin HRP-conjugate antibody were

incubated for 1 h at room temperature and β-actin HRP-conjugate was diluted in 5% skim milk. Following washing of primary antibody with TBS-T, membranes were incubated with IgG HRP-linked antibodies diluted in 5% skim milk for 1 h at room temperature (except membranes probed with β-actin HRP-conjugate antibody), washed again with TBS-T, and exposed to ECL-2 western blotting substrate (ThermoFisher) and imaged on a Carestream Image Station 4000mm Pro (Carestream) using the chemifluorescence setting (excitation/emission of 430/510). Table 2.2 lists all the antibodies used in this thesis.

2.9 XBP1 RT-PCR Splicing Assay

RNA was isolated from TREx BCBL1-RTA cells with the RNeasy Plus Kit (Qiagen) and 500 ng total RNA was reverse transcribed with qScript cDNA SuperMix (Quanta) according to manufacturers' protocols. Based on the Ron Lab protocol (http://ron.cimr.cam.ac.uk/protocols/XBP-1.splicing.06.03.15.pdf) and minor modifications, a 473 bp amplicon overlapping the IRE1 splice site was generated by PCR from 10% of cDNA mixture with XBP1 forward (5'-AAACAGAGTAGCAGCTCAGACTGC-3') and reverse (5'-TCCTTCTGGGTAGACCTCTGGGAG-3') primers, and 30 amplification cycles. For amplifying XBP1 from CHO cells the following forward and reverse XBP1 primers were used to generate a 480 bp PCR product: 5'-AAACAGAGTAGCAGCGCAGACTGC-3' and 5'-AGGTCCTGGGTAGACCTCTGGGAG-3'. The amplified PCR product was digested overnight with 40 units of High Fidelity PstI (PstI-HF®; New England Biolabs) to cleave unspliced XBP1 cDNA. The PCR products were resolved on a 2.5% agarose gel made with 1x TAE (Tris-acetate-EDTA) buffer and stained with SYBR Safe (ThermoFisher) and visualized on a ChemiDoc Imaging Station (Bio-Rad). Percent XBP1 mRNA splicing was calculated by densitometry analysis with Image Lab software ver. 6.0.0 (Bio-Rad) and calculated using the following formula:

$$\%\ \mathbf{XBP1\ mRNA\ splicing} = \frac{\mathbf{0.5{*}xbp1hybrid{+}xbp1s}}{\mathbf{xbp1hybrid{+}xbp1s{+}xbp1u1{+}xbp1u2}} * \mathbf{100},$$

in which "xbp1hybrid" corresponds to XBP1u-XBP1s hybrid cDNA, and "xbp1u1" and "xbp1u2" correspond to the larger and shorter fragments of PstI-cleaved XBP1u cDNA.

2.10 Quantitative Reverse-Transcription PCR (RT-qPCR)

RNA was isolated from TREx BCBL1-RTA cells with the RNeasy Plus Kit (Qiagen) and 500 ng total RNA was reverse transcribed with qScript cDNA SuperMix (Quanta) according to manufacturers' protocols. cDNA was diluted 1:10 or 1:100 depending on the primer sets used. CFX96 Touch Real-Time PCR Detection System (Bio-Rad) and GoTaq qPCR MasterMix (Promega) was used to perform Real-Time PCR. Changes in mRNA levels were calculated by the ΔΔCt method and normalized using 18S rRNA or β-actin as a reference gene. 2 or 3 technical replicates of each sample were measured. Table 2.3 lists the primer sets used in this thesis and the cellular gene targets were all designed based off of the human gene.

2.11 Viral Genome Amplification

DNA was harvested from iSLK.219 cells with DNeasy Blood & Tissue Kit (Qiagen) according to manufacturer's protocol. RT-qPCR (or qPCR) was carried out as described previously with primers specific to KSHV ORF26 and β-actin (as listed previously). Changes in KSHV genome copy number was calculated by the ΔΔCt method and normalized to β-actin.

2.12 DNAse I-Protected Virus Titer

Virus-containing cell supernatants were processed by first pelleting floating cells and debris and then 180 μL cleared supernatant was treated with 20 μL of 3 mg/mL DNase I (Sigma) for 30 minutes at 37˚C. Viral genomic DNA was purified from the supernatant with DNeasy Blood & Tissue Kit (Qiagen) according to the manufacturer's protocol with the following modifications: 10 μg of salmon sperm DNA (Invitrogen) and 1 ng of luciferase plasmid pGL4.26[*luc2*/minP/Hygro] (Promega) were added to the lysis buffer. qPCR was performed as described previously with primers specific to KSHV ORF26 (as listed previously) and *luc2* (Fwd: 5'-TTCGGCAACCAGATCATCCC-3'; Rev: 5'-TGCGCAAGAATAGCTCCTCC-3'). Changes in virus titer was calculated by the ΔΔCt method and normalized to *luc2* DNA.

2.13 rKSHV.219 Infection and Quantification of Virus Titer

Virus-containing supernatant was harvested from iSLK.219 cells at the indicated times by pelleting cellular debris at 3300 x g for 5 minutes and then stored at -80˚C until ready to titer the virus. $1x10^5$ 293A cells/well were seeded in 12-well plates to obtain a confluent monolayer two days later. The thawed viral inoculum was briefly vortexed and centrifuged again at 3300 x g for 5 minutes. Two-fold serial dilutions of 1 mL viral supernatants were applied to the monolayer containing 4 μg/mL polybrene and 25 mM HEPES (ThermoFisher) and centrifuged at 800 x g for 2 h at 30˚C. The total cell count per well was also determined from an uninfected well. Fresh media was applied immediately after spinoculation. 20-24 h post-infection, two different dilutions that resulted in less than 30% GFP-positive cells (the linear range for infection [data not shown]) were trypsinized, washed once with PBS and fixed with 1% paraformaldehyde in PBS. GFP-positivity was measured with BD FACSCalibur™ cell analyzer and CellQuest Pro software or BD FACSCanto ™ cell analyzer and BD FACSDiva software (Beckton Dickinson) and by gating on FSC/SSC and counting 10000-15000 "live" events. Gating and % GFP positive events were determined with FCS Express 6 Flow Cytometry Software (ver.6.0; De Novo). Virus titer was calculated as IU/mL with the following formula:

$$\textbf{Virus titre (IU/mL)} = \%\ \textbf{GFP positive events} * \textbf{dilution factor} * \textbf{cell count} * \textbf{100}$$

The two different virus dilutions measured were averaged for the final titer value.

2.14 KSHV ORF Lentiviral Vector Library Generation and Flow Cytometry Analysis with the UPR Reporter Cell Line

The KSHV ORFs used to generate the lentivirus ORF library were obtained from multiple sources and multiple members of the McCormick Lab were involved in the cloning process, with myself conducting the majority of the cloning. The ORFs were restriction digested from a variety of sources (KSHV ORFs in a yeast expression plasmid, PCR of cDNA from lytic TREx BCBL-RTA cells, or PCR of BAC16 genomic DNA) and ligated into the MCS of pLJM1 B* Puro. Successful cloning of KSHV ORFs into the lentiviral vector were confirmed by Sanger sequencing using CMV forward sequencing primer.

CHO-7.1 cells containing CHOP::GFP and XBP1-mCherry reporter plasmids were previously generated in the laboratory of David Ron (University of Cambridge) and generously donated. The CHO-7.1 reporter cell line is akin to a UPR reporter CHO cell line previously published by the Ron Lab (Sekine et al., 2015), except that mCherry replaced the mTurquoise and the puromycin resistance marker was removed through recombination. The CHOP::GFP plasmid contains an 8.5kb fragment of the murine CHOP gene fragment that terminates 9 nucleotides upstream of the CHOP coding sequence and is fused to GFP (Novoa et al., 2001). When the ISR is activated, including activation of PERK following ER stress, GFP will be expressed. The XBP1-mCherry reporter plasmid contains mCherry fused out of frame and downstream of a 252-nucleotide fragment of human XBP1 that contains the IRE1 splice site but is missing a portion of the N- terminal DNA binding domain and the C-terminal transactivation domain. Expression of the reporter is driven by a chicken actin promoter. Cells exposed to ER stress will express mCherry due to the excision of the intron and subsequent shift in reading frame. Stable integration of the plasmids was obtained through antibiotic selection and serial passaging. FACS (flow cytometry-associated cell sorting) was used to isolate CHO-7.1 and was selected for future experimentation based on low basal fluorescence and high inducibility upon exposure to pharmacological UPR activators.

I conducted the majority of the KSHV ORF lentivirus generation, transduction of the UPR reporter cell line and screening of ORFs using flow cytometry in the laboratory of David Ron at the University of Cambridge during an eight-week research study. In small batches of 8 to 12 KSHV ORF lentiviral vectors plus an empty vector control for normalization, lentiviruses were generated as previously described except that (1) HEK293T cells were seeded in 6-well plates, and (2) after filtering through a 0.45 μM SCFA (surfactant-free cellulose acetate) filter, the lentivirus stocks were used immediately or stored at 4˚C for up to one week. $7.2x10^3$ CHO-7.1 cells were seeded per well of a 12-well plate. The following day, the cells were transduced with 6, 2-fold dilutions (range of 1:2 to 1:64) of lentiviral vectors (two KSHV ORFs per 12-well plate) plus 10 μg/mL polybrene. 48 h post-transduction, cells were selected for with 6 μg/mL puromycin and the least concentrated lentivirus dilution that resulted in minimal cell death was either further passaged or seeded in 12-well plate at $3.2x10^4$ cells/well, which yields an optimal cell density of approximately 20-30% confluency the following day to

ensure minimal basal fluorescence during flow cytometry analysis. Cells are left untreated or treated for approximately 16 to 24 h with 500 nM Tg and immediately before analysis were washed once with PBS and then detached from the well with gentle pipetting up and down with 1mM EDTA diluted in PBS and transferred to 5 mL polypropylene tubes on ice.

CHOP:GFP and XBP1-mCherry fluorescence signals were measured on approximately 10,000 cells/sample (expression of some viral ORFs caused cell toxicity and therefore less events were measured) using a BD LSRFortessa cell analyzer and BD FACSDiva software (Beckton Dickinson Biosciences) with a blue laser (488 nM excitation; 530/30 nM filter) to measure GFP and a yellow-green laser (561 nM excitation; 610/20 nM filter) to measure mCherry. FlowJo (FlowJo, LLC) and FCS Express 6 software were used for data analysis and visualization. For each batch of KSHV ORFs, the median fluorescence intensity (MFI) of GFP::CHOP and mCherry-XBP1 was determined for each ORF and normalized to the empty vector control pertaining to that batch. CHO-7.1 cells expressing KSHV ORFs that showed a discernible increase or decrease in either GFP or mCherry fluorescence compared to empty vector and viral ORFs that had no effect were re-seeded and re-screened by flow cytometry to confirm activation or inhibition of the UPR reporters.

2.15 Graphing and Statistical Analysis

Prism7 (GraphPad) was used for generating graphs and performing statistical analysis. Unpaired Student's t-tests were used to determine significance between two groups. One-way or two-way ANOVA was used to compare multiple samples or between grouped samples respectively, and an appropriate *post hoc* test was done to determine differences between groups. p-values <0.05 were considered significant and denoted as the following: <0.05 (*), <0.01 (**), <0.001 (***), <0.0001 (****)

Table 2.1 pLKO.1-Blast and -Puro shRNA lentiviral vectors

Vector name	Target gene	TRC Clone ID	Targeting Sequence
NS	Non-targeting	N/A	N/A
shATF6α-1	ATF6α	TRCN0000416318	ACAGAGTCTCTCAGGTTAAAT
shIRE1α-2	IRE1α	TRCN0000356305	TCAACGCTGGATGGAAGTTTG
shIRE1α-3	IRE1α	TRCN0000235529	AGAGGAGGGAATCGTACATTT
PERK-3	PERK	TRCN0000262374	TTTGTCCCTGGCGGGTAAATT

Table 2.2 Antibodies and dilutions used for immunoblots

Target	Company	Catalog #	Dilution
ATF4	Santa Cruz	sc-200	1:1000
ATF6α	Abcam	ab122897	1:1000
BiP	Cell Signaling	#3177	1:1000
CHOP	Cell Signaling	#2895	1:1000
eIF2α	Cell Signaling	#5324	1:1000
FLAG-tag (DYDDDDK-tag)	Cell Signaling	#8146	1:1000
HA-tag	Cell Signaling	#2367	1:2000
IRE1α	Cell Signaling	#3294	1:1000
Kaposin B & C	A kind gift from Don Ganem	N/A	1:4000
Myc-tag	Cell Signaling	#2278	1:2000
ORF45	Thermo-Fisher	MA5-14769	1:2000
ORF65	a kind gift from Shou-Jiang Gao	N/A	1:500
p-eIF2α (Ser51)	Abcam	ab32157	1:2000
p-eIF4B (Ser422)	Cell Signaling	#3591	1:1000
PERK	Cell Signaling	#5683	1:1000
RTA	a kind gift from David Lukac	N/A	1:2000
XBP1	Cell Signaling	#12782	1:2000
β-actin HRP-linked	Cell Signaling	#5125	1:5000
Anti-rabbit IgG HRP-linked	Cell Signaling	#7074	1:5000
Anti-rabbit IgG HRP-linked	Cell Signaling	#7076	1:5000

Table 2.3 Sequences of primer sets used for RT-qPCR

Gene Target	Forward primer (5' -> 3')	Reverse primer (5' -> 3')
18S	TTCGAACGTCTGCCCTATCAA	GATGTGGTAGCCGTTTCTCAGG
β-actin	CTTCCAGCAGATGTGGATCA	AAAGCCATGCCAATCTCATC
CHOP	ATGAACGGCTCAAGCAGGAA	GGGAAAGGTGGGTAGTGTGG
ERdj4	CGCCAAATCAAGAAGGCCT	CAGCATCCGGGCTCTTATTTT
EDEM1	TTGACAAAGATTCCACCGTCC	TGTGAGCAGAAAGGAGGCTTC
BiP	GCCTGTATTTCTAGACCTGCC	TTCATCTTGCCAGCCAGTTG
HERPUD1	AACGGCATGTTTTGCATCTG	GGGGAAGAAAGGTTCCGAAG
K8.1	AGATACGTCTGCCTCTGGGT	AAAGTCACGTGGGAGGTCAC
ORF26	CAGTTGAGCGTCCCAGATGA	GGAATACCAACAGGAGGCCG
ORF45	TGATGAAATCGAGTGGGCGG	CTTAAGCCGCAAAGCAGTGG
RTA	GATTACTGCGACAACGGTGC	TCTGCGACAAAACATGCAGC
XBP1 *(total)*	TAGCAGCTCAGACTGCCAGA	CCAAGCGCTGTCTTAACTCC

CHAPTER 3 KSHV LYTIC REPLICATION ACTIVATES UPR SENSOR PROTEINS BUT THE DOWNSTREAM TRANSCRIPTIONAL RESPONSES ARE INHIBITED

3.1 Introduction

The endoplasmic reticulum (ER) is the largest organelle in the eukaryotic cells that exhibits diverse roles in cellular function, such as lipid synthesis, calcium storage, and protein synthesis (Klaips et al., 2018). The ER is the gateway to the secretory pathway and one-third of the entire proteome is translated in the ER. These newly translated proteins need to be folded, modified, and sorted. Folding is central to protein function. Proteins in the ER undergo complex folding and re-folding events by disulfide bond formation and isomerization, as well as membrane insertion of single and multi-pass transmembrane proteins. ER proteins can also undergo complex co- and post-translational modifications, such as glycosylation, which are important for regulating protein sorting and function. The cell dedicates many enzymes, such as chaperones, foldases, protein disulfide isomerases, and oxidoreductases to help facilitate protein folding. If a protein becomes terminally misfolded then a host of different ER proteins coordinate the proteasomal degradation of the misfolded protein through a process called ERAD (ER-associated degradation) (Ruggiano et al., 2014).

Disruption of these cellular processes can lead to the accrual of unfolded or misfolded proteins that can aggregate and become toxic to the cell (Holmes et al., 2014). This increase in misfolded proteins is defined as ER stress. Eukaryotic cells have evolved a fail-safe signaling response to mitigate ER stress known as the unfolded protein response (UPR) (reviewed in Ron & Walter, 2007). Through transcriptional and translational reprograming the UPR aims to restore ER protein homeostasis. This is accomplished by transiently attenuating bulk protein translation, while increasing chaperone and foldase synthesis, expanding ER surface area by increasing phospholipid synthesis, and degrading terminally misfolded proteins. Persistent or irremediable ER stress causes the UPR to transition from an adaptive response to a pro-apoptotic response to prevent further damage to the host.

In metazoans, the UPR is carried out by PERK, ATF6, and IRE1, three ER transmembrane proteins which are normally maintained in an inactive state by the

abundant ER chaperone BiP (Grp78) (Bertolotti et al., 2000; K. Ma et al., 2002). During ER stress, it is believed that the higher affinity for hydrophobic domains of unfolded proteins titrate out BiP, allowing for activation of the sensors.

IRE1 is a type I ER transmembrane protein that has both kinase and endoribonuclease activity and is the only ER stress sensor conserved in all eukaryotes (Calfon et al., 2002; Cox et al., 1993). IRE1 has two isoforms in mammals, IRE1α and IRE1β . IRE1α is expressed in all tissues, whereas IRE1β expression is primarily restricted to bronchial and intestinal epithelia (Bertolotti et al., 2001). For simplicity, throughout the thesis, IRE1 refers to IRE1α. Upon release from BiP, the luminal domains of two monomers dimerize, which brings the kinase domains into close proximity. These in turn promote one of the monomers to phosphorylate one another through *trans*-autophosphorylation (K. P. K. Lee et al., 2008). IRE1 dimers subsequently form higher-order oligomers, which are essential for IRE1 activity (Welihinda & Kaufman, 1996). Phosphorylation of IRE1 facilitates ADP or ATP binding, which induces a conformational change that activates the C-terminal ribonuclease (RNase) domain (Sidrauski & Walter, 1997). The activated RNase has specific activity for the mRNA that encodes XBP1 (Calfon et al., 2002; Yoshida et al., 2001). IRE1 cleaves out a short intron (26-nucleotides in mammalian cells) and re-ligation by the tRNA ligase RtcB results in a translational frameshift generating spliced-XBP1 (XBP1s) (Jurkin et al., 2014; Y. Lu et al., 2014). This isoform has an extended C-terminus, which is an activation domain and converts XBP1 into an active bZIP transcription factor that upregulates genes involved in protein folding, ERAD, and lipid biosynthesis (Ron & Walter, 2007). IRE1 can also cleave a subset of ER-translating mRNAs that have only one XBP1-like cleavage site (Hollien & Weissman, 2006; Maurel et al., 2014). These mRNAs are subsequently degraded by the exonuclease XRN1 in a process called RIDD (regulated IRE1-dependent decay). RIDD is thought to reduce the protein burden in the ER, and has also been shown to promote apoptosis (Hollien et al., 2009).

The ER stress sensor PERK is also a kinase and is one of four kinases that phosphorylate eIF2α as part of the integrated stress response (ISR) (Pakos-Zebrucka et al., 2016). Similar to IRE1, upon dimerization, PERK undergoes *trans*-autophosphorylation, inducing a conformational change that allows it to bind and phosphorylate the translation initiation factor, eIF2α (Cui et al., 2011; Harding et al.,

1999). Phospho-eIF2α has a higher affinity for the rate limiting GEF eIF2B, thereby eventually blocking GTP cycling and resulting in the attenuation of bulk translation (Krishnamoorthy et al., 2001; Pavitt et al., 1998). eIF2α phosphorylation also results in the preferential translation of stress-related mRNAs, due to the presence of uORFs in the 5'UTR (Harding et al., 2000; Vattem & Wek, 2004). Central to the ISR is the translation of the uORF-containing mRNA that encodes ATF4. ATF4 is a bZIP transcription factor and a master regulator of the ISR. Following phosphorylation of eIF2α and activation of the ISR, ATF4 upregulates genes involved in amino acid biosynthesis, the anti-oxidant response and autophagy-related genes (Harding et al., 2003). ATF4 also transactivates the pro-apoptotic transcription factor CHOP (Harding et al., 2000).

The third sensor of ER stress is ATF6, a type II transmembrane glycoprotein with two isoforms ATF6α and ATF6β (K Haze et al., 2001; Kyosuke Haze et al., 1999; C. Zhu et al., 1997). Both isoforms are expressed in all tissue types, and may have some redundant roles, but ATF6α is primarily considered to have a dominant role in UPR signaling (Keisuke Yamamoto et al., 2007). I will often refer to ATF6α as ATF6. Similar to IRE1 and PERK, in the absence of stress BiP binds ATF6 to inhibit signaling (Shen et al., 2005). ATF6 can also form dimers and oligomers through intra-disulfide bonds, which are also thought to contribute to inhibition (Nadanaka et al., 2007). Upon exposure to ER stress, ATF6 inter- and intra-disulfide bonds are reduced and BiP is released. This allows ATF6 to traffic to the Golgi where it undergoes regulated intramembrane proteolysis (RIP) by Site-1 and Site-2 proteases (S1P and S2P) (J. Ye et al., 2000). RIP releases the cytosolic N-terminal fragment, ATF6-N, which is an active bZIP transcription factor that translocates to the nucleus to upregulate chaperones, foldases and lipid synthesis enzymes (Shoulders et al., 2013). ATF6-N also has been shown to upregulate XBP1 to promote XBP1 splicing (Yoshida et al., 2001).

Much of what we know regarding the UPR is from the use of ER stress-inducing drugs that have gross deleterious effects on the ER and the cell. These include tunicamycin, which inhibits N-linked glycosylation; thapsigargin, which depletes ER Ca^{2+} levels by inhibiting the SERCA (sarco/endoplasmic reticulum Ca^{2+}-ATPase) pump; and reducing agents dithiothreitol (DTT) and β-mercaptoethanol, which disrupt disulfide bonds.

The physiological cues of ER stress, however, are not well understood, but UPR signaling is linked to both physiological processes and disease (S. Wang & Kaufman, 2012). The UPR is important for the development and differentiation of professional secretory cells, including insulin-secreting β cells, granulocytic eosinophils, and antibody-secreting plasma cells. Importantly, XBP1s is essential for differentiation of B cells into plasma cells (Reimold et al., 2001). Overexpression of XBP1s can promote the plasma cell malignancy multiple myeloma (Carrasco et al., 2007). XBP1 and the UPR are implicated in other cancers, such as breast cancer (X. Chen et al., 2014) and ovarian cancer (M. Song et al., 2018), as well as protein misfolding neurodegenerative disorders like Huntington's disease (Roussel et al., 2013). Due to the importance of the UPR in insulin secretion by pancreatic β cells, dysregulated UPR signaling is also linked to type II diabetes (Back & Kaufman, 2012).

The UPR is also activated in multiple different virus infections, including coronavirus, flavivirus, influenza, and herpesvirus infection (J. A. Smith, 2014). However, the precise cause of UPR activation during virus infection is not well understood. Enveloped viruses may activate the UPR by triggering ER stress due to the burst in the synthesis of viral glycoproteins. Markedly, there are increasing examples of viruses or viral proteins that can activate or inhibit one or multiple UPR sensors or the downstream signaling events, suggesting that viruses can fine-tune the UPR. However, the mechanistic details of how and why viruses modulate the UPR are largely unknown.

Kaposi's sarcoma-associated herpesvirus (KSHV) is the infectious cause of Kaposi's sarcoma and two rare B cell lymphoproliferative disorders, plasmablastic multicentric Castleman's disease (MCD) and primary effusion lymphoma (PEL) (Ganem, 2007). PEL and MCD have a pre-plasma cell phenotype and some UPR markers are marginally upregulated in PEL cells (Jenner et al., 2003). KSHV is an enveloped virus with a large DNA genome that allows for the expression of many viral accessory proteins that are important for pathogenesis. Importantly, the virus encodes multiple oncogenes, which promote tumorigenesis through the secretion of pro-inflammatory cytokines and growth factors (Mesri et al., 2010).

KSHV has both a latent and lytic replication cycle but the default is latency. During latency, a subset of viral genes are expressed (i.e. latent genes), and the viral genome is maintained as a circular episome tethered to the host chromatin. The precise

physiological cues that trigger the switch from latency to lytic are not well understood, but certain types of cellular stress (including ER stress), can trigger reactivation *in vitro*. These stresses upregulate the immediate early protein RTA, a sufficient and necessary viral protein to induce the lytic replication cycle (Lukac et al., 1998; Ren Sun et al., 1998). Through the use of host and viral factors, RTA induces a temporal and coordinated lytic gene expression program through the expression of early and late viral genes. Collectively, these gene products facilitate viral genome replication, subversion of host innate immune defense mechanisms, and the assembly of infectious virus particles that are released from the cell (Aneja & Yuan, 2017).

RTA expression is responsive to ER stress through the presence of at least one XBP1s binding site in the RTA promoter (Dalton-Griffin et al., 2009). Therefore, in response to ER stress, RTA is upregulated to initiate lytic replication. Presumably, this allows the virus to escape a cell that may undergo cell death.

KSHV also has been reported to undergo lytic reactivation in B cells following activation of the B cell receptor (BCR) by IgM crosslinking (Kati et al., 2013). This activation is analogous to B cell differentiation into plasma cells following antigen recognition by the BCR, which stimulates plasma cell differentiation. Consistently, BCR-mediated lytic reactivation was also dependent on XBP1s (Kati et al., 2013). Since XBP1s is activated during plasma cell differentiation, KSHV reactivation in PEL cells may be linked to plasma cell differentiation, which may have important implications for PEL and MCD pathogenesis. vIL-6 is also highly associated with PEL and MCD pathology and has recently been shown to contain XBP1 binding sites in its promoter (D. Hu et al., 2016).

Following lytic reactivation, a large number of viral proteins, both structural and non-structural proteins, are expressed in the ER. In addition to this, KSHV lytic replication causes an upregulation of cytokines and growth factors that are also translated in the ER. This burst in ER protein synthesis could potentially overwhelm the ER protein folding machinery and induce ER stress. The activation status of the ER stress sensors (IRE1, PERK, and ATF6) and their potential requirement during KSHV lytic replication are currently unknown.

In this chapter, I demonstrate that KSHV lytic replication in a PEL cell model activates all three UPR sensors: ATF6 is proteolytically cleaved, PERK and eIF2α are

phosphorylated, and IRE1 is activated and XBP1 mRNA is spliced. Despite activation of the UPR sensors, accumulation of the downstream effectors, XBP1s and ATF4 are inhibited, and ATF6-N does not transactivate its canonical UPR genes. Furthermore, activation of IRE1, PERK, and ATF6 is likely required for robust virus replication since pharmacological or genetic inhibition of each of the sensors reduced virus titer.

3.2 Results

3.2.1 KSHV Lytic Replication Activates IRE1, PERK, but the Downstream Transcription Factors XBP1s and ATF4 are Inhibited

ER stress and activation of the UPR triggers KSHV lytic reaction through the direct binding of XBP1s to the promoter of the immediate early protein RTA, thereby initiating the lytic replication cascade (Wilson et al., 2007; F. Yu et al., 2007). I confirmed these findings by measuring RTA expression by qPCR in the PEL cell line BCBL1, following pharmacological induction of ER stress with the SERCA inhibitor thapsigargin (Tg) (Fig 3.1A). Combined treatment of BCBL1 with the HDAC inhibitor sodium butyrate (NaB) and the phorbol ester TPA, known inducers of KSHV reactivation, showed similar induction of RTA expression compared to Tg treatment. To corroborate that XBP1s can induce RTA expression through direct binding to its promoter, Hela Tet-Off cells were co-transfected an XBP1s expression vector and a luciferase reporter plasmid that contains four copies of the XBP1s binding site found in the RTA promoter (Dalton-Griffin et al., 2009). Cells transfected with the luciferase reporter were also treated with Tg to induce XBP1s expression. Both XBP1s and Tg exposure increased RTA promoter activity confirming that XBP1s can transactivate RTA (Fig 3.1B).

Although a role for the UPR during viral reactivation in response to ER stress is established, the role of the UPR during lytic replication is largely unknown. I hypothesized that the burst in ER-synthesized proteins, the change in lipid composition, or rearrangement of membranes during viral egress was sufficient to trigger ER stress to activate the UPR. To determine the activation status of the UPR during KSHV lytic replication, I used the PEL cell line TREx BCBL1-RTA cells (H. Nakamura et al., 2003). These cells have been engineered to express RTA from a dox-inducible promoter to induce robust lytic replication without the confounding pleiotropic effects of HDAC inhibitors or phorbol esters. TREx BCBL1-RTA cells were treated with dox for 24 or 48

h to induce early and late lytic replication, respectively, while others were left untreated as a control for latency. Two hours prior to harvesting for RNA and protein, cells were treated with Tg to induce ER stress to ensure that UPR signaling was intact in this cell line, and to determine whether lytic replication had any impact on UPR signaling following drug-induced ER stress.

Treatment of latent cells with Tg resulted in activation of IRE1α as determined by a migration shift in a total protein blot (Fig 3.2). Semiquantitative RT-PCR XBP1 splicing assay showed that the majority of XBP1 mRNA was spliced, which corresponded to an increase in spliced-XBP1 (XBP1s) protein. The PERK branch of the UPR was also activated by phosphorylation following Tg treatment, as determined by a migration shift in a total protein blot, as well as phosphorylation at Ser51 in the downstream target eIF2α. Phosphorylation of eIF2α attenuates global translation while preferentially translating a subset of stress-related genes including ATF4. Tg treatment in BCBL1 cells resulted in a robust upregulation of ATF4, while it was largely undetectable in latent cells, which corresponded with low basal levels of phospho-eIF2α. ATF6 immunoblot analysis only revealed full-length ATF6 (ATF6α-FL) and the cleaved ATF6-N isoform could not be detected after 2 h Tg treatment. However, ATF6 immunoblotting is fraught with difficulty, primarily because it is highly unstable and the lack of available high-quality antibodies. Therefore, it is challenging to clearly detect ATF6-N.

Treatment with dox for 24 h or 48 h resulted in early and late viral gene expression as shown by the detection of the early protein ORF45 and the late protein ORF65, respectively (Fig 3.2). This induction of gene expression corresponded with an activation of IRE1, as determined by a shift in total protein migration and induction of XBP1 mRNA splicing that persisted throughout the lytic cycle. Interestingly, there was minimal induction of XBP1s protein and Tg was unable to overcome this inhibition. There was also a slight, but noticeable increase in unspliced XBP1 mRNA after Tg treatment in the 24 h dox sample, which corresponded with reduced IRE1 accumulation. This decrease in IRE1 was most evident after 48 h. Full-length ATF6 increased after 24 h dox, but by 48 h the levels of ATF6 were greatly reduced, possibly due to ATF6 cleavage by S1P and S2P. Alternatively the reduction of ATF6 at the late time point may be the result of host shut-off or cell toxicity. During lytic replication there was also a slight upward shift in migration of total PERK immunoblot with concomitant increase in eIF2α

phosphorylation. Surprisingly, even though there were equivalent levels of eIF2α phosphorylation compared to Tg treatment alone, there was minimal ATF4 production during the lytic cycle. Furthermore, Tg treatment during lytic replication had minimal impact on the ability to upregulate ATF4 even though PERK activity was likely still intact as indicated by a further increase in phospho-eIF2α, most notably after 24 h post-dox. One hypothesis as to why ATF4 is not upregulated during lytic is that phospho-eIF2α does not inhibit eIF2B and so global protein synthesis is not inhibited. One study shows that TLR signaling inhibits the ISR following induction of ER stress by dephosphorylation of the ε subunit of eIF2B by protein phosphatase 2 A (PP2A) (Woo et al., 2012). Potentially, KSHV hijacks PP2A during lytic replication to block protein inhibition by eIF2α phosphorylation.

The presence of a truncated fragment of total eIF2α is likely due to a previously identified caspase cleavage event (Marissen, Guo, Thomas, Matts, & Lloyd, 2000). However, the impact that the truncated eIF2α isoform has on the ISR and ATF4 translation is not known. vIRF-2 has been reported to activate caspase-3 (Aresté, Mutocheluh, & Blackbourn, 2009), and lytic replication has been shown to activate caspase-7 and caspase-8 (Majerciak, Kruhlak, Dagur, McCoy, & Zheng, 2010). Therefore, KSHV-activated caspases may cleave eIF2α to prevent activation of the ISR during lytic replication. Treatment with the pan-caspase inhibitor Z-VAD-FMK during lytic replication reduced the levels of truncated eIF2α in both total protein and phospho-eIF2α, as expected, but this did not restore ATF4 accumulation (Fig 3.3).

3.2.2 KSHV Lytic Replication Triggers ATF6 Processing but ATF6 Transcriptional Activity is Inhibited

Upon the disruption of protein homeostasis, ATF6 traffics to the Golgi where it is cleaved by S1P and S2P releasing the cytosolic N-terminal fragment of ~ 55 kDa (J. Ye et al., 2000). ATF6-N is an active bZIP transcription factor that upregulates chaperones, ERAD machinery, and lipid biosynthetic enzymes (Bommiasamy et al., 2009; Shoulders et al., 2013; Keisuke Yamamoto et al., 2007). Since cleavage of endogenous ATF6 is classically difficult to detect by immunoblot, TREx BCBL1-RTA cells were transduced with a HA-epitope tagged full-length ATF6 lentiviral expression vector (HA-ATF6 WT), which can be readily detected with anti-HA antibody. The N-terminal cleavage product

was detected after 4 h Tg treatment (Fig 3.4A). Induction of lytic replication with dox for 24 h resulted in an increase in full length ATF6 similar to what was observed for endogenous ATF6 (Fig 3.2). There was also a corresponding increase in cleaved ATF6 which was more prominent than with the Tg treatment alone (Fig 3.4A). By 48 h post-dox, the levels of ATF6 were significantly reduced but the HA-ATF6-N could still be detected. Interestingly, during lytic replication there was a band that migrated slightly faster than the N-terminal fragment that was not as prominent in cells treated with only Tg. Based on a comparative analysis with one of the first studies characterizing the ATF6 cleavage events (J. Ye et al., 2000), it is possible that the smaller protein isoform is in fact the active ATF6 N-terminal product and the prominent cleaved species observed with Tg treatment alone still retains the ER transmembrane portion, and is therefore inactive. Careful biochemical analysis will need to be conducted to ascertain which protein species correspond to the nuclear active transcription factor and the intermediate membrane bound species.

To determine the extent of ATF6 transcriptional activity during lytic replication, mRNA levels of ATF6 target genes, BiP and HERPUD1 (homocysteine-responsive endoplasmic reticulum-resident ubiquitin-like domain member 1), were measured by qPCR (Fig 3.4B). Surprisingly, even though there was a clear production of the cleaved ATF6-N isoform after 24 h dox treatment, there was no upregulation in BiP and HERPUD1 mRNA levels. Furthermore, lytic replication also repressed Tg-induced ATF6 transcriptional activity, for there was no significant upregulation of these ATF6 target genes compared to Tg-treated latent cells.

3.2.3 PERK Dependent Phosphorylation of eIF2α During Lytic Replication

eIF2α can be phosphorylated by four different kinases that make up the ISR (Pakos-Zebrucka et al., 2016). Nutrient stress activates GCN2, dsRNA from virus infections activates PKR, oxidative stress or heme stress activates HRI, and ER stress activates PERK. As there is a clear increase in eIF2α phosphorylation during lytic replication and only a modest increase in PERK phosphorylation compared to latent cells, I wanted to determine the level of PERK contribution to eIF2α phosphorylation during lytic replication. TREx BCBL1-RTA cells were treated with the PERK inhibitor GSK2606414 (PERKi) (Harding, Zyryanova, & Ron, 2012) simultaneously with dox for 24 and 48 h.

As a positive control for PERK activity, 2 h prior to lysis, cells were also treated with Tg. Combined treatment of PERKi and Tg resulted in complete inhibition of PERK activity due to the lack of a protein migration shift in a total PERK blot. PERKi treatment also restored eIF2α phosphorylation to basal levels and blocked ATF4 expression (Fig 3.5). Treatment with the PERKi was specific to PERK as it did not inhibit IRE1 phosphorylation. Consistent with Fig 3.2, lytic replication did not induce ATF4 expression even though there were similar levels of eIF2α phosphorylation compared to Tg-treated latent cells. Importantly, treatment with PERKi in cells undergoing lytic replication reduced eIF2α phosphorylation; however, phospho-eIF2α levels did not return to baseline even though PERK phosphorylation was completely inhibited. This suggests that PERK is possibly not the only eIF2α kinase that is activated during lytic replication.

3.2.4 Lytic Replication Inhibits ATF4 and XBP1s Regardless of the Type and Duration of ER Stress

I previously demonstrated that ATF4 and XBP1s are not upregulated during the lytic cycle after a 2-h pulse with the SERCA inhibitor Tg (Fig 3.2). To ensure that the apparent UPR signaling blockade during lytic replication is not specific to either the type of stress or to a delay in response to ER stress, I treated lytic TREx BCBL1-RTA cells for 1, 4, and 8 h with either Tm, which triggers ER stress by blocking N-linked glycosylation, or Tg. Tm treatment induces ER stress slower than Tg because Tm requires new protein synthesis to accumulate misfolded proteins, whereas inhibiting the ER calcium import almost immediately disrupts protein folding (A.-H. Lee et al., 2003a). This can be observed by RT-PCR XBP1 mRNA splicing where the majority of splicing following Tg treatment occurred by the one-hour mark, whereas the bulk of splicing with Tm treatment was not observed until after 4 h (Fig 3.6). ATF4 also accumulated more rapidly with Tg treatment compared to Tm. Importantly, regardless of the duration or type of stress, XBP1s and ATF4 did not accumulate to the same levels during lytic replication even though IRE1 was activated by phosphorylation as determined by a migration shift in total protein blot, and PERK was activated based on the increase in phosphorylation of its substrate eIF2α. Consistent with Fig 3.2, even though IRE1 was phosphorylated, IRE1 did not accumulate to the same level after drug-induced ER stress during lytic replication

compared to latently treated cells (Fig 3.6). Again, there was a noticeable increase in XBP1u mRNA after Tg treatment. This difference was not observed after Tm treatment, indicating that the lower levels of IRE1 was likely not the reason for the decreased XBP1 splicing efficiency after Tg treatment, but may still play a role in the failure of XBP1s protein to accumulate. Consistent with Fig 3.2, full-length ATF6 also accumulated by 24 h post-dox and treatment with Tm resulted in a decrease in size due to de-glycosylation (denoted as ATF6α-FL*) (C. Zhu et al., 1997). This time probing for ATF6 with anti-ATF6 sera revealed a protein species that was the appropriate size for ATF6-N after Tg and Tm treatment and was absent in untreated latent cells. This protein species, which is likely the cleaved isoform ATF6-N, was also detected after dox treatment, indicating that endogenous ATF6 is cleaved during lytic replication and that cleavage of ectopic HA-ATF6 in Fig 3.4 was likely not the result of ATF6 overexpression. Taken together, these data confirm that the UPR sensors are active during lytic replication while the downstream effectors, most notably XBP1s and ATF4, are inhibited. Furthermore, exposure to pharmacological inducers of ER stress cannot overcome this inhibition.

3.2.5 XBP1s Target Genes are not Transactivated During Lytic Replication

Since the IRE1-XBP1s pathway can induce KSHV reactivation (Wilson et al., 2007), I wanted to more carefully analyze the activation status during early lytic replication. Induction of lytic replication in TREx BCBL1-RTA with dox over a 24-h time course, revealed that IRE1 activation began as early as 6 h post-dox treatment as determined by the increase in spliced XBP1 mRNA and XBP1s protein compared to the latent control (Fig 3.7A and B). This activation of IRE1 at 6 h corresponded with an increase in ORF45 protein. By 18 h post-dox, which roughly coincides with viral genome replication in this cell model (H. Nakamura et al., 2003), IRE1 activity peaked as determined by the observed maximum levels of XBP1s protein and mRNA. IRE1 phosphorylation continued until 24 h post-dox but IRE1 protein levels began to decrease, which corresponded to a minor decrease in XBP1 mRNA levels, consistent with previous results.

Since there is an increase in XBP1s protein in early lytic, even if this is nominal, I wanted to test if XBP1s had any transcriptional activity. mRNA levels of the XBP1s target genes ERdj4 (endoplasmic reticulum–localized DnaJ 4) and EDEM1 (ER degradation-enhancing alpha-mannosidase-like protein 1) in lytic TREx BCBL1-RTA

cells showed no change in expression compared to the latent control (Fig 3.8A and B). Furthermore, XBP1 target genes were significantly reduced during lytic replication following Tg or Tm treatment compared to the Tg- or Tm-treated latent samples even though XBP1 splicing was intact. This indicates that the low levels of XBP1s protein during lytic replication is not enough to induce transcription of genes involved in restoring protein homeostasis.

XBP1s induces RTA expression after exposure to ER stress by directly binding to the RTA promoter (Dalton-Griffin et al., 2009). As such, it is possible, due to the multiple copies of viral genomes, that during lytic replication the RTA promoter may titrate out the available XBP1s and prevent transcription of cellular genes. To test whether the pool of XBP1s induced during lytic replication can transactivate RTA as a feed-forward based mechanism, RTA mRNA levels were measured in wild type BCBL1 cells treated with NaB and TPA or Tg in the presence or absence of the IRE1 inhibitor 4μ8c (Cross et al., 2012). 4μ8c potently inhibited IRE1 activity as determined by a loss of spliced XBP1 mRNA, which inhibited Tg-induced RTA mRNA as expected (Fig 3.9A and B). However, even though spliced XBP1 was inhibited in NaB- and TPA-treated cells there was no significant inhibition of RTA expression, suggesting that similar to that of XBP1 target genes, the available pool of XBP1s does not induce RTA expression. Collectively, these data demonstrate that even though there is an increase in XBP1s during lytic, the low levels of XBP1s protein does not cause a detectable increase in transcriptional activity.

3.2.6 UPR Sensors are Required for Robust Virus Production

Since all three sensors of the UPR are engaged during lytic replication, I next wanted to determine their relative impact on virus production, using genetic and pharmacologic approaches. To determine the role of ATF6 during lytic, ATF6 expression was silenced in TREx BCBL1-RTA cells with an shRNA lentiviral vector. Immunoblots of ATF6 and the ATF6 target gene BiP demonstrated a significant reduction in ATF6 expression and decrease in BiP following exposure to Tm (Fig 3.10A). Virus-containing supernatants were harvested 48 h post-dox and relative virus titer was determined by measuring the level of DNase I-protected genomes in the supernatant by qPCR. ATF6 knockdown resulted in an approximate 2-fold reduction in titer compared to virus harvested from cells expressing the non-targeting shRNA control (Fig 3.10B).

To determine the role of PERK and the ISR for virus replication, TREx BCBL1-RTA cells were co-treated with dox and either PERKi or the ISR inhibitor ISRIB, which binds to eIF2B and prevents the high affinity binding of phospho-eIF2α (Sekine et al., 2015; Sidrauski et al., 2013). Both PERKi and ISRIB inhibited virus production by approximately 2-fold compared to the untreated control as measured by qPCR (Fig 3.11).

The IRE1-XBP1 pathway likely does not play a role in RTA expression or XBP1-specific cellular gene expression during lytic replication. However, IRE1 can also induce RIDD, which may be important for robust virus production. The IRE1 inhibitor 4μ8c, which covalently modifies the RNase domain rendering it inactive, inhibited virus titer in a dose-dependent manner in TREx BCBL1-RTA cells as measured by qPCR (Fig 3.12A). I confirmed this inhibition of titer by IRE1 inhibition in another KSHV model cell line, iSLK.219 cells (Myoung & Ganem, 2011b), which also express RTA from a dox-inducible promoter. These cells contain a recombinant latent KSHV with a genome that harbors a GFP cassette under a constitutively active promoter to enable titering by flow cytometry. 96 h post-dox, virus containing supernatants were spinfected onto a monolayer of 293A cells and the following day, infected GFP-expressing cells were enumerated by flow cytometry to calculate virus titer. The inhibition of virus titer from iSLK.219 cells following 4μ8c treatment was not as robust as seen in TREx BCBL1-RTA cells and required a higher concentration of 4μ8c to observe a significant inhibition (Fig 3.12B). To better understand if IRE1 activation is required for virus replication in iSLK.219 cells, IRE1 expression was silenced with shRNA lentiviral vectors using two different hairpins. Immunoblot analysis of IRE1 and its downstream target XBP1s shows a significant reduction in IRE1 expression and a corresponding decrease in XBP1 splicing, with the hairpin *IRE1-3* showing a slightly stronger suppression (Fig 3.12C). Virus titer was again determined by flow cytometry, and there was a significant reduction in virus production consistent with the strength of IRE1 knockdown: *IRE1-3* shRNA had a stronger inhibitory effect on virus titer compared to the *IRE1-2* shRNA (Fig 3.12D). Collectively these data demonstrate that all three of the UPR sensors are important for maximum virus production.

3.3 Discussion

Accumulating evidence suggests that viruses hijack the UPR to promote replication. KSHV uses the IRE1-XBP1 pathway to transactivate RTA and induce lytic replication in response to ER stress (Wilson et al., 2007), but little is known about the activation status of the UPR and its importance during KSHV lytic replication in the absence of ER stress. This chapter of the thesis shows that all three branches of the UPR are activated during lytic replication but that the UPR transcriptional response is stymied. Furthermore, pharmacologic or genetic inhibition of the UPR sensors reduces virus production, suggesting that during lytic replication KSHV may repurpose the UPR sensors for a different role other than restoring protein homeostasis.

These data (and other data not shown) indicate that all 3 UPR sensors are activated at the same time in TREx BCBL1-RTA cells (~ 12 h post-dox), indicating that the UPR may be activated by ER stress rather than specific targeting of each of the UPR branches. Multiple viral proteins are synthesized in the ER during lytic replication, including a collection of glycoproteins, which in theory could overwhelm the cellular folding machinery and cause ER stress. However, the majority of envelope glycoproteins are synthesized in the late phase of the replication cycle, and since the timing of UPR sensor activation occurs in the early phase, it is implausible that a burst in viral glycoproteins are the trigger for ER stress in this model. There are other early non-structural viral proteins synthesized in the ER that could induce ER stress. vGPCR is a constitutively active seven-transmembrane signaling protein that upregulates multiple chemokines and cytokines that are synthesized in the ER, and thus the combined protein load of vGPCR and its cellular signaling molecules may induce ER stress. The level of expression of vGPCR during lytic replication is not known, and thus it is difficult to speculate if it could in fact saturate the folding machinery. vGPCR has also been reported to bind and inhibit SERCA2b (J. Zhang et al., 2015). Therefore, vGPCR may act analogous to thapsigargin to activate ER stress by decreasing ER calcium levels.

If lytic replication activates the UPR sensors due to classical ER stress, why would KSHV evolve to promote protein misfolding? And if KSHV specifically induces ER stress, why would the virus also block the adaptive transcriptional reprograming in response to this stress? This assumption that KSHV blocked UPR signaling is based on classical gene targets of ATF6 (BiP and HERPUD1) and XBP1s (ERdj4 and EDEM1). However, it is possible that KSHV has modified ATF6 and XBP1s to no longer bind their

canonical DNA binding sequences, and thus potentially changing their gene expression profile. ATF6 and XBP1s are bZIP transcription factors that can homo- and hetero-dimerize with other bZIP transcription factors. KSHV K8 is also called K-bZIP due to the presence of a bZIP domain. K-bZIP is a transcriptional repressor and can repress cellular and viral genes, including RTA (Liao, Tang, Lin, Kung, & Giam, 2003; Park et al., 2000). Therefore, one possible hypothesis for the lack of upregulation of ATF6- or XBP1s target genes during lytic replication is that these stress-responsive transcription factors heterodimerize with K-bZIP or other potential cellular bZIP transcription factors, which changes the gene targets or represses their activity. K-bZIP is also an SUMO2/3 E3 ligase that is important for repression of its target genes (P.-C. Chang et al., 2013; W.-S. Yang, Hsu, Campbell, Cheng, & Chang, 2015). RTA has also been reported to ubiquitinate SUMOylated proteins targeting them for proteasomal degradation (Izumiya et al., 2013). Interestingly, XBP1s can be SUMOylated and mutating the SUMOylated lysine residues increases transcriptional activity indicating that SUMOylated XBP1s is less active (H. Chen & Qi, 2010). Based on these studies, one theory is that K-bZIP and RTA may act in concert to promote the proteasomal degradation of XBP1s during lytic.

ATF6 is normally very unstable and during lytic replication, full length ATF6 protein levels are enhanced and ATF6 is cleaved to ATF6-N. The levels of ATF6-N are higher during lytic replication compared to cells treated with Tg or Tm alone. Surprisingly, ATF6 target genes are not upregulated with or without treatment with ER stressors. ATF6 binding to its target sequences is dependent on the heterotrimeric transcription factor NF-Y (Yoshida et al., 2000); therefore, NF-Y may be inhibited or re-purposed during lytic replication which would subsequently block ATF6 target gene expression. Alternatively, like the acquisition of XBP1 binding sequences in the RTA promoter, KSHV may also have acquired ATF6 binding sequences such as ERSE (ER stress response element) or ERSE-II and therefore use ATF6 to promote expression of viral genes.

As well as trying to resolve ER stress, the UPR can also promote apoptosis. ATF4 induces CHOP, a pro-apoptotic transcription factor and together promote apoptosis (J. Han et al., 2013). This is evident in CHOP knockout cells, which survive longer than wild type cells following ER stress (Marciniak et al., 2004). Therefore, KSHV may silence ATF4 and CHOP to extend cell survival. ATF4 and CHOP are also essential for

autophagy (B'chir et al., 2013), and there are multiple links for the role of the IRE1-XBP1 pathway in regulating autophagy (Margariti et al., 2013; Pehar, Jonas, Hare, & Puglielli, 2012; Vidal et al., 2012; Zhao et al., 2013). In the context of KSHV replication, autophagy is thought to be anti-viral. Along these lines, KSHV encodes vFLIP, K7, and vBCL2, which have been shown to inhibit the autophagic pathway (E et al., 2009; J.-S. Lee et al., 2009; Q. Liang et al., 2013). Potentially KSHV inhibits ATF4 and XBP1s as another mechanism for suppressing autophagy during lytic. ATF6 and XBP1s are important for the increase in degradation of misfolded proteins in the ER through ERAD (A.-H. Lee et al., 2003a; Shoulders et al., 2013; Yamamoto et al., 2007). HCV and IAV glycoproteins have been shown to be targeted for degradation by ERAD (Frabutt et al., 2018; Saeed et al., 2011). By blocking ATF6 and XBP1s activity, KSHV may prevent the degradation of viral proteins synthesized in the ER.

The UPR is also linked to multiple inflammatory diseases including Crohn's disease and diabetes (S. Wang & Kaufman, 2012). Furthermore, the UPR, specifically XBP1, mediates a robust inflammatory response following TLR2 activation in macrophages (Martinon et al., 2010). Thus, KSHV may block downstream UPR signaling events to negate any of the potentially harmful inflammatory molecules that would normally be upregulated by the UPR.

Like all viruses, KSHV requires the host translation machinery to synthesize viral protein. During lytic replication there is a robust and prolonged phosphorylation of eIF2α, which should attenuate translation and activate the ISR. Surprisingly, ATF4 does not accumulate and translation of viral proteins ensues. This may suggest that high levels of phospho-eIF2α during lytic has a minimal impact on viral translation. Phospho-eIF2α binds eIF2B GEF with high affinity preventing cycling of GDP to GTP on eIF2 (Krishnamoorthy et al., 2001; Pavitt et al., 1998). The recently identified small molecule ISRIB binds to eIF2B and blocks this inhibition by phospho-eIF2α (Zyryanova et al., 2018). One mechanism that KSHV could employ to bypass the ISR is to prevent the high affinity binding of phospho-eIF2α to eIF2B and allow the cycling of GDP to GTP to continue. This could be mediated by direct binding of a viral protein to eIF2B or potentially dephosphorylation of Ser539 on the ε subunit of eIF2B, as previously discussed (Woo et al., 2012). Inhibiting the ISR is a not a unique feature for viruses. HSV-1 encodes $\gamma_1$34.5, which is a GADD34 mimic that can bridge PP1 (protein

phosphatase 1) to eIF2α to promote dephosphorylation (He et al., 1997). HSV-1 has also been reported to prevent PERK activation through the direct binding of glycoprotein gB (Matthew Mulvey, Arias, & Mohr, 2007)

ATF4 translation occurs through a decrease in available eIF2-GTP-tRNAi^{Met} ternary complexes, which in turn causes the small ribosomal subunit to bypass uORFs present in the 5'UTR (Vattem & Wek, 2004). Host shutoff by the viral nuclease SOX causes a global decrease in translating cellular mRNAs (Glaunsinger et al., 2005; Glaunsinger & Ganem, 2004b), would could theoretically increase the amount of eIF2B inhibition required to establish bypass of uORFs in order to translate stress-responsive genes. However, if this is the case then further increases in eIF2α phosphorylation should likely promote ATF4 translation, which is not what is observed following Tg treatment during lytic replication.

Recently, there has been a link between post-transcriptional modifications (PTMs) and the ISR. Specifically, activation of the ISR results in N^6-methyladenosine (m^{6}A) modification of ATF4 mRNA by the methyltransferase ALKBH5, which is important for robust ATF4 translation (Jun Zhou et al., 2018). Recent reports have also shown that m^{6}A and the m^{6}A machinery are required for efficient KSHV translation (Hesser, Karijolich, Dominissini, He, & Glaunsinger, 2018; F. Ye, Chen, & Nilsen, 2017). Thus, it is possible that during lytic replication the m^{6}A machinery, which normally promotes the ISR, may be subverted by KSHV to promote translation of viral mRNAs.

Like ATF4, the KSHV genome also contain uORFs that control translation of viral genes. There are uORFs that control expression of the genes in the ORF35-ORF36-ORF37 tricistronic mRNA and are required for maximum translation of ORF36 (Kronstad, Brulois, Jung, & Glaunsinger, 2013). Although the mechanisms of how these uORFs impact translation following activation of the ISR have not been analyzed, it is still possible that increased eIF2α phosphorylation during lytic is important for controlling the relative levels of proteins expressed from this polycistronic mRNA.

Why is it that IRE1 is activated but XBP1s protein fails to accumulate during lytic replication? It is thought that normally during the UPR, ATF6 upregulates XBP1 transcriptionally (Yoshida et al., 2001), and recently ATF4 was shown to upregulate IRE1 to promote XBP1 mRNA splicing (Tsuru et al., 2016). Since ATF6 and ATF4 are both inhibited during KSHV lytic replication this may contribute to the low levels of

IRE1 and XBP1 observed in this system. If this is the case, then overexpression of ATF4 and/or ATF6 may reverse the phenotype and restore XBP1s protein levels.

Although, XBP1 mRNA is the primary target of IRE1, IRE1 can also cleave mRNAs with XBP1-like stem loop sequences through RIDD (Maurel et al., 2014). An *in vitro* study of IRE1 RNase activity showed that oligomeric IRE1 preferentially induces XBP1 splicing but IRE1 dimers preferentially induce RIDD (Tam et al., 2014). Therefore, it is possible that the reduced levels of activated IRE1 during the lytic cycle primarily induces RIDD activity, which is important for robust virus production. I have attempted to characterize RIDD activity during lytic replication in TREx BCBL1-RTA cells but due to the small decreases in mRNA levels of canonical RIDD substrates in the positive control samples and the extent of variability between replicates in the qPCR data, I was unable to confidently determine if RIDD was activated (data not shown).

IRE1 also acts as a signaling platform and it is possible that KSHV usurps this function of IRE1 to promote replication. IRE1 activates the JNK signaling through the recruitment and activation of the TRAF2-ASK1 pathway (Nishitoh et al., 2002). IRE1-TRAF2 was also shown to recruit pro-caspase-12 and induce cleavage to initiate apoptosis (Yoneda et al., 2001). A recent study showed that HSV-1 infection can activate JNK through IRE1 (Su et al., 2017), and the JNK pathway has been shown to be involved in virus replication. Multiple KSHV proteins have been reported to activate JNK signaling, including vGPCR, ORF36, and K15 (Bais et al., 1998; Brinkmann et al., 2003; Hamza et al., 2004), and therefore, KSHV may activate IRE1 to promote JNK signaling.

The IRE-XBP1 pathway is modulated by multiple different virus families, which may be important for viral replication. HCV can suppress IRE1-XBP1 signaling and HCV translation is higher in IRE1 knockout MEFs (Tardif et al., 2004). IAV specifically activated the IRE1 pathway (without engaging PERK or ATF6), and chemical inhibition of IRE1 diminished influenza A virus replication (Hassan et al., 2012). IRE1 signaling is also modulated by herpesviruses. HCMV activated PERK and IRE1 in human fibroblasts, inducing XBP1 mRNA splicing but the XBP1 target gene EDEM1 was not upregulated (Isler et al., 2005). Future studies should investigate if HCMV, like KSHV, also inhibits XBP1s protein accumulation. A recent study linked HCMV-mediated UPR activation to the ER resident glycoprotein UL148, presumably by causing ER stress directly (Siddiquey et al., 2018). In another CMV study, HCMV UL50 and the MCMV ortholog

M50 bind and inhibit IRE1 protein accumulation, thereby blocking ER stress-induced XBP1 mRNA splicing (Stahl et al., 2013). HSV-1 promoted IRE1 protein accumulation but the RNase activity was reduced; while treatment with the IRE1 inhibitor STF-083010 inhibited HSV-1 replication (Su et al., 2017). Importantly ectopic expression of XBP1s inhibited HSV-1 titer, indicating that similar to the data I have presented, IRE1 activity in HSV-1 infection is also likely rededicated to promote virus production. Thus, there is accumulating evidence that many viruses, which now includes KSHV, usurp or fine-tune UPR signaling to promote replication.

The lack of XBP1s observed during lytic replication is intriguing due to the strong link between XBP1 signaling during B cell differentiation and the pre-plasma cell expression profile in KSHV-positive PEL cells (Jenner et al., 2003). Immunohistochemistry of patient PEL samples were also negative for XBP1s in contrast to many different plasmablastic lymphomas (Montes-Moreno, Montalban, & Piris, 2012). This lack of XBP1s in PEL tumor samples is consistent with the *in vitro* lytic replication data described here. However, the apparent lack of XBP1s from patient-derived KSHV-positive pre-plasma cells could also be due to the intimate link between XBP1s and reactivation through RTA transactivation. Along these lines, any cell differentiating into plasma cell-like lymphomas would undergo lytic replication and presumably cell death. Due to the established link between KSHV replication and XBP1s, and my observations that XBP1s is inhibited during lytic replication, I decided to investigate the impact that XBP1s expression has on KSHV replication. This will be the focus of the next chapter.

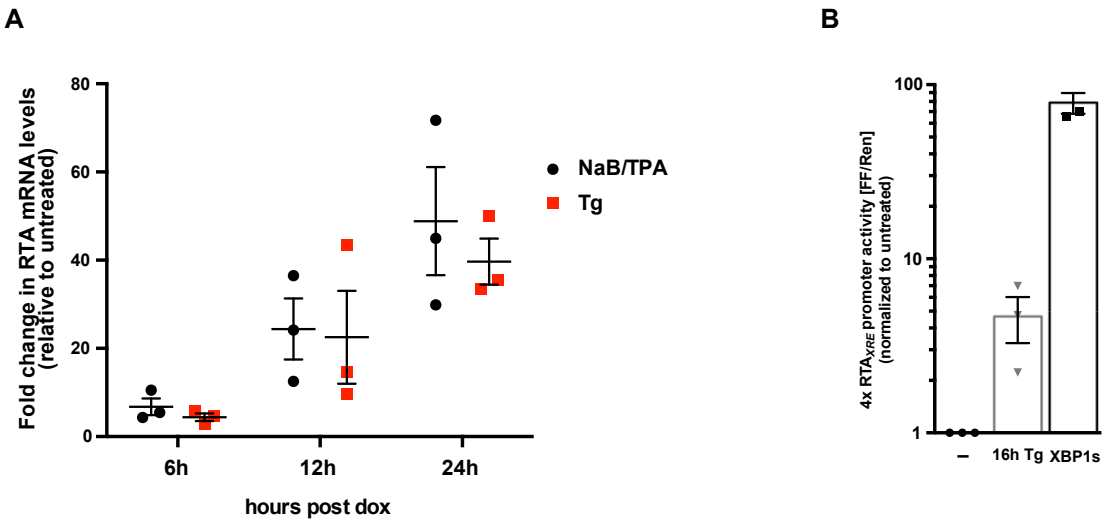

Fig 3.1 XBP1s transactivates KSHV immediate early gene RTA
(A) BCBL1 wild type cells were treated with 1 mM NaB and 20 ng/ml TPA or 150 nM Tg for 6, 12, or 24 hours or left untreated and harvested for total RNA. RTA mRNA levels were measured by qPCR and the change in mRNA levels compared to the untreated control was calculated by the ΔΔCt method using β-actin as a reference gene. The means of 3 independent experiments were calculated and the error bars denote the SEM. (B) Hela Tet-Off cells were transfected with pCMV2B-XBP1s or pCR3.1 vector control and a firefly luciferase expression construct that is driven by 4 tandem XBP1 target sequences that are derived from the promoter of RTA (4xRTA$_{XRE}$). A renilla luciferase plasmid was added for normalization and 24 hours later the vector control samples were treated with 500 nM Tg for 16h. Approximately 48 hours post transfection, relative luciferase units were measured to determine promoter activity.

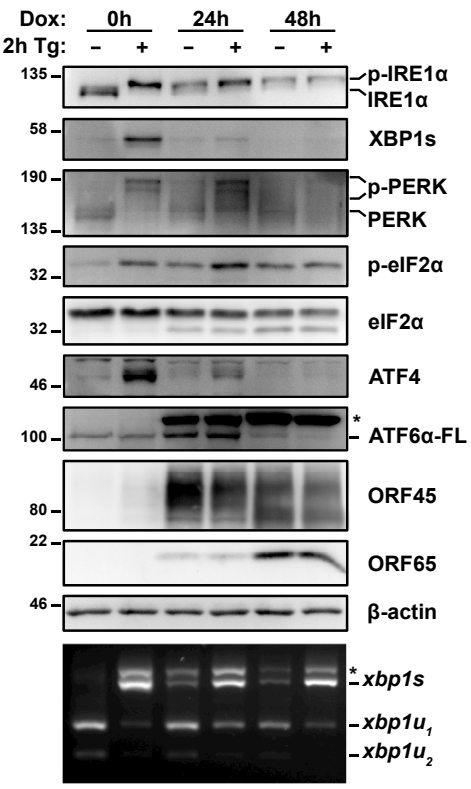

Fig 3.2 KSHV lytic replication activates IRE1 and PERK but their downstream transcription factors are inhibited

TREx BCBL1-RTA cells were treated with 1 μg/mL dox for 0, 24 and 48 h to induce lytic replication followed by 75nM Tg for 2 h prior to harvesting for protein and total RNA. Whole cell lysates were analyzed by immunoblots for UPR markers (IRE1α, XBP1s, PERK, phospho- and total eIF2α, ATF4, and full length ATF6α. Migration shift in PERK and IRE1α immunoblots correspond to phosphorylation. KSHV proteins ORF45 and ORF65 were probed for to indicate induction of early lytic and late lytic, respectively. β-actin was used as a loading control. The asterisk (*) corresponds to an unknown protein species that cross-reacts with ATF6 anti-sera. (Bottom) XBP1 mRNA was amplified by RT-PCR, digested with PstI (cleaves unspliced XBP1 isoform only), and resolved on a SYBR Safe-stained agarose gel. The asterisk (*) corresponds to xbp1u-xbp1s hybrid cDNA. Representative immunoblots and agarose gel of two independent experiments are shown.

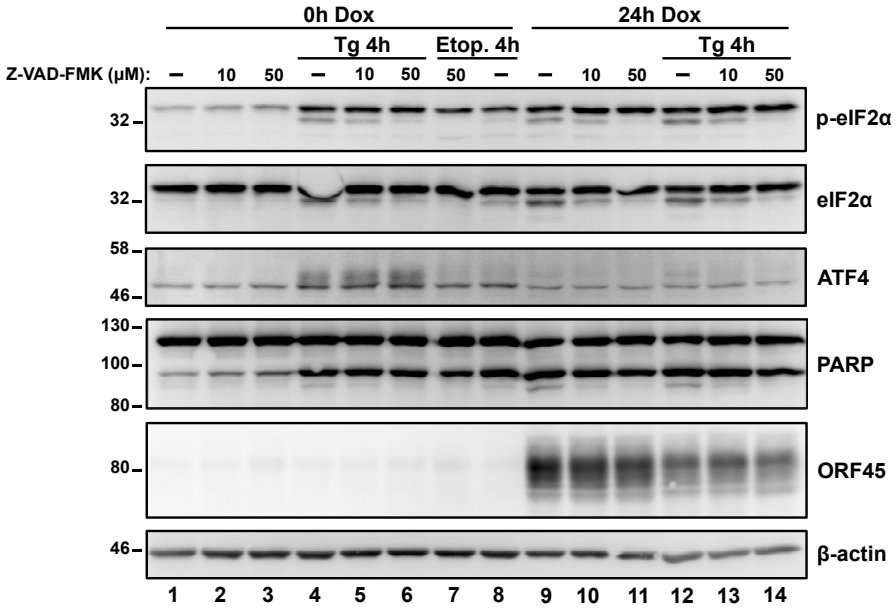

Fig 3.3 Caspase cleavage of eIF2α is not responsible for inhibition of ATF4 expression

TREx BCBL1-RTA cells were treated with 1 μg/ml dox or left untreated for 24 hours (lane 1 vs lane 9) with or without the combined treatment of the pan-caspase inhibitor Z-VAD-FMK (10 or 50 μM) (lanes 2 & 3 vs lanes 10 & 11). 4 hours prior to harvesting for total protein, cells were treated with 75 nM Tg (lanes 4-7 vs lanes 12-14). Cells were also treated 25 μM etoposide as a positive control for caspase activity (lane 7 vs lane 8). Immunoblot analysis of phospho- and total eIF2α, ATF4 were completed. PARP immunoblot was used as a positive control to demonstrate changes in caspase activity. β-actin was used as a loading control. ORF45 was used to confirm lytic induction. Immunoblots were completed once.

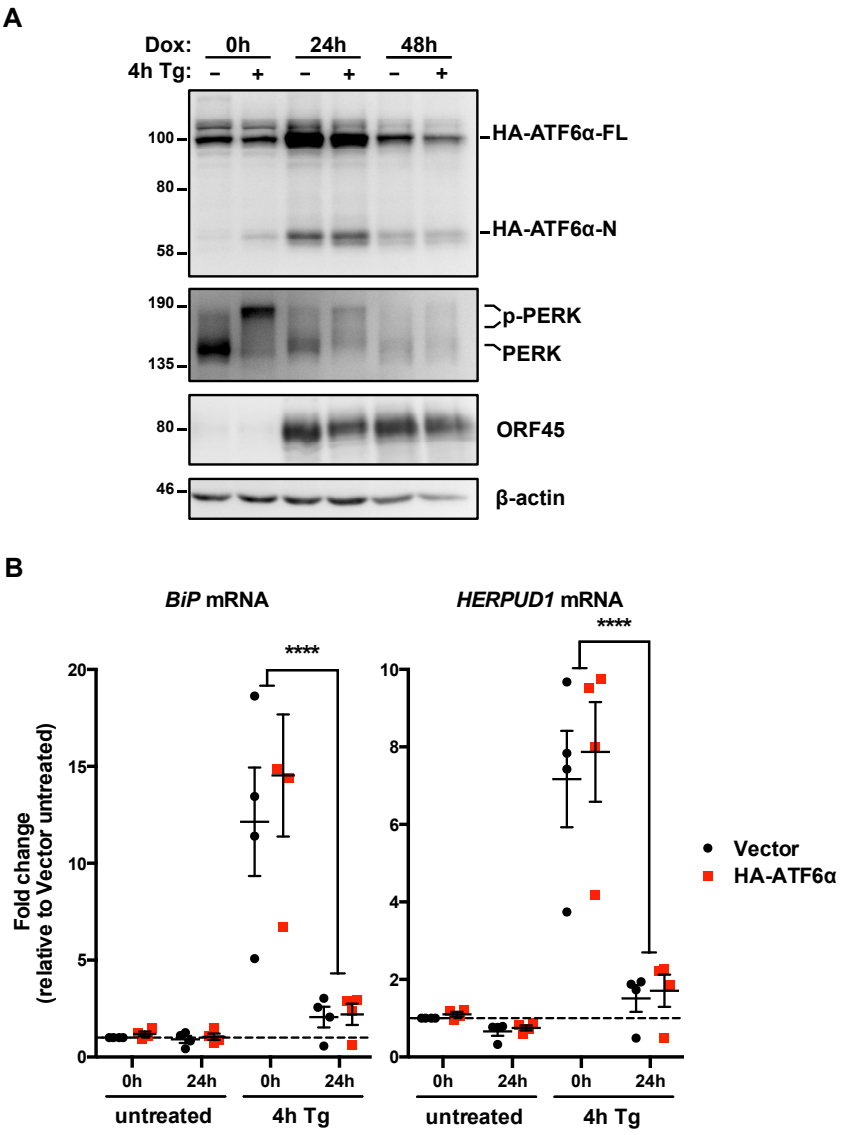

Fig 3.4 KSHV lytic replication activates ATF6α intra-membrane proteolytic cleavage but downstream gene targets are inhibited

(A) TREx BCBL1-RTA cells were transduced with a lentiviral expression vector encoding HA-ATF6α and selected for with puromycin. Following selection, cells were treated with 1 μg/mL dox for 0, 24 and 48 h and treated with 75nM Tg for 4 h prior to harvest. Whole cell lysates were analyzed by immunoblots for HA epitope tag, PERK, ORF45 and β-actin (loading control). Immunoblots shown are representative of two independent experiments. (B) As in (A), HA-ATF6α-transduced TREx BCBL1-RTA were treated with dox for 0 and 24 h and then treated with 75nM Tg for 4 h prior to total RNA isolation. mRNA levels of ATF6α target genes BiP and HERPUD1 were measured by qPCR. Changes in mRNA levels were calculated by the ΔΔCt method and normalized using 18S rRNA as a reference gene. An average of 3 independent experiments are graphed and error bars denote SEM. Two-way ANOVA and a *post hoc* multiple comparisons test was done to determine statistical significance (****, p value < 0.0001).

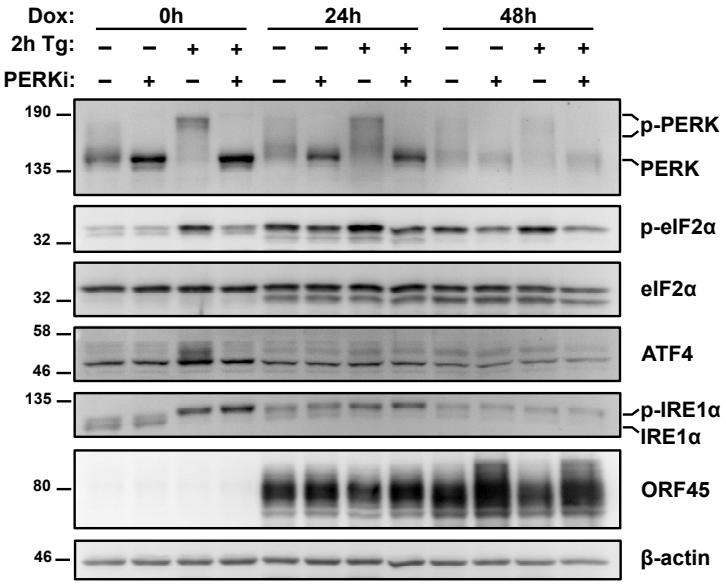

Fig 3.5 PERK-dependent eIF2α phosphorylation during lytic replication
TREx BCBL1-RTA cells were treated with 1 μg/mL dox with or without 500 nM PERK inhibitor GSK2606414 (PERKi) for 0, 24 and 48 h. 2 h prior to harvesting cell lysates, cells were treated with or without 75 nM Tg. Whole cell lysates were analyzed by immunoblots for PERK, phospho- and total eIF2α, ATF4, IRE1α, and ORF45. Migration shift in PERK and IRE1α immunoblots correspond to phosphorylation. β-actin was used as a loading control. Immunoblots shown are representative of two independent experiments.

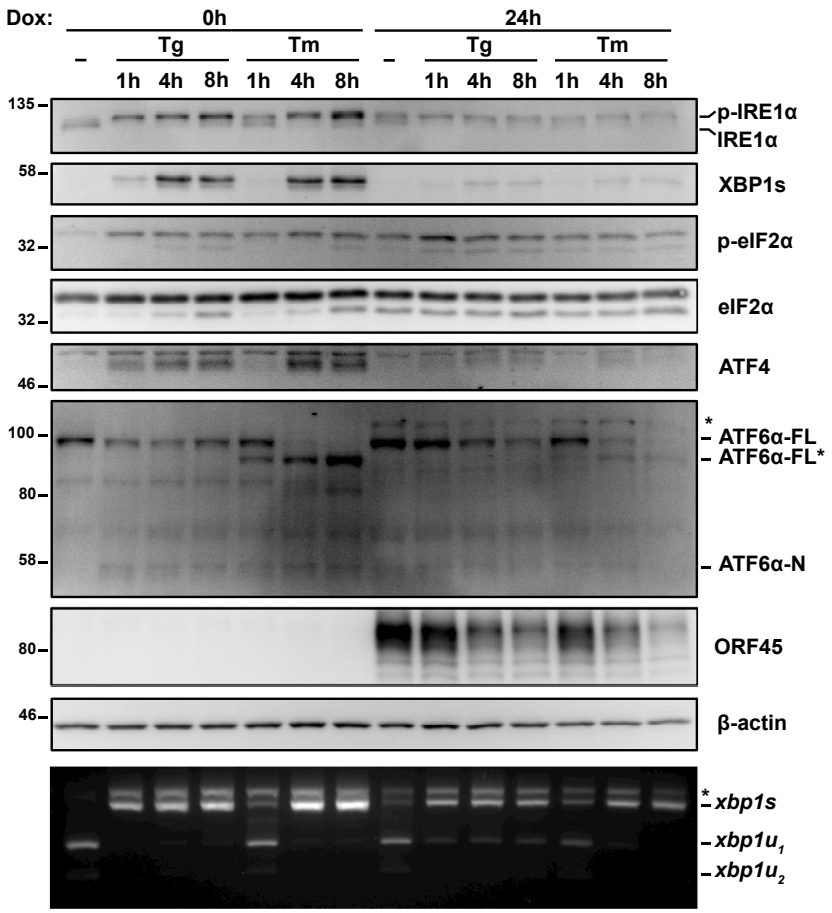

Fig. 3.6 Lytic replication inhibits ATF4 and XBP1s in response to different inducers of ER stress

TREx BCBL1-RTA cells were treated with dox for 0 or 24 h with 75nM Tg or 5 μg/mL Tm for 1, 4, or 8 h prior to harvesting for either protein or RNA. Whole cell lysates were analyzed by immunoblots for UPR markers (IRE1α, XBP1s, phospho- and total eIF2α, ATF4, and ATF6α). (*) in ATF6 immunoblot is likely a non-specific band that is upregulated during lytic replication. ATF6-FL* is generated as a result of ATF6 deglycosylation by Tm treatment. KSHV protein ORF45 was probed to show lytic replication and β-actin was used as a loading control. (Bottom) Total RNA was analyzed for XBP1 mRNA splicing using the XBP1 RT-PCR splicing assay as previously indicated. (*) corresponds to xbp1u-xbp1s hybrid cDNA. Immunoblots and agarose gels are representative of two independent experiments.

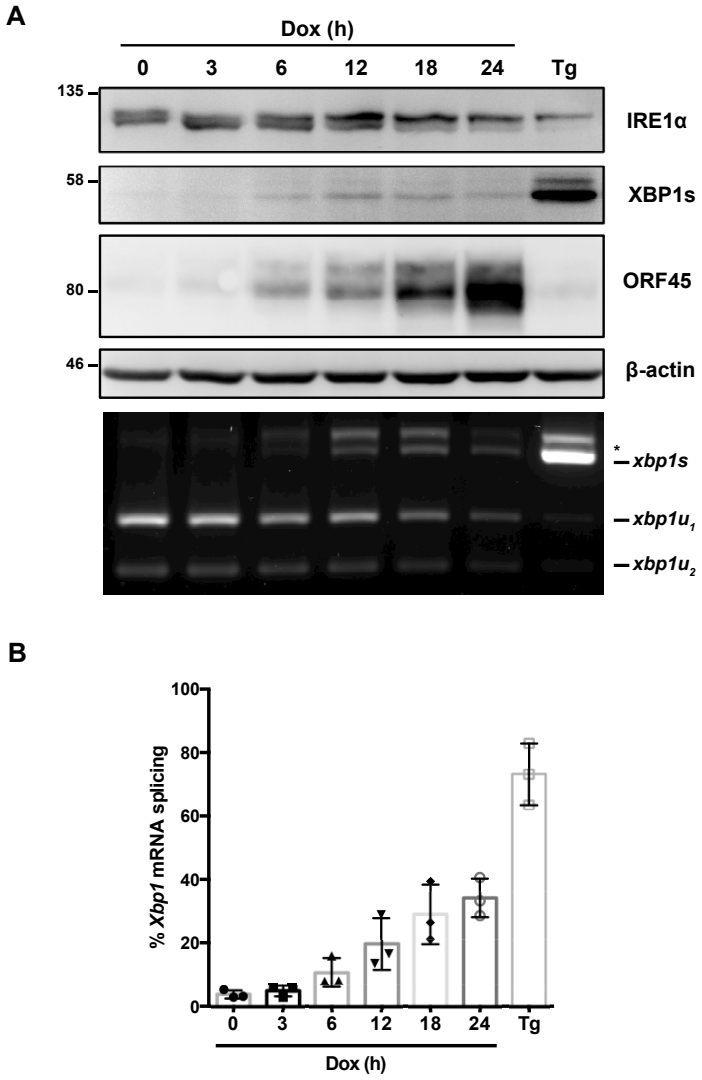

Fig 3.7 Low levels of XBP1s protein are induced during lytic replication
(A) TREx BCBL1-RTA cells were treated with 1 μg/mL dox for the indicated times or treated with 75nM Tg for 4 h as a positive control and harvested for either protein or RNA. Immunoblot analysis of IRE1α, XBP1s, ORF45 and β-actin (loading control) were completed. (Bottom) An XBP1 RT-PCR splicing assay was performed to determine extent of XBP1 mRNA splicing. (*) corresponds to xbp1u-xbp1s hybrid cDNA. Representative immunoblots and agarose gel for three independent experiments are shown. (B) Densitometry analysis from semi-quantitative XBP1 RT-PCR splicing assay in (A) was performed to calculate the percentage of XBP1 in the spliced isoform. The mean of three independent experiments are graphed and error bars represent the standard deviation (SD) of the mean.

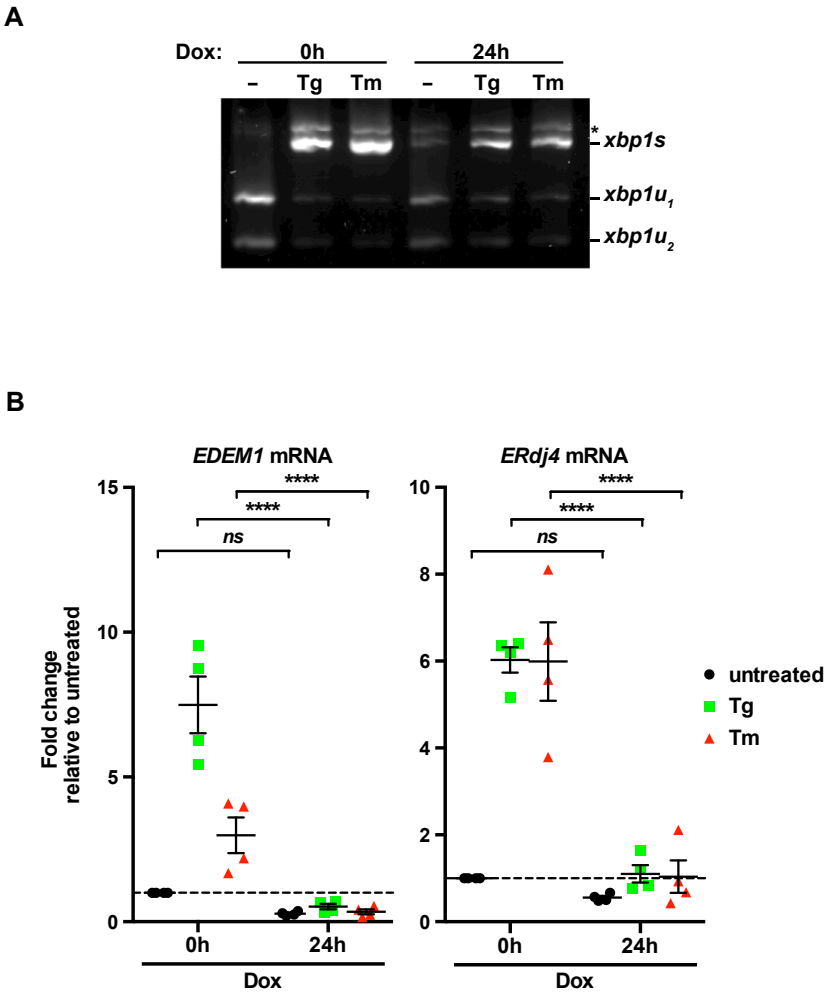

Fig 3.8 XBP1s target genes are not upregulated during lytic replication
(A) TREx BCBL1-RTA cells were treated with 1 μg/ml dox for 0 or 24 h and treated with 75nM Tg or 5 μg/mL Tm for 4 h prior to RNA isolation. XBP1 mRNA splicing was determined by semi-quantitative RT-PCR splicing assay as previously described. The gel shown is representative of two independent experiments. (B) Total RNA samples from (A) were used to measure the mRNA levels of XBP1 target genes EDEM1 and ERdj4 by qPCR. Changes in mRNA levels were calculated by the ΔΔCt method and normalized using 18S rRNA as a reference gene. An average of 4 independent experiments are graphed and error bars denote SEM. Two-way ANOVA and a *post hoc* multiple comparisons test was done to determine statistical significance (****, p value < 0.0001).

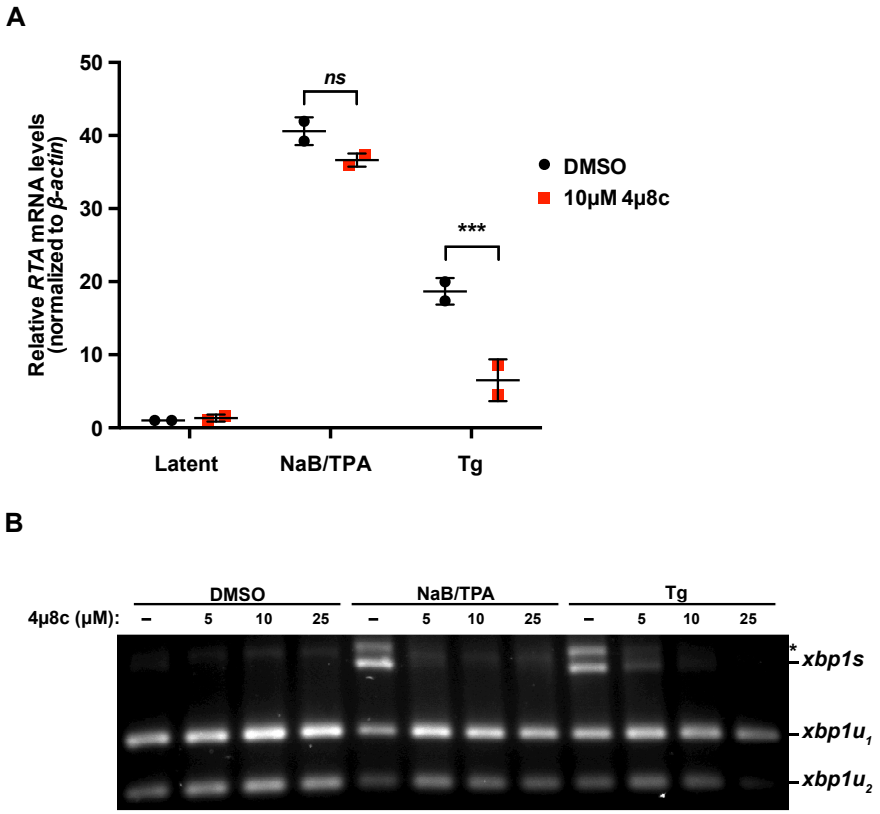

Fig 3.9 Tg-induced RTA but not Nab/TPA-induced RTA is dependent on XBP1 splicing

(A) BCBL1 wild type cells were treated with 1 mM sodium butyrate (NaB) and 20 ng/mL TPA or 150 nM Tg for 24 h with 10 μM IRE1 inhibitor 4μ8c or DMSO vehicle control prior to RNA isolation. mRNA levels of RTA levels were measured by qPCR and changes in mRNA levels compared to DMSO-treated latent BCBL1 cells were calculated by the ΔΔCt method and normalized using β-actin mRNA as a reference gene. An average of 2 independent experiments are graphed and error bars denote SD. (B) Similar to (A), but wild type BCBL1 were treated with increasing concentrations of 4μ8c and semi quantitative RT-PCR XBP1 splicing assay was done to confirm inhibition of XBP1 splicing by the 4μ8c.

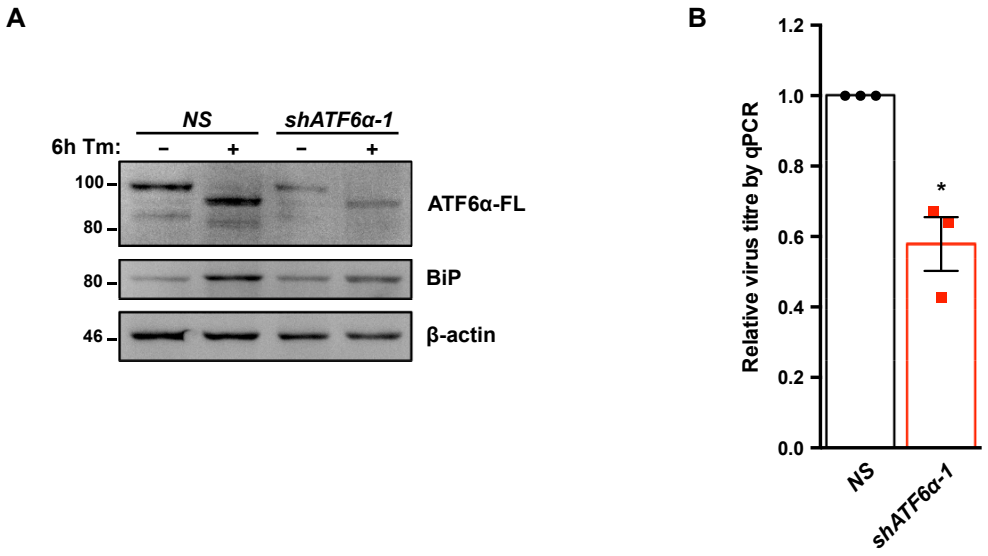

Fig 3.10 ATF6α activation supports robust KSHV replication
(A) TREx BCBL1-RTA cells were transduced with lentivirus expressing either non-targeting shRNA (NS) or shRNA against ATF6 and selected for with 1 μg/mL puromycin. Following selection, cells were treated with 5 μg/mL Tm for 6 h and harvested for immunoblot analysis to confirm ATF6 knockdown. The immunoblot shown is representative of two independent experiments performed. (B) TREx BCBL1-RTA cells from (A) were treated with 1 μg/ml dox for 48 h and virus-protected genomic DNA from supernatants were column purified to determine virus titer by qPCR using primers against KSHV ORF26. Firefly luciferase plasmid DNA was added during DNA purification to use for normalization with luciferase primers using the ΔΔCt method. The mean of 3 independent experiments are graphed and error bars denote SEM. One-way ANOVA and a *post hoc* multiple comparisons test was done to determine statistical significance. (*, p value <0.05).

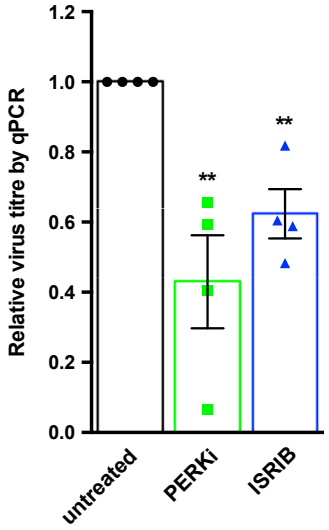

Fig 3.11 PERK activation supports robust KSHV replication
TREx BCBL1-RTA cells were treated with 1 µg/mL dox for 48 h with or without 500 nM PERKi GSK2606414 or 250 nM ISRIB, and virus-protected genomic DNA from supernatants were column purified to determine virus titer by qPCR using primers against KSHV ORF26. Firefly luciferase plasmid DNA was added during DNA purification to use for normalization with luciferase primers using the ΔΔCt method. The mean of 4 independent experiments are graphed and error bars denote SEM. One-way ANOVA and a *post hoc* multiple comparisons test was done to determine statistical significance. (**, *p* value <0.01).

Fig 3.12 IRE1α activation supports robust KSHV replication
(A) TREx BCBL1-RTA cells were treated with 1 μg/mL dox for 48 h without or with increasing concentrations of IRE1 inhibitor 4μ8c and virus-protected genomic DNA from supernatants were column purified to determine virus titer by qPCR as previously described. The mean of four independent experiments are graphed and error bars represent the SEM. (B) iSLK.219 cells were treated with 1 μg/mL dox without or with 10 or 25 μM 4μ8c for 96 h and virus-containing supernatants were serially-diluted and spinfected onto a monolayer of 293A cells. GFP-positive cells (infected) were quantified by flow cytometry the following day and virus titer was calculated as described in the Materials & Methods. The mean of four independent experiments are graphed and error bars denote the SEM. (C) iSLK.219 cells were transduced with two different pLKO.1-blast shRNA lentiviruses targeting IRE1α or a non-targeting control and selected for with blasticidin. Following selection, cells were treated with 150nM Tg for 4 h and harvested for immunoblot analysis of IRE1 and XBP1 were performed to confirm IRE1α knockdown. The immunoblots shown are representative of two independent experiments. (D) Lentivirus-transduced iSLK.219 cells from (C), were treated with dox for 96h and virus titer was determined in 293A cells by flow cytometry as previously described. The data are represented as the change in virus titer relative to the non-targeting shRNA control sample and the mean of three independent experiments are graphed. Error bars represent the SEM. One-way ANOVA and multiple comparisons test were done to determine statistical significance in (A), (B), and (D). (ns, not statistically significant; *, p value < 0.05; **, p value < 0.01; ***, p value < 0.001)

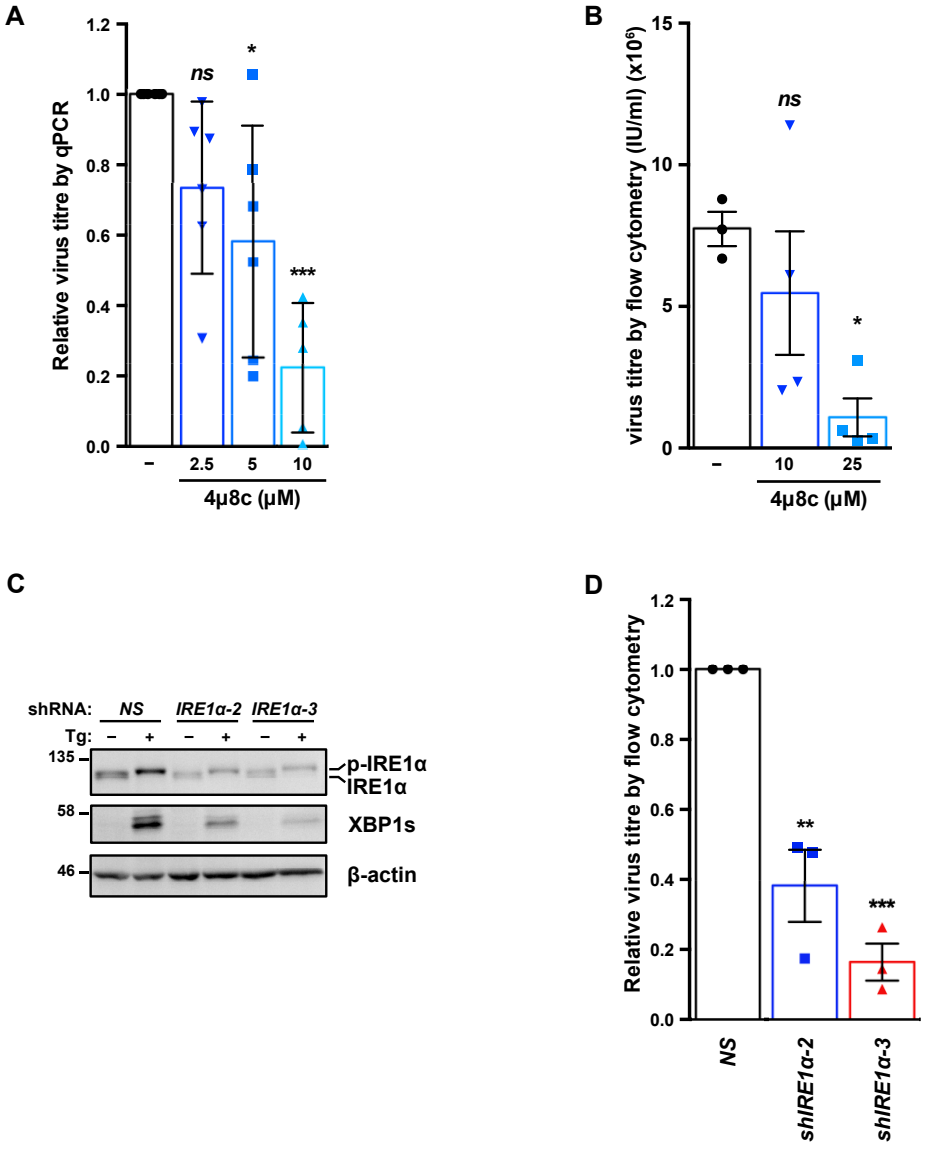
A
Relative virus titre by qPCR
1.2
1.0
0.8
0.6
0.4
0.2
0.0
ns
*
***
–
2.5
5
10
4μ8c (μM)
B
virus titre by flow cytometry (IU/ml) (x10⁶)
15
10
5
0
ns
*
–
10
25
4μ8c (μM)
C
shRNA:
NS
IRE1α-2
IRE1α-3
Tg:
–
+
–
+
–
+
135
58
46
p-IRE1α
IRE1α
XBP1s
β-actin
D
Relative virus titre by flow cytometry
1.2
1.0
0.8
0.6
0.4
0.2
0.0
**
***
NS
shIRE1α-2
shIRE1α-3

CHAPTER 4 SELECTIVE INHIBITION OF KSHV LYTIC REPLICATION BY XBP1S

4.1 Introduction

X box binding protein 1 (XBP1), as the name suggests, was discovered because of its ability to bind to a region in the HLA-DRα promoter called the X box and promote MHC class II expression (Liou et al., 1990). It wasn't until almost 15 years after its discovery that IRE1 was found to activate XBP1 into a potent transcription factor by mRNA splicing as part of the unfolded protein response (UPR) (Calfon et al., 2002; Yoshida et al., 2001). In response to ER stress, XBP1s (Hac1p in yeast) upregulates genes to mitigate the stress such as chaperones and genes involved in protein degradation through ERAD (A.-H. Lee et al., 2003a; Shoulders et al., 2013).

XBP1s also has a role in developmental biology and normal physiology. One of the first identified physiological roles for XBP1s was in hepatocyte growth and survival; knocking out XBP1 in mice resulted in embryonic lethality due to extreme liver hyperplasia (Reimold et al., 2000). XBP1s has also been shown to be important for memory formation (Martínez et al., 2016), adipogenesis (Sha et al., 2009), and the differentiation of various cell types that have a high translational burden in the ER, most notably professional secretory cells. This include insulin-secreting pancreatic β cells (A.-H. Lee et al., 2011), granulocytic eosinophils (Bettigole et al., 2015), and antibody-secreting plasma cells (PCs) (Reimold et al., 2001).

In the case of PC differentiation, mature B cells bind foreign antigens through the B cell receptor (BCR), which elicits a cytokine-driven response and coordinated transcriptional reprogramming to differentiate into terminally-differentiated PCs (Shaffer et al., 2002). Importantly, XBP1s is upregulated by the plasma cell master transcriptional regulator Blimp-1 and XBP1s can upregulate IL-6, an important cytokine that drives terminal differentiation of mature B cells into PCs (Iwakoshi et al., 2003b). Blimp-1 also represses PAX-5, a transcriptional repressor of XBP1, and BCL-6, a repressor of Blimp-1 (Shaffer et al., 2002). XBP1 knockout cells, stimulated by various inducers of PC differentiation, failed to express PC markers like CD138 (Syndecan-1), and had reduced IgM secretion (Reimold et al., 2001). XBP1 knockout B cells also have increased c-myc expression, which drives cell cycle progression. Mice with XBP1 knockout B cells had fewer plasma cells even though germinal center formation was unaffected and these mice

were more susceptible to polyoma virus infection than wild type mice (Reimold et al., 2001).

Dysregulated XBP1 is also implicated in multiple diseases, either due to a lack of XBP1s or hyperactive XBP1s, including ischemia reperfusion injury (Z. V. Wang et al., 2014), Huntington's disease (Vidal et al., 2012), breast cancer (X. Chen et al., 2014), and multiple myeloma (Carrasco et al., 2007). Interestingly the above examples do not involve activation of UPR but rather a specific engagement of the IRE1-XBP1 pathway.

XBP1s is a basic leucine zipper (bZIP) domain transcription factor that belongs to the CREB subfamily of transcription factors and binds to CRE-like sequences that have an ACGT core (Clauss et al., 1996). This ACGT core is essential for XBP1 transactivation. During ER stress, XBP1 can bind to a consensus binding sequence TGACGTGG/A, which is referred to as the UPRE (unfolded protein response element) (Yoshida et al., 2001). XBP1 can also transactivate other genes which contain sequence motifs that diverge from the UPRE, including the ERSE-II (K. Yamamoto et al., 2004). Multiple groups have used various techniques to identify XBP1 target genes (Acosta-Alvear et al., 2007; A.-H. Lee et al., 2003a; Shoulders et al., 2013). Some of these studies rely on overexpression of XBP1 or pharmacological induction of stress, and therefore, depending on the model used, the XBP1s target genes may vary. These XBP1s target genes may also differ from the ones that are induced in response to physiological triggers of ER stress or if the IRE1-XBP1 pathway is specifically engaged independent of ER stress. XBP1s target genes may also be cell type-dependent. For example, following TLR2 or TLR4 activation in macrophages, XBP1s upregulates inflammatory cytokines such as IL-6 and TNFα (Martinon et al., 2010). XBP1s can also heterodimerize with ATF6 in response to ER stress, which changes the gene expression profile of XBP1 (Reinke et al., 2013; Keisuke Yamamoto et al., 2007). There is also evidence that XBP1s expression can promote or inhibit replication of multiple different viruses and during infection the genes that are transcriptionally upregulated may be different than classical ER stress-induced genes.

KSHV is a lymphotropic gamma-herpesvirus that is the infectious cause of two B cell lymphoproliferative disorders, primary effusion lymphoma (PEL), and multicentric Castleman's disease (MCD) (Cesarman et al., 1995; Y. Chang et al., 1994; Soulier et al., 1995). KSHV causes disease primarily in patients who are immunosuppressed and thus

there is strong co-morbidity in HIV-infected individuals. It is thought that KSHV primarily infects naïve B cells and causes them to differentiate into cells that have a plasmablast phenotype (M. Q. Du et al., 2001), with PEL cells having a late plasmablast phenotype (Hassman et al., 2011). One of the striking differences between PEL cells and PC gene expression profile is that PEL cells have a much lower expression level of UPR related genes (Jenner et al., 2003). PEL cells are also defective in Ig production (Di Bartolo et al., 2009).

Some of the shared phenotypic features between PEL and MCD cells are that they are both PAX-5 and BCL-6 negative, but Blimp-1, IRF4, and Ki67 positive (A Chadburn et al., 2008). MCD differs from PEL due to the presence of OCT-2 and cytoplasmic Igλ and they lack expression of PC marker Syndecan-1 (CD138). MCD cells are EBV negative, whereas approximately 75 % of PEL cells are co-infected with EBV, which greatly correlates with the incidence of AIDS (Drexler, Uphoff, Gaidano, & Carbone, 1998).

As its name indicates, KSHV has also evolved to expand its cellular repertoire, including endothelial cells, which are thought to be the precursor spindle cells in a KS lesion cells. *In vitro*, KSHV can also infect a wide variety of human and non-human transformed cells, as well as non-transformed cell lines (Bechtel et al., 2003). There is also *in vivo* evidence that KSHV can infect epithelial cells (Yarchoan & Davis, 2002), which are likely important for viral transmission, since saliva is the primary source of person-to-person transmission (Myoung & Ganem, 2011a).This is analogous to EBV infection, where the presumed source of virus in the oropharynx is tonsillar B cells (Hatton, Harris-Arnold, Schaffert, Krams, & Martinez, 2014). Interestingly, even though KSHV is a B cell virus, the efficiency of *in vitro* KSHV infection of primary or transformed B cells is low compared to other non-B cell lineages. Currently the reason for this paradox is unknown. Similar to a model of viral transmission from oral epithelial to tonsillar B cells, infecting B cells *in vitro* can be circumvented with the use of co-culture systems involving the B cell and a KSHV-infected adherent cell line that generates high viral titer (Myoung & Ganem, 2011c).

Following infection, KSHV undergoes latency and the viral genome is normally maintained as a circular episome tethered to the host chromatin by the latent protein LANA (Ballestas et al., 1999). However, in a laboratory setting, a stable persistent

infection is rarely achieved and continual cell passaging results in gradual elimination of the viral episome (Grundhoff & Ganem, 2004). For this reason, PEL and MCD tumors isolated from patients, which stably maintain the viral episome, are primarily used for understanding KSHV biology. This includes the EBV-negative PEL cell line BCBL1.

Although the default replication program of KSHV is latency, approximately 1-2 % of cells in a PEL tumor undergo spontaneous lytic replication and the cause of this reactivation is not known (Ganem, 2007). RTA is the immediate early protein and its expression is sufficient and necessary to induce the lytic gene cascade (Lukac et al., 1998; Ren Sun et al., 1998). Following expression, RTA uses different cellular transcription factors, including RBP-J-κ, to mediate a temporally regulated cascade that follows a classical herpesvirus gene expression profile: early gene expression, delayed gene expression, genome replication, and late gene expression (Staudt & Dittmer, 2007). Following late gene expression, replicated linear genomes are packaged into icosahedral capsids in the nucleus, which then bud out of the nuclear envelope and appropriate lipid membranes at the *trans*-Golgi network (TGN) as it acquires its tegument proteins (Mettenleiter, 2002). The virions then bud out of the cell membrane into the extracellular milieu.

When lytic replication was first being studied, sodium butyrate (NaB) and/or TPA, which were first used to reactivate EBV (Luka et al., 1979), were also used to reactivate KSHV (Black et al., 1999). Although the precise details of how these drugs trigger reactivation are not known, NaB is an HDAC inhibitor and thus increases global transcription of both cellular and viral genes by loosening chromatin from histones (Riggs, Whittaker, Neumann, & Ingram, 1977). TPA is thought to activate replication through the ERK and PKCδ pathways (Cohen et al., 2006). These drugs have pleiotropic effects and thus to clearly understand the cellular and viral gene interactions during the lytic cycle, a more directed approach for reactivating the virus from latency was required. Because of this, groups have transfected RTA or engineered recombinant adenoviral or baculoviral vectors to express RTA upon infection (Bechtel et al., 2003). To eliminate the requirement for infecting or transfecting cells every time to induce lytic reactivation, H. Nakamura, *et al.* (2003) engineered BCBL1 cells to express RTA from a dox-inducible promoter, generating the cell line TREx BCBL1-RTA. These cells produce large amounts of virus, which is likely due to the large number of genome copies. On average, a BCBL1

cell harbors > 50 viral episomes (Asahi-Ozaki et al., 2006). Some of the downsides to using these cells are that they undergo spontaneous lytic replication in a small percentage of cells, which cannot be easily identified. These cells are also suspension cells, and thus experimental assays (like immunofluorescence imaging) are not ideal. Furthermore, there is not an easy method to measure the titer of the virus.

Vieira & O'Hearn (2004) overcame some of these limitations by engineering a recombinant KSHV genome, rKSHV.219. This recombinant viral genome contains RFP under the control of the abundant early lytic promoter PAN to allow for detecting cells that are undergoing lytic reactivation, as well as a constitutively active EF-1α promoter that drives GFP expression to identify infected cells. Constitutive GFP expression can also be used to easily measure virus titer. This recombinant virus also expresses a puromycin resistance gene to minimize shedding of viral episomes during cell passaging, as discussed previously. Vero cells, containing rKSHV.219, generated robust virus titers only when transduced with an RTA-bearing baculovirus along with NaB treatment. The rKSHV.219 system typically displayed tight control of latency following infection (Vieira & O'Hearn, 2004). However, many of the rKSHV.219 infected cell lines tested were not biologically-relevant cell models for KSHV infection. In an attempt to create a more biologically relevant cell model, SLK cells isolated from a KS tumor in 1990 and believed to be of endothelial origin, were infected with rKSHV.219 (Myoung & Ganem, 2011b). Although still a relevant cell model for studying KSHV lytic replication, SLK cells were eventually found to be a contaminant from the renal-cell carcinoma cell line Caki-1 (Stürzl et al., 2013).

These latently infected SLK cells were also engineered to induce lytic reactivation, via a dox-inducible promoter, and were renamed iSLK.219. Clones were isolated based on their ability to maintain tight control of latency (i.e., no spontaneous reactivation based on RFP expression) and produce high viral titers following dox or combined dox and NaB treatment. The selected clones displayed 100-fold higher titer compared to dox-inducible Vero cells and showed titers similar to that obtained from BCBL-1 cells (Myoung & Ganem, 2011b).

Some of the main differences that I have observed between the two different cell models is that the majority of BCBL1 and TREx BCBL1-RTA cells undergo lytic replication following exposure to reactivation stimuli, whereas only 30-40% undergo

lytic reactivation in iSLK.219 cells following dox treatment. The other noticeable difference is that the duration of lytic replication is faster in TREx BCBL1-RTA cells compared to iSLK.219 cells. Following dox treatment of TREx BCBL1-RTA cells, early lytic and late lytic replication begin at 6 and 24 h, respectively, whereas early and late lytic replication in BCBL1 cells treated with TPA occur at approximately 12-16 h and 36-48 h, respectively, and virus can be detected in the supernatant by 48 h. iSLK.219 cells replicate even slower; following dox treatment, early and late gene expression begins at 8-24 h and 48-72 h, respectively, with the bulk of virus secretion into the supernatant occurring from 72 to 96 h. In both TREx BCBL1-RTA and iSLK.219 cells, the amount of virus produced, and onset of gene expression can be augmented with the addition of NaB and/or TPA. Both cell lines have been useful for studying and understanding the molecular mechanisms of lytic replication and both cell lines have obvious advantages and disadvantages in regard to their use. Although BCBL1 cells are a more relevant cell line for KSHV infection, iSLK.219 tight control or latency, robust titers and their ease of measuring titer, still makes these cells a tractable model for studying lytic replication *in vitro.*

Although these model cell lines have easy ways to induce RTA expression and lytic reactivation, the physiological and environmental factors that induce RTA expression and consequently lytic replication are not well defined. As discussed in Chapter 3, various forms of stress can reactivate the virus *in vitro.* One mechanism of linking reactivation in response to stress is through the co-option of stress-dependent transcription factors by incorporating their DNA targeting sequences within the RTA promoter. This includes the presence of multiple hypoxia-response elements (HREs) in the RTA promoter to facilitate HIF-1-dependent RTA expression following exposure to low oxygen levels (Q. Cai et al., 2006). Similar to XBP1 binding sites (i.e. UPREs), HREs can also contain a conserved ACGT core motif. An originally defined HRE (5'-ATGAC<u>ACGT</u>CCC-3', with the ACGT core underlined) is located immediately upstream of the RTA transcription start site and showed stronger transactivation activity by XBP1s than HIF-1 (Dalton-Griffin et al., 2009). As a result, this *cis*-acting element was reclassified as an XBP1 binding site and facilitates virus reactivation following exposure to ER stress. XBP1s-mediated reactivation is not specific to KSHV, as the closely related EBV and MHV68 gamma herpesviruses reactivate from XBP1s

expression through the direct binding and transcriptional activation of their respective immediate early genes (Bhende et al., 2007; Matar et al., 2014). Interestingly, even though XBP1s can reactivate MHV68 *in vitro*, it does not seem to be important for reactivation *in vivo,* at least by standard reactivation protocols (Matar et al., 2014). XBP1s was also shown to reactivate rKSHV.219 from a latently infected mature B cell line following crosslinking of the BCR with IgM antibody, consistent with the fact that XBP1s is important for PC differentiation in response to antigen-activated BCR signaling (Kati et al., 2013). Ectopic XBP1s can also force reactivation in the absence of ER stress or BCR stimulation but there is little evidence that XBP1s-mediated reaction can complete the replication cycle and produce infectious progeny virions. Since XBP1s protein does not accumulate in KSHV lytic replication, despite efficient XBP1 mRNA splicing (Chapter 3), I sought to determine the effect that ectopic XBP1s expression has on the lytic replication cycle.

4.2 Results

4.2.1 Viral Gene Expression is Enhanced Early by XBP1s Overexpression

The results from Chapter 3 indicate that the UPR sensors are important for lytic replication but the downstream transcription factors, including XBP1s, are inhibited, suggesting that KSHV may re-dedicate the UPR for a role other than resolving ER stress to support virus production. Upon initial inspection, these findings appear inconsistent with the evidence that XBP1s promotes virus replication through RTA transactivation. For this reason, I wanted to test the effects of ectopic XBP1s expression on virus gene expression.

I created a lentiviral vector bearing a myc-tagged XBP1s driven by a tetracycline response element (TRE), which contains 7 tandem Tet operators (TetO; 7xTetO). The addition of dox results in robust gene expression (Gossen et al., 1995). This allows for tight control of XBP1s expression in order to prevent spontaneous lytic reactivation upon lentivirus transduction, unlike if XBP1s expression was driven from a constitutively active promoter like CMV. iSLK.219 cells were transduced with 7xTetO myc-XBP1s lentiviral vector followed by the addition of dox, which drives virus reactivation from both RTA and myc-XBP1s transgene expression. mRNA levels of the viral gene transcripts RTA (immediate early), ORF45 (early), and K8.1 (late) were measured over a

4-d time course. To confirm that K8.1 is a late gene, cells were also treated with a viral DNA polymerase inhibitor PAA. mRNA levels of XBP1s target gene ERdj4 were also measured to confirm myc-XBP1s expression. By 24 h post-dox there was a clear upregulation of ERdj4 mRNA with the overexpression of XBP1s (Fig 4.1), but interestingly these mRNA levels returned to baseline levels by 48 h. There was also a marked increase in RTA, ORF45, and K8.1 mRNA levels compared to empty vector control by 24 h.

In this cell model, genome replication normally begins between 36 and 48 h post-dox, which precedes late gene expression (Myoung & Ganem, 2011b). Based on the gene expression profile of the late gene K8.1, genome replication in XBP1s likely begins around 24 h post-dox, indicating the replication cycle is accelerated with XBP1s overexpression. This may be due to an overall enhancement of viral gene expression. By 72 h post-dox, the mRNA levels of viral transcripts are significantly lower in XBP1s-expressing cells compared to empty vector control, which may be due to increased toxicity due to this vigorous replication cycle.

This accelerated and enhanced viral gene expression profile can also be seen at the protein level. iSLK.219 cells were transduced with 7xTetO myc-XBP1s as well as a lentiviral vector that expressed myc-XBP1 under the control of a single TetO (1xTetO), which results in lower levels of XBP1s expression. This low level of XBP1s expression only had a nominal impact on RTA, ORF45, and ORF65 (a late protein) expression, which was not apparent until 96 h post-dox (Fig 4.2A). By contrast, cells expressing myc-XBP1s from the 7xTetO showed significantly enhanced RTA, ORF45, and ORF65 expression by 48 h post-dox. There was also a noticeable change in the banding pattern of XBP1s in these cells. At 48 h a potential XBP1 protein species of ~ 75 kDa appears and persists up to 96 h.

After 96 h of high XBP1s expression, there was a markedly obvious decrease in ORF45 levels, as well as the ~ 19 kDa ORF65. Interestingly, an ~ 35 kDa protein species that cross-reacts with ORF65 antisera can be detected in all samples at 96 h, which may potentially be a post-translationally modified version of ORF65. As of yet this potentially modified version of ORF65 has not been characterized. There are also protein bands that migrate at ~ 28 kDa and ~ 58 kDa, in which the former is unlikely a modified species of ORF65, because it can be detected at 24 h post-dox in the empty vector control, which is

before late gene expression has occurred. Measuring the levels of intracellular viral DNA by qPCR showed that genome replication was occurring in cells expressing 7xTetO myc-XBP1s but was also enhanced approximately 2-fold compared to the empty vector control (Fig 4.2B). These data demonstrate that XBP1s overexpression can augment viral gene expression, but at later stages in the replication cycle high levels of XBP1s attenuate viral gene expression.

4.2.2 XBP1s Ectopic Expression Suppresses Virus Production in iSLK.219 Cells

Since combined RTA and XBP1s expression can enhance virus gene expression, I wanted to determine if this also resulted in enhanced virus production. The recombinant KSHV genome in iSLK.219 cells bears a GFP gene driven by the strong EF-1α promoter, which can be used to measure virus titer (Myoung & Ganem, 2011b). Serially-diluted virus-containing supernatants from iSLK.219 cells treated with dox for 48, 72, and 96 h were inoculated onto a monolayer of 293A cells and GFP-positive cells were enumerated by flow cytometry the following day. Surprisingly, although viral gene expression was enhanced in cells transduced with 7xTetO myc-XBP1s construct after 48 h (Figs 4.1 and 4.2A), virus titer was similar to empty vector control and cells expressing myc-XBP1s from 1xTetO promoter (Fig 4.3A). Strikingly, by 72 and 96 h post-dox, there was an approximately 10- and 40-fold decrease in virus titer, respectively, from the cells expressing high levels of XBP1s. There was a 2-fold decrease in titer from cells expressing lower levels of XBP1s, which did not have a significant impact on viral gene expression. This virus titering assay measures the level of infectious progeny virions; to determine if the decrease in virus titer was due to a failure to generate infectious virus particles or a block in virus release or an earlier step in the replication cycle, DNAse I-resistant viral genomic DNA from cell supernatant were measured by qPCR. This exhibited a 20-fold decrease in release of virus particles in cells expressing high levels of XBP1s compared to empty vector control, indicating that XBP1s does inhibit the release of virus particles (Fig 4.3B). To test if the inhibition of KSHV by XBP1 was dependent on its C-terminal activation domain, iSLK.219 cells were also transduced with myc-XBP1u, which can be spliced to form active XBP1s, and an XBP1u mutant (XBP1u*G519A*) that has a mutation in a conserved guanine residue in one of the stem loops of XBP1 mRNA that blocks splicing by IRE1 (Yoshida et al., 2001). Expression of the spliceable XBP1u isoform following 72 and 96 h dox treatment resulted in potent

inhibition of virus titer, although not as robust as XBP1s (Fig 4.3C). Importantly, overexpression of the non-spliceable XBP1u mutant had no impact on virus production, indicating that it is only the XBP1 isoform with transactivating capabilities that can inhibit virus replication. Collectively, these data reveal that XBP1s and not XBP1u overexpression inhibits KSHV at a late stage of the replication cycle.

4.2.3 XBP1s Inhibition of KSHV is not due to Enhanced RTA Expression

Since XBP1s transactivates RTA, the tet-inducible myc-XBP1s expressing iSLK.219 cells show a hyperactivation of RTA, which may be contributing to the XBP1-dependent decrease in virus production, due to increased apoptosis (Nishimura et al., 2003). To test if higher levels of RTA expression inhibit virus production, iSLK.219 cells were also transduced with 7xTetO FLAG-tagged RTA. After the addition of dox these cells will express RTA from two different tet-inducible promoters. iSLK.219 cells express RFP under the early lytic PAN promoter and so to ensure that RTA and XBP1s tet-inducible cell lines had similar reactivation profiles, RFP positive cells were visualized by fluorescence microscopy after 48 h post-dox. XBP1s and RTA showed similar levels of RFP-positive cells and were significantly more RFP-positive than the vector control, reflecting enhanced early viral gene expression (Fig 4.4A). Virus titer was measured over a 4-d time course by flow cytometry, as described previously. By 24 h post-dox there was a significant increase in progeny virus in 7xTetO RTA-expressing cells. By contrast, it took 48 h for accumulation of similar titers of progeny virus from the 7xTetO myc-XBP1s-expressing cells or empty vector control, indicating that the presence of two RTA ORFs driven by two different tet-inducible promoters can accelerate virus production (Fig 4.4B). This increase in virus titer in 7xTetO RTA expressing cells continued until 72 h post-dox, and by 96 h the virus titer plateaued, possibly due to cell toxicity. Consistent with previous results, virus titer from cells expressing 7xTetO myc-XBP1s was dramatically reduced compared to empty vector. These data demonstrate that KSHV inhibition by XBP1s overexpression is not due to off-target effects of enhanced RTA expression, while the lack of enhanced or accelerated virus production that was observed for RTA overexpression, suggests that there may be an XBP1s-dependent factor that is preventing viral progeny release.

4.2.4 KSHV Titer is not Enhanced in iSLK.219 with Increasing Levels of XBP1s

These findings indicate that XBP1s can be both pro-viral (by promoting RTA expression and enhancing viral gene expression) and anti-viral (by inhibiting lytic replication at a late phase). Since the previous data was based on using dox-inducible XBP1s, I wanted to determine if XBP1s-mediated reactivation alone could generate infectious virions. To do this, myc-XBP1s was expressed from a constitutive CMV promoter rather than the tet-inducible promoter. iSLK.219 cells were transduced with increasing concentrations of myc-XBP1s or FLAG-RTA lentiviral vectors for 5 d, and for a subset of the lentivirus dilutions RFP-positive cells were imaged by fluorescence microscopy, which demonstrated similar levels of lytic replication from XBP1s and RTA expression (Fig 4.5A). As a positive control, RFP-positive cells were visualized from untransduced cells that were treated with dox for 48 h. 24 h later, virus-containing supernatants were harvested and flow cytometry was used to calculate virus titer. There was a dose-dependent increase in virus titer from RTA lentiviral vector expression in iSLK.219 cells and the levels were similar to 72 h post-dox in the most concentrated lentivirus stock (Fig 4.5B). Interestingly, even though there was a dose-dependent increase in lytic reactivation as approximated by RFP-positive cells (Fig 4.5A), increasing XBP1s levels did not enhance virus production and the levels were similar to that of cells expressing 7xTetO myc-XBP1s (Fig 4.3A).

Immunoblot analysis of matched lysates showed that although there was a dose-dependent increase in myc-XBP1s expression, there was not the same increase in RTA expression. Likewise, the predominant 85 kDa ORF45 protein species was consistently not enhanced with increasing levels of XBP1s, unlike in cells expressing increasing levels of CMV-driven RTA (Fig 4.5C). Interestingly, the banding pattern of ORF45 immunoblot was dramatically different in the XBP1s samples compared to the RTA-transduced or dox-treated control samples. As XBP1s expression increases there was a corresponding decline in a minor ORF45 protein species that is ~ 70 kDa and an increase in a higher MW species of ~ 100 kDa, which may represent changes in PTMs that impact ORF45 function. There is another protein species directly below the 70 kDa ORF45 species in RTA-transduced and dox-treated samples, which is absent in XBP1s-expressing cells. ORF65 immunoblot also showed striking differences in XBP1s-expressing cells compared to RTA-expressing cells; while there was a dose dependent

increase in the ~19 kDa ORF65 protein species in RTA-expressing cells, this protein species was not detected in XBP1s-expressing cells. There was however, a corresponding increase in the ~ 35 kDa ORF65 species with increasing XBP1s expression, which I observed previously (Fig 4.2A). This protein species was also observed in the dox-treated control sample and the FLAG-RTA transduced cells (Fig 4.5C). Curiously, there was a higher MW XBP1s protein species ~15 to 20 kDa larger than the unmodified XBP1s protein that was detected at all lentivirus dilutions and is possibly a PTM. This PTM likely corresponds to the PTM also observed previously (Fig 4.2A). These data are consistent with previous results that propose that XBP1s is both pro- and anti-viral and that increased XBP1s levels may trigger PTMs of viral proteins that could inhibit late stages of lytic replication.

4.2.5 XBP1s Overexpression does not Inhibit Virus Production in TREx BCBL1-RTA Cells

I next wanted to test if XBP1s also had the same inhibitory effect on titer in the TREx BCBL1-RTA cells as in iSLK.219 cells. TREx BCBL1-RTA cells were transduced with increasing concentrations of CMV-driven XBP1s or RTA for 72 h or treated with dox for 72 h as a positive control. These cells needed to be transduced with a more concentrated stock of XBP1s lentivirus compared to in iSLK.219 cells to express approximately similar levels of myc-XBP1s. This discrepancy in lentivirus concentration may be due to a decrease in susceptibility to transduction compared to iSLK.219 cells and could explain why RTA lentivirus concentrations, which did not change between cell types, resulted in much lower RTA expression in TREx BCBL1-RTA cells (Fig 4.6A). In contrast to iSLK.219 cells, XBP1s increased RTA, ORF45, and ORF65 in a dose-dependent manner similar to RTA expressing cells, concomitant with a dose-dependent increase in virus titer as determined by qPCR of DNase I-resistant extracellular viral DNA (Fig 4.6A and B). Interestingly, the lower MW species of ORF45 that were reduced in iSLK.219 were unaffected in XBP1s-expressing TREx BCBL1-RTA. ORF65 immunoblots were also different between the two cell lines. In the dox-treated control and the transduced TREx BCBL1-RTA cells, the 35 kDa ORF65 species detected in iSLK.219 cells was not present (Fig 4.6A). In fact, the 19 kDa ORF65 protein appears to be the only unique band detected in TREx BCBL1-RTA. These data indicate that unlike iSLK.219 cells, XBP1s is not anti-viral in TREx BCBL1-RTA cells and the differences in length of replication

cycle and/or potential PTMs of viral proteins (i.e., ORF65) may provide clues to the mechanism of action of XBP1s inhibition of KSHV.

4.2.6 The HDAC Inhibitor NaB Reverses XBP1s Suppression of KSHV Lytic Replication

Since the inhibitory effect of tet-inducible XBP1s observed in iSLK.219 cells does not occur until 72 h and XBP1s does not inhibit virus production in TREx BCBL1-RTA cells, which has a replication cycle of 48-72 h, I hypothesized that one possible reason for the discrepancy between cell lines is that XBP1s expression requires a significant amount of time to be inhibitory to KSHV. Therefore, I wanted to test if accelerating viral gene expression even more in iSLK.219 cells could circumvent the inhibitory effect of XBP1s. I measured virus production from 7xTetO myc-XBP1s iSLK.219 cells co-treated with both dox and the HDAC inhibitor NaB, which is known to enhance gene expression thereby accelerating the lytic replication cycle. Indeed, after combined dox and NaB treatment for 48 h in the empty vector control there was a robust increase in virus titer compared to 24 h (Fig 4.7A); normally virus production does not peak until 72 h in this cell model (Myoung & Ganem, 2011b). Strikingly, while XBP1s expression induced by dox alone for 96 h inhibits virus titer by ~ 20-fold (Fig 4.3A), combined treatment of dox and NaB in 7xTetO XBP1s-expressing cells had a similar virus titer profile as the vector control, indicating that XBP1s expression was no longer anti-viral when NaB was added (Fig 4.7A). Immunoblot analysis of the empty vector control corresponded with the titer data and 48 h post-dox and -NaB treatment of empty vector transduced cells resulted in robust expression of the late protein ORF65, which was not detected until 72 h with dox alone (Fig 4.7B). The lack of inhibitory effect of XBP1s on virus titer also corresponded with a clear restoration of ORF65 protein by 72 h with dox and NaB treatment compared to dox alone. The restoration of ORF65 levels by the addition of NaB is not due to a lack of XBP1s expression; in fact, NaB enhanced XBP1s levels. XBP1s is likely still active with NaB treatment, for there was a lack of lower MW species of ORF45 that was observed in iSLK.219 cells expressing CMV-driven XBP1s. By 72 h post-dox treatment of XBP1s-expressing cells there was a significant decrease in the 19 kDa ORF65 protein, and an accumulation of the 35 kDa species as seen previously. Both of these protein species were enhanced with NaB treatment. The changes in potential ORF45 protein species likely does not play a role in virus production, since XBP1s, in the presence or

absence of NaB, displayed an attenuation in the lower MW species, even though NaB abrogated the inhibitory effect of XBP1s on virus production.

4.3 Discussion

These findings show a contrasting phenotype of XBP1s-induced lytic replication and virus production depending on the cell model used and type of reactivation stimuli. See Appendix E for a summary of the different effects that XBP1 has on titer in the different cell models. XBP1s can induce lytic replication in the PEL cell line TREx BCBL1-RTA cells resulting in production of virus, whereas XBP1s potently blocks robust accumulation of infectious virions in iSLK.219 cells, even though XBP1s can still initiate the replication cycle by transactivating RTA. Furthermore, combined ectopic XBP1s expression with dox can enhance viral gene expression (analogous to NaB or TPA treatment) in iSLK.219 cells but this does not correspond to enhanced or accelerated virus production. This was not the case when RTA was expressed from a tet-inducible lentiviral vector; RTA strongly enhanced and accelerated production of infectious virus. These data also indicate that the inhibitory effect of XBP1s overexpression is not due to more pronounced RTA expression. RTA could have cytotoxic effects, due to either accelerated gene expression and premature apoptosis, or by directly increasing toxicity.

Curiously, the addition of NaB reversed the inhibitory effect of XBP1s on virus production. Although it may look like the combined treatment of XBP1s and NaB does not accelerate the replication cycle, this conclusion cannot be adequately made because the method of virus titer quantification that was used measures percent GFP-positive cells and has a smaller dynamic range compared to the other titering method used for iSLK.219 cells, which measures IU/mL. In the iSLK.219 model, the inhibitory effect of XBP1s is not evident until 72 h post-dox, which presents as a plateau in virus titer. If XBP1s-mediated inhibition of KSHV is occurring at a specific stage of the replication cycle, it is possible that NaB acceleration of viral gene expression makes it so that the event that XBP1s normally inhibits has occurred before XBP1s is ready to execute the inhibitory effect. Along these lines, the lytic cycle in TREx BCBL1-RTA is mostly complete by 48-72 h post-dox, and if XBP1s inhibition does not occur until 72 h post-dox then that may be one of the reasons why XBP1s is not anti-viral in TREx BCBL1-RTA cells.

There are also clear decreases in mRNA levels of multiple viral genes in the 7xTetO-XBP1s-expressing iSLK.219 cells. However, this attenuation in viral gene expression is likely not the only mechanism of virus inhibition. Low levels of XBP1s from a 1xTetO promoter did not have this impact on viral gene expression but still inhibited virus production by over 2-fold. If anything, viral gene expression may be enhanced with low XBP1s expression based on ORF45 and ORF65 immunoblots. Besides RTA upregulation, ectopic XBP1s also upregulates cellular genes, such as ERdj4, that are involved in ER protein homeostasis (A.-H. Lee et al., 2003a; Shoulders et al., 2013). ERdj4 expression in iSLK.219 cells is potently upregulated by 24 h post-dox in XBP1s-expressing cells but its expression returns to baseline by 48 h. Although this strong inhibition of virus titer is not evident until 72 h, the repertoire of XBP1s target genes may be conditioning the ER early on to promote an anti-viral environment, which is not evident until 72 h. By this time, the majority of ER-targeted viral glycoproteins are being synthesized and virus particles are transiting through the secretory pathway. In light of this, it would be interesting to determine if this transient burst in XBP1s-dependent cellular genes still elicited a function during the time when virus production is inhibited.

XBP1s can undergo PTMs including SUMOylation and acetylation (H. Chen & Qi, 2010; F.-M. Wang, Chen, & Ouyang, 2011). Although the precise function of these PTMs are not clear, it is thought they may impact protein stability and/or transcriptional activity. For example, mutations of the SUMO-modified lysine residues result in increased XBP1s transcriptional activity (H. Chen & Qi, 2010). Interestingly, the banding pattern of tet-inducible XBP1s immunoblot changes as lytic replication progresses. At 24 h there is a protein species ~85 kDa that likely corresponds to SUMOylated XBP1s. By 48 h, when ERdj4 is no longer transcriptionally upregulated, the potential SUMOylated XBP1s species begins to decrease while a new potential XBP1s PTM that migrates at 75 kDa begins to form, and it is maintained throughout the rest of lytic replication. This potentially modified version of XBP1s could theoretically change the transcriptional landscape of XBP1s or possibly impact the function of XBP1s, which may play a role in its anti-viral function. Although there may be a similar banding pattern in XBP1s immunoblots from TREx BCBL1-RTA cells, which does not inhibit virus production, the relative level of this PTM compared to total XBP1s is much smaller. This PTM is also

found in tet-inducible XBP1s iSLK.219 cells treated with dox and NaB, where XBP1s no longer inhibits the virus. A potential explanation for this discrepancy, is that since the modified form of XBP1s inhibits replication at a late stage event, NaB could accelerate replication so that this aforementioned event has occurred before XBP1s acquires this PTM. Therefore, it is important to identify this potential PTM of XBP1s in order to determine its role during lytic replication.

ORF65 immunoblot also show an interesting banding pattern in iSLK.219 cells, and to my knowledge has not been previously described. Endogenous ORF65 is 170 amino acids and is ~ 19 kDa, which is detected by immunoblot. In iSLK.219 cells, there are also protein species that cross-react with ORF65 antisera that migrate approximately at 32 and 58 kDa. These proteins appear to be specific to ORF65 as they are only found during late lytic replication. Strikingly, even though these higher MW protein species can be detected in both dox-inducible and RTA transduced cells, the 32 kDa species is the main ORF65 protein detected in CMV-driven XBP1s-expressing iSLK.219 cells. Importantly, ORF65 immunoblots from TREx BCBL1-RTA cells do not display these potential PTMs. Large PTMs by ubiquitin, or ubiquitin-like proteins, could account for these large changes in MW. SUMO is 11 kDa but can appear ~ 15-17 kDa on SDS-PAGE (Hilgarth & Sarge, 2005). Since XBP1s is also modified by SUMO, it will be interesting to identify if some of these different protein species are SUMOylated ORF65. ORF45 immunoblots also show a varying banding pattern in iSLK.219 cells expressing CMV-driven XBP1s, which is not observed in TREx BCBL1-RTA cells. ORF45 is 407 amino acids and is predicted to migrate at ~ 43 kDa (Fan Xiu Zhu & Yuan, 2003); however, SDS-PAGE reveals that the predominant species is twice that size and migrates at ~ 85 kDa with multiple banding patterns. ORF45 is heavily phosphorylated but this does not completely account for this discrepancy in MW (Fan Xiu Zhu & Yuan, 2003). Increasing levels of XBP1s did not impact the levels of the predominant ORF45 protein species, whereas increasing levels of RTA did. Furthermore, XBP1s expression resulted in a decrease in a protein species that migrates at ~ 75 kDa and an increase in an ~ 100 kDa species, both of which are detected in dox-treated or RTA-transduced cells. ORF45 has been shown to be mono-ubiquitinated (X. Wang et al., 2015). This is thought to be important for ORF45 trafficking to lipid rafts in order to facilitate the maturation and egress of virus particles. The shift in expression of the larger MW species may

correspond to the mono-ubiquitin moiety, which could mean that XBP1s inhibits KSHV by altering LR dynamics and egress. This is particularly intriguing, since XBP1s can transcriptionally upregulate lipid biosynthetic enzymes during ER stress. Possibly XBP1s expression changes the lipid during lytic replication, and as a result, disrupts a step in the viral maturation pathway, such as envelopment at the TGN.

PEL cells have a plasma cell-like phenotype but interestingly the gene expression profile of the UPR is markedly reduced compared to plasma cell lines or plasma tumor cells, like multiple myeloma (Jenner et al., 2003). This may partially explain why XBP1s fails to efficiently block virus production in BCBL1 cells; the virus may have evolved in these cells to specifically dampen UPR signaling. By contrast, the virus may be more susceptible to the anti-viral effects of the UPR and XBP1s in SLK cells, which are not a natural host to KSHV. Furthermore, KSHV belongs to the gamma-herpesvirus family, which are known as lymphotropic viruses and therefore may be better attuned to circumventing potential anti-viral responses, including the UPR, in B cells as compared to other cell types.

Other herpesviruses have been shown to disrupt the IRE1-XBP1 pathway and block XBP1s activity. HCMV infection of fibroblasts can trigger XBP1 mRNA splicing but canonical XBP1s target genes such as EDEM1 are not upregulated (Isler et al., 2005). This study did not address whether the inhibition is due to an attenuation of XBP1s protein or to a block in transcriptional activity. Another study showed that Tm-induced XBP1s is blocked by MCMV (Qian et al., 2012). Stahl *et al.* (2013) showed that this is through the downregulation of IRE1 by the direct binding of M50, a protein that along with M53 make up the nuclear egress complex. This was also conserved in HCMV, as the M50 ortholog UL50 also attenuated IRE1 protein levels (Stahl et al., 2013). Although it is unclear why the IRE1-XBP1 pathway is targeted by CMV, it would be interesting to test if XBP1s overexpression can also inhibit CMV production, which could explain why this herpesvirus inhibits IRE1.

HSV-1 was also shown to attenuate IRE1 RNase activity resulting in decreased XBP1 levels (Su et al., 2017). Importantly XBP1s overexpression also inhibited HSV-1 production, possibly indicating a conserved anti-viral role for XBP1s in herpesvirus biology.

One potential anti-viral mechanism of XBP1 is that XBP1s has been shown to induce an inflammatory response by promoting cytokine and IFN production (F. Hu et al., 2011; Martinon et al., 2010; J. A. Smith et al., 2008). Interestingly, Fink *et al.* (2017) found that replication of HSV and two other unrelated viruses, VSV and HCV, was higher in XBP1 knockout MEFs than their matched wild type MEFs. Surprisingly, IFNs and ISGs were higher in XBP1 deficient MEFs compared to matched wild type MEFs, indicating that the anti-viral role of XBP1 is not due to a heightened IFN response. They discovered that the increase in virus replication was due to a decrease in apoptosis. Since XBP1 is not expressed in these cells to protect the cells from ER stress, IRE1 is hyperactive and cleaves other cellular mRNAs through RIDD. They found that the increase in cell survival was partially mediated by IRE1 cleavage of the pro-apoptotic miRNA miR-125a (Fink et al., 2017). This finding conflicts with other studies that show that IRE1 can promote apoptosis by cleaving miRNAs that inhibit apoptosis (D. Han et al., 2009; John-Paul Upton et al., 2012). These inconsistencies may be due to differences in cell models or the sources of ER stress. Understanding the global changes in cellular and viral gene expression during infection of cells either deficient of XBP1 or overexpressing XBP1s will likely help identify key signaling nodes that are important for regulating viral replication.

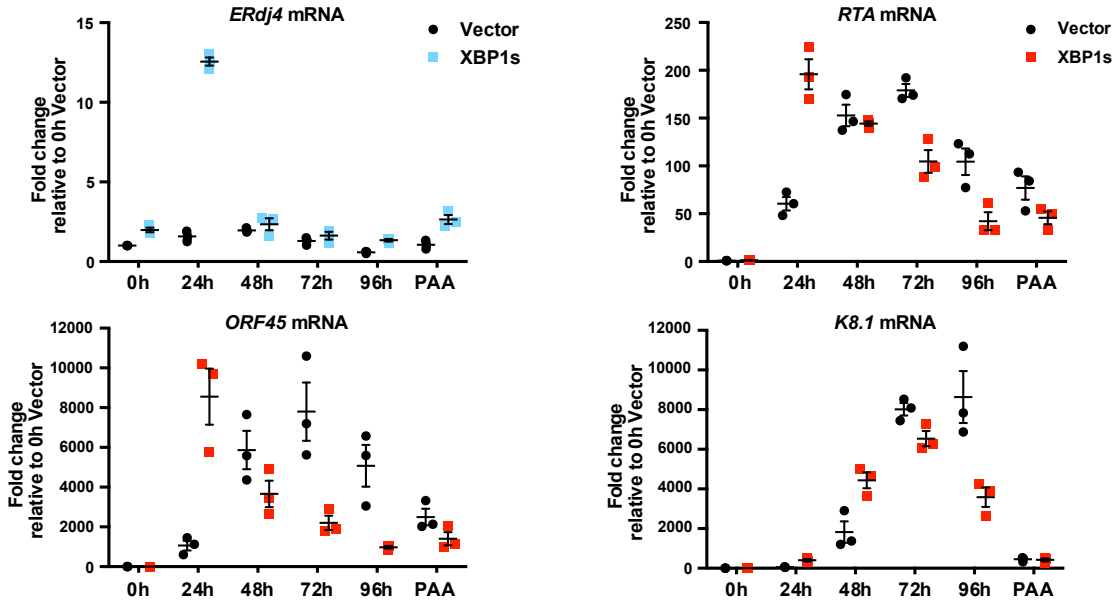

Fig 4.1 XBP1s overexpression enhances accelerates viral gene expression
iSLK.219 cells were transduced with lentiviral dox-inducible expression vectors encoding myc-XBP1s. The promoter contains 7-tandem tet operator (7xTetO) for robust gene expression. Following blasticidin selection, lytic replication and myc-XBP1s expression were induced with 1 μg/mL dox over a 4-d time course or for 96 h with 500 nM PAA to inhibit genome replication. Cells were harvested for total RNA and mRNA levels of XBP1s target gene ERdj4 and viral genes RTA, ORF45, and K8.1 were measured by qPCR and 18S rRNA was as a reference gene normalization. Using the ΔΔCt method, changes in mRNA levels were calculated based on normalizing to 0h vector control. An average of 3 independent experiments are graphed and error bars denote SEM.

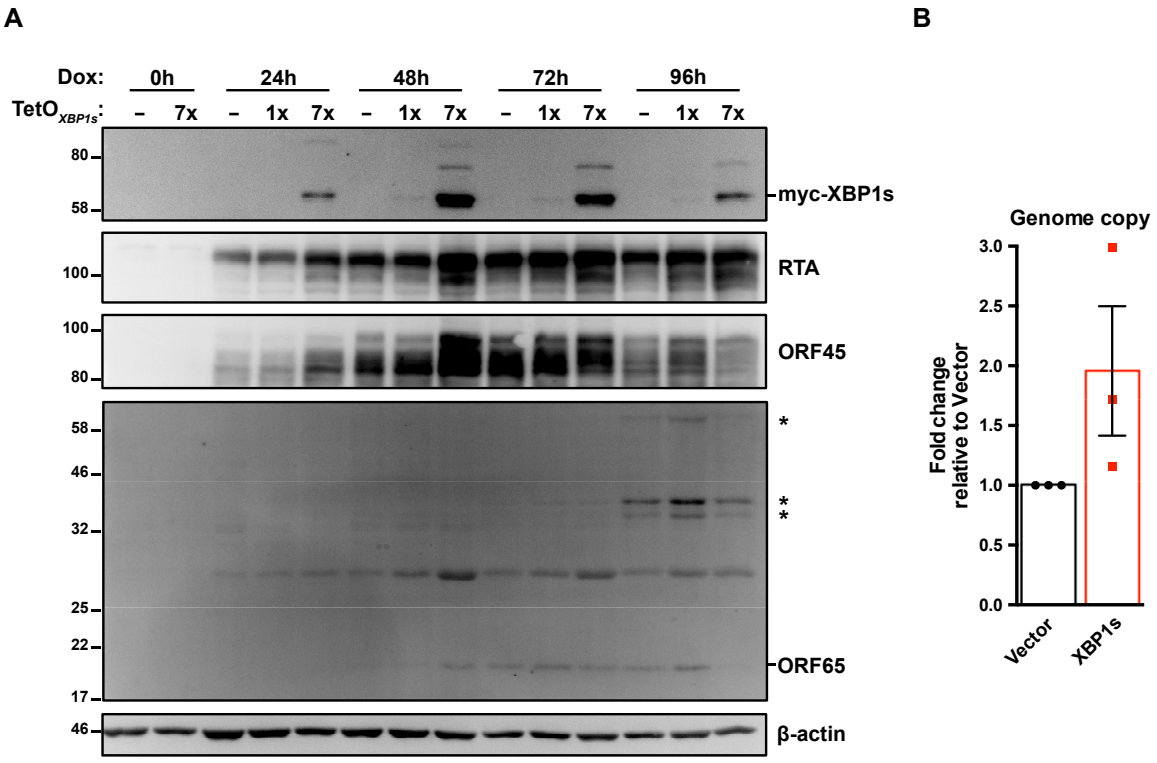

Fig 4.2 XBP1s overexpression inhibits KSHV replication at a late stage
(A) iSLK.219 cells were transduced with lentiviral dox-inducible expression vectors encoding myc-XBP1s with expression driven from either 1xTetO (weak expression) or 7xTetO (robust expression). Following antibiotic selection, cells were treated with 1 μg/mL dox over a 4-d time course and harvested for total cell lysates. Immunoblot analysis of myc-epitope tag (XBP1s), and the viral proteins RTA, ORF45, and ORF65 were completed. β-actin was used as a loading control. (*) denote potential modified ORF65 protein species. The immunoblots shown are representative of 2 independent experiments. (B) 7xTetO myc-XBP1s and vector transduced iSLK.219 cells were treated with dox for 96 h and intracellular DNA was purified. The relative change in viral genome replication was measured by qPCR using primers specific for ORF26 and normalized to β-actin DNA using the ΔΔCt method. The mean of 3 independent experiments is shown and error bars represent the SEM.

Fig 4.3 XBP1s ectopic expression inhibits KSHV production in iSLK.219 cells
(A) iSLK.219 cells were transduced with lentiviral dox-inducible expression vectors encoding myc-XBP1s with expression driven from either 1xTetO (weak expression) or 7xTetO (robust expression). Transduced cells were treated with 1 μg/mL dox for 48, 72, and 96 h and virus-containing supernatants were serially diluted and spinfected onto a confluent monolayer of 293A cells. GFP-positive cells were quantified by flow cytometry the following day and used to calculate virus titer (IU/mL). The values graphed are the mean virus titer of 4 independent experiments and error bars represent the SEM. (B) 7xTetO myc-XBP1s and vector transduced iSLK.219 cells were treated with 1 μg/mL dox for 96 h and DNase I-protected viral genomic DNA from the supernatant were column purified. Firefly luciferase plasmid DNA was added during DNA purification for normalization. The relative change in virus titer (infectious and non-infectious) was quantified by qPCR using ORF26 primers and normalized to luciferase DNA using the ΔΔCt method. The mean of 4 independent experiments was graphed and error bars denote the SEM. (C) iSLK.219 cells were transduced with 7xTetO myc-XBP1u (which can be spliced), myc-XBP1s, or myc-XBP1u*G519A*, which cannot be spliced due to a guanine to adenine mutation at nucleotide position 519 of the XBP1u ORF. Transduced cells were untreated or treated with 1 μg/mL dox for 72, and 96 h and virus-containing supernatants were diluted 1 in 10 and spinoculated onto a confluent 293A monolayer. GFP-positive cells were quantified by flow cytometry 24 h post-infection. The means of 3 independent experiments are graphed as percent GFP-positive cells and the error bars represent the SEM.

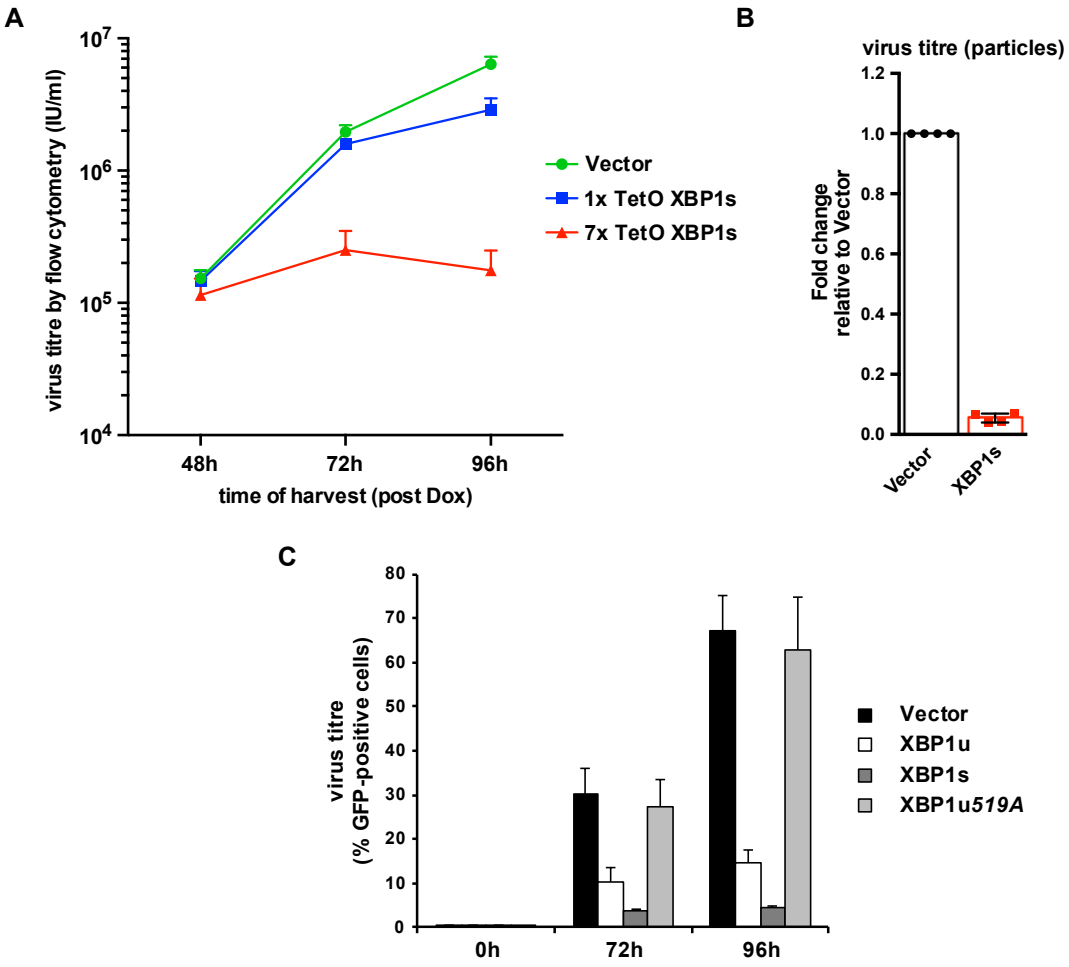
A
virus titre by flow cytometry (IU/ml)
10^7
10^6
10^5
10^4
48h
72h
96h
time of harvest (post Dox)
Vector
1x TetO XBP1s
7x TetO XBP1s
B
virus titre (particles)
Fold change relative to Vector
1.2
1.0
0.8
0.6
0.4
0.2
0.0
Vector
XBP1s
C
virus titre (% GFP-positive cells)
80
70
60
50
40
30
20
10
0
0h
72h
96h
Vector
XBP1u
XBP1s
XBP1u519A

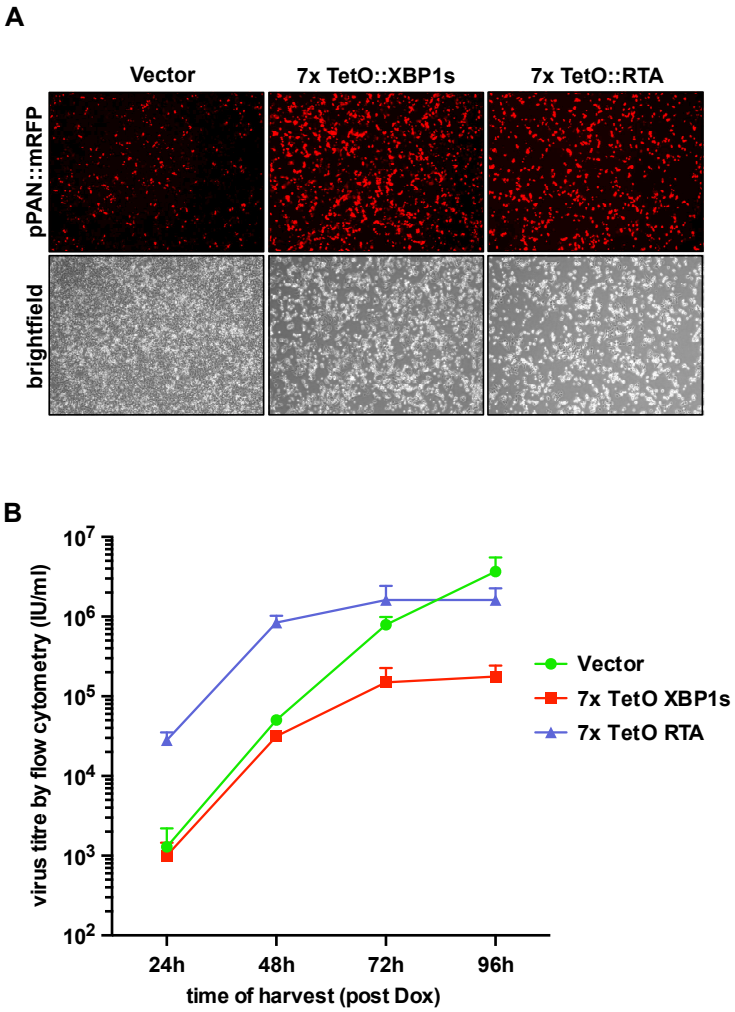

Fig 4.4 Inhibition of KSHV replication in iSLK.219 cells by XBP1s is not due to increased RTA expression

(A and B) iSLK.219 cells were transduced with lentiviral expression vectors encoding either dox-inducible 7xTetO myc-XBP1s or 7xTetO FLAG-RTA. Following blasticidin selection, lytic replication was induced with 1 μg/mL dox for (A) 48 h and fluorescence microscopy was used to image RFP-positive cells (cells undergoing lytic replication) or (B) 24, 48, 72, and 96 h and virus supernatants were harvested to measure titer by flow cytometry. The mean virus titer of 3 independent experiments was graphed and the error bars denote the SEM.

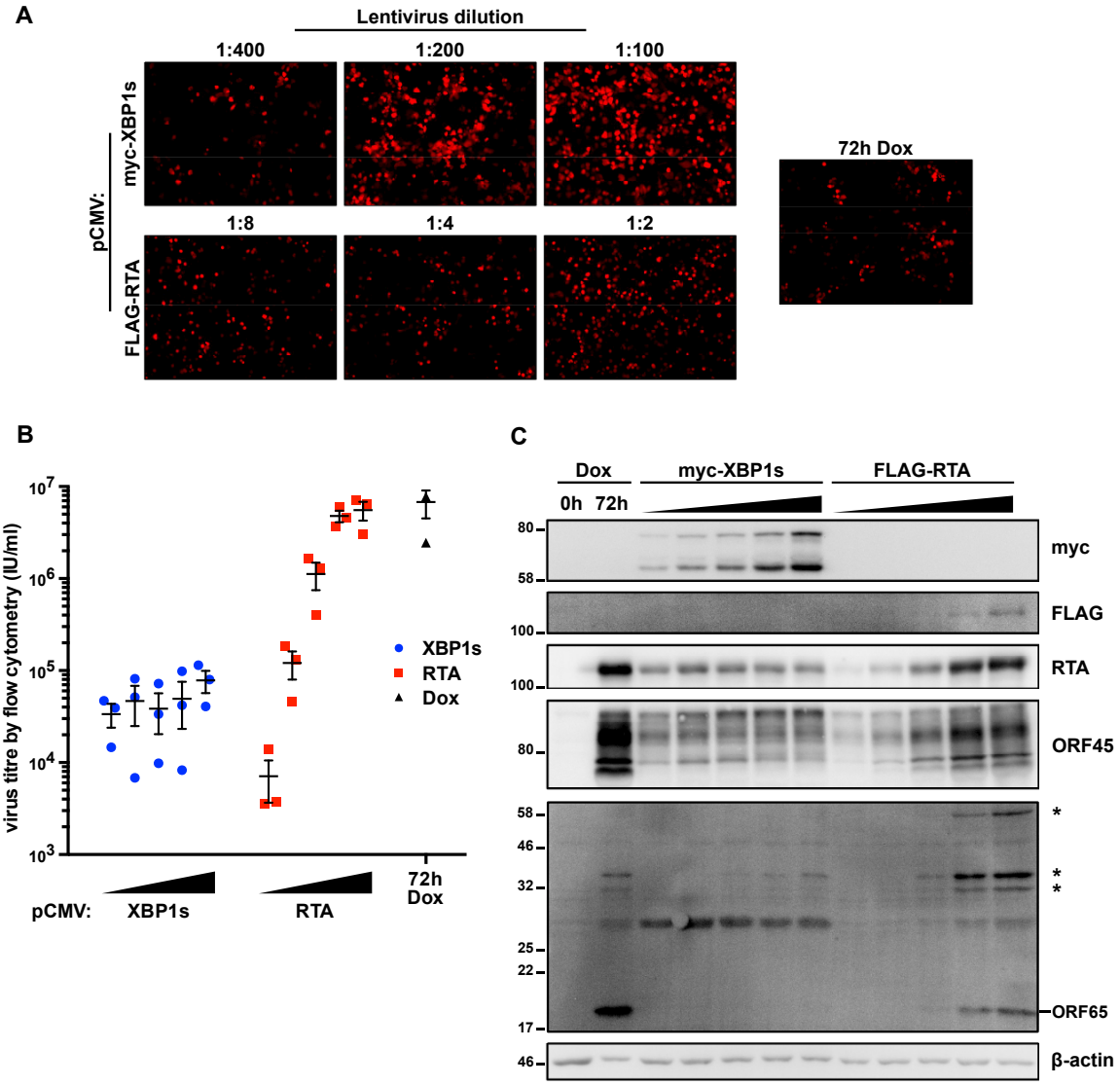

Fig 4.5 KSHV replication does not increase with increasing levels of XBP1s in iSLK.219 cells

(A,B, and C) iSLK.219 cells were transduced with increasing concentrations of lentiviral expression vectors encoding CMV-driven myc-XBP1s (lentiviral dilutions: 1:400, 1:200, 1:100, 1:50, 1:25) or FLAG-RTA (lentiviral dilutions: 1:32, 1:16, 1:8, 1:4, 1:2) for 5 d or treated with dox for 48 h (as a positive control). (A) For a subset of the lentiviral dilutions, cells were imaged a day earlier for RFP-positive cells by fluorescence microscopy. (B) 24 h later, virus-containing supernatants were harvested and virus titer was measured by flow cytometry. (C) Cell lysates from samples in (B) were analyzed by immunoblots for myc-epitope tag (XBP1s), FLAG-epitope tag (RTA) and the viral proteins RTA, ORF45, and ORF65. β-actin was used as a loading control. Microscopy images and immunoblot analysis shown are representative of two independent experiments and the virus titer is an average of 3 independent experiments and the error bars correspond to the SEM.

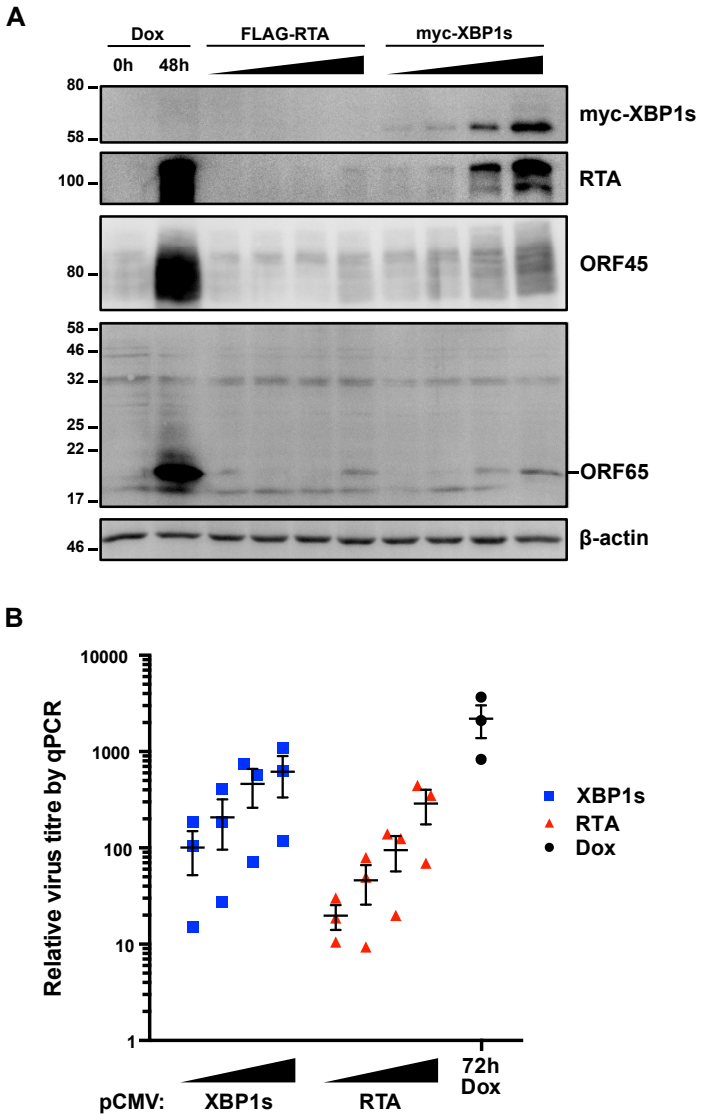

Fig 4.6 XBP1s over-expression does not inhibit KSHV replication in TREx BCBL1-RTA cells

(A) TREx BCBL1-RTA cells were treated with 1 μg/mL dox or transduced with increasing concentrations of lentiviral vectors encoding CMV-driven expression of FLAG-RTA (lentivirus dilutions: 1:16, 1:8, 1:4, and 1:2) or myc-XBP1s (lentivirus dilutions: 1:32, 1:16, 1:8, and 1:4) for 48 h. Cell lysates were harvested for immunoblot analysis for myc-epitope tag (XBP1s) and the viral proteins RTA, ORF45, and ORF65. β-actin was used as a loading control. The immunoblots shown are representative of two independent experiments. (B) TREx BCBL1-RTA cells were treated with dox or transduced with the same lentivirus concentrations of FLAG-RTA or myc-XBP1s as in (A). 72 h post-transduction or post-dox, the supernatant was harvested and DNase I-protected viral genomic DNA was measured by qPCR using primers against ORF26. Firefly luciferase plasmid DNA was added during DNA purification for normalization using the ΔΔCt method. The mean of 3 independent experiments is shown and the error bars correspond to the SEM.

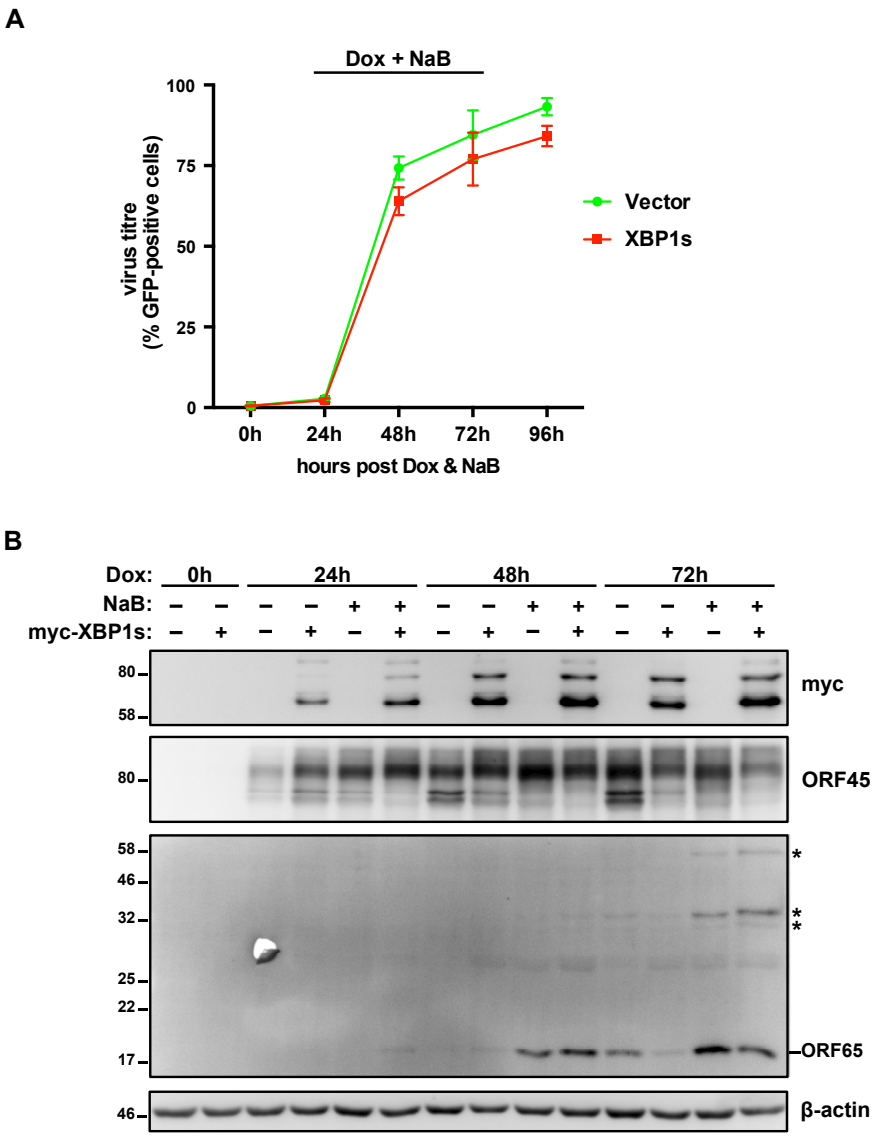

Fig 4.7 XBP1s does not inhibit KSHV replication in iSLK.219 cells when co-treated with sodium butyrate

(A) iSLK.219 cells were transduced with empty vector or dox-inducible expression vector encoding myc-XBP1s with expression driven from a 7-tandem tet operator (7xTetO) for robust gene expression. XBP1s expression and lytic replication was induced with 1 µg/mL dox and 1 mM sodium butyrate (NaB) over a 4-d time course. Virus-containing cell supernatants were spinoculated onto a confluent 293A monolayer and 24 hours post infection GFP-positive cells were quantified by flow cytometry. The means of 3 independent experiments are graphed and the error bars represent the SEM. (B) As in (A), cells were transduced with empty vector and 7xTetO myc-XBP1s and treated with 1 µg/mL dox with or without 1 mM NaB for 24, 48, and 72 h. Cells were harvested for immunoblot analysis of the viral proteins ORF45 and ORF65, and myc tag to detect XBP1s ectopic expression. The immunoblots are representative of 2 independent experiments.

CHAPTER 5 IDENTIFICATION OF VIRAL PROTEINS THAT MODULATE THE UPR

5.1 Introduction

In Chapter 3 I demonstrated that KSHV lytic replication triggers the activation of the UPR sensors PERK, IRE1, and full length ATF6 (ATF6-FL), but their downstream transcription factors ATF4, XBP1s, and ATF6-N, respectively, are inhibited. These transcription factors are also inhibited following pharmacological induction of ER stress during lytic replication. In addition, inhibition of the sensors by genetic or pharmacological treatment significantly reduced virus production. These intriguing findings suggest that the UPR sensors may be reprogrammed during lytic replication to promote viral replication instead of enhancing ER protein folding capacity. Because of this, it is vital to gain a better understanding of the cellular and viral events that are involved in the reprogramming of the UPR.

Over the past 15 years there has been accumulating evidence that many viruses can activate and/or suppress different branches of the UPR, and that some of these responses are carried out by a specific viral protein or multiple proteins. Some viral proteins, such as the HCMV ER resident glycoprotein UL148, have been shown to globally upregulate all branches of the UPR (Siddiquey et al., 2018). While other viral proteins have been specifically shown to activate or inhibit only one UPR sensor. For example, HSV-1 gB was reported to selectively bind PERK and block its activation, likely to maintain robust translation of HSV-1 proteins (Matthew Mulvey et al., 2007). nsP4 of the Togaviruses Chikungunya and Sindbis virus can also inhibit eIF2α phosphorylation (Rathore, Ng, & Vasudevan, 2013), which like HSV-1 gB, may enable robust translation of viral proteins. MCMV M50 and its HCMV homolog UL50 have been shown to bind IRE1 resulting in a reduction in IRE1 protein levels (Stahl et al., 2013). The molecular details of how these viral proteins modulate UPR signaling is currently unknown.

UPR modulation by KHSV is largely unexplored. P.-J. Chang *et al.* (2014) demonstrated that UPR activation may be linked to isoforms of ORF45. They showed that during lytic replication, a tricistronic mRNA is expressed containing ORF47, 46, and 45, which encodes glycoprotein L (gL), uracil DNA glycosylase, and a tegument protein, respectively. Northern blotting analysis revealed shorter mRNA variants of this original

mRNA, including two mRNAs that were generated by alternative splicing. These mRNAs lacked introns encompassing the entire ORF46 gene and different lengths of the 3'end of ORF47. *In silico* translation of these mRNAs results in the generation of two different isoforms of ORF45, ORF47/ORF45A and ORF47/ORF45B, which contain 114 and 56 amino acids from the N-terminus of ORF47, respectively. ORF47 encodes gL and contains an N-terminal ER signal sequence. Consequently, these ORF45 isoforms were shown to be localized in the ER (P.-J. Chang et al., 2014), whereas ORF45 is cytoplasmic (Fan Xiu Zhu & Yuan, 2003).

Ectopic expression of these ORF45 variants, surprisingly, resulted in protein products that were all the same size as determined by immunoblot analysis (P.-J. Chang et al., 2014). The predicted MWs of ORF45, ORF47/ORF45A, and ORF47/ORF45B are 43 kDa, 57 kDa, and 50 kDa, respectively; however, they all had a MW of 75 kDa. Ectopic expression of the tricistronic mRNA also showed that this 75 kDa protein is the only obvious protein expressed. These confounding data indicates that there is likely something unique that regulates the expression of these ORFs that we currently do not understand. ORF45 is heavily phosphorylated (Fan Xiu Zhu & Yuan, 2003) and has also been shown to be mono-ubiquitinated (X. Wang et al., 2015); however, these PTMs likely do not fully account for this size discrepancy observed on immunoblots, and currently it is unknown why ORF45 presents with this MW.

Interestingly, ectopic expression of ORF47/ORF45A and ORF47/ORF45B, but not ORF45 were shown to activate some of the downstream effectors of the UPR, primarily BiP and XBP1s; while PERK and ATF6 were largely unaffected. It was proposed that the upregulation of these UPR markers were due to ER localization of the ORF45 isoforms. Although the role that these alternative ORF45 isoforms play during lytic replication is unclear, silencing BiP resulted in significant reduction in KSHV titer but had nominal impact on viral gene expression (P.-J. Chang et al., 2014). This suggests that BiP may be important for viral glycoprotein folding in the ER. Alternatively, inhibition of BiP causes ER stress and activates the UPR; therefore, it may be UPR signaling and not the protein folding activity of BiP that inhibits virus production.

ORF45 is likely not the only KSHV viral protein that modulates UPR signaling, since I have shown that during lytic replication, BiP transcription is inhibited despite

ATF6 proteolytic processing, and PERK and IRE1 are activated, but XBP1s protein does not accumulate.

Bioluminescent or fluorescent UPR reporters have been useful tools to identify cellular proteins involved in controlling UPR signaling or to identify small molecule activators or inhibitors of the UPR sensors (Gallagher & Walter, 2016; Plate et al., 2016; Sekine et al., 2015; Z. Yang et al., 2018). UPR reporters have also been used to identify viral modulators of the UPR. Indeed, an IRE1 reporter that expresses the firefly luciferase gene downstream of unspliced XBP1 (XBP1u) and out of frame was used to identify Dengue virus NS2b-NS3 fusion protein and E glycoprotein as activators of IRE1 (C.-Y. Yu, Hsu, Liao, & Lin, 2006). To identify potential KSHV proteins with UPR modulating activity, I used a UPR dual-fluorescent reporter cell line to screen our KSHV ORF library. This screen revealed multiple potential "hits", including Kaposin C and ORF45, which were further validated for UPR-modulating activity.

5.2 Results

5.2.1 Flow Cytometry-based Screen of a KSHV Lentiviral ORF Library using a Dual Fluorescent UPR Reporter

In the previous chapters, I showed that the UPR sensors IRE1, PERK, and ATF6-FL are activated during lytic replication but that the downstream transcription factors XBP1s and ATF4 do not accumulate, and ATF6 is cleaved to ATF6-N, but does not upregulate its target genes. I also showed that in one KSHV cell model, XBP1s can thwart virus production.

To better understand how KSHV may be modulating the UPR to prevent potential deleterious effects of UPR signaling, we collaborated with David Ron (University of Cambridge) to screen the McCormick Lab's KSHV lentiviral ORF library with a fluorescent UPR reporter CHO cell line. The KSHV ORF library was generated by ligating untagged ORFs (except for HA-vGPCR and FLAG-ORF45) into pLJM1 B* Puro lentiviral vector plasmid, which is modified version of pLJM1 (Sancak et al., 2010). pLJM1 contains a puromycin resistance cassette for selection of positively transduced clones.

While the ORF library is comprehensive, we decided to exclude several ORFs based on a few important factors. Due to alternative splicing or alternative translation start sites primarily revealed by ribosomal footprinting, multiple potential isoforms of a

subset of viral ORFs may be expressed during infection, including K3A, K8.1B/long, ORF54A, and ORF57A. Ribosomal footprinting also revealed potential translated ORFs in viral lncRNAs, Although these potential isoforms and novel proteins may be functionally important for virus replication, their expression during infection is not clear and so they are currently excluded from the ORF library. ORF64, which encodes a deubiquitinase (DUB), is too large to be packaged into the lentiviral vector, and so using protein domain secondary structure as a guide (Gredmark, Schlieker, Quesada, Spooner, & Ploegh, 2007), ORF64 was cloned into two fragments, as well as the active DUB N-terminal domain (C. M. Gonzalez, Wang, & Damania, 2009). With all of these factors taken into account, the library contains all of the ORFs originally identified when the genome was first sequenced, plus Kaposin B and Kaposin C. This brings the total number of ORFs in the library to 92. For a list of the protein ORFs in the library and their primary functions, see Appendix B.

We realize our decision to leave the large majority of ORFs untagged prevents us from easily confirming expression by immunoblot analysis because very few high-quality KSHV antibodies are available either commercially or from colleagues. Nevertheless, we opted not to put epitope tags on most proteins in the library to maximize chances of producing native, functional proteins that traffic to the right subcellular compartments and bind to the right host substrates. Epitope-tagged vGPCR and ORF45 were previously generated by our lab and shown by us (unpublished data) and others (Kuang, Fu, Liang, Myoung, & Zhu, 2011; Y. Wang et al., 2013) to maintain proper localization and function, so we were confident including these clones in the library. Other groups have generated KSHV ORF libraries, such as a pcDNA Strep-tagged ORF library (Davis et al., 2015) or a lentiviral ORF library (Vart et al., 2007). However, unlike our lentiviral vector, the plasmid used for constructing this library does not contain a selectable marker like ours did. We believe that including a puromycin cassette, as well as expressing primarily untagged ORF provides a library that is more amenable to carefully-controlled functional screens.

The reporter cells that we used is a modified CHO cell line that has dual fluorescent UPR reporter activity and is called CHO-7.1. This is modified version of the CHO reporter cell line CHO-S21 previously published by the Ron Lab (Sekine et al., 2015). CHO-7.1 cells stably express mCherry (instead of mTurquoise in CHO-S21 cells)

fused to a fragment of XBP1 downstream of the IRE1 splice site and is ligated out of frame (XBP1-mCherry). The cells also express GFP under the control of a mouse CHOP promoter (CHOP::GFP). Cells with low basal fluorescence in the absence of stress were selected for and these cells showed tight control of expression of these reporters. However, mCherry expression is slightly higher than GFP, likely due to low levels of spontaneous IRE1 activation (data not shown). ER stress results in upregulation of both GFP and mCherry fluorescence. This is mediated through ATF4 (and possibly ATF6) binding to the mouse CHOP promoter to transactivate GFP and IRE1-dependent splicing of the XBP1-mCherry reporter, which shifts the reading frame to express XBP1-mCherry fusion protein. Exposure to a stress that activates an eIF2α kinase other than PERK, such as amino acid starvation or exposure to dsRNA, would result in increased GFP expression only. To confirm functionality, CHO-7.1 cells were treated with thapsigargin (Tg) for ~ 20 h to activate both PERK and IRE1 and fluorescence was measured by flow cytometry. Tg treatment induced a 2-log increase in GFP fluorescence and a 1-log increase in mCherry fluorescence, respectively (Fig 5.1A).

Using this dual reporter cell line, we sought to determine if there are KSHV ORFs that activate the UPR (or ISR only) or KSHV ORFs that can inhibit UPR activity following pharmacological induction of ER stress. In batches of 10-12 ORFs, CHO-7.1 cells were transduced with KSHV ORF lentiviral vectors or an empty vector control and selected for with puromycin. Following positive selection, cells were left untreated or treated with Tg for ~ 20 h and changes in fluorescence were monitored by flow cytometry. The change in relative median fluorescence intensity (MFI) was normalized to empty vector control. KSHV ORFs that showed potential UPR-modulating activity were re-screened by flow cytometry. The criteria for re-screening was loosely based on showing a clear increase or decrease from both empty vector and the bulk of the ORFs that did not impact fluorescence.

Of the 92 ORFs, 10 ORFs (K2, K3, K11, KapC, ORF16, ORF45, ORF50, ORF72, ORF74, and ORF75) showed discernible and repeatable activation or inhibition of UPR/ISR fluorescent reporters (Fig 5.2B and C; see Appendix C for the relative MFI values). Potential activators were highlighted in green and potential inhibitors were highlighted in red. Of these ORFs, ORF16 (vBcl-2) and ORF75 (vFGARAT) were extremely toxic to the cells (text highlighted in grey) and excluded from further analysis.

In untreated cells, ORF74 (vGPCR) expression resulted in slightly increased XBP1-mCherry levels and therefore may be a candidate IRE1 activator. Conversely, ORF72 (vCyclin) preferentially induces CHOP::GFP expression and therefore is likely not activating the UPR but instead may be activating an eIF2α kinase other than PERK. ORF45 enhanced both GFP and mCherry fluorescence and therefore may activate classical UPR signaling due to potential ER stress. This finding conflicts with the aforementioned study that showed that only the ORF47/ORF45A and B isoforms of ORF45 activated XBP1s, while ORF45 had no effect (P.-J. Chang et al., 2014).

KapC had a modest inhibition of XBP1-mCherry fluorescence, however only in the absence of Tg treatment. K11 (vIRF-2) expression resulted in a slight decrease in CHOP::GFP and K3 reduced both GFP and mCherry fluorescence approximately 2-fold following Tg treatment, however this inhibition is more selective for CHOP::GFP since XBP1-mCherry was also slightly decreased in the untreated K3-expressing cells. Interestingly K2 (vIL-6), which had a negligible impact on either fluorescent reporter in the untreated sample, triggered an almost 2-fold increase in XBP1-mCherry fluorescence following Tg treatment, suggesting that vIL-6 is not an activator but rather an enhancer of IRE1 activity. The ORF with the most dramatic impact on the IRE1 reporter was ORF50 (RTA), which caused a 4-fold decrease in XBP1-mCherry fluorescence regardless of Tg treatment. This robust inhibition by RTA warranted further analysis to determine if the inhibition was also observed with endogenous IRE1 activity.

5.2.2 RTA is not an Inhibitor of IRE1α

From the ORF library screen, RTA showed the most dramatic modulation of the UPR reporters, with a specific inhibition of the IRE1 reporter XBP1-mCherry. This, coupled with the finding that during lytic replication there is an obvious decrease in IRE1 which may impact XBP1 mRNA splicing (Chapter 3), led me to conclude that it is possible that RTA may be the viral gene product responsible for this phenotype observed during lytic replication.

To confirm RTA inhibition of the IRE1 fluorescent reporter, CHO-7.1 cells were re-transduced with RTA lentiviral vector or empty vector control and treated with Tg. In addition, the IRE1 RNase inhibitor 4μ8c was included to determine the extent of RTA-dependent inhibition of the IRE1 reporter in this assay. The results were similar to the

previous findings and revealed that RTA expression caused a 5-fold reduction in the IRE1 reporter regardless of Tg treatment compared to empty vector control (Fig 5.2A and B). This reduction in mCherry fluorescence by RTA expression was similar to empty vector control cells treated with both Tg and 4μ8c, indicating that RTA may be a robust inhibitor of IRE1. RTA inhibition of the IRE1 reporter was specific since there was a minimal impact on CHOP::GFP levels, implying that RTA may directly inhibit IRE1 rather than suppressing UPR activation altogether.

This potential robust and selective inhibition of the IRE1 reporter prompted me to test if RTA can inhibit endogenous IRE1 activity. The RTA-transduced CHO-7.1 cells that were seeded for flow cytometry in Fig 5.2A were also seeded for both immunoblot analysis and semi-quantitative RT-PCR of XBP1 mRNA. The immunoblot analysis confirmed that RTA had no impact on Tg-induced PERK phosphorylation, as determined by a migration shift of a total protein blot (Fig 5.2C). Also consistent with the flow cytometry data, 4μ8c potently inhibited IRE1 RNase activity as determined by a reduction in spliced XBP1 mRNA and protein (Fig 5.2C and D). However, in contrast to the inhibition of the IRE1 fluorescent reporter, RTA had no effect on either XBP1 mRNA splicing or XBP1s protein accumulation following Tg treatment. IRE1 phosphorylation was also not inhibited in these cells and was similar to empty vector control as determined by a similar migration shift in a total IRE1 protein immunoblot (Fig 5.2C). This discrepancy between flow cytometry data and immunoblot analysis is not due to a lack of RTA expression, since RTA could be detected by immunoblot and these cells were from the same batch of cells used for flow cytometry in Fig 5.2A. Based on these data, it is clear that RTA does not inhibit IRE1 as the IRE1 fluorescent reporter suggested and RTA may directly be impacting expression of the XBP1-mCherry fusion protein. Since RTA is a DNA binding protein and has transactivating potential, one potential conclusion is that RTA inhibits the XBP1-mCherry construct at the transcriptional level. Based on these findings, there is possibly another viral protein that is responsible for attenuating IRE1 signaling as observed during replication.

5.2.3 Kaposin C Downregulates IRE1α

Kaposin C (KapC) also showed a decrease in XBP1-mCherry fluorescence in untreated cells, although not as robust as RTA. This inhibition was also specific to IRE1 since the CHOP::GFP levels were largely unaffected. KapC was also an appealing target to

investigate because unlike RTA, which is nuclear, KapC is translated in the ER, which places it in the right compartment to interact with IRE1. Furthermore, nothing is known about the function of KapC and so the potential of ascribing it as an IRE1 inhibitor would greatly benefit our understanding of the role of KapC during KSHV infection.

To test the impact of KapC on IRE1 activity, 293A cells were transduced with increasing concentrations of a KapC lentiviral vector followed by treatment with either Tg or Tm. KapC caused a dose-dependent decrease in IRE1 protein levels, which corresponded with a subtle decrease in spliced XBP1 mRNA and protein after Tg or Tm treatment (Fig 5.3A and B). KapC inhibition of IRE1 was specific since it did not impact PERK levels, which is also consistent with the flow cytometry data.

In untreated samples, I consistently observe IRE1 as a doublet by SDS-PAGE. The identity of the higher molecular weight (MW) species is not known but could be a hypo-phosphorylated version of IRE1. Interestingly, this higher MW species appears to be more sensitive to KapC expression. Identifying these different IRE1 protein species may provide insight into the mechanism of IRE1 inhibition by KapC.

KapC is expressed from a tricistronic mRNA that also encodes KapA and B. Although the function of KapC is not known its protein domains are essentially composed of Kaposin A (KapA; K12) and Kaposin B (KapB) due to the unique coding sequence of its mRNA. KapB and KapC are translated from near-cognate CUG start codons that are located in close proximity but in different reading frames. KapB translation terminates upstream of KapA and is a nuclear/cytoplasmic protein that is composed of two domains, DR1 and DR2, each of which are comprised of distinct 23-amino acid repeats. Due to the degenerate coding sequence of the DR1 and DR2, the majority KapB and KapC share the same protein coding sequence but KapC translation terminates at the same codon as KapA thus incorporating KapA into its C-terminal domain. KapA is a small type II ER- and Golgi-localized transmembrane protein. Therefore, KapC is essentially a fusion of KapA and KapB. Although KapA and KapB did not score with the IRE1 reporter, I wanted to confirm if KapA or KapB had an effect on endogenous IRE1 which will help reveal the important features required by KapC to inhibit IRE1. 293A cells were transduced with increasing concentrations of lentiviral vectors expressing either KapA, KapB, or KapC. Immunoblots using Kaposin anti-sera specific to the DR1 region (which cannot detect KapA) showed that increasing lentiviral

inoculum caused matching increases in accumulation of KapB and KapC proteins (Fig 5.3C). KapA was unable to be confirmed for expression but based on the assumption that it was expressed in these cells, KapA or KapB had no impact on IRE1 levels and therefore, it appears that inhibition of IRE1 requires both the DRs and the ER transmembrane domain present in KapC. IRE1 is reduced during lytic replication and therefore KapC may be a key contributor to this attenuation (Fig 3.2). XBP1s is also attenuated during lytic replication in the absence or presence of drug-induced ER stress; however, it is likely that KapC is not the only factor involved in this inhibition of XBP1s, since KapC expression following Tg or Tm treatment had a nominal effect on XBP1s levels (Fig 5.3A & B). Nonetheless, KapC reduction of IRE1 is striking and reduced IRE1 levels may have alternative consequences other than XBP1 splicing.

5.2.4 ORF45 Upregulates Components of the UPR

During lytic replication the UPR sensors are activated with the onset of ORF45 expression (Chapter 3) and the ORF screen identified ORF45 as an activator of both CHOP::GFP and XBP1-mCherry expression. Therefore, ORF45 may be at least partly responsible for UPR activation during lytic replication. This conflicts with a previous report that showed that ORF45 isoforms ORF47/45A and ORF47/ORF45B, but not wild type ORF45, upregulated UPR proteins XBP1s and BiP (P.-J. Chang et al., 2014). Therefore, there are many key issues that need to be resolved to understand these discrepancies between findings.

To determine if ORF45 could activate the UPR, 293A cells were transduced with ORF45 lentiviral vector or an empty vector control and at 3 d post-transduction, cells were treated with Tg or Tm as positive controls for UPR activation. To confirm that ORF45 was functional, phospho-Ser422 of eIF4B, a known substrate of ORF45 (Kuang et al., 2011), was probed for via immunoblotting (Fig 5.4A). Indeed, ORF45 expression correlated with an increase in levels of phospho-eIF4B (Fig 5.4A). ORF45 expression also increased total IRE1 protein levels, although IRE1 was not phosphorylated based on the lack of migration shift in the total IRE1 immunoblot. This lack of IRE1 phosphorylation also corresponded with minimal induction of XBP1s. Interestingly, ORF45 caused an increase in levels of XBP1u protein, which is not commonly observed during canonical activation of the UPR. Consistent with the flow cytometry data, ORF45 activated the ISR as determined by a modest increase in phospho-eIF2α, ATF4, and

CHOP. Surprisingly, there was no obvious shift in PERK migration, indicating that PERK may not be activated and that eIF2α may be phosphorylated by a different eIF2α kinase. Interestingly, ORF45 cells treated with Tg or Tm displayed reduced ATF4 and XBP1s expression potentially indicating that a further increase in eIF2α phosphorylation can inhibit ISR activation.

Based on immunoblot analysis, I have found that HeLa cells seem to express slightly higher levels of XBP1 compared to 293A cells (data not shown), and therefore may be a more tractable cell line to determine the impact of ORF45 on XBP1 splicing. HeLa cells were transduced with an ORF45 lentiviral vector for 48 and 72 h or treated with Tm for 6 h as a positive control. XBP1 mRNA splicing was measured by semi-quantitative PCR and revealed a time-dependent increase in XBP1 splicing upon ORF45 expression (Fig 5.4B). Curiously, unlike cells treated with Tm, ORF45 expression did not cause an obvious decrease in XBP1u mRNA levels. This suggests that total XBP1 mRNA levels may increase with ORF45 expression. Consistent with these data, increased levels of XBP1u protein were observed in ORF45-expressing 293A cells (Fig 5.4A). Indeed, qPCR of XBP1 mRNA revealed that ORF45 caused an approximately 5-fold increase in total XBP1, which was comparable to Tm treatment (Fig 5.4C).

XBP1u mRNA and protein are normally highly unstable (Calfon et al., 2002; Majumder et al., 2012) and therefore, ORF45 may be increasing total XBP1 mRNA levels due to an increase in XBP1u mRNA stability. Furthermore, mRNA stability is intimately linked to its translation (L. Y. Chan, Mugler, Heinrich, Vallotton, & Weis, 2018). Theoretically, the increased level of total XBP1 mRNA observed in ORF45-expressing cells may be due to increased translation. Alternatively, ATF6 can also directly upregulate XBP1 transcription (Yoshida et al., 2001), which could also account for the ORF45-dependent increase in total XBP1.

To determine if ORF45 activates ATF6, mRNA levels of ATF6 target genes BiP and HERPUD1 were measured by qPCR. At 48 h there was not a significant increase in these ATF6 target genes, but by 72 h post-transduction there was an approximately 4-fold increase in both BiP and HERPUD1 compared to empty vector control (Fig 5.5A). This increase in mRNAs levels was nominal compared to the increase observed following Tm treatment; Tm increased BiP and HERPUD1 mRNA levels approximately 25- and 60-fold, respectively. This suggests that there may be a slight activation of ATF6 in response

to ORF45 expression but is unlikely enough to facilitate the observed increase in XBP1 mRNA. mRNA levels of the XBP1s target gene ERdj4, and the ATF4 target gene CHOP were also measured in ORF45-expressing cells. 72 h post-transduction, ORF45 induced an approximately 4-fold increase in ERdj4 mRNA and an approximately 20-fold increase in CHOP mRNA compared to empty vector (Fig 5.5A). The induction of ERdj4 was considerably lower than in cells treated with Tm (~ 15-fold). Although based on the differences between ORF45- and Tg-induced XBP1 splicing (Fig 5.4B), the corresponding differences in ERd4 mRNA levels are not surprising. The robust increase in CHOP mRNA levels concomitant with the apparent lack of PERK phosphorylation in ORF45-expressing 293A cells (Fig 5.4A), further indicates that an eIF2α kinase other than PERK is activated by ORF45.

Since there appears to be a time-dependent increase in UPR signaling with ORF45 expression, UPR activation was monitored over a 5-d time course in ORF45-expressing HeLa cells. As a positive control, untransduced cells were treated with Tm for 3 and 6 h. Consistent with previous data, by 48 h there was robust ORF45 expression with concomitant upregulation of BiP, ATF4, and CHOP (Fig 5.5B). Interestingly, the levels of phospho-eIF2α were comparable between ORF45 and empty vector-transduced cells. This may be due to dephosphorylation of eIF2α through GADD34, which is a gene target of CHOP. Unlike in 293A cells (Fig 5.3A), XBP1s can also be detected by 48 h, concomitant with an increase in both IRE1 and XBP1u expression. IRE1 and XBP1u, along with other protein markers of the UPR, accumulate with time until expression peaks by 96 h. By 5 d post-dox, expression of these markers began to wane, which may be due to ORF45-induced cytotoxicity, since microscopy analysis revealed that a portion of the cells displayed delayed cell growth, gross morphological changes, and cell rounding (data not shown). Consistent with previous results, even though IRE1 expression was markedly induced by ORF45, IRE1 did not undergo the same extent of phosphorylation as seen with Tm treatment. These differences were also reflected in the differences between the protein levels of XBP1u and XBP1s; XBP1u was the major isoform in ORF45 expressing cells, whereas XBP1s was the major isoform following Tm treatment.

Another striking feature in ORF45 expressing cells was the large increase in BiP. By 72 h, BiP levels were similar to cells treated with Tm for 6 h even though the mRNA

levels were vastly lower in ORF45-transduced cells (Fig 5.5B). These data indicate that the ORF45 mediated increase in BiP protein is likely not due to a transcriptional response, which is normally observed following drug-induced UPR activation through ATF6-N transactivation. Collectively, these data show that ORF45 can activate components of the UPR but that the expression profiles of many of these proteins differ compared to activation of the UPR following drug-induced ER stress. KSHV is especially good at hijacking stress responses during infection, and therefore it is not surprising that KSHV-encoded proteins like ORF45 can control UPR signaling.

5.2.5 ATF6 Expression Constructs Impact ORF45 Expression

In response to ER stress, ATF6 transcriptionally upregulates BiP. However, in ORF45-expressing cells, despite a robust increase in BiP at the protein level, there was a minimal change in BiP mRNA expression. Based on these striking differences, it was necessary to test if ORF45 expression activated ATF6 through proteolytic cleavage. As previously mentioned, due to the lack of adequate ATF6 antibodies and ATF6's highly labile nature, endogenous full-length and cleaved ATF6 are difficult to detect by immunoblot. To overcome this obstacle, HeLa cells were co-transduced with ORF45 or empty vector lentiviral vectors along with either HA epitope-tagged full-length ATF6 (WT), constitutively active (CA) ATF6 (HA-ATF6 1-373), or dominant negative (DN) ATF6 (HA-ATF6 1-373m1). HA-ATF6 1-373 expresses the first 373 amino acids of ATF6, which contains the bZIP transcription factor, and DN ATF6 was generated by inserting point mutations in HA-ATF6 1-373 to prevent DNA binding. After 48 and 72 h post-transduction, the empty vector control cells expressing constitutively active ATF6 but not full length or DN ATF6 upregulated BiP (Fig 5.6). This also coincided with an increase in XBP1u, which is consistent with evidence that ATF6 can transcriptionally upregulate XBP1 (Yoshida et al., 2001). ORF45 alone or co-expressed with full-length ATF6 also upregulated XBP1u, as well as XBP1s, as previously demonstrated. Interestingly, ORF45 induction of XBP1s was blocked with the expression of CA ATF6, suggesting that ATF6 transcriptional reprogramming of the ER may protect against ORF45-induced ER stress.

These data should be interpreted with caution because co-expression of either CA and DN ATF6 diminished total ORF45 levels to an extent that may impact its ability to cause stress. Furthermore, the banding pattern of ORF45 changed with ATF6 expression, which may also impact ORF45 function. Co-expression of ORF45 and full-length HA-

ATF6 resulted in a striking enrichment in ATF6 protein levels with multiple protein species detected, including the 60 kDa cleaved N-terminal transcription factor HA-ATF6-N, which coincided with enhanced BiP expression. ORF45 also enhanced BiP expression when co-expressed with CA ATF6. Surprisingly, DN ATF6 did not fully block ORF45-induced BiP suggesting that in the absence of ATF6 overexpression, ORF45 may not upregulate BiP through ATF6-dependent transactivation. This is consistent with the nominal increase in BiP mRNA levels previously observed. Alternatively, the HA-ATF6 1-373m1 construct may not be a true dominant negative of ATF6 and therefore, further experiments are needed to test this.

5.2.6 ORF45 does not Induce Conventional UPR Signaling

The previous data highlight some subtle UPR signaling differences between classical ER stress-inducing drugs and ORF45 expression. Specifically, ORF45 elicited a strong upregulation of BiP with minimal changes in transcription, induced CHOP expression with minimal PERK phosphorylation, and upregulated IRE1 with minimal phosphorylation. This ORF45-dependent increase in IRE1 corresponded to increased levels of XBP1u but not XBP1s. This suggests that ORF45 may upregulate UPR protein marker but not through some of the ER stress sensors.

To determine if ORF45 is indeed activating CHOP and BiP independent of PERK and ATF6, respectively, expression of the ER stress sensors was silenced individually with shRNA lentiviral vectors followed by transduction with ORF45. Tg was used as a positive control to confirm that each of the UPR branches are inhibited following ER stress. Immunoblot analysis showed that treatment with Tg in the non-targeting shRNA control sample resulted in the upregulation of BiP, which corresponded with the faint detection of an ATF6 protein species that had the appropriate MW to be ATF6-N (Fig 5.7A). Importantly, this ATF6 protein species disappeared with the knockdown of ATF6 expression, corresponding with decreased BiP expression. This putative ATF6-N protein species does not appear to be present in ORF45-expressing cells, and surprisingly ATF6 knockdown enhanced, rather than reduced, BiP protein levels in these cells. These data indicate that ORF45 does not upregulate BiP in an ATF6-dependent manner.
Silencing ATF6 expression also inhibited Tg-induced CHOP likely due to the presence of an ERSE in the CHOP promoter (Y. Ma et al., 2002; Yoshida et al., 2000). Interestingly, ATF6 silencing in ORF45-expressing cells increased ATF4 and CHOP expression, which

corresponded with a slight migration shift in the total PERK immunoblot, indicating potential activation. This suggests that even though ATF6 may not be potently activated by ORF45, ATF6 may provide a buffer for suppressing ER stress. ATF6 silencing in the vector control sample also resulted in a slight increase in PERK phosphorylation, although this may not be enough to activate the ISR, since there was no obvious increase in ATF4 or CHOP. Silencing PERK blocked Tg-induced CHOP and ATF4 expression, whereas silencing PERK in ORF45-expressing cells had the opposite effect: CHOP and ATF4 expression was enhanced. This further supports the idea that ORF45 may induce stress that activates an eIF2α kinase other than PERK, and PERK silencing may enhance this stress to further promote ISR activation. However, since this is only a knockdown of PERK expression, an alternative hypothesis is that PERK silencing may be self-activating in ORF45-expressing cells, which promotes ATF4 and CHOP. Expressing ORF45 in PERK knockout MEFs will clarify some of these theories. Unfortunately, phospho-eIF2α immunoblot did not reveal any noticeable changes in phospho-eIF2α levels among samples, which may be partly attributed to the high basal levels in the untreated, non-targeting shRNA control. These high levels may be due to the length of time the cells spent in the same cell culture media, which may activate the eIF2α kinase GCN2 due to amino acid depletion (P. Zhang et al., 2002).

Consistent with the data shown previously, ORF45 also upregulated IRE1 and XBP1u, as well as low levels of XBP1s (Fig 5.7A). IRE1 silencing in both Tg-treated and ORF45-expressing cells decreased XBP1s confirming that ORF45-dependent activation of IRE1 causes XBP1 splicing. Interestingly, similar to ATF6 silencing, the decrease in IRE1 levels also enhanced ORF45-mediated BiP, ATF4, and CHOP expression. This is likely a result of enhanced ER stress by the loss of IRE1, which promotes ATF6 and PERK activation and their downstream effectors.

To corroborate the immunoblot data, mRNA levels of ATF6-N, XBP1s, and ATF4 target genes from matched total RNA lysates were measured by qPCR. Consistent with immunoblot data, ATF6 knockdown reduced BiP and HERPUD1 mRNA levels in Tg-treated cells but not ORF45-expressing cells (Fig 5.7B). CHOP mRNA was also reduced in ATF6-silenced cells following Tg treatment indicating that ATF6 induces CHOP transcription likely through binding the ERSE in the CHOP promoter. PERK silencing also elicited a strong reduction in CHOP mRNA levels following Tg treatment.

Conversely, PERK silencing in ORF45 expressing cells resulted in an approximately 3-fold increase in CHOP mRNA compared to the non-targeting control, which was also observed when IRE1 or ATF6 expression was silenced. These findings are consistent with the immunoblot data and suggest that an eIF2α kinase may be more active when the ER stress sensors are silenced. This conclusion may indicate that even though activation of the sensors are not detected by experimental assays in ORF45-expressing cells, they could still play a protective role.

Silencing IRE1 had a minimal effect on ERdj4 mRNA levels in ORF45-expressing cells but this was not surprising due to the minimal transcriptional upregulation in the non-targeting shRNA control sample and the residual XBP1s transcriptional activity following IRE1 knockdown in Tg-treated cells.

Based on immunoblot analysis and the qPCR data, it is also evident that knockdown of one of the UPR sensors impacts the robustness of the signaling of the other two branches, which highlights the importance of the coordination between the UPR sensors in order to effectively respond to ER stress. Along these lines, ATF4 has been shown to transcriptionally upregulate IRE1 to promote robust XBP1 mRNA splicing (Tsuru et al., 2016). To determine if ORF45 activation of ATF4 is responsible for the upregulation of IRE1, ISR-deficient Hela eIF2α Ser51Ala CRISPR knock-in mutant cells and their matched wild type control cells were transduced with ORF45 or an empty vector control. Vector-transduced eIF2α Ser51Ala mutant cells treated with Tg confirmed the lack of eIF2α phosphorylation and resulted in slightly lower levels of IRE1 compared to wild type Hela cells (Fig 5.8). While this decrease in IRE1 corresponded with a nominal decrease in XBP1u, XBP1s protein levels were largely unaffected. ORF45-expressing wild type cells showed an increase in IRE1 levels as observed previously, which corresponded with an increase in XBP1u and slight increase in XBP1s. This increase in IRE1 by ORF45 was abolished in the eIF2α Ser51Ala mutant cells, which corresponded to a decrease in both XBP1s and XBP1u, although XBP1u levels did not return to basal levels. This block in IRE1 and XBP1 accumulation in ORF45-expressing eIF2α mutant cells was also observed following Tg treatment, although this may be partly attributed to cellular toxicity as there was an observed increase in cell rounding and detachment (data not shown). These data indicate that the ISR promotes

IRE1 signaling, which can be exemplified by ORF45 expression. For further evidence that the ISR is important for IRE1/XBP1 signaling, please see Appendix A.

5.2.7 BiP is not Upregulated during Lytic Replication

Chapter 3 showed that ATF6 accumulates and is proteolytically cleaved during lytic replication, but ATF6-N was likely inactive since it did not upregulate BiP at the transcriptional level. However, these recent data demonstrated that ORF45 upregulated BiP in an ATF6-independent manner and was likely not due to increases in transcription (Fig 5.7). Conversely, overexpression of full-length ATF6 in the context of ORF45 expression resulted in a further enhancement of BiP, concomitant with ATF6 accumulation and ATF6 cleavage (Fig 5.6). Intriguingly, P.-J Chang *et al.* (2014) showed that BiP is upregulated in various PEL cell lines following induction of lytic replication with NaB and/or TPA and silencing BiP attenuated virus production. I therefore wanted to determine if BiP is upregulated at the protein level during lytic replication in an ATF6-independent manner.

TREx BCBL1-RTA cells were stably transduced with full length HA-ATF6 or empty vector control and these cells were used to monitor ATF6 activation status and BiP expression levels from 12 to 24 h post-dox with SDS-PAGE. Latent and 24 h post-dox samples were also treated with Tg 4 h prior to harvesting as controls. Treatment of latent cells with Tg elicited a clear induction of BiP concomitant with cleavage of endogenous ATF6 and ectopic HA-ATF6 (Fig 5.9). By 12 h post-dox, ORF45 was expressed, which corresponded with robust upregulation of full length ATF6 and proteolytic cleavage to generate ATF6-N. Strikingly, even though ATF6-N was more pronounced in lytic cells compared to Tg-treated control, BiP expression was not induced. Consistent with qPCR data in Chapter 3, lytic cells treated with Tg displayed a pronounced level of ATF6-N but BiP was significantly reduced compared to Tg-treated latent cells. Therefore, while ectopic expression of ORF45 stimulated a robust accumulation of BiP, this was not observed during lytic replication, suggesting that either ORF45 behaves differently in these different models or that BiP protein expression is actively being inhibited during lytic replication. Collectively these data indicate that KSHV encodes multiple viral proteins to modulate the UPR and ISR during lytic replication.

5.3 Discussion

A screen of KSHV ORFs for UPR-modulating activity using a dual-fluorescence cell reporter for IRE1 or ISR modulation revealed multiple ORFs with activating or inhibiting potential (Fig 5.1). Of the approximately dozen ORFs that showed changes in UPR activity based on the reporters, a few were selected for confirmation of true UPR-modulating activity.

RTA showed a dramatic decrease in XBP1-mCherry fluorescence in the absence or presence of Tg suggesting that RTA may inhibit IRE1 activity. Surprisingly, this observation was not reflected with endogenous IRE1; XBP1 mRNA splicing or XBP1s protein accumulation was unchanged in Tg-treated RTA expressing cells compared to empty vector indicating a discrepancy between the reporter and endogenous IRE1 activity following RTA expression (Fig 5.2). RTA is the immediate early protein that, along with multiple cellular factors including the transcription factor RBP-Jκ, is responsible for initiating lytic replication by directly transactivating multiple viral genes (Y. Liang, Chang, Lynch, Lukac, & Ganem, 2002). Although RTA is an activator of viral gene expression, RTA may suppress transcription of the XBP1-mCherry fusion construct, which would explain why RTA appeared as an IRE1 inhibitor. The expression of XBP1-mCherry is driven by the chicken actin promoter. Therefore, RTA may bind to the chicken actin promoter and repress transcription. Based on comparisons of the RTA binding sequences in viral promoters there is not an obvious RTA targeting sequence (Staudt & Dittmer, 2007) and therefore identifying a potential RTA consensus sequence in chicken actin promoter is not feasible. Alternatively, RTA may inhibit XBP1-mCherry at the protein level. RTA has been shown to have SUMO-targeted ubiquitin ligase (STUbl) activity and can promote the degradation of SUMOylated proteins, including PML and the viral protein K-bZIP (Izumiya et al., 2013). There are likely other SUMOylated host proteins targeted by the E3 ubiquitin ligase activity of RTA but currently this is unknown. XBP1s has been reported to be SUMOylated at distinct lysine residues (H. Chen & Qi, 2010), however these lysine residues are not contained within the fragment of XBP1 that is fused to mCherry. Comparing mRNA and protein levels of this fluorescent reporter may help identify the source of inhibition in RTA-expressing cells.

Another inhibitor of IRE1 activity identified from the screen was KapC. KapC expression caused a decrease in IRE1 and a slight decrease in XBP1 mRNA splicing,

however this inhibition was mostly evident in untreated cells (Fig 5.3). Currently, nothing is known about KapC function. KapC is expressed from a tricistronic mRNA along with KapB and KapA (Sadler et al., 1999). The mRNA that encodes the Kaposins is abundantly expressed during latency by a constitutively active promoter found directly downstream of LANA (Hong Li et al., 2002). The Kaposins are also upregulated during the lytic cycle by RTA due to RTA-responsive elements located upstream of the latent promoter (P.-J. Chang et al., 2002). KapB and KapC translation is unique and is initiated from CUG start codons (Sadler et al., 1999). The mRNA is composed of repetitive nucleotide sequence that when translated results in two regions of repetitive 23 amino acid sequence regardless of reading frame called direct repeats (DR) 1 and 2. Depending on the reading frame, translation will result in either KapB or KapC. Termination of translation upstream of the KapA ORF generates nuclear/cytoplasmic Kaposin B (Corcoran, Johnston, & McCormick, 2015). Translation in a different reading frame bypasses the stop codon for KapB and translates the longer KapC isoform, which contains the same amino acid sequence as KapA at its C-terminus. KapA is a type-II transmembrane protein that localizes primarily to the ER and Golgi (Muralidhar et al., 1998). Although nothing is known about Kaposin C, since its C-terminus is shared with KapA, it is likely that KapC is also found in the ER and Golgi with the N-terminal DRs exposed in the cytosol. Therefore, based on KapC localization in the same organelle as IRE1, it is theoretically possible that KapC may facilitate IRE1 downregulation via a direct interaction.

I consistently observe IRE1 as a doublet in immunoblots. Although the precise identity of these two isoforms, the higher MW species could be a phosphorylated IRE1 species. Preliminary data suggests that KapC prioritizes the downregulation of the higher molecular weight species. In response to ER stress, IRE1 is auto-phosphorylated at Serines 724, 726, and 729 in the activation loop of the kinase domain, which is important for dimerization and total activation of the RNase domain (Prischi, Nowak, Carrara, & Ali, 2014). This fully phosphorylated, active IRE1 migrates as a higher MW species than the observed doublet in untreated cells as determined by immunoblot analysis. The top band in the IRE1 doublet may be a hypo-phosphorylated species that has low XBP1 splicing activity and could explain why KapC inhibition of IRE1 is only obvious in non-ER stressed cells. KapC is thought to be expressed during latency and since XBP1s

induces lytic replication, this inhibition of quasi-active IRE1 by KapC may be a mechanism that KSHV uses to prevent non-essential reactivation during low levels of ER stress. However, following exposure to toxic levels of ER stress, KapC is in ineffective at repressing fully activated IRE1, allowing KSHV to reactivate. Generating a KapC knockout virus will be essential to test these hypotheses.

The KSHV ORF screen revealed that ORF45 activates both the IRE1 reporter (XBP1-mCherry) and the ISR reporter (CHOP::GFP) suggesting that ORF45 causes ER stress and activates all 3 branches of the UPR. Analyzing expression of endogenous markers of UPR activity revealed that ORF45 upregulated the canonical marker of ER stress, BiP, as well as the ISR-dependent transcription factor CHOP (Figs 5.4 and 5.5). ORF45 also promoted IRE1 accumulation, which corresponded with low levels of spliced XBP1 mRNA. However, it does not appear that ORF45 is inducing classical UPR signaling. This is largely based on shRNA studies that showed that silencing PERK and ATF6 did not inhibit ORF45-induced CHOP and BiP expression, respectively (Fig 5.7). Surprisingly, ORF45 did upregulate ectopically expressed full length ATF6 which corresponded to ATF6 cleavage and increased BiP expression, but since ORF45 does not seem to impact endogenous ATF6, this phenotype is likely a result of ATF6 overexpression (Fig 5.6). Interestingly, overexpression of the constitutively active ATF6 or its DNA binding defective mutant caused a significant decrease in ORF45 protein levels suggesting that ATF6 may play a role in ORF45 signaling. Along these lines, ORF45 immunoblot banding pattern in full length ATF6 expressing cells showed a striking difference compared to vector control. However, ATF6 silencing did not impact this ORF45 banding pattern, and therefore, further studies are needed to determine the relationship between ORF45 and ATF6 signaling.

BiP is transcriptionally activated during ER stress and in mammalian cells this is mainly driven by ATF6-N, although there are some reports that XBP1s and ATF4 can also promote BiP transcription. Interestingly, in ORF45-expressing cells there was a minimal increase in BiP mRNA levels despite a robust increase in protein levels, suggesting that accumulation of BiP may be regulated by a transcription-independent mechanism. However, a more careful analysis of BiP transcription following ORF45 expression is required to fully comprehend the signaling involved. Interestingly, although BiP appears to be upregulated by ORF45 in an ATF6-independent manner, during lytic

replication BiP mRNA and protein levels do not change, even though ATF6 is cleaved. This suggests that KSHV may suppress both ATF6-dependent and -independent mechanisms of BiP upregulation. There are other non-transcriptional regulatory methods of BiP but these are less well understood. BiP mRNA contains a putative IRES but this IRES did not impact BiP expression following ER stress (Fernandez et al., 2002; Q. Yang & Sarnow, 1997). Interestingly, HCMV infection upregulated BiP in an ATF6 independent manner, which was reported to be mediated through IRES-dependent translation (N. J. Buchkovich et al., 2010; Nicholas J Buchkovich et al., 2008; Isler et al., 2005). Although HCMV does not express an ortholog of ORF45, it will be interesting to identify if these herpesviruses have evolved similar mechanisms to enhance translation of BiP. ORF45 activates the ERK-RSK pathway to phosphorylate eIF4B and stimulate the translation of mRNAs with complex 5'UTRs in a cap-dependent mechanism (Avey, Tepper, Li, Turpin, & Zhu, 2015). Therefore, ORF45 may be upregulating BiP translation independent of its IRES. A recent study showed that robust BiP translation during ER stress is dependent on the presence of uORFs in the 5'UTR, which contain CUG start sites (Starck et al., 2016). This mechanism of BiP translation was also dependent on the alternative translation initiation factor eIF2A, which does not depend on GTP cycling from eIF2B (Golovko et al., 2016). Therefore, it is possible that ORF45 promotes BiP translation though a uORF- and eIF2A-dependent mechanism.

ORF45 activated the ISR but this is likely independent of PERK activity; in fact, PERK silencing increased CHOP expression (Fig 5.7). This suggests that ORF45 activates the ISR through one of the other eIF2α kinases. ORF45 stimulates cell growth through RSK dependent activation of eIF4B, mTORC1 and mTORC2 (Avey et al., 2015; H. H. Chang & Ganem, 2013). Potentially this increase in cell growth rapidly depletes the cell of amino acids and growth factors which could activate GCN2 (P. Zhang et al., 2002). Alternatively, UV induces a DNA Damage response (DRR) which activates GCN2, reportedly through the DDR effector DNA-PKcs (Powley et al., 2009). Using this rationale, rapid cell growth and replication by ORF45 could lead to the accumulation of DNA damage, thereby activating the ISR through GCN2. I consistently observed high amounts of cell of toxicity in cells overexpressing ORF45, which may be consistent with hyperproliferation and activation of DDR. Careful analysis of the ISR activation status

following genetic silencing of each of the eIF2α kinases will help elucidate how ORF45 is activating the ISR.

ORF45 also induced low levels of XBP1 splicing, which was dependent on IRE1. Interestingly, IRE1 was not obviously phosphorylated as determined by a lack of mobility shift in an immunoblot that XBP1 splicing can occur without a clear induction of activation based on phosphorylation. Although ORF45 did not induce an observable increase in IRE1 phosphorylation, there was a significant accumulation of total IRE1 that corresponded to a robust accumulation of XBP1u mRNA and protein. XBP1 transcription has shown to be upregulated by ATF6 (Yoshida et al., 2001), however this is likely not playing a role in ORF45-expressing cells since ATF6 does not appear to be active. IRE1 was also reported to be transcriptionally upregulated by ATF4 (Tsuru et al., 2016). Since IRE1 levels decreased in ISR-deficient eIF2α Ser51Ala mutant cells expressing ORF45, it is plausible that IRE1 accumulation by ORF45 is due to increased ATF4 (Fig 5.8). XBP1u protein levels were also reduced in these mutant cells suggesting that the ISR may also be playing a role in XBP1u accumulation. See Appendix A for further evidence that the ISR regulates XBP1u levels.

The precise role of XBP1u is largely unknown. In unstressed cells its expression level is quite low in part due to its highly labile nature (Calfon et al., 2002). Therefore, in most situations XBP1u function may be innocuous. Much of the ascribed roles for XBP1u have been based on ectopic expression. One study showed that XBP1u can bind and promote XBP1s degradation (Yoshida et al., 2006). Another group proposed that XBP1u can promote degradation of the autophagy-dependent transcription factor FoxO1, which results in the attenuation of autophagy (Vidal et al., 2012; Zhao et al., 2013). Potentially, ORF45-induced XBP1u can also inhibit XBP1s and/or FoxO1.

Many of these UPR-related phenotypes observed during ORF45 ectopic expression do not occur during lytic replication. This may be because ORF45 behaves differently depending on if its expressed alone or in the context of lytic replication. During infection, ORF45 may be regulated by other viral genes, which could impact ORF45-dependent upregulation of BiP or activation of the ISR. For example, ORF45 was reported to interact with the viral protein kinase ORF36 (Avey et al., 2016), which could influence ORF45 cellular localization and/or signaling. Therefore, it may be useful to conduct a KSHV ORF counter-screen for inhibitors of ORF45-induced UPR markers.

ORF45 is a tegument protein that gets incorporated into the budding virus (Fan Xiu Zhu & Yuan, 2003). Therefore, another potential explanation for this discrepancy between ectopic ORF45 and ORF45 expressed during lytic replication, is that virus-associated ORF45 may induce these UPR-like effects upon entry. BiP is normally located in the ER but there are reports that it can be found elsewhere in the cell including the plasma membrane (Y. Zhang et al., 2010). It was recently reported that BiP binds the glycoprotein of the flavivirus JEV, and blocking plasma membrane-localized BiP reduced viral entry (Nain et al., 2017; Y.-P. Wu et al., 2011). Polyomavirus SV40 entry involves penetrating the ER to reach the cytoplasm, which requires multiple ER enzymes required for protein quality control, including BiP (Geiger et al., 2011). Although KSHV does not enter the ER during entry, some of the UPR markers that ORF45 upregulates may play a key role in the delivery of the viral genome to the nucleus. Therefore, future studies identifying the impact that ORF45 has on the UPR during entry are necessary.

ORF45 upregulation of UPR markers differs from the study by P.-J Chang *et al.* (2014), which proposes that the larger isoforms of ORF45, ORF47/45A and ORF47/45B, but not ORF45, are responsible for this induction. The data presented in their study is puzzling because immunoblots of all three ORF45 variants show protein species that are the same size, even though ORF47/45A and ORF47/45B are 114 and 56 amino acids longer than ORF45, respectively. They also showed that BiP is upregulated during the lytic cycle, which I did not observe. I also found that BiP is further suppressed with drug-induced ER stress. These discrepancies regarding BiP expression during the lytic cycle could be explained by the different cell models used and/or method of inducing lytic reactivation. Whereas, I used the dox-inducible TREx BCBL1-RTA cells, P.-J. Chang *et al.* used NaB or TPA to induce lytic reactivation, which can have off-targets and may impact BiP expression. Evidently, further understanding of the mechanisms in which these different ORF45 isoforms are expressed, and their potential function in regulating the UPR during lytic replication are necessary to clarify some of these discrepancies.

A handful of other viral ORFs were identified from the screen as potential modulators of UPR activity, which requires further investigation. These include K2 (vIL-6), the E3 Ubiquitin ligase K3, ORF72 (vCyclin), and ORF74 (vGPCR). vIL-6 enhanced mCherry fluorescence following treatment with Tg, which was unique to this ORF. All of

the other viral ORFs that showed IRE1 activity had reduced XBP1-mCherry expression following Tg.

Like human IL-6, vIL-6 is expressed in the ER, however it constitutively signals through gp130, whereas human IL-6 requires both gp130 and IL-6 receptor engagement for signaling (Molden et al., 1997). Interestingly, vIL-6 was recently shown to bind to HYOU1 (GRP170) (Giffin, Yan, Ben Major, & Damania, 2014), which is one of the two BiP-specific nucleotide exchange factors (NEFs), and is important for BiP chaperone activity (Behnke, Feige, & Hendershot, 2015). *In vitro* studies showed that HYOU1 promoted BiP activity to bind and break up IRE1 dimers (Amin-Wetzel et al., 2017). Therefore, vIL-6 may block IRE1 monomerization by BiP through sequestration of HYOU1 to promote robust IRE1 activation. vIL-6 is latently expressed in many plasmablast tumors and is important for tumorigenesis (Giffin & Damania, 2014). One potential model for the role of vIL-6 enhancement of IRE1 signaling is that in response to ER stress, vIL-6 promotes robust IRE1 activation of XBP1s to ensure efficient viral reactivation in these cells. In addition, XBP1 binding sites were found in the vIL-6 promoter and therefore ER stress may promote a positive feedback loop for upregulating vIL-6 via IRE1 activation.

The ORF screen revealed that K3 can inhibit CHOP:GFP expression. Interestingly, K3 did not affect GFP levels following treatment of L-histidinol (data not shown), an inhibitor of the His-tRNA synthetase that activates GCN2 (P. Zhang et al., 2002). This suggests that K3 may directly impact PERK signaling. K3 is an E3 ubiquitin ligase that can promote degradation of MHC class I and other immune modulator molecules such as Cd1d, PECAM, and IFN-γR1, to help the virus evade detection by the immune system (Brulois et al., 2014). One provocative hypothesis is that K3 ubiquitinates and degrades PERK in its active dimeric conformation. PERK levels are attenuated as lytic replication progresses, which corresponds to a decrease in eIF2α phosphorylation following treatment with Tg (Fig 3.3). This inhibition largely occurs during the late lytic phase of the replication cycle, which roughly corresponds with when K3 is expressed (Arias et al., 2014). Late lytic replication is also when the bulk of the viral glycoproteins are translated in the ER. Therefore, during late phases of lytic replication, K3 may degrade PERK to block attenuation of the synthesis of viral proteins. However, if K3-mediated degradation is specific towards activated PERK, then blocking

PERK phosphorylation with PERKi should presumably restore PERK levels, which does not seem to be the case (Fig 3.3).

vGPCR is a mutant ortholog of human CXCR1/CXCR2 and signals independent of ligand binding and thus is constitutively active (Bais et al., 1998). vGPCR upregulates neo-angiogenic growth factors and cytokines such as IL-6 (Montaner et al., 2004), which has shown to promote XBP1 expression (Wen et al., 1999). XBP1s has also been reported to upregulate IL-6 (Iwakoshi et al., 2003b; Martinon et al., 2010). vGPCR has also been reported to bind and inhibit SERCA2b, resulting in decreased ER Ca^{2+} levels (J. Zhang et al., 2015). Therefore, vGPCR may act analogous to Tg and impede chaperone function, which triggers ER stress. Identifying SERCA2b binding mutants of vGPCR will be important for testing if vGPCR can induce ER stress by inhibiting SERCA2b.

vCyclin is a latent protein but is also expressed during the lytic cycle (Cannell & Mittnacht, 1999). vCyclin is an ortholog of the cell cycle regulator cyclin-D and forms a heterodimer with CDK6 to promote hyperproliferation. Analogous to the oncogene Ras, v-Cyclin also causes DNA damage which in some cells initiates a cell cycle arrest program known as oncogene-induced senescence (Koopal et al., 2007). Since GCN2 is activated in response to DNA damage (Anda et al., 2017), it is possible that the large increase in CHOP:GFP by vCyclin is due to the activation of GCN2.

All or some of these viral ORFs identified by this screen may play a role in modulation of the UPR and ISR during virus replication and therefore further investigation is required to tease out their specific roles during infection. The KSHV lentiviral ORF library used in this screen also does not contain newly identified KSHV protein isoforms or miRNAs and lncRNAs. These viral factors may have unidentified roles in modulating the UPR. Of importance, the lncRNA PAN is the most abundant viral RNA during lytic replication and was shown through ribosomal footprinting to encode 3 peptides, one of which has a putative ER signal sequence. Translation of this peptide may have an effect on UPR signaling. Clearly, there is much to be learned about how KSHV and its arsenal of effectors can control UPR signaling to promote replication and disease.

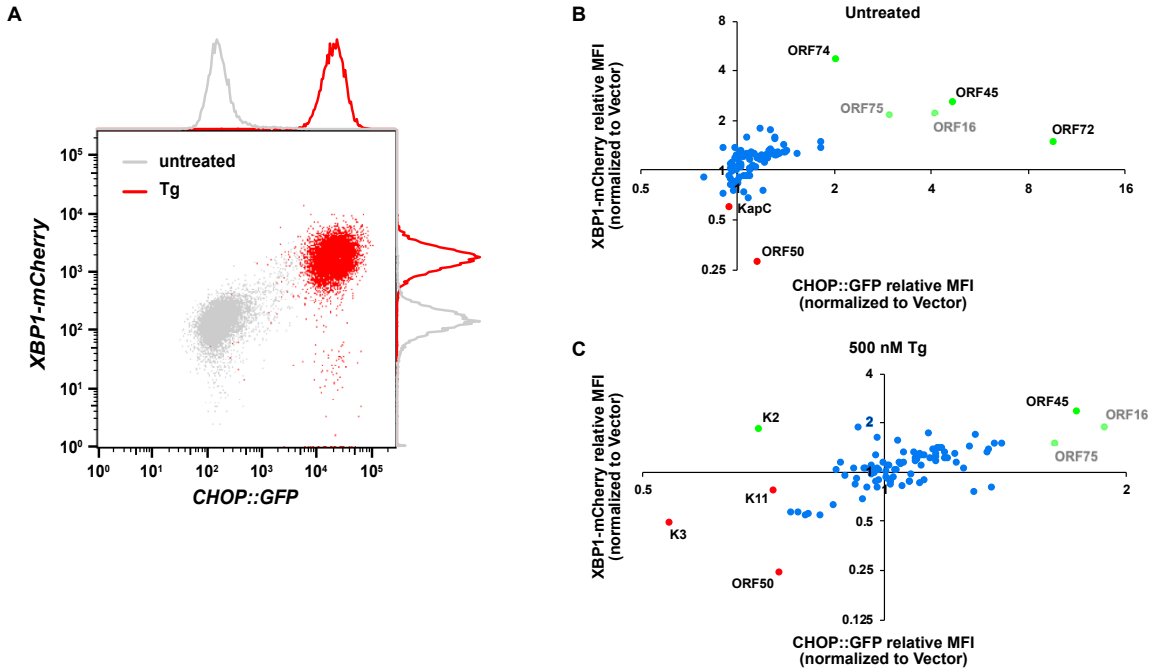

Fig 5.1 KSHV lentiviral ORF screen for modulators of the ISR and IRE1 using a dual fluorescence cell reporter

(A) Flow cytometry analysis of CHOP::GFP and XBP1-mCherry dual reporter CHO-7.1 cells untreated or treated with 500 nM Tg for 20 h. (B and C) CHO-7.1 reporter cell line was transduced with empty vector control and KSHV ORF lentiviral vectors (in batches of 8-12 ORFs per batch plus an empty vector control) and selected for with puromycin. Following selection, transduced cells were untreated or treated with 500 nM Tg for ~ 20 h and CHOP:GFP and XBP1-mCherry signal was measured by flow cytometry and normalized relative to the matched empty vector control. Based on observable deviation from the majority of viral ORFs, potential UPR activators (green) and inhibitors (red) are highlighted. ORFs highlighted in grey were highly toxic to the reporter cell line. Viral ORFs with potential UPR activation or inhibition were re-screened by flow cytometry to confirm result (data not shown).

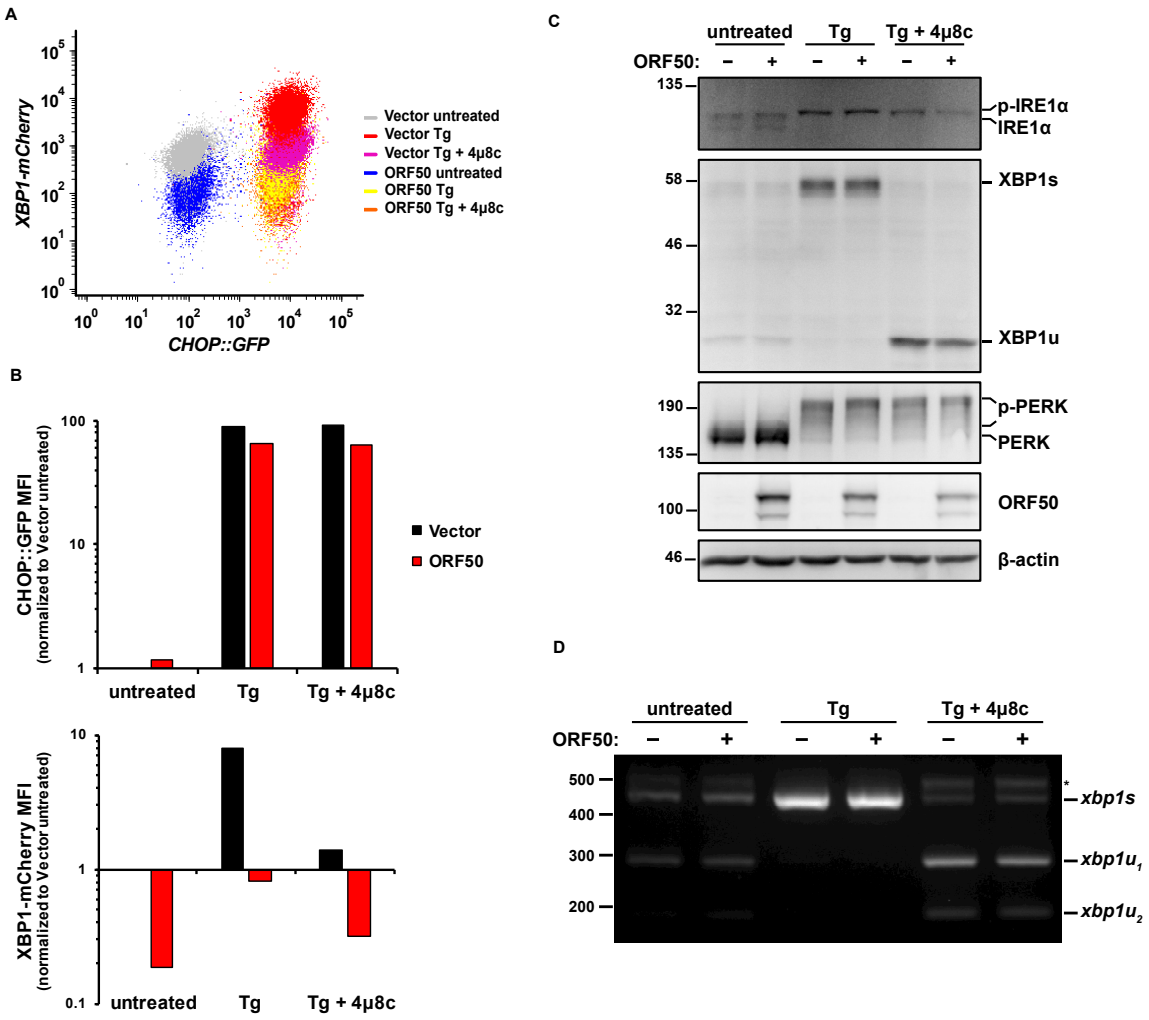

Fig 5.2 A discrepancy between IRE1 fluorescence reporter and endogenous IRE1 activity in RTA-expressing CHO-7.1 cells

(A) Flow cytometry analysis of CHOP::GFP and XBP1-mCherry dual reporter CHO-7.1 cells transduced with ORF50 or empty vector control. The cells were untreated or treated with 500nM Tg with or without 10μM 4μ8c for 20 h. (B) CHOP::GFP MFI and XBP1-mCherry MFI were determined from (A) and normalized to MFI of vector untreated cells. (C) Immunoblot of IRE1α, XBP1, PERK, ORF50 and β-actin (loading control) in ORF50- and Vector-transduced CHO-7.1 cell lysate. The cells were treated as in (A) but for 8 h instead. Monoclonal XBP1 antibody recognize epitope surrounding Leu64 and detects both spliced and unspliced XBP1 but does not cross react with XBP1-mCherry. The migration shifts in IRE1α and PERK blots correspond to phosphorylation. (D) PstI-treated PCR of XBP1 cDNA from CHO-7.1 cells treated as in (C). The primers were designed to specifically amplify CHO xbp1 cDNA. (*) corresponds to xbp1u-xbp1s hybrid cDNA. All data in panel were conducted once.

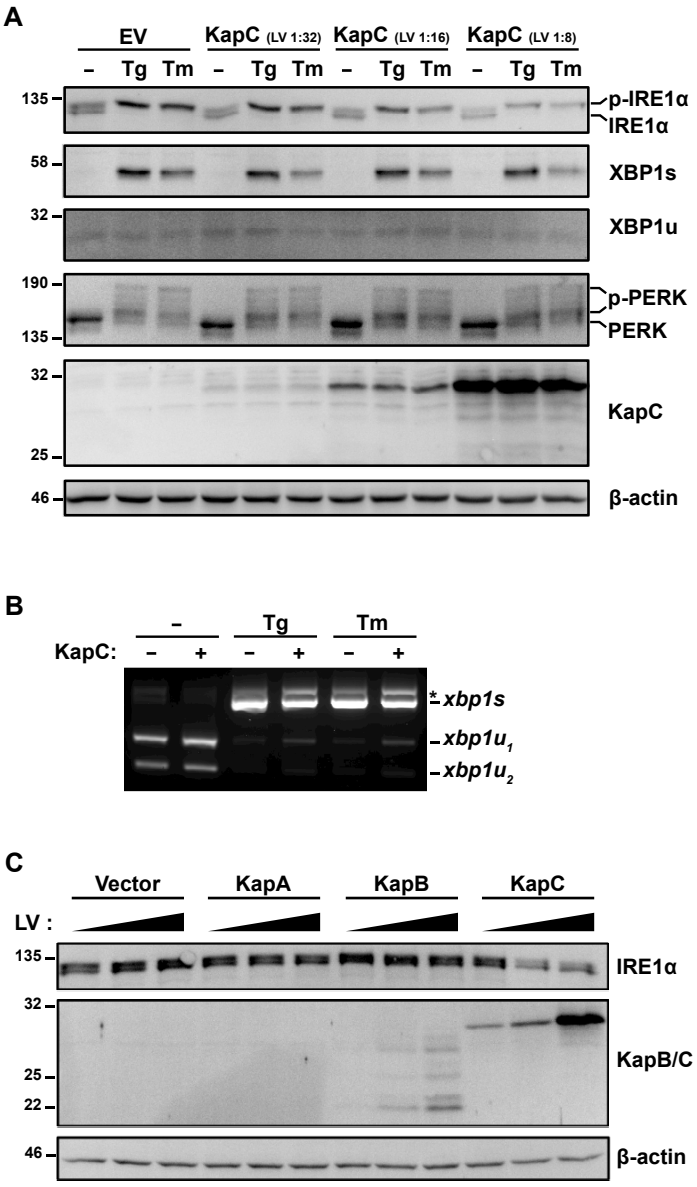

Fig 5.3 Kaposin C decreases IRE1α expression

(A) 293A cells were transduced with increasing concentration of CMV-driven Kaposin C lentiviral vectors (lentivirus [LV] dilutions: 1:32, 1:16, 1:8) or empty vector control and treated with 150 nM Tg or 5 μg/mL Tm for 4 h followed by harvesting cell lysate for immunoblot analysis of UPR markers and Kaposin C. β-actin was used as a loading control. (B) XBP1 cDNA from 293A cells transduced with Kaposin C lentiviral vector (1:8 dilution) treated with Tg, Tm or untreated were PstI-digested and resolved on an agarose gel. (*) corresponds to xbp1u-xbp1s hybrid cDNA. (C) 293A cells were transduced with increasing titer of Kaposin A, B, or C lentiviral vectors (lentivirus dilutions: 1:32, 1:16, 1:8) or empty vector control and whole cell lysates were analyzed by immunoblots for IRE1α and an anti-Kaposin antibody that recognizes Kaposin B and C but not Kaposin A. β-actin was used as a loading control. All experiments in the panel were conducted once (N=1).

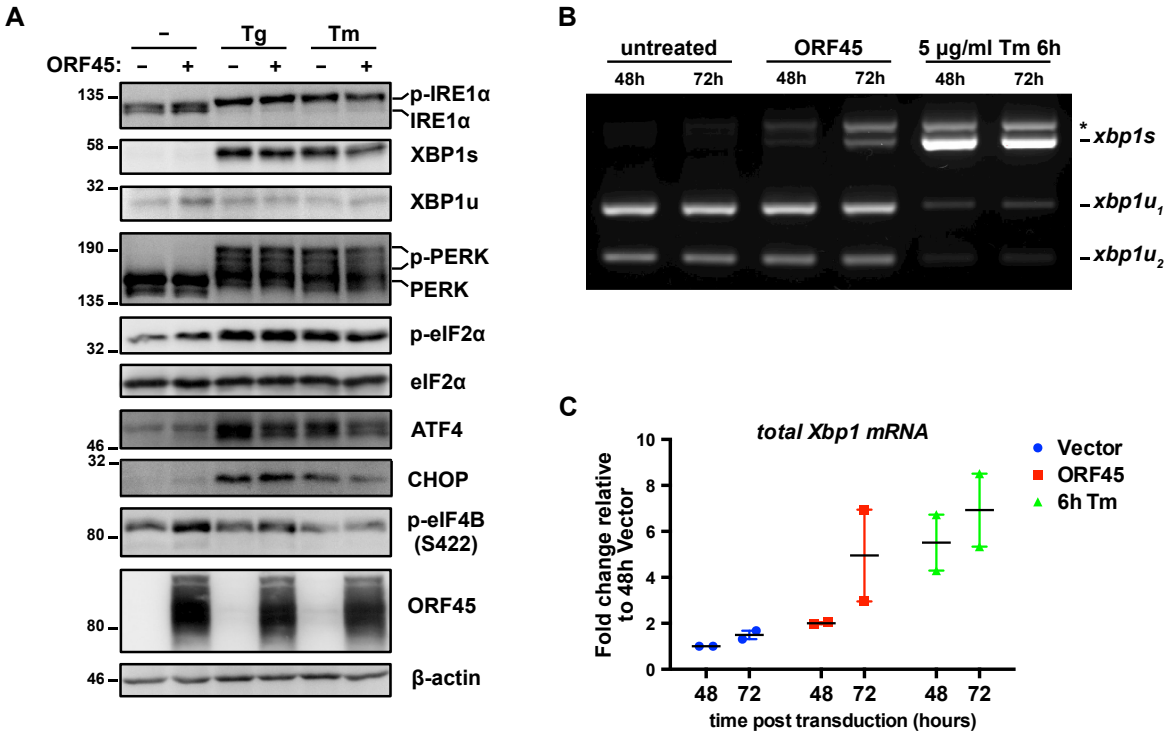

Fig 5.4 ORF45 upregulates IRE1 and XBP1 and activates the ISR
(A) 293A cells were transduced with ORF45 lentiviral vector or empty vector control and treated with 150 nM Tg or 5 μg/mL Tm for 4 h followed by harvesting cell lysate for immunoblot analysis. A panel of UPR protein markers, ORF45, and phospho-ser422 eIF4B were probed for. XBP1u and XBP1s blots were from the same membrane but cropped to allow for changes in digital contrast that will not saturate the signal of either protein. β-actin was used as a loading control. (B) Hela cells were transduced with ORF45 lentiviral vector or empty vector control for 2 and 3 d or matched untransduced HeLa cells treated with 5 μg/mL Tm followed by harvesting for total RNA. PstI-treated XBP1 cDNA was resolved on an agarose gel and visualized with SYBR Safe. (*) corresponds to xbp1u-xbp1s hybrid cDNA. The agarose gel is representative of 2 independent experiments. (C) Total RNA from (B) was used to quantify total XBP1 mRNA levels by qPCR. The mean of 2 independent experiments are graphed and the error bars denote the SEM.

Fig 5.5 ORF45 upregulates components of the UPR in a time-dependent manner
(A) HeLa cells were transduced with ORF45 lentiviral vector or empty vector control for 2 and 3 d or matched untransduced HeLa cells were treated with 5μg/mL Tm followed by harvesting for total RNA. mRNA levels of ATF6 target genes BiP and HERPUD1, XBP1s target gene ERdj4, and ATF4 target gene CHOP, were measured by qPCR. The means of 2 independent experiments are graphed and the error bars denote the SEM. (B) HeLa cells were transduced with ORF45 lentiviral expression vector or empty vector control over a 5-d time course and harvested for immunoblot analysis. Untransduced cells treated with 5 μg/mL Tm for 3 or 6 h used as positive controls. The immunoblots of the time course were conducted in one independent experiment (N=1).

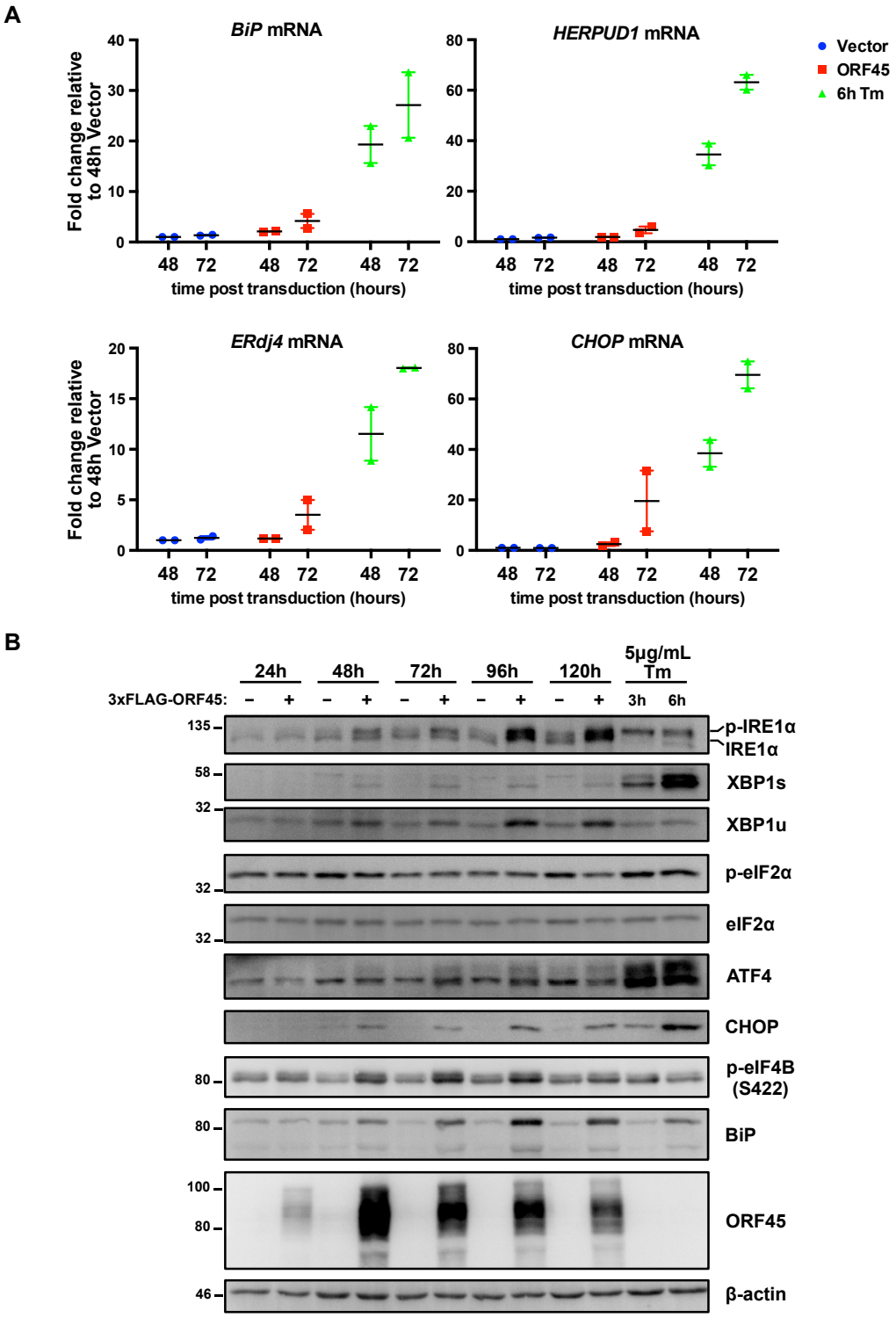
A
BiP mRNA
HERPUD1 mRNA
ERdj4 mRNA
CHOP mRNA
Fold change relative to 48h Vector
time post transduction (hours)
Vector
ORF45
6h Tm
B
24h
48h
72h
96h
120h
5μg/mL Tm
3xFLAG-ORF45:
3h
6h
p-IRE1α
IRE1α
XBP1s
XBP1u
p-eIF2α
eIF2α
ATF4
CHOP
p-eIF4B (S422)
BiP
ORF45
β-actin

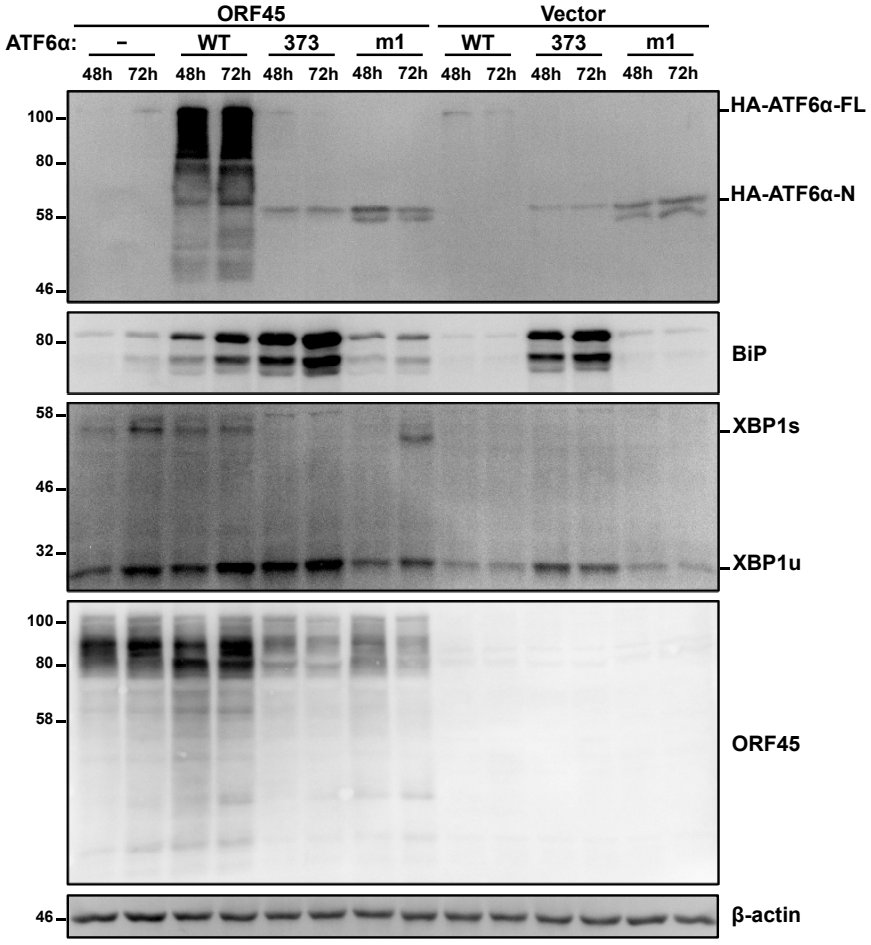

Fig 5.6 ORF45 enhances HA-ATF6 expression to promote BiP accumulation
HeLa cells were co-transduced with lentiviral vectors expressing full length HA-ATF6α (WT), constitutively active HA-ATF6α (N-terminal fragment 1-373 amino acids [373]), or dominant negative HA-ATF6α (DNA binding mutant of N-terminal fragment 1-373 amino acids [m1]) and either 3xFLAG-ORF45 or empty vector control lentiviruses. 3 d post-transduction cells were harvested for immunoblot analysis of HA-ATF6α, ATF6 target genes BiP and XBP1s, and ORF45. β-actin was included as a loading control. Immunoblots shown are representative of two independent experiments, except XBP1 was only completed once.

Fig 5.7 ORF45 does not induce canonical ER stress-induced UPR signaling
(A and B) HeLa cells were transduced with lentiviral vectors expressing either a non-targeting shRNA (NS) or shRNAs targeting each of the sensors of the UPR (ATF6α, IRE1α, and PERK). Following puromycin selection, cells were transduced with empty vector control lentivirus or 3xFLAG-ORF45 for 3 d. Untransduced cells were treated with 500 nM Tg for 4 h prior to harvesting for either (A) immunoblot analysis or (B) total RNA for qPCR. (A) Immunoblot analysis of UPR marker proteins and ORF45. β-actin was analyzed for a loading control. Immunoblots shown are representative of two independent experiments. (B) mRNA levels of ATF6 target genes BiP and HERPUD1, IRE1 target gene ERdj4, and ISR gene CHOP were measured by qPCR and change in levels was calculated using the ΔΔCt method and compared relative to the empty vector and non-targeting shRNA control cells. 18S rRNA was used as the reference gene. The mean of two independent experiments are shown and the error bars correspond to the standard deviation of the mean.

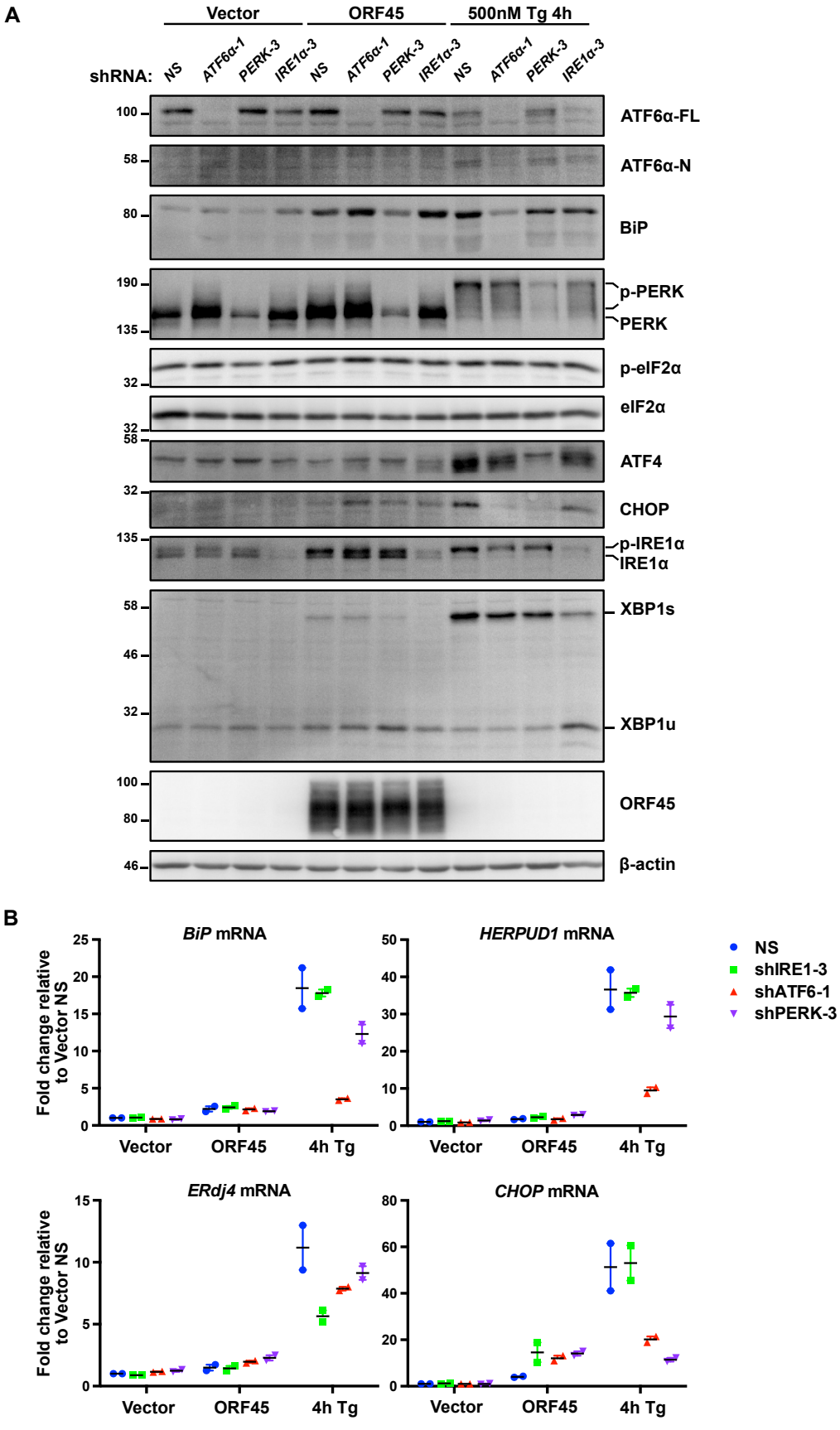
A
Vector
ORF45
500nM Tg 4h
shRNA:
NS
ATF6α-1
PERK-3
IRE1α-3
ATF6α-FL
ATF6α-N
BiP
p-PERK
PERK
p-eIF2α
eIF2α
ATF4
CHOP
p-IRE1α
IRE1α
XBP1s
XBP1u
ORF45
β-actin
B
BiP mRNA
HERPUD1 mRNA
ERdj4 mRNA
CHOP mRNA
Fold change relative to Vector NS
Vector
ORF45
4h Tg
NS
shIRE1-3
shATF6-1
shPERK-3

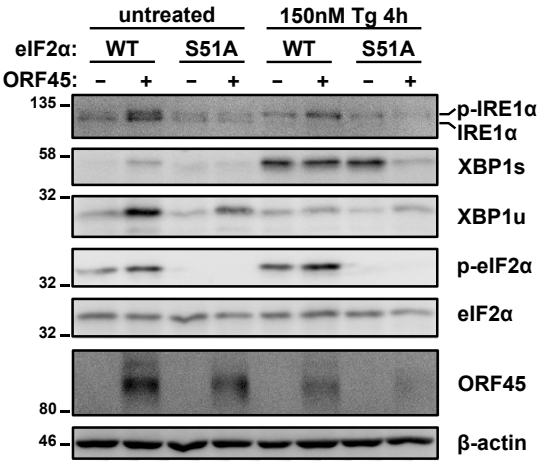

Fig 5.8 ORF45 upregulation of IRE1 and XBP1 may be dependent on the ISR
CRISPR eIF2α Ser51Ala knock-in mutant HeLa cells or matched control cells were transduced with 3xFLAG-ORF45 or empty vector control for 3 d and left untreated or treated with 150 nM Tg for 4 h. Whole cell lysates were processed for immunoblot analysis of IRE1, XBP1, phospho- and total eIF2α. ORF45 was analyzed to confirm expression and β-actin was used for a loading control. Immunoblots are N=1.

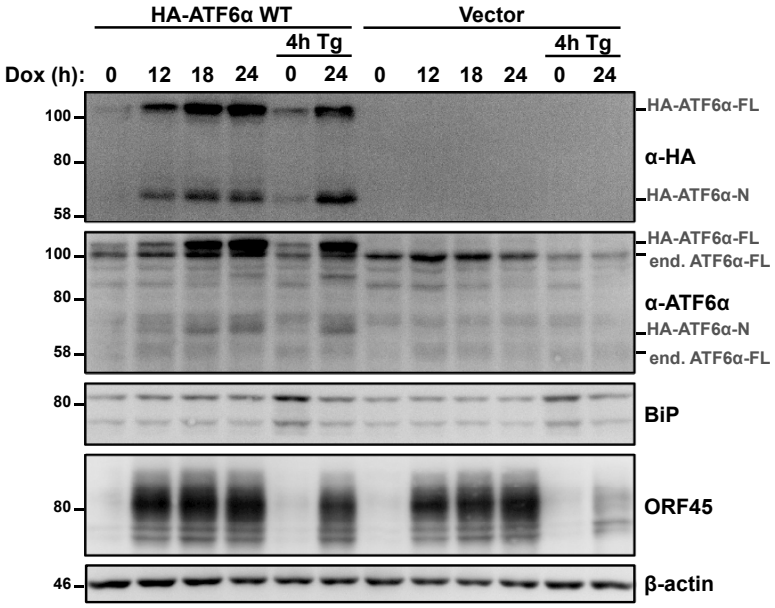

Fig 5.9 ATF6 is activated but BiP is not upregulated during lytic replication
TREx BCBL1-RTA cells were transduced with lentivirus encoding full length HA-ATF6α (WT) or empty vector control and transduced cells were selected for with puromycin. Following selection, cells were left untreated or treated with 1 μg/mL dox for 0, 12, 18, and 24 h to induce lytic replication. 0 and 24 h dox-treated samples were also treated with 75 nM Tg for 4 h prior to harvesting. Immunoblots were analyzed for HA-ATF6α, ATF6α (detects ectopic and endogenous ATF6α), ATF6 target gene BiP, and ORF45. β-actin was included as a loading control. The immunoblots are N=1.

CHAPTER 6 CONCLUSIONS

6.1 Summary

Disruption of ER protein homeostasis due to environmental or physiological factors can lead to the accumulation of unfolded or misfolded proteins, which is called ER stress. Eukaryotic cells have evolved a signaling response called the UPR to mitigate ER stress. In metazoans, the UPR consists of three ER transmembrane proteins, IRE1, PERK and ATF6, that sense increased protein misfolding and become activated. Together, these activated sensors attenuate the translational burden, and signal to the nucleus through the activation of bZIP transcription factors XBP1s, ATF4, and ATF6-N. These stress-responsive transcription factors upregulate genes that encode chaperones, foldases, lipid biosynthetic enzymes, and anti-oxidant factors. Catabolic machinery involved in ERAD and autophagy are also upregulated to degrade misfolded proteins. However, if ER stress persists, then the UPR switches from an adaptive response to a pro-apoptotic response (Walter & Ron, 2011).

Many physiological processes require UPR activation. Professional secretory cells, such as insulin-secreting β cells and antibody-secreting plasma cells, activate the UPR to prepare the cell for the increase in ER protein load. Inflammatory responses specifically activate the IRE1-XBP1 pathway. However, persistent ER stress or dysregulated UPR signaling is also associated with various types of diseases such as cancer, neurological disorders, inflammatory bowel disease, and type II diabetes (S. Wang & Kaufman, 2012).

UPR signaling is also implicated in infection, both bacterial and viral. Based on the different effects of UPR activation, it can likely have both pro- and anti-viral properties. Interestingly, there is increasing evidence that different viruses may selectively activate certain UPR sensors while inhibiting other sensors or their downstream transcription factors. Viruses are extremely adept at hijacking cellular processes, including stress responses, to promote infection. Thus, some viruses may have also evolved to fine-tune UPR signaling to activate the pro-viral signaling of the UPR while suppressing the potential anti-viral components.

KSHV is a large, enveloped human oncogenic herpesvirus that primarily infects B cells and can cause primary effusion lymphoma and multicentric Castleman's disease. KSHV has expanded its repertoire of cellular targets and can cause Kaposi's sarcoma

through the infection of endothelial cell. Like all herpesviruses, KSHV has latent and lytic cycles, but latency is the default replication program. Importantly, both latent and lytic cycles contribute to pathogenesis and in a KS lesion approximately 10% of infected cells express lytic markers. Through the production of multiple oncogenes and homologs of human cytokines and chemokines, KSHV lytic replication promotes a pro-inflammatory and neo-angiogenic environment that drives tumor growth (Ganem, 2007).

The *in vivo* signals that trigger the switch from latency to the lytic cycle are unknown, but *in vitro*, different types of stress can reactivate the virus through upregulation of the immediate early viral protein RTA (Lukac et al., 1998). ER stress can induce RTA expression through direct transactivation by XBP1s (Wilson et al., 2007), but it is unknown if lytic replication itself can cause ER stress. Multiple lytic viral genes are expressed in the ER, and the combination of upregulated inflammatory molecules in the ER may saturate the protein folding machinery and activate the UPR. The aim of this thesis was to identify the status of UPR activation during lytic replication and evaluate its impact on virus replication.

Chapter 3 demonstrated that the induction of lytic replication activated all three sensors of the UPR. The RNase IRE1 was phosphorylated and its substrate XBP1 mRNA was spliced. PERK and eIF2α were phosphorylated, and ATF6 was proteolytically cleaved. Surprisingly, the downstream transcription factors were not active. XBP1s did not accumulate and XBP1starget genes were not upregulated; eIF2α phosphorylation did not induce ATF4 expression; and ATF6-N, although detected, did not upregulate its canonical target genes. I further showed that activation of UPR sensors is likely important for KSHV replication, since chemical inhibition or genetic silencing resulted in decreased virus production.

The inhibition of XBP1s was somewhat surprising since it has been shown to induce lytic reactivation by upregulating RTA. However, XBP1s may have other UPR-associated roles, such as upregulating ERAD, which may have a deleterious effect on the replicating virus. Chapter 4 revealed that ectopic XBP1s expression activated early stages of lytic replication but potently blocked virus production. Interestingly, this was only seen in a non-KSHV adapted tumor cell line, whereas in a PEL cell line, XBP1s promoted virus production. Since KSHV can infect multiple different cell types, these

contrasting findings may have important implications for the role of XBP1s in different cell contexts.

Activating the ER stress sensors, while simultaneously inhibiting the downstream transcription factors during lytic replication, suggests that KSHV may encode viral proteins dedicated to re-programming UPR signaling. Chapter 5 demonstrated that there are multiple KSHV proteins that can activate or suppress UPR signaling, and some of these proteins may show specificity toward one of the branches. Collectively, these findings suggest that KSHV likely encodes different viral proteins to usurp the ER stress sensors to promote virus production instead of resolving ER stress.

6.2 KSHV Modulates UPR Signaling

During lytic replication, IRE1 was activated and XBP1s mRNA was spliced, but XBP1s gene targets were not upregulated. Treatment with drugs that induce ER stress, such as Tg or Tm, also failed to upregulate XBP1s protein even though there were increased levels of splicing. Normally, IRE1 is upregulated in response to ER stress, however the opposite was observed in response to lytic replication: IRE1 levels became attenuated as the lytic cycle progressed. IRE1 undergoes dimerization, followed by oligomerization, which is necessary for its XBP1 splicing activity (Shamu & Walter, 1996). As well as inducing XBP1 splicing, IRE1 can also degrade ER-targeted mRNAs by RIDD (Hollien et al., 2009). At least *in vitro*, it has been reported that IRE1 formed higher-order oligomers preferentially spliced XBP1, whereas dimeric forms of IRE1 had a more relaxed substrate specificity and engaged RIDD (Tam et al., 2014). Therefore, reduced IRE1 levels during the lytic cycle may prevent the formation of IRE1 oligomers, preferentially inducing RIDD. Furthermore, XBP1 deficiency can cause IRE1 hyperactivation to increase RIDD activity (A.-H. Lee et al., 2011), which may also be contributing to RIDD during lytic replication. RIDD may be used by KSHV (and other viruses) as a form of host shutoff to prioritize translation of viral glycoproteins over cellular proteins. I have attempted to measure RIDD activity during lytic replication and preliminary results showed that a few canonical RIDD substrates were consistently attenuated during lytic replication. However, treatment with the IRE1 inhibitor 4μ8c did not reliably restore mRNA levels of these IRE1 substrates. This is likely due to variability between qPCR replicates, as well as off-target toxic effects from 4μ8c.

Therefore, more careful analysis of the role of RIDD during lytic replication is required and RIDD reporters or IRE1 knockout cell lines will likely be beneficial for this endeavor.

IRE1 can also activate the MAPK JNK pathway through the binding and oligomerization of TRAF2, which recruits the MAP3K ASK1 to phosphorylate JNK (Nishitoh et al., 2002). XBP1 deficiency may also promote JNK phosphorylation through hyperactivation of IRE1 (Olivares & Henkel, 2015). JNK signaling has been reported to be activated during KSHV infection and there are multiple viral proteins that can promote JNK phosphorylation (Bais et al., 1998; Brinkmann et al., 2003; Hamza et al., 2004). Therefore, one potential model is that KSHV activates IRE1 while suppressing XBP1 to activate JNK signaling, which can promote virus replication. Analogous to this theory, HSV-1 has also been reported to activate JNK signaling through activation of IRE1 kinase activity while suppressing its RNase activity. Importantly, inhibition of either IRE1 or JNK reduced HSV-1 replication (Su et al., 2017). Both HCV and HCMV activate IRE1 but suppress expression of XBP1s-dependent genes (Isler et al., 2005; Tardif, Mori, & Siddiqui, 2002). The impact on RIDD or JNK phosphorylation was not investigated in these infection models but it would be interesting to determine if multiple different viruses have evolved a common mechanism of impeding the IRE1-XBP1s signaling to repurpose IRE1 for RIDD and/or JNK phosphorylation.

During lytic replication, eIF2α is phosphorylated but the master regulator of the ISR, ATF4, is not upregulated. ATF4 normally upregulates CHOP, and together they can upregulate genes to promote autophagy and apoptosis (B'chir et al., 2013; J. Han et al., 2013). Autophagy and apoptosis can be activated by multiple different mechanisms and these processes are generally considered inhibitory to KSHV. As a result, the virus encodes multiple different proteins to suppress both autophagy and apoptosis (Cirone, 2018; Patrick S. Moore, 2007). In this light, it seems plausible that KSHV has evolved to suppress autophagy and apoptosis by dismantling the ISR via ATF4 inhibition.

In the absence of stress, translation of ATF4 and other stress-responsive genes is inhibited due to the presence of uORFs in the 5'UTR of their mRNAs. Phosphorylation of eIF2α reduces the pool of active TCs, which prolongs translation re-initiation allowing translation of ATF4 (Vattem & Wek, 2004). During lytic replication the pool of cellular translating mRNAs is reduced by the viral protein SOX (ORF37) (Glaunsinger & Ganem,

2004b), which may increase the threshold for phospho-eIF2α-dependent ATF4 translation. There are also translation-regulating uORFs in a few KSHV mRNAs. Importantly, there are two uORFs in the tricistronic mRNA encoding ORF35-ORF36-ORF37 that are essential for robust translation of ORF36 (Kronstad et al., 2013). Potentially, SOX may regulate ORF36 expression through host-shutoff-dependent control of uORF-mediated translation.

Unlike XBP1s and ATF4, ATF6-N is not inhibited at the protein level during lytic replication, but its transcriptional activity is suppressed based on its inability to upregulate canonical target genes, such as BiP and HERPUD1. ATF6 is a bZIP transcription factor and a characteristic feature of this family of transcription factors is that they can heterodimerize (Reinke et al., 2013). KSHV encodes the bZIP transcription factor, K-bZIP, which is generally considered a transcriptional repressor (W.-S. Yang et al., 2015). Tentatively, K-bZIP may heterodimerize with ATF6-N and represses its activity. Alternatively, ATF6 binding to its target genes may be inhibited. ATF6 binding to cis-elements, such as ERSE and ERSE-II motifs, is dependent on the presence of the transcription factor NF-Y (K. Yamamoto et al., 2004). During lytic replication, KSHV hijacks multiple cellular transcription factors such as RBP-J-κ and C/EBPα to promote lytic replication (Aneja & Yuan, 2017). NF-Y may be recruited to the KSHV genome to promote viral gene expression, thereby preventing ATF6 from binding and upregulating UPR-dependent genes. There may also be ERSE and ERSE-II motifs in the promoters of KSHV genes, which could titrate out the available pool of ATF6-N. Further examination of how ATF6-N (and the other branches of the UPR) may regulate viral gene expression is clearly warranted.

6.3 XBP1s Promotes Lytic Reactivation but can Inhibit Replication at a Late Phase

Ectopic expression of XBP1s induced lytic replication in both TREx BCBL1-RTA cells and iSLK.219 cells. Conversely, robust virus production was stymied in iSLK.219 cells but was intact in the PEL cell line. The replication cycle is approximately twice as fast in the TREx BCBL1-RTA cells compared to iSLK.219, which may not provide XBP1s with enough time to carry out its inhibitory effect on virus replication. Consistently, accelerating lytic replication in iSLK.219 with NaB abolished XBP1s-mediated virus inhibition. However, NaB likely has other effects on the virus other than accelerating

replication. Further analysis is required to determine if the duration of replication cycle is a pre-determining factor for XBP1s sensitivity.

PTMs may also contribute to the observed differences in virus inhibition in cells ectopically expressing XBP1s. XBP1s, ORF45, and ORF65 showed various differences in protein banding patterns following expression of XBP1s that seem to be cell type-specific. Notably, the potential ORF65 PTMs in iSLK.219 cells were not detected in TREx BCBL1-RTA cells. ORF65 is a capsid protein and is important for virus production (Dai et al., 2015; Perkins et al., 2008). Modification of ORF65 may block virus assembly, which could explain the selective inhibition of virus production in iSLK.219 cells by XBP1s. Therefore, it is important to identify the nature of these PTMs to determine if they play a role in XBP1s-mediated virus inhibition.

KSHV is a lymphotropic virus that infects B cells and re-programs them to have a plasmablast-like phenotype (Chadburn et al., 2017). Unlike KS spindle cells, the viral genome is stably maintained in PEL cells (Grundhoff & Ganem, 2004), suggesting that the virus may be better adapted to re-programming B cells than spindle cells to provide a favorable environment for a persistent latent cycle. Furthermore, infection of SLK cells and other tumor cells are not the natural host cell and so it is possible that the virus has not fully adapted to replicate in these cells. Therefore, KSHV in PEL cells may have a selective advantage to subvert cellular factors such as XBP1s.

XBP1s is also an important B cell factor required for PC differentiation (Reimold et al., 2001). During the differentiation process, XBP1s also coordinates with other B cell-specific transcription factors to regulate transcriptional reprogramming of the B cell (Shaffer et al., 2004). Thus, the cellular genes that XBP1s upregulates in PEL may be different than iSLK.219 cells. This could have important implications on the anti-viral effects of XBP1s. Therefore, transcriptome and proteome analysis of XBP1s-expressing iSLK.219 and PEL cells may reveal selective expression of anti-viral factors in iSLK.219 cells but not PEL cells.

There is accumulating evidence that there is extensive cross-talk among the three branches of the UPR to facilitate a coordinated UPR and to regulate the switch from an adaptive response to pro-apoptotic. Both ATF6 and PERK-dependent activation of the ISR have been shown to be important for robust XBP1 expression. ATF6 can transcriptionally upregulate XBP1 to promote mRNA splicing, while the ISR can

promote XBP1s mRNA stability and upregulate IRE1 transcription via ATF4 (Majumder et al., 2012; Tsuru et al., 2016; Yoshida et al., 2001). Appendix A provides further support that the ISR can promote XBP1 splicing through the upregulation of XBP1u. Thus, part of the reason for the suppression of XBP1s expression during lytic replication may be due to the blockade in the signaling of the other two branches. Re-establishing ATF4 and ATF6-N activity during the lytic cycle may facilitate XBP1s-dependent inhibition of virus production.

6.4 Multiple KSHV Proteins Control the UPR Sensors

A KSHV ORF screen for modulators of the UPR revealed multiple potential hits, including KapC and ORF45. Further characterization showed that KapC inhibited IRE1 protein levels, which attenuated basal XBP1 splicing. However, KapC expression had no significant impact on the IRE1-XBP1 pathway following drug-induced ER stress. KapC is expressed during latency and upregulated during lytic replication. I showed that IRE1 expression is attenuated during lytic replication, and therefore, KapC may facilitate this attenuation. As previously mentioned, the reduction in IRE1 levels may promote RIDD. Based on this theory, it will be interesting to determine if KapC can also promote RIDD during lytic replication.

IRE1 immunoblot analysis revealed that in non-ER stress-induced cells, IRE1 appeared as a doublet. KapC seems to preferentially suppress the higher MW species. The identity of this possible isoform of IRE1 is not known, but it may be hypo-phosphorylated IRE1 due to basal levels of ER stress, which in the context of KSHV infection may be sufficient to induce low levels of RTA expression. Therefore, KapC may maintain latency by repressing XBP1s expression in response to low levels of ER stress. However, in response to lethal forms of ER stress, which causes IRE1 to be fully phosphorylated, KapC no longer has an effect. As a result, this would permit XBP1-dependent RTA expression so that the virus can escape the stressed cell.

ORF45 was also shown to modulate UPR signaling. Interestingly, ORF45 activated the ISR and BiP in a PERK- and ATF6-independent manner, respectively. BiP mRNA has been reported to contain an IRES in the 5'UTR to mediate translation (Q. Yang & Sarnow, 1997). IRES-dependent translation of BiP has been demonstrated during HCMV infection, and BiP was required for virus replication (N. J. Buchkovich et al.,

2009, 2010). Alternatively, the ISR has also been reported to regulate BiP expression through translation of uORFs in its mRNA, which is facilitated by the alternative initiation factor eIF2A (Starck et al., 2016). Therefore, ORF45 may upregulate BiP in an IRES- or eIF2A-dependent manner.

I also demonstrated that BiP was not upregulated at the protein level during the lytic cycle in TREx BCBL1-RTA cells, suggesting that KSHV may encode other viral proteins to suppress ORF45-induced BiP. P.-J. Chang *et al.* (2014) reported that BiP was upregulated during lytic replication in different PEL models and genetic silencing of BiP attenuated virus production. However, the method of induction was with NaB and/or TPA and these drugs alone may promote BiP expression. Alternatively, dox-induced lytic replication in TREx-BCBL1-RTA cells is more robust than lytic replication induced with NaB or TPA (H. Nakamura et al., 2003). Therefore, the enhanced expression of certain viral proteins following dox treatment may be responsible for BiP inhibition. Further exploration of the role of ORF45-mediated expression of BiP in the context of the lytic cycle will help clarify some of these differences.

ORF45 also upregulated IRE1 and XBP1 expression and their upregulation was likely dependent on the ISR. This is consistent with results from Appendix A, which provides evidence that the ISR promotes activation of the IRE1-XBP1 pathway. Through ATF4, the ISR also can upregulate BiP (Luo et al., 2003). The reasons why ORF45 upregulates UPR markers, such as ATF4, XBP1s, and BiP, are not clear since they are inhibited during lytic replication. ORF45 is expressed during lytic but is also a tegument protein and is present in virus particles (Fan Xiu Zhu & Yuan, 2003). Therefore, these UPR effectors may be upregulated during viral entry, which may be important for delivery of the viral genome to the nucleus or establishment of latency. It has been reported that there is a burst in lytic gene expression immediately following *de novo* infection, which may be important for establishing latency (Krishnan et al., 2004). Theoretically, ORF45 activation of the IRE1-XBP1 pathway upon entry could help facilitate this induction of lytic gene expression. BiP has also been shown to play a role in viral entry of other viruses (Geiger et al., 2011; Nain et al., 2017) and may also promote KSHV entry. *De novo* infection with an ORF45 knockout virus will help elucidate some of the potential roles of these UPR-related proteins during entry.

There were other viral proteins that showed UPR or ISR-modulating activity that will need to be characterized in the future. These include vIL-6, K3, vCyclin, and vGPCR. vGPCR is intriguing due to its localization in the ER as well as its ability to upregulate multiple pro-inflammatory genes (Bais et al., 1998). In theory this could trigger ER stress, which would be consistent with the UPR reporter data. Furthermore, vGPCR has been reported to deplete ER calcium levels by binding and inhibiting SERCA2b (J. Zhang et al., 2015), which may further promote ER stress. vGPCR is an early gene (R Sun et al., 1999) and its timing of expression is consistent with the onset of activation of the UPR sensors. Therefore, vGPCR is a prime candidate for activation of the three ER stress sensors during lytic replication. Further analyses of vGPCR, and the other viral gene targets, are necessary to determine the full extent of UPR modulation by KSHV proteins.

6.5 Future Investigations

This thesis has identified a central role for the UPR during lytic replication. However, further understanding of the mechanistic details of how KSHV infection modulates the UPR will likely greatly enhance our appreciation of this intimate relationship between virus and an evolutionary conserved stress response. Characterizing how some of these viral gene products, like ORF45 and KapC, activate or inhibit different branches of the UPR or ISR will help inform both how and why KSHV modulates UPR signaling during infection. Identifying the role of the ISR in regulating viral gene expression, especially viral mRNAs with uORFs, will advance our knowledge of how the ISR can be hijacked by viruses to promote infection. Clarifying roles that RIDD and IRE1-dependent JNK signaling have during the lytic cycle will help us to better understand potential roles of IRE1 signaling during virus infection.

Currently, the mechanism of ATF6 trafficking to the Golgi to undergo proteolytic cleavage is unclear. Viruses are amazing teachers and much of what we know about cellular biology has been from studying how viruses have evolved to use these cellular processes to facilitate replication. Studying ATF6 during KSHV lytic replication may help identify some of the key proteins that regulate ATF6 trafficking that are normally involved in response to ER stress. The ORF screen conducted in Chapter 5 only addressed the PERK and IRE1 branch of the UPR. Conducting an ORF screen in an

ATF6 reporter cell line will hopefully reveal viral proteins that can also modulate ATF6 signaling, which could help identify the cellular components that regulate ATF6 activation.

The ATF6 target gene BiP has been shown to be upregulated during lytic replication in some PEL cell lines, but in this case is independent of ATF6 (P.-J. Chang et al., 2014). However, I showed that in the TREx BCBL1-RTA lytic replication model, BiP is not upregulated. As well as being regulated at the transcriptional level by ATF6, BiP has also been shown to be regulated at the translational level due to an IRES in the 5'UTR of its mRNA. BiP translation has also been shown to be regulated through CUG-mediated translation of uORFs by the alternative initiation factor eIF2A. However, the precise mechanisms of how these translation regulatory elements control BiP in different cellular contexts is unclear. Upregulation of BiP by ORF45 may be dependent on some of these alternative translation control mechanisms, but in the context of lytic replication, they become inhibited. Therefore, understanding how ectopic ORF45 upregulates BiP may help identify the potential viral and/or cellular factors that suppress BiP expression during lytic replication.

Currently there is no targeted treatment option for PEL, which contributes to its poor prognosis (Boulanger et al., 2005). Drug-targeting of essential viral proteins is a common strategy, however due to an inherent ability of viruses to rapidly mutate, it is well appreciated that viral adaptation can occur in response to virus-targeted anti-virals. Because of this, there has been an increasing focus on host-targeting anti-virals (HTAs) (K. Lin & Gallay, 2013). Since the UPR is likely important for tumor initiating events by KSHV, my research suggests that HTAs focused on manipulating UPR signaling may be a potential approach for treating PEL. There is increasing evidence that multiple different viruses usurp the UPR to promote infection. Therefore, a UPR-focused HTA may also have pan-anti-viral potential. Currently our understanding of viral modulation of UPR signaling is in its infancy, but my hope is that this thesis will be used to inspire future research in this exciting and important field.

BIBLIOGRAPHY

Abel, E. D., Peroni, O., Kim, J. K., Kim, Y.-B., Boss, O., Hadro, E., … Kahn, B. B. (2001). Adipose-selective targeting of the GLUT4 gene impairs insulin action in muscle and liver. *Nature*, *409*(6821), 729–733. doi:10.1038/35055575

Abuaita, B. H., Burkholder, K. M., Boles, B. R., & O'Riordan, M. X. (2015). The endoplasmic reticulum stress sensor inositol-requiring enzyme 1α augments bacterial killing through sustained oxidant production. *MBio*, *6*(4), e00705. doi:10.1128/mBio.00705-15

Acosta-Alvear, D., Zhou, Y., Blais, A., Tsikitis, M., Lents, N. H., Arias, C., … Dynlacht, B. D. (2007). XBP1 controls diverse cell type- and condition-specific transcriptional regulatory networks. *Molecular Cell*, *27*(1), 53–66. doi:10.1016/j.molcel.2007.06.011

Adachi, Y., Yamamoto, K., Okada, T., Yoshida, H., Harada, A., & Mori, K. (2008). ATF6 is a transcription factor specializing in the regulation of quality control proteins in the endoplasmic reticulum. *Cell Structure and Function*, *33*(1), 75–89. doi:10.1247/csf.07044

Adang, L. A., Parsons, C. H., & Kedes, D. H. (2006). Asynchronous progression through the lytic cascade and variations in intracellular viral loads revealed by high-throughput single-cell analysis of Kaposi's sarcoma-associated herpesvirus infection. *Journal Of Virology*, *80*(20), 10073–10082. doi:10.1128/JVI.01156-06

Adolph, T. E., Tomczak, M. F., Niederreiter, L., Ko, H.-J., Böck, J., Martinez-Naves, E., … Blumberg, R. S. (2013). Paneth cells as a site of origin for intestinal inflammation. *Nature*, *503*(7475), 272–276. doi:10.1038/nature12599

Aguirre, V., Uchida, T., Yenush, L., Davis, R., & White, M. F. (2000). The c-Jun NH(2)-terminal kinase promotes insulin resistance during association with insulin receptor substrate-1 and phosphorylation of Ser(307). *The Journal of Biological Chemistry*, *275*(12), 9047–9054. doi:10.1074/jbc.275.12.9047

Akiyama, M., Liew, C. W., Lu, S., Hu, J., Martinez, R., Hambro, B., … Kulkarni, R. N. (2013). X-box binding protein 1 is essential for insulin regulation of pancreatic-cell function. *Diabetes*, *62*(7), 2439–2449. doi:10.2337/db12-1747

Ambrose, R. L., & Mackenzie, J. M. (2013). ATF6 signaling is required for efficient West Nile virus replication by promoting cell survival and inhibition of innate immune responses. *Journal of Virology*, *87*(4), 2206–2214. doi:10.1128/JVI.02097-12

Amin-Wetzel, N., Saunders, R. A., Kamphuis, M. J., Rato, C., Preissler, S., Harding, H. P., & Ron, D. (2017). A J-protein co-chaperone recruits BiP to monomerize IRE1 and repress the unfolded protein response. *Cell*, *171*(7), 1625–1637.e13. doi:10.1016/J.CELL.2017.10.040

An, J., Sun, Y., & Rettig, M. B. (2004). Transcriptional coactivation of c-Jun by the KSHV-encoded LANA. *Blood*, *103*(1), 222–228. doi:10.1182/blood-2003-05-1538

Anda, S., Zach, R., & Grallert, B. (2017). Activation of Gcn2 in response to different stresses. *PLOS ONE*, *12*(8), e0182143. doi:10.1371/journal.pone.0182143

Anderson, P., & Kedersha, N. (2008). Stress granules: the Tao of RNA triage. *Trends in Biochemical Sciences*, *33*(3), 141–150. doi:10.1016/j.tibs.2007.12.003

Aneja, K. K., & Yuan, Y. (2017). Reactivation and lytic replication of Kaposi's sarcoma-associated herpesvirus: an update. *Frontiers in Microbiology*, *8*, 613-613. doi:10.3389/fmicb.2017.00613

Aoki, Y., Tosato, G., Fonville, T. W., & Pittaluga, S. (2001). Serum viral interleukin-6 in AIDS-related multicentric Castleman disease. *Blood*, *97*(8), 2526-2527. doi:10.1182/blood.V97.8.2526

Aragón, T., Van Anken, E., Pincus, D., Serafimova, I. M., Korennykh, A. V, Rubio, C. A., & Walter, P. (2009). Messenger RNA targeting to endoplasmic reticulum stress signalling sites. *Nature*, *457*(7230), 736-740. doi:10.1038/nature07641

Araki, K., & Nagata, K. (2011). Protein folding and quality control in the ER. *Cold Spring Harbor Perspectives in Biology*, *3*(11), a007526–a007526. doi:10.1101/cshperspect.a007526

Aresté, C., Mutocheluh, M., & Blackbourn, D. J. (2009). Identification of caspase-mediated decay of interferon regulatory factor-3, exploited by a Kaposi sarcoma-associated herpesvirus immunoregulatory protein. *Journal of Biological Chemistry*, *284*(35), 23272–23285. doi:10.1074/jbc.M109.033290

Arias, C., Weisburd, B., Stern-Ginossar, N., Mercier, A., Madrid, A. S., Bellare, P., … Ganem, D. (2014). KSHV 2.0: A comprehensive annotation of the Kaposi's sarcoma-associated herpesvirus genome using next-generation sequencing reveals novel genomic and functional features. *PLoS Pathogens*, *10*(1), e1003847. doi:10.1371/journal.ppat.1003847

Asada, R., Kanemoto, S., Kondo, S., Saito, A., & Imaizumi, K. (2011). The signalling from endoplasmic reticulum-resident bZIP transcription factors involved in diverse cellular physiology. *Journal of Biochemistry*, *149*(5), 507–518. doi:10.1093/jb/mvr041

Asahi-Ozaki, Y., Sato, Y., Kanno, T., Sata, T., & Katano, H. (2006). Quantitative analysis of kaposi sarcoma–associated herpesvirus (KSHV) in KSHV-Associated diseases. *The Journal of Infectious Diseases*, *193*(6), 773–782. doi:10.1086/500560

Averous, J., Bruhat, A., Jousse, C., Carraro, V., Thiel, G., & Fafournoux, P. (2004). Induction of *CHOP* expression by amino acid limitation requires both ATF4 expression and ATF2 phosphorylation. *Journal of Biological Chemistry*, *279*(7), 5288–5297. doi:10.1074/jbc.M311862200

Avey, D., Tepper, S., Li, W., Turpin, Z., & Zhu, F. (2015). Phosphoproteomic analysis of KSHV-infected cells reveals roles of ORF45-activated RSK during lytic replication. *PLOS Pathogens*, *11*(7), e1004993. doi:10.1371/journal.ppat.1004993

Avey, D., Tepper, S., Pifer, B., Bahga, A., Williams, H., Gillen, J., … Zhu, F. (2016). Discovery of a coregulatory interaction between Kaposi's sarcoma-associated herpesvirus ORF45 and the viral protein kinase ORF36. *Journal of Virology*, *90*(13), 5953–5964. doi:10.1128/JVI.00516-16

Avril, T., Vauléon, E., & Chevet, E. (2017). Endoplasmic reticulum stress signaling and chemotherapy resistance in solid cancers. *Oncogenesis*, *6*(8), e373.

doi:10.1038/oncsis.2017.72

B'chir, W., Maurin, A.-C., Carraro, V., Averous, J., Jousse, C., Muranishi, Y., … Bruhat, A. (2013). The eIF2alpha/ATF4 pathway is essential for stress-induced autophagy gene expression. *Nucleic Acids Research*, *41*(16), 7683–7699. doi:10.1093/nar/gkt563

Back, S. H., & Kaufman, R. J. (2012). Endoplasmic reticulum stress and type 2 diabetes. *Annual Review of Biochemistry*, *81*, 767–793. doi:10.1146/annurev-biochem-072909-095555

Bais, C., Santomasso, B., Coso, O., Arvanitakis, L., Raaka, E. G., Gutkind, J. S., … Mesri, E. A. (1998). G-protein-coupled receptor of Kaposi's sarcoma-associated herpesvirus is a viral oncogene and angiogenesis activator. *Nature*, *391*(6662), 86–89. doi:10.1038/34193

Ballestas, M. E., Chatis, P. A., & Kaye, K. M. (1999). Efficient persistence of extrachromosomal KSHV DNA mediated by latency-associated nuclear antigen. *Science*, *284*(5414), 641–644. doi:10.1126/science.284.5414.641

Ballon, G., Chen, K., Perez, R., Tam, W., & Cesarman, E. (2011). Kaposi sarcoma herpesvirus (KSHV) vFLIP oncoprotein induces B cell transdifferentiation and tumorigenesis in mice. *Journal of Clinical Investigation*, *121*(3), 1141–1153. doi:10.1172/JCI44417

Barbera, A. J., Chodaparambil, J. V, Kelley-Clarke, B., Joukov, V., Walter, J. C., Luger, K., & Kaye, K. M. (2006). The nucleosomal surface as a docking station for Kaposi's sarcoma herpesvirus LANA. *Science*, *311*(5762), 856–861. doi:10.1126/science.1120541

Bechtel, J. T., Liang, Y., Hvidding, J., & Ganem, D. (2003). Host range of Kaposi's sarcoma-associated herpesvirus in cultured cells. *Journal of Virology*, *77*(11), 6474–6481. doi:10.1128/JVI.77.11.6474-6481.2003

Behnke, J., Feige, M. J., & Hendershot, L. M. (2015). BiP and its nucleotide exchange factors Grp170 and Sil1: mechanisms of action and biological functions. *Journal of Molecular Biology*, *427*(7), 1589–1608. doi:10.1016/j.jmb.2015.02.011

Bellare, P., & Ganem, D. (2009). Regulation of KSHV lytic switch protein expression by a virus-encoded microRNA: an evolutionary adaptation that fine-tunes lytic reactivation. *Cell Host & Microbe*, *6*(6), 570–575. doi:10.1016/j.chom.2009.11.008

Benhamron, S., Hadar, R., Iwawaky, T., So, J.-S., Lee, A.-H., & Tirosh, B. (2014). Regulated IRE1-dependent decay participates in curtailing immunoglobulin secretion from plasma cells. *European Journal of Immunology*, *44*(3), 867–876. doi:10.1002/eji.201343953

Bergman, R. N., & Ader, M. (2000). Free fatty acids and pathogenesis of type 2 diabetes mellitus. *Trends in Endocrinology and Metabolism*, *11*(9), 351–356. doi:10.1016/S1043-2760(00)00323-4

Berlanga, J. J., Santoyo, J., & De Haro, C. (1999). Characterization of a mammalian homolog of the GCN2 eukaryotic initiation factor 2alpha kinase. *European Journal of Biochemistry*, *265*(2), 754–762. doi:10.1046/j.1432-1327.1999.00780.x

Bertolotti, A., Wang, X., Novoa, I., Jungreis, R., Schlessinger, K., Cho, J. H., … Ron, D. (2001). Increased sensitivity to dextran sodium sulfate colitis in IRE1β-deficient mice. *Journal of Clinical Investigation*, *107*(5), 585–593. doi:10.1172/JCI11476

Bertolotti, A., Zhang, Y., Hendershot, L. M., Harding, H. P., & Ron, D. (2000). Dynamic interaction of BiP and ER stress transducers in the unfolded-protein response. *Nature Cell Biology*, *2*(6), 326–332. doi:10.1038/35014014

Bettigole, S. E., Lis, R., Adoro, S., Lee, A.-H., Spencer, L. A., Weller, P. F., & Glimcher, L. H. (2015). The transcription factor XBP1 is selectively required for eosinophil differentiation. *Nature Immunology*, *16*(8), 829–837. doi:10.1038/ni.3225

Bhattacharyya, S. (2014). Can't RIDD off viruses. *Frontiers in Microbiology*, *5*, 292. doi:10.3389/fmicb.2014.00292

Bhattacharyya, S., Sen, U., & Vrati, S. (2014). Regulated IRE1-dependent decay pathway is activated during Japanese encephalitis virus-induced unfolded protein response and benefits viral replication. *Journal of General Virology*, *95*(Pt_1), 71–79. doi:10.1099/vir.0.057265-0

Bhende, P. M., Dickerson, S. J., Sun, X., Feng, W.-H., & Kenney, S. C. (2007). X-box-binding protein 1 activates lytic Epstein-Barr virus gene expression in combination with protein kinase D. *Journal of Virology*, *81*(14), 7363–7370. doi:10.1128/JVI.00154-07

Bi, M., Naczki, C., Koritzinsky, M., Fels, D., Blais, J., Hu, N., … Koumenis, C. (2005). ER stress-regulated translation increases tolerance to extreme hypoxia and promotes tumor growth. *The EMBO Journal*, *24*(19), 3470–3481. doi:10.1038/sj.emboj.7600777

Bieleski, L., & Talbot, S. J. (2001). Kaposi's sarcoma-associated herpesvirus vcyclin open reading frame contains an internal ribosome entry site. *Journal of Virology*, *75*(4), 1864–1869. doi:10.1128/JVI.75.4.1864-1869.2001

Black, J. B., Browning, P. J., Offermann, M. K., Goldsmith, C. S., Yu, Y., & Bhalla, K. (1999). Induction of human herpesvirus-8 DNA replication and transcription by butyrate and TPA in BCBL-1 cells. *Journal of General Virology*, *80*(1), 83–90. doi:10.1099/0022-1317-80-1-83

Blais, J. D., Addison, C. L., Edge, R., Falls, T., Zhao, H., Wary, K., … Bell, J. C. (2006). Perk-dependent translational regulation promotes tumor cell adaptation and angiogenesis in response to hypoxic stress. *Molecular and Cellular Biology*, *26*(24), 9517–9532. doi:10.1128/MCB.01145-06

Bommiasamy, H., Back, S. H., Fagone, P., Lee, K., Meshinchi, S., Vink, E., … Brewer, J. W. (2009). ATF6 induces XBP1-independent expansion of the endoplasmic reticulum. *Journal of Cell Science*, *122*(10), 1626–1636. doi:10.1242/jcs.045625

Boshoff, C., Schulz, T. F., Kennedy, M. M., Graham, A. K., Fisher, C., Thomas, A., … O'Leary, J. J. (1995). Kaposi's sarcoma-associated herpesvirus infects endothelial and spindle cells. *Nature Medicine*, *1*(12), 1274–1278. doi:10.1038/nm1295-1274

Boulanger, E., Gérard, L., Gabarre, J., Molina, J.-M., Rapp, C., Abino, J.-F., … Oksenhendler, E. (2005). Prognostic factors and outcome of human herpesvirus 8–associated primary effusion lymphoma in patients with AIDS. *Journal of Clinical Oncology*, *23*(19), 4372–4380. doi:10.1200/JCO.2005.07.084

Bratton, S. B., & Salvesen, G. S. (2010). Regulation of the Apaf-1-caspase-9 apoptosome. *Journal of Cell Science*, *123*(Pt 19), 3209–3214. doi:10.1242/jcs.073643

Brinkmann, M. M., Glenn, M., Rainbow, L., Kieser, A., Henke-Gendo, C., & Schulz, T. F. (2003). Activation of mitogen-activated protein kinase and NF-kappaB pathways by a Kaposi's sarcoma-associated herpesvirus K15 membrane protein. *Journal of Virology*, *77*(17), 9346–9358.

Bronner, D. N., Abuaita, B. H., Chen, X., Fitzgerald, K. A., Nuñez, G., He, Y., … O'Riordan, M. X. D. (2015). Endoplasmic reticulum stress activates the inflammasome via NLRP3- and caspase-2-driven mitochondrial damage. *Immunity*, *43*(3), 451–462. doi:10.1016/j.immuni.2015.08.008

Brulois, K., Toth, Z., Wong, L.-Y., Feng, P., Gao, S.-J., Ensser, A., & Jung, J. U. (2014). Kaposi's sarcoma-associated herpesvirus K3 and K5 ubiquitin e3 ligases have stage-specific immune evasion roles during lytic replication. *Journal of Virology*, *88*(16), 9335–9349. doi:10.1128/JVI.00873-14

Brunt, J. J., Khan, S., & Heikkila, J. J. (2012). Sodium arsenite and cadmium chloride induction of proteasomal inhibition and HSP accumulation in Xenopus laevis A6 kidney epithelial cells. *Comparative Biochemistry and Physiology. Toxicology & Pharmacology : CBP*, *155*(2), 307–317. doi:10.1016/j.cbpc.2011.09.011

Bucciantini, M., Giannoni, E., Chiti, F., Baroni, F., Formigli, L., Zurdo, J., … Stefani, M. (2002). Inherent toxicity of aggregates implies a common mechanism for protein misfolding diseases. *Nature*, *416*(6880), 507–511. doi:10.1038/416507a

Buchkovich, N. J., Maguire, T. G., Paton, A. W., Paton, J. C., & Alwine, J. C. (2009). The endoplasmic reticulum chaperone BiP/GRP78 is important in the structure and function of the human cytomegalovirus assembly compartment. *Journal of Virology*, *83*(22), 11421–11428. doi:10.1128/JVI.00762-09

Buchkovich, N. J., Maguire, T. G., Yu, Y., Paton, A. W., Paton, J. C., & Alwine, J. C. (2008). Human cytomegalovirus specifically controls the levels of the endoplasmic reticulum chaperone BiP/GRP78, which is required for virion assembly. *Journal of Virology*, *82*(1), 31–39. doi:10.1128/JVI.01881-07

Buchkovich, N. J., Yu, Y., Pierciey, F. J., & Alwine, J. C. (2010). Human cytomegalovirus induces the endoplasmic reticulum chaperone BiP through increased transcription and activation of translation by using the BiP internal ribosome entry site. *Journal of Virology*, *84*(21), 11479–11486. doi:10.1128/JVI.01330-10

Burnett, H. F., Audas, T. E., Liang, G., & Lu, R. R. (2012). Herpes simplex virus-1 disarms the unfolded protein response in the early stages of infection. *Cell Stress & Chaperones*, *17*(4), 473–483. doi:10.1007/s12192-012-0324-8

Byrd, A. E., Aragon, I. V., & Brewer, J. W. (2012). MicroRNA-30c-2* limits expression of proadaptive factor XBP1 in the unfolded protein response. *Journal of Cell Biology*, *196*(6), 689–698. doi:10.1083/JCB.201201077

Cai, Q., Lan, K., Verma, S. C., Si, H., Lin, D., & Robertson, E. S. (2006). Kaposi's sarcoma-associated herpesvirus latent protein LANA interacts with HIF-1 to upregulate RTA expression during hypoxia: latency control under low oxygen

conditions. *Journal of Virology*, *80*(16), 7965–7975. doi:10.1128/JVI.00689-06

Cai, Q., Murakami, M., Si, H., & Robertson, E. S. (2007). A potential alpha-helix motif in the amino terminus of LANA encoded by Kaposi's sarcoma-associated herpesvirus is critical for nuclear accumulation of HIF-1alpha in normoxia. *Journal of Virology*, *81*(19), 10413–10423. doi:10.1128/JVI.00611-07

Cai, Q., Verma, S. C., Lu, J., & Robertson, E. S. (2010). Molecular biology of Kaposi's sarcoma-associated herpesvirus and related oncogenesis. *Advances in virus research*, *78*, 87–142. doi:10.1016/B978-0-12-385032-4.00003-3

Calfon, M., Zeng, H., Urano, F., Till, J. H., Hubbard, S. R., Harding, H. P., … Ron, D. (2002). IRE1 couples endoplasmic reticulum load to secretory capacity by processing the XBP-1 mRNA. *Nature*, *415*(6867), 92–96. doi:10.1038/415092a

Cannell, E., & Mittnacht, S. (1999). Viral encoded cyclins. *Seminars in Cancer Biology*, *9*(3), 221–229. doi:10.1006/scbi.1999.0090

Carrara, M., Prischi, F., Nowak, P. R., & Ali, M. M. (2015). Crystal structures reveal transient PERK luminal domain tetramerization in endoplasmic reticulum stress signaling. *The EMBO Journal*, *34*(11), 1589–1600. doi:10.15252/embj.201489183

Carrasco, D. R., Sukhdeo, K., Protopopova, M., Sinha, R., Enos, M., Carrasco, D. E., … DePinho, R. A. (2007). The differentiation and stress response factor XBP-1 drives multiple myeloma pathogenesis. *Cancer Cell*, *11*(4), 349–360. doi:10.1016/j.ccr.2007.02.015

Casas-Tinto, S., Zhang, Y., Sanchez-Garcia, J., Gomez-Velazquez, M., Rincon-Limas, D. E., & Fernandez-Funez, P. (2011). The ER stress factor XBP1s prevents amyloid-β neurotoxicity. *Human Molecular Genetics*, *20*(11), 2144–2160. doi:10.1093/hmg/ddr100

Casas, C. (2017). GRP78 at the centre of the stage in cancer and neuroprotection. *Frontiers in Neuroscience*, *11*, 177. doi:10.3389/fnins.2017.00177

Casper, C., Nichols, W. G., Huang, M.-L., Corey, L., & Wald, A. (2004). Remission of HHV-8 and HIV-associated multicentric Castleman disease with ganciclovir treatment. *Blood*, *103*(5), 1632–1634. doi:10.1182/blood-2003-05-1721

Castañeda, A. F., & Glaunsinger, B. A. (2018). The Interaction between ORF18 and ORF30 Is Required for Late Gene Expression in Kaposi's Sarcoma-Associated Herpesvirus. *Journal of Virology*, *93*(1). doi:10.1128/JVI.01488-18

Castleman, B., Iverson, L., & Menendez, V. P. (1956). Localized mediastinal lymph-node hyperplasia resembling thymoma. *Cancer*, *9*(4), 822–830. doi: 10.1002/1097-0142(195607/08)9:4<822::AID- CNCR2820090430>3.0.CO;2-4

Cesarman, E., Chang, Y., Moore, P. S., Said, J. W., & Knowles, D. M. (1995). Kaposi's sarcoma-associated herpesvirus-like DNA sequences in AIDS-related body-cavity-based lymphomas. *The New England Journal of Medicine*, *332*(18), 1186–1191. doi:10.1056/NEJM199505043321802

Chadburn, A., Hyjek, E. M., Tam, W., Liu, Y., Rengifo, T., Cesarman, E., & Knowles, D. M. (2008). Immunophenotypic analysis of the Kaposi sarcoma herpesvirus (KSHV; HHV-8)-infected B cells in HIV+ multicentric Castleman disease (MCD). *Histopathology*, *53*(5), 513–524. doi:10.1111/j.1365-2559.2008.03144.x

Chadburn, A., Said, J., Gratzinger, D., Chan, J. K. C., de Jong, D., Jaffe, E. S., … Goodlad, J. R. (2017). HHV8/KSHV-Positive lymphoproliferative disorders and the spectrum of plasmablastic and plasma cell neoplasms: 2015 SH/EAHP workshop report-Part 3. *American Journal of Clinical Pathology*, *147*(2), 171–187. doi:10.1093/ajcp/aqw218

Chakraborty, S., Veettil, M. V., & Chandran, B. (2012). Kaposi's sarcoma associated herpesvirus entry into target cells. *Frontiers in Microbiology*, *3*, 6. doi:10.3389/fmicb.2012.00006

Chan, L. Y., Mugler, C. F., Heinrich, S., Vallotton, P., & Weis, K. (2018). Non-invasive measurement of mRNA decay reveals translation initiation as the major determinant of mRNA stability. *ELife*, *7*, e32536. doi:10.7554/eLife.32536

Chan, S.-W. (2014). The unfolded protein response in virus infections. *Frontiers in Microbiology*, *5*, 518. doi:10.3389/fmicb.2014.00518

Chan, S.-W., & Egan, P. A. (2005). Hepatitis C virus envelope proteins regulate CHOP via induction of the unfolded protein response. *The FASEB Journal*, *19*(11), 1510–1512. doi:10.1096/fj.04-3455fje

Chandriani, S., & Ganem, D. (2007). Host transcript accumulation during lytic kshv infection reveals several classes of host responses. *PLoS ONE*, *2*(8), e811. doi:10.1371/journal.pone.0000811

Chandriani, S., Xu, Y., & Ganem, D. (2010). The lytic transcriptome of Kaposi's sarcoma-associated herpesvirus reveals extensive transcription of noncoding regions, including regions antisense to important genes. *Journal of Virology*, *84*(16), 7934–7942. doi:10.1128/JVI.00645-10

Chang, H. H., & Ganem, D. (2013). A unique herpesviral transcriptional program in KSHV-infected lymphatic endothelial cells leads to mTORC1 activation and rapamycin sensitivity. *Cell Host & Microbe*, *13*(4), 429–440. doi:10.1016/j.chom.2013.03.009

Chang, P.-C., Cheng, C.-Y., Campbell, M., Yang, Y.-C., Hsu, H.-W., Chang, T.-Y., … Kung, H.-J. (2013). The chromatin modification by SUMO-2/3 but not SUMO-1 prevents the epigenetic activation of key immune-related genes during Kaposi's sarcoma associated herpesvirus reactivation. *BMC Genomics*, *14*(1), 824. doi:10.1186/1471-2164-14-824

Chang, P., Hung, C., Wang, S., Tsai, P., Shih, Y., Huang, H., ... Chen, L. (2014). Identification and characterization of two novel spliced genes located in the orf47-orf46-orf45 gene locus of Kaposi's sarcoma-associated herpesvirus. *Journal of Virology, 88*(17), 10092-10109. doi:10.1128/JVI.01445-14

Chang, P.-J., Shedd, D., Gradoville, L., Cho, M.-S., Chen, L.-W., Chang, J., & Miller, G. (2002). Open reading frame 50 protein of Kaposi's sarcoma-associated herpesvirus directly activates the viral PAN and K12 genes by binding to related response elements. *Journal of Virology*, *76*(7), 3168–3178. doi:10.1128/JVI.76.7.3168-3178.2002

Chang, R. C. C., Wong, A. K. Y., Ng, H.-K., & Hugon, J. (2002). Phosphorylation of eukaryotic initiation factor-2alpha (eIF2alpha) is associated with neuronal degeneration in Alzheimer's disease. *Neuroreport*, *13*(18), 2429–2432.

doi:10.1097/01.wnr.0000048020.74602.bb

Chang, S., Wooden, S., Nakaki, T., Kim, Y., Lin, A., Kung, L., . . . Lee, A. (1987). Rat gene encoding the 78-kDa glucose-regulated protein GRP78: its regulatory sequences and the effect of protein glycosylation on its expression. *Proceedings of the National Academy of Sciences of the United States of America*, 84(3), 680-684. doi:10.1073/pnas.84.3.680

Chang, T.-K., Lawrence, D. A., Lu, M., Tan, J., Harnoss, J. M., Marsters, S. A., … Ashkenazi, A. (2018). Coordination between two branches of the unfolded protein response determines apoptotic cell fate. *Molecular Cell*, *71*(4), 629–636.e5. doi:10.1016/J.MOLCEL.2018.06.038

Chang, Y., Cesarman, E., Pessin, M. S., Lee, F., Culpepper, J., Knowles, D. M., & Moore, P. S. (1994). Identification of herpesvirus-like DNA sequences in AIDS-associated Kaposi's sarcoma. *Science*, *266*(5192), 1865–1869. doi:10.1126/science.7997879

Chen, H.-S., De Leo, A., Wang, Z., Kerekovic, A., Hills, R., & Lieberman, P. M. (2017). BET-inhibitors disrupt Rad21-dependent conformational control of KSHV latency. *PLOS Pathogens*, *13*(1), e1006100. doi:10.1371/journal.ppat.1006100

Chen, H., & Qi, L. (2010). SUMO modification regulates the transcriptional activity of XBP1. *Biochemical Journal*, *429*(1), 95–102. doi:10.1042/BJ20100193

Chen, J. J., Throop, M. S., Gehrke, L., Kuo, I., Pal, J. K., Brodsky, M., & London, I. M. (1991). Cloning of the cDNA of the heme-regulated eukaryotic initiation factor 2 alpha (eIF-2 alpha) kinase of rabbit reticulocytes: homology to yeast GCN2 protein kinase and human double-stranded-RNA-dependent eIF-2 alpha kinase. *Proceedings of the National Academy of Sciences of the United States of America*, *88*(17), 7729–7733. doi:10.1073/pnas.88.17.7729

Chen, X., Iliopoulos, D., Zhang, Q., Tang, Q., Greenblatt, M. B., Hatziapostolou, M., … Glimcher, L. H. (2014). XBP1 promotes triple-negative breast cancer by controlling the HIF1α pathway. *Nature*, *508*(7494), 103–107. doi:10.1038/nature13119

Cheng, G., Feng, Z., & He, B. (2005). Herpes simplex virus 1 infection activates the endoplasmic reticulum resident kinase PERK and mediates eIF-2alpha dephosphorylation by the gamma(1)34.5 protein. *Journal of Virology*, *79*(3), 1379–1388. doi:10.1128/JVI.79.3.1379-1388.2005

Cheng, J.-H., Sun, Y.-J., Zhang, F.-Q., Zhang, X.-R., Qiu, X.-S., Yu, L.-P., … Ding, C. (2016). Newcastle disease virus NP and P proteins induce autophagy via the endoplasmic reticulum stress-related unfolded protein response. *Scientific Reports*, *6*(1), 24721. doi:10.1038/srep24721

Chew, G.-L., Pauli, A., & Schier, A. F. (2016). Conservation of uORF repressiveness and sequence features in mouse, human and zebrafish. *Nature Communications*, *7*(1), 11663. doi:10.1038/ncomms11663

Choi, Y., Bowman, J. W., & Jung, J. U. (2018). Autophagy during viral infection — a double-edged sword. *Nature Reviews Microbiology*, *16*(6), 341–354. doi:10.1038/s41579-018-0003-6

Cirone, M. (2018). EBV and KSHV infection dysregulates autophagy to optimize viral

replication, prevent immune recognition and promote tumorigenesis. *Viruses*, *10*(11), 599. doi:10.3390/v10110599

Clauss, I. M., Chu, M., Zhao, J. L., & Glimcher, L. H. (1996). The basic domain/leucine zipper protein hXBP-1 preferentially binds to and transactivates CRE-like sequences containing an ACGT core. *Nucleic Acids Research*, *24*(10), 1855–1864. doi:10.1093/nar/24.10.1855

Cnop, M., Foufelle, F., & Velloso, L. A. (2012). Endoplasmic reticulum stress, obesity and diabetes. *Trends in Molecular Medicine*, *18*(1), 59–68. doi:10.1016/j.molmed.2011.07.010

Cohen, A., Brodie, C., & Sarid, R. (2006). An essential role of ERK signalling in TPA-induced reactivation of Kaposi's sarcoma-associated herpesvirus. *Journal of General Virology*, *87*(4), 795–802. doi:10.1099/vir.0.81619-0

Colla, E., Coune, P., Liu, Y., Pletnikova, O., Troncoso, J. C., Iwatsubo, T., … Lee, M. K. (2012). Endoplasmic reticulum stress is important for the manifestations of -synucleinopathy In Vivo. *Journal of Neuroscience*, *32*(10), 3306–3320. doi:10.1523/JNEUROSCI.5367-11.2012

Corcoran, J. A., Johnston, B. P., & McCormick, C. (2015). Viral activation of MK2-hsp27-p115RhoGEF-RhoA signaling axis causes cytoskeletal rearrangements, P-body disruption and ARE-mRNA stabilization. *PLoS Pathogens*, *11*(1), e1004597. doi:10.1371/journal.ppat.1004597

Covarrubias, S., Gaglia, M. M., Kumar, G. R., Wong, W., Jackson, A. O., & Glaunsinger, B. A. (2011). Coordinated destruction of cellular messages in translation complexes by the gammaherpesvirus host shutoff factor and the mammalian exonuclease Xrn1. *PLoS Pathogens*, *7*(10), e1002339. doi:10.1371/journal.ppat.1002339

Covino, R., Hummer, G., & Ernst, R. (2018). Integrated functions of membrane property sensors and a hidden side of the unfolded protein response. *Molecular Cell*, *71*(3), 458–467. doi:10.1016/j.molcel.2018.07.019

Cox, J. S., Shamu, C. E., & Walter, P. (1993). Transcriptional induction of genes encoding endoplasmic reticulum resident proteins requires a transmembrane protein kinase. *Cell*, *73*(6), 1197–1206. doi:10.1016/0092-8674(93)90648-A

Cox, J. S., & Walter, P. (1996). A novel mechanism for regulating activity of a transcription factor that controls the unfolded protein response. *Cell*, *87*(3), 391–404. doi:10.1016/S0092-8674(00)81360-4

Credle, J. J., Finer-Moore, J. S., Papa, F. R., Stroud, R. M., & Walter, P. (2005). On the mechanism of sensing unfolded protein in the endoplasmic reticulum. *Proceedings of the National Academy of Sciences*, *102*(52), 18773–18784. doi:10.1073/pnas.0509487102

Credle, J. J., Forcelli, P. A., Delannoy, M., Oaks, A. W., Permaul, E., Berry, D. L., … Sidhu, A. (2015). α-Synuclein-mediated inhibition of ATF6 processing into COPII vesicles disrupts UPR signaling in Parkinson's disease. *Neurobiology of Disease*, *76*, 112–125. doi:10.1016/j.nbd.2015.02.005

Cross, B. C. S., Bond, P. J., Sadowski, P. G., Jha, B. K., Zak, J., Goodman, J. M., … Harding, H. P. (2012). The molecular basis for selective inhibition of

unconventional mRNA splicing by an IRE1-binding small molecule. *Proceedings of the National Academy of Sciences of the United States of America*, *109*(15), E869-78. doi:10.1073/pnas.1115623109

Cubillos-Ruiz, J. R., Silberman, P. C., Rutkowski, M. R., Chopra, S., Perales-Puchalt, A., Song, M., … Glimcher, L. H. (2015). ER stress sensor XBP1 controls anti-tumor immunity by disrupting dendritic cell homeostasis. *Cell*, *161*(7), 1527–1538. doi:10.1016/j.cell.2015.05.025

Cui, W., Li, J., Ron, D., & Sha, B. (2011). The structure of the PERK kinase domain suggests the mechanism for its activation. *Acta Crystallographica Section D Biological Crystallography*, *67*(5), 423–428. doi:10.1107/S0907444911006445

Cullinan, S. B., Zhang, D., Hannink, M., Arvisais, E., Kaufman, R. J., & Diehl, J. A. (2003). Nrf2 is a direct PERK substrate and effector of PERK-dependent cell survival. *Molecular and Cellular Biology*, *23*(20), 7198–7209. doi:10.1128/MCB.23.20.7198-7209.2003

Dai, X., Gong, D., Wu, T.-T., Sun, R., & Zhou, Z. H. (2014). Organization of capsid-associated tegument components in Kaposi's sarcoma-associated herpesvirus. *Journal of Virology*, *88*(21), 12694–12702. doi:10.1128/JVI.01509-14

Dai, X., Gong, D., Xiao, Y., Wu, T.-T., Sun, R., & Zhou, Z. H. (2015). CryoEM and mutagenesis reveal that the smallest capsid protein cements and stabilizes Kaposi's sarcoma-associated herpesvirus capsid. *Proceedings of the National Academy of Sciences of the United States of America*, *112*(7), E649-56. doi:10.1073/pnas.1420317112

Dalton-Griffin, L., Wilson, S. J., & Kellam, P. (2009). X-box binding protein 1 contributes to induction of the Kaposi's sarcoma-associated herpesvirus lytic cycle under hypoxic conditions. *Journal of Virology*, *83*(14), 7202–7209. doi:10.1128/JVI.00076-09

Datan, E., Roy, S. G., Germain, G., Zali, N., McLean, J. E., Golshan, G., … Zakeri, Z. (2016). Dengue-induced autophagy, virus replication and protection from cell death require ER stress (PERK) pathway activation. *Cell Death & Disease*, *7*(3), e2127. doi:10.1038/cddis.2015.409

Davis, Z. H., Hesser, C. R., Park, J., & Glaunsinger, B. A. (2016). Interaction between ORF24 and ORF34 in the Kaposi's Sarcoma-Associated Herpesvirus Late Gene Transcription Factor Complex Is Essential for Viral Late Gene Expression. *Journal of Virology*, *90*(1), 599–604. doi:10.1128/JVI.02157-15

Davis, Z. H., Verschueren, E., Jang, G. M., Kleffman, K., Johnson, J. R., Park, J., … Glaunsinger, B. A. (2015). Global mapping of herpesvirus-host protein complexes reveals a transcription strategy for late genes. *Molecular Cell*, *57*(2), 349–360. doi:10.1016/j.molcel.2014.11.026

Davison, A. J., Eberle, R., Ehlers, B., Hayward, G. S., McGeoch, D. J., Minson, A. C., … Thiry, E. (2009). The order herpesvirales. *Archives of Virology*, *154*(1), 171–177. doi:10.1007/s00705-008-0278-4

De Leo, A., Chen, H.-S., Hu, C.-C. A., & Lieberman, P. M. (2017). Deregulation of KSHV latency conformation by ER-stress and caspase-dependent RAD21-cleavage. *PLOS Pathogens*, *13*(8), e1006596. doi:10.1371/journal.ppat.1006596

Dejeans, N., Manié, S., Hetz, C., Bard, F., Hupp, T., Agostinis, P., … Chevet, E. (2014). Addicted to secrete – novel concepts and targets in cancer therapy. *Trends in Molecular Medicine*, *20*(5), 242–250. doi:10.1016/j.molmed.2013.12.003

Delépine, M., Nicolino, M., Barrett, T., Golamaully, M., Mark Lathrop, G., & Julier, C. (2000). EIF2AK3, encoding translation initiation factor 2-α kinase 3, is mutated in patients with Wolcott-Rallison syndrome. *Nature Genetics*, *25*(4), 406–409. doi:10.1038/78085

Deng, J., Lu, P. D., Zhang, Y., Scheuner, D., Kaufman, R. J., Sonenberg, N., … Ron, D. (2004). Translational repression mediates activation of nuclear factor Kappa B by phosphorylated translation initiation factor 2. *Molecular and Cellular Biology*, *24*(23), 10161–10168. doi:10.1128/MCB.24.23.10161-10168.2004

Desai, P. J., Pryce, E. N., Henson, B. W., Luitweiler, E. M., & Cothran, J. (2012). Reconstitution of the Kaposi's sarcoma-associated herpesvirus nuclear egress complex and formation of nuclear membrane vesicles by coexpression of ORF67 and ORF69 gene products. *Journal of Virology*, *86*(1), 594–598. doi:10.1128/JVI.05988-11

Dever, T. E., Feng, L., Wek, R. C., Cigan, A. M., Donahue, T. F., & Hinnebusch, A. G. (1992). Phosphorylation of initiation factor 2 alpha by protein kinase GCN2 mediates gene-specific translational control of GCN4 in yeast. *Cell*, *68*(3), 585–596.

Devi, L., & Ohno, M. (2014). PERK mediates eIF2α phosphorylation responsible for BACE1 elevation, CREB dysfunction and neurodegeneration in a mouse model of Alzheimer's disease. *Neurobiology of Aging*, *35*(10), 2272–2281. doi:10.1016/j.neurobiolaging.2014.04.031

Dewson, G., & Kluck, R. M. (2009). Mechanisms by which Bak and Bax permeabilise mitochondria during apoptosis. *Journal of Cell Science*, *122*(Pt 16), 2801–2808. doi:10.1242/JCS.038166

Di Bartolo, D. L., Hyjek, E., Keller, S., Guasparri, I., Deng, H., Sun, R., … Cesarman, E. (2009). Role of defective Oct-2 and OCA-B expression in immunoglobulin production and Kaposi's sarcoma-associated herpesvirus lytic reactivation in primary effusion lymphoma. *Journal of Virology*, *83*(9), 4308–4315. doi:10.1128/JVI.02196-08

Dittmer, D., Lagunoff, M., Renne, R., Staskus, K., Haase, A., & Ganem, D. (1998). A cluster of latently expressed genes in Kaposi's sarcoma-associated herpesvirus. *Journal of Virology*, *72*(10), 8309–8315. Retrieved from http://www.ncbi.nlm.nih.gov/pubmed/9733875

Dittmer, D. P., Damania, B., & Sin, S.-H. (2015). Animal models of tumorigenic herpesviruses--an update. *Current Opinion in Virology*, *14*, 145–150. doi:10.1016/j.coviro.2015.09.006

Domsic, J. F., Chen, H.-S., Lu, F., Marmorstein, R., & Lieberman, P. M. (2013). Molecular basis for oligomeric-DNA binding and episome maintenance by KSHV LANA. *PLoS Pathogens*, *9*(10), e1003672. doi:10.1371/journal.ppat.1003672

Drexler, H. G., Uphoff, C. C., Gaidano, G., & Carbone, A. (1998). Lymphoma cell lines: in vitro models for the study of HHV-8+ primary effusion lymphomas (body

cavity-based lymphomas). *Leukemia*, *12*(10), 1507–1517. 10.1038/sj.leu.2401160

Drori, A., Messerle, M., Brune, W., & Tirosh, B. (2014). Lack of XBP-1 impedes murine cytomegalovirus gene expression. *PloS One*, *9*(10), e110942. doi:10.1371/journal.pone.0110942

Du, M.-Q., Diss, T. C., Liu, H., Ye, H., Hamoudi, R. A., Cabeçadas, J., … Isaacson, P. G. (2002). KSHV- and EBV-associated germinotropic lymphoproliferative disorder. *Blood*, *100*(9), 3415–3418. doi:10.1182/blood-2002-02-0487

Du, M. Q., Liu, H., Diss, T. C., Ye, H., Hamoudi, R. A., Dupin, N., … Isaacson, P. G. (2001). Kaposi sarcoma-associated herpesvirus infects monotypic (IgM lambda) but polyclonal naive B cells in Castleman disease and associated lymphoproliferative disorders. *Blood*, *97*(7), 2130–2136.

Duennwald, M. L., & Lindquist, S. (2008). Impaired ERAD and ER stress are early and specific events in polyglutamine toxicity. *Genes & Development*, *22*(23), 3308–3319. doi:10.1101/gad.1673408

Dünn-Kittenplon, D. (Dana), Kalt, I., Lellouche, J.-P. (Moshe), & Sarid, R. (2019). The KSHV portal protein ORF43 is essential for the production of infectious viral particles. *Virology*, *529*, 205–215. doi:10.1016/j.virol.2019.01.028

E, X., Hwang, S., Oh, S., Lee, J.-S., Jeong, J. H., Gwack, Y., … Liang, C. (2009). Viral Bcl-2-mediated evasion of autophagy aids chronic infection of γherpesvirus 68. *PLoS Pathogens*, *5*(10), e1000609. doi:10.1371/journal.ppat.1000609

Elmore, S. (2007). Apoptosis: A review of programmed cell death. *Toxicologic Pathology*, *35*(4), 495–516. doi:10.1080/01926230701320337

Elphick, D. A., & Mahida, Y. R. (2005). Paneth cells: their role in innate immunity and inflammatory disease. *Gut*, *54*(12), 1802–1809. doi:10.1136/gut.2005.068601

Fagone, P., & Jackowski, S. (2009). Membrane phospholipid synthesis and endoplasmic reticulum function. *Journal of Lipid Research*, *50*(Supplement), S311–S316. doi:10.1194/jlr.R800049-JLR200

Farina, A., Santarelli, R., Bloise, R., Gonnella, R., Granato, M., Bei, R., … Faggioni, A. (2013). KSHV ORF67 encoded lytic protein localizes on the nuclear membrane and alters emerin distribution. *Virus Research*, *175*(2), 143–150. doi:10.1016/j.virusres.2013.04.001

Farrell, P. J., Balkow, K., Hunt, T., Jackson, R. J., & Trachsel, H. (1977). Phosphorylation of initiation factor elF-2 and the control of reticulocyte protein synthesis. *Cell*, *11*(1), 187–200. doi:10.1016/0092-8674(77)90330-0

Feng, J., Gong, D., Fu, X., Wu, T., Wang, J., Chang, J., … Sun, R. (2015). M1 of murine gamma-herpesvirus 68 induces endoplasmic reticulum chaperone production. *Scientific Reports*, *5*, 17228. doi:10.1038/srep17228

Fernandez, J., Yaman, I., Sarnow, P., Snider, M. D., & Hatzoglou, M. (2002). Regulation of internal ribosomal entry site-mediated translation by phosphorylation of the translation initiation factor eif2α. *Journal of Biological Chemistry*, *277*(21), 19198–19205. doi:10.1074/jbc.M201052200

Fink, S. L., Jayewickreme, T. R., Molony, R. D., Iwawaki, T., Landis, C. S., Lindenbach, B. D., & Iwasaki, A. (2017). IRE1α promotes viral infection by conferring

resistance to apoptosis. *Science Signaling*, *10*(482), eaai7814. doi:10.1126/scisignal.aai7814

Forte, E., Raja, A. N., Shamulailatpam, P., Manzano, M., Schipma, M. J., Casey, J. L., & Gottwein, E. (2015). MicroRNA-mediated transformation by the Kaposi's sarcoma-associated herpesvirus Kaposin locus. *Journal of Virology*, *89*(4), 2333–2341. doi:10.1128/JVI.03317-14

Frabutt, D. A., Wang, B., Riaz, S., Schwartz, R. C., & Zheng, Y.-H. (2018). Innate sensing of Influenza A virus hemagglutinin glycoproteins by the host endoplasmic reticulum (ER) stress pathway triggers a potent antiviral response via ER-associated protein degradation. *Journal of Virology*, *92*(1). doi:10.1128/JVI.01690-17

Frisan, T., Levitsky, V., Masucci, M. (2001). Generation of lymphoblastoid cell lines (LCLs). *Methods in Molecular Biology, 174*, 125-127. doi:10.1385/1-59259-227-9:125

Fu, S., Yang, L., Li, P., Hofmann, O., Dicker, L., Hide, W., … Hotamisligil, G. S. (2011). Aberrant lipid metabolism disrupts calcium homeostasis causing liver endoplasmic reticulum stress in obesity. *Nature*, *473*(7348), 528–531. doi:10.1038/nature09968

Gachon, F., Gaudray, G., Thébault, S., Basbous, J., Koffi, J. A., Devaux, C., & Mesnard, J. (2001). The cAMP response element binding protein-2 (CREB-2) can interact with the C/EBP-homologous protein (CHOP). *FEBS Letters*, *502*(1–2), 57–62. doi:10.1016/S0014-5793(01)02646-1

Gallagher, C. M., Garri, C., Cain, E. L., Ang, K. K.-H., Wilson, C. G., Chen, S., … Walter, P. (2016). Ceapins are a new class of unfolded protein response inhibitors, selectively targeting the ATF6alpha branch. *ELife*, *5*. doi:10.7554/eLife.11878

Gallagher, C. M., & Walter, P. (2016). Ceapins inhibit ATF6α signaling by selectively preventing transport of ATF6α to the Golgi apparatus during ER stress. *ELife*, *5*. doi:10.7554/eLife.11880

Ganem, D. (2007). KSHV-induced oncogenesis. In A. Arvin, B. Roizman, E. Mocarski, G. Campadelli Fiume, K. Yamanishi, P.S. Moore, & R. Whitley. (Eds.), *Human herpesviruses: biology, therapy, and immunoprophylaxis*. Cambridge: Cambridge University Press. Retrieved from https://www.ncbi.nlm.nih.gov/books/NBK47373/

Gardner, B. M., & Walter, P. (2011). Unfolded proteins are IRE1-activating ligands that directly induce the unfolded protein response. *Science (New York, N.Y.)*, *333*(6051), 1891–1894. doi:10.1126/science.1209126

Gardner, M. R., & Glaunsinger, B. A. (2018). Kaposi's sarcoma-associated herpesvirus ORF68 is a DNA binding protein required for viral genome cleavage and packaging. *Journal of Virology*, *92*(16). doi:10.1128/JVI.00840-18

Geiger, R., Andritschke, D., Friebe, S., Herzog, F., Luisoni, S., Heger, T., & Helenius, A. (2011). BAP31 and BiP are essential for dislocation of SV40 from the endoplasmic reticulum to the cytosol. *Nature Cell Biology*, *13*(11), 1305–1314. doi:10.1038/ncb2339

Gething, M. J., McCammon, K., & Sambrook, J. (1986). Expression of wild-type and

mutant forms of influenza hemagglutinin: the role of folding in intracellular transport. *Cell*, *46*(6), 939–950. doi:10.1016/0092-8674(86)90076-0

Giffin, L., & Damania, B. (2014). KSHV: pathways to tumorigenesis and persistent infection. *Advances in Virus Research*, *88*, 111–159. doi:10.1016/B978-0-12-800098-4.00002-7

Giffin, L., Yan, F., Ben Major, M., & Damania, B. (2014). Modulation of Kaposi's sarcoma-associated herpesvirus interleukin-6 function by hypoxia-upregulated protein 1. *Journal of Virology*, *88*(16), 9429–9441. doi:10.1128/JVI.00511-14

Gillespie, L. K., Hoenen, A., Morgan, G., & Mackenzie, J. M. (2010). The endoplasmic reticulum provides the membrane platform for biogenesis of the flavivirus replication complex. *Journal of Virology*, *84*(20), 10438–10447. doi:10.1128/JVI.00986-10

Glab, J. A., Doerflinger, M., Nedeva, C., Jose, I., Mbogo, G. W., Paton, J. C., … Puthalakath, H. (2017). DR5 and caspase-8 are dispensable in ER stress-induced apoptosis. *Cell Death & Differentiation*, *24*(5), 944–950. doi:10.1038/cdd.2017.53

Glaunsinger, B., Chavez, L., & Ganem, D. (2005). The exonuclease and host shutoff functions of the SOX protein of Kaposi's sarcoma-associated herpesvirus are genetically separable. *Journal of Virology*, *79*(12), 7396–7401. doi:10.1128/JVI.79.12.7396-7401.2005

Glaunsinger, B., & Ganem, D. (2004a). Highly selective escape from KSHV-mediated host mRNA shutoff and its implications for viral pathogenesis. *The Journal of Experimental Medicine*, *200*(3), 391–398. doi:10.1084/jem.20031881

Glaunsinger, B., & Ganem, D. (2004b). Lytic KSHV infection inhibits host gene expression by accelerating global mRNA turnover. *Molecular Cell*, *13*(5), 713–723.

Golovko, A., Kojukhov, A., Guan, B.-J., Morpurgo, B., Merrick, W. C., Mazumder, B., … Komar, A. A. (2016). The eIF2A knockout mouse. *Cell Cycle*, *15*(22), 3115–3120. doi:10.1080/15384101.2016.1237324

Gonzalez, C. M., Wang, L., & Damania, B. (2009). Kaposi's sarcoma-associated herpesvirus encodes a viral deubiquitinase. *Journal of Virology*, *83*(19), 10224–10233. doi:10.1128/JVI.00589-09

Gonzalez, T. N., Sidrauski, C., Dörfler, S., & Walter, P. (1999). Mechanism of non-spliceosomal mRNA splicing in the unfolded protein response pathway. The EMBO Journal, 18(11), 3119-3132. doi:10.1093/emboj/18.11.3119

Görlach, A., Bertram, K., Hudecova, S., & Krizanova, O. (2015). Calcium and ROS: A mutual interplay. *Redox Biology*, *6*, 260–271. doi:10.1016/j.redox.2015.08.010

Gossen, M., Freundlieb, S., Bender, G., Müller, G., Hillen, W., & Bujard, H. (1995). Transcriptional activation by tetracyclines in mammalian cells. *Science (New York, N.Y.)*, *268*(5218), 1766–1769. doi:10.1093/nar/27.2.708

Gredmark, S., Schlieker, C., Quesada, V., Spooner, E., & Ploegh, H. L. (2007). A functional ubiquitin-specific protease embedded in the large tegument protein (ORF64) of murine gammaherpesvirus 68 is active during the course of infection. *Journal of Virology*, *81*(19), 10300–10309. doi:10.1128/JVI.01149-07

Grootjans, J., Kaser, A., Kaufman, R. J., & Blumberg, R. S. (2016). The unfolded protein response in immunity and inflammation. *Nature Publishing Group*, *16*. doi:10.1038/nri.2016.62

Grundhoff, A., & Ganem, D. (2004). Inefficient establishment of KSHV latency suggests an additional role for continued lytic replication in Kaposi sarcoma pathogenesis. *The Journal of Clinical Investigation*, *113*(1), 124–136. doi:10.1172/JCI17803

Guasparri, I., Keller, S. A., & Cesarman, E. (2004). KSHV vFLIP is essential for the survival of infected lymphoma cells. *The Journal of Experimental Medicine*, *199*(7), 993–1003. doi:10.1084/jem.20031467

Günther, T., & Grundhoff, A. (2010). The epigenetic landscape of latent Kaposi sarcoma-associated herpesvirus genomes. *PLoS Pathogens*, *6*(6), e1000935. doi:10.1371/journal.ppat.1000935

Gurlo, T., Rivera, J. F., Butler, A. E., Cory, M., Hoang, J., Costes, S., & Butler, P. C. (2016). CHOP contributes to, but is not the only mediator of, IAPP induced β-Cell apoptosis. *Molecular Endocrinology (Baltimore, Md.)*, *30*(4), 446–454. doi:10.1210/me.2015-1255

Haas, I. G., & Wabl, M. (1983). Immunoglobulin heavy chain binding protein. *Nature*, *306*(5941), 387–389. doi:10.1038/306387a0

Hai, T., & Hartman, M. G. (2001). The molecular biology and nomenclature of the activating transcription factor/cAMP responsive element binding family of transcription factors: activating transcription factor proteins and homeostasis. *Gene*, *273*(1), 1–11. doi:10.1016/S0378-1119(01)00551-0

Hajnóczky, G., Davies, E., & Madesh, M. (2003). Calcium signaling and apoptosis. *Biochemical and Biophysical Research Communications*, *304*(3), 445–454. doi:10.1016/S0006-291X(03)00616-8

Halbleib, K., Pesek, K., Covino, R., Hofbauer, H. F., Wunnicke, D., Hänelt, I., … Ernst, R. (2017). Activation of the unfolded protein response by lipid bilayer stress. *Molecular Cell*, *67*(4), 673–684.e8. doi:10.1016/j.molcel.2017.06.012

Hamza, M. S., Reyes, R. A., Izumiya, Y., Wisdom, R., Kung, H.-J., & Luciw, P. A. (2004). ORF36 protein kinase of Kaposi's sarcoma herpesvirus activates the c-Jun N-terminal kinase signaling pathway. *Journal of Biological Chemistry*, *279*(37), 38325–38330. doi:10.1074/jbc.M400964200

Han, A.-P., Yu, C., Lu, L., Fujiwara, Y., Browne, C., Chin, G., … Chen, J. J. (2001). Heme-regulated eIF2alpha kinase (HRI) is required for translational regulation and survival of erythroid precursors in iron deficiency. *The EMBO Journal*, *20*(23), 6909–6918. doi:10.1093/emboj/20.23.6909

Han, D., Lerner, A. G., Vande Walle, L., Upton, J.-P., Xu, W., Hagen, A., … Papa, F. R. (2009). IRE1α kinase activation modes control alternate endoribonuclease outputs to determine divergent cell fates. *Cell*, *138*(3), 562–575. doi:10.1016/J.CELL.2009.07.017

Han, J., Back, S. H., Hur, J., Lin, Y.-H., Gildersleeve, R., Shan, J., … Kaufman, R. J. (2013). ER-stress-induced transcriptional regulation increases protein synthesis leading to cell death. *Nature Cell Biology*, *15*(5), 481–490. doi:10.1038/ncb2738

Haque, M., Davis, D. A., Wang, V., Widmer, I., & Yarchoan, R. (2003). Kaposi's

sarcoma-associated herpesvirus (human herpesvirus 8) contains hypoxia response elements: relevance to lytic induction by hypoxia. *Journal of Virology*, *77*(12), 6761–6768. doi:10.1128/JVI.77.12.6761-6768.2003

Haque, M., & Kousoulas, K. G. (2013). The Kaposi's Sarcoma-Associated Herpesvirus ORF34 Protein Binds to HIF-1 and Causes Its Degradation via the Proteasome Pathway. *Journal of Virology*, *87*(4), 2164–2173. doi:10.1128/JVI.02460-12

Haque, M., Wang, V., Davis, D. A., Zheng, Z.-M., & Yarchoan, R. (2006). Genetic organization and hypoxic activation of the Kaposi's sarcoma-associated herpesvirus ORF34-37 gene cluster. *Journal of Virology*, *80*(14), 7037–7051. doi:10.1128/JVI.00553-06

Harding, H. P., Novoa, I., Zhang, Y., Zeng, H., Wek, R., Schapira, M., & Ron, D. (2000). Regulated translation initiation controls stress-induced gene expression in mammalian cells. *Molecular Cell*, *6*(5), 1099–1108. doi:10.1016/S1097-2765(00)00108-8

Harding, H. P., Zeng, H., Zhang, Y., Jungries, R., Chung, P., Plesken, H., ... Ron, D. (2001). Diabetes mellitus and exocrine pancreatic dysfunction in perk-/- mice reveals a role for translational control in secretory cell survival. Molecular cell, 7(6), 1153-1163.

Harding, H. P., Zhang, Y., & Ron, D. (1999). Protein translation and folding are coupled by an endoplasmic-reticulum-resident kinase. *Nature*, *397*(6716), 271–274. doi:10.1016/S1097-2765(01)00264-7

Harding, H. P., Zhang, Y., Zeng, H., Novoa, I., Lu, P. D., Calfon, M., … Ron, D. (2003). An integrated stress response regulates amino acid metabolism and resistance to oxidative stress. *Molecular Cell*, *11*(3), 619–633.

Harding, H. P., Zyryanova, A. F., & Ron, D. (2012). Uncoupling proteostasis and development *in Vitro* with a small molecule inhibitor of the pancreatic endoplasmic reticulum kinase, PERK. *Journal of Biological Chemistry*, *287*(53), 44338–44344. doi:10.1074/jbc.M112.428987

Hassan, I., Gaines, K. S., Hottel, W. J., Wishy, R. M., Miller, S. E., Powers, L. S., … Monick, M. M. (2014). Inositol-requiring enzyme 1 inhibits respiratory syncytial virus replication. *The Journal of Biological Chemistry*, *289*(11), 7537–7546. doi:10.1074/jbc.M113.510594

Hassan, I. H., Zhang, M. S., Powers, L. S., Shao, J. Q., Baltrusaitis, J., Rutkowski, D. T., … Monick, M. M. (2012). Influenza A viral replication is blocked by inhibition of the inositol-requiring enzyme 1 (IRE1) stress pathway. *The Journal of Biological Chemistry*, *287*(7), 4679–4689. doi:10.1074/jbc.M111.284695

Hassman, L. M., Ellison, T. J., & Kedes, D. H. (2011). KSHV infects a subset of human tonsillar B cells, driving proliferation and plasmablast differentiation. *Journal of Clinical Investigation*, *121*(2), 752–768. doi:10.1172/JCI44185

Hatton, O. L., Harris-Arnold, A., Schaffert, S., Krams, S. M., & Martinez, O. M. (2014). The interplay between Epstein-Barr virus and B lymphocytes: implications for infection, immunity, and disease. *Immunologic Research*, *58*(2–3), 268–276. doi:10.1007/s12026-014-8496-1

Hausen, H. Zur, O'neill, F. J., Freese, U. K., & Hecker, E. (1978). Persisting oncogenic

herpesvirus induced by the tumour promoter TPA. *Nature*, *272*(5651), 373–375. doi:10.1038/272373a0

Haze, K., Okada, T., Yoshida, H., Yanagi, H., Yura, T., Negishi, M., & Mori, K. (2001). Identification of the G13 (cAMP-response-element-binding protein-related protein) gene product related to activating transcription factor 6 as a transcriptional activator of the mammalian unfolded protein response. *The Biochemical Journal*, *355*(Pt 1), 19–28. doi:10.1042/0264-6021:3550019

Haze, K., Yoshida, H., Yanagi, H., Yura, T., & Mori, K. (1999). Mammalian Transcription Factor ATF6 Is Synthesized as a Transmembrane Protein and Activated by Proteolysis in Response to Endoplasmic Reticulum Stress. *Molecular Biology of the Cell*, *10*(11), 3787–3799. doi:10.1091/mbc.10.11.3787

He, B., Gross, M., & Roizman, B. (1997). The gamma(1)34.5 protein of herpes simplex virus 1 complexes with protein phosphatase 1alpha to dephosphorylate the alpha subunit of the eukaryotic translation initiation factor 2 and preclude the shutoff of protein synthesis by double-stranded RNA-activated protein kinase. *Proceedings of the National Academy of Sciences of the United States of America*, *94*(3), 843–848. doi:10.1073/pnas.94.3.843

He, B., Gross, M., & Roizman, B. (1998). The gamma134.5 protein of herpes simplex virus 1 has the structural and functional attributes of a protein phosphatase 1 regulatory subunit and is present in a high molecular weight complex with the enzyme in infected cells. *The Journal of Biological Chemistry*, *273*(33), 20737–20743. doi:10.1074/jbc.273.33.20737

Hellert, J., Weidner-Glunde, M., Krausze, J., Lünsdorf, H., Ritter, C., Schulz, T. F., & Lührs, T. (2015). The 3D structure of Kaposi sarcoma herpesvirus LANA C-terminal domain bound to DNA. *Proceedings of the National Academy of Sciences*, *112*(21), 6694–6699. doi:10.1073/pnas.1421804112

Hempstead, A. D., & Isberg, R. R. (2015). Inhibition of host cell translation elongation by Legionella pneumophila blocks the host cell unfolded protein response. *Proceedings of the National Academy of Sciences of the United States of America*, *112*(49), E6790-7. doi:10.1073/pnas.1508716112

Herber, D. L., Cao, W., Nefedova, Y., Novitskiy, S. V, Nagaraj, S., Tyurin, V. A., … Gabrilovich, D. I. (2010). Lipid accumulation and dendritic cell dysfunction in cancer. *Nature Medicine*, *16*(8), 880–886. doi:10.1038/nm.2172

Hesser, C. R., Karijolich, J., Dominissini, D., He, C., & Glaunsinger, B. A. (2018). N6-methyladenosine modification and the YTHDF2 reader protein play cell type specific roles in lytic viral gene expression during Kaposi's sarcoma-associated herpesvirus infection. *PLoS Pathogens*, *14*(4), e1006995. doi:10.1371/journal.ppat.1006995

Hetz, C., & Papa, F. R. (2018). The unfolded protein response and cell fate control. *Molecular Cell*, *69*(2), 169–181. doi:10.1016/j.molcel.2017.06.017

Hilgarth, R. S., & Sarge, K. D. (2005). Detection of sumoylated proteins. *Methods in Molecular Biology (Clifton, N.J.)*, *301*, 329–338. doi:10.1385/1-59259-895-1:329

Hinnebusch, A. G. (1984). Evidence for translational regulation of the activator of general amino acid control in yeast. *Proceedings of the National Academy of*

Sciences of the United States of America, *81*(20), 6442–6446. doi:10.1073/pnas.81.20.6442

Hinnebusch, A. G. (1997). Translational regulation of yeast GCN4. A window on factors that control initiator-trna binding to the ribosome. *The Journal of Biological Chemistry*, *272*(35), 21661–21664. doi:10.1074/jbc.272.35.21661

Hirosumi, J., Tuncman, G., Chang, L., Görgün, C. Z., Uysal, K. T., Maeda, K., … Hotamisligil, G. S. (2002). A central role for JNK in obesity and insulin resistance. *Nature*, *420*(6913), 333–336. doi:10.1038/nature01137

Hollien, J., Lin, J. H., Li, H., Stevens, N., Walter, P., & Weissman, J. S. (2009). Regulated IRE1-dependent decay of messenger RNAs in mammalian cells. *The Journal of Cell Biology*, *186*(3), 323–331. doi:10.1083/jcb.200903014

Hollien, J., & Weissman, J. S. (2006). Decay of endoplasmic reticulum-localized mRNAs during the unfolded protein response. *Science (New York, N.Y.)*, *313*(5783), 104–107. doi:10.1126/science.1129631

Holmes, W. M., Klaips, C. L., & Serio, T. R. (2014). Defining the limits: Protein aggregation and toxicity in vivo. *Critical Reviews in Biochemistry and Molecular Biology*, *49*(4), 294–303. doi:10.3109/10409238.2014.914151

Hong, M., Luo, S., Baumeister, P., Huang, J.-M., Gogia, R. K., Li, M., & Lee, A. S. (2004). Underglycosylation of ATF6 as a novel sensing mechanism for activation of the unfolded protein response. *Journal of Biological Chemistry*, *279*(12), 11354–11363. doi:10.1074/jbc.M309804200

Hsiao, J.-R., Chang, K.-C., Chen, C.-W., Wu, S.-Y., Su, I.-J., Hsu, M.-C., … Chang, Y. (2009). Endoplasmic reticulum stress triggers XBP-1-mediated up-regulation of an EBV oncoprotein in nasopharyngeal carcinoma. *Cancer Research*, *69*(10), 4461–4467. doi:10.1158/0008-5472.CAN-09-0277

Hu, D., Wang, V., Yang, M., Abdullah, S., Davis, D. A., Uldrick, T. S., … Yarchoan, R. (2016). Induction of Kaposi's sarcoma-associated herpesvirus-encoded viral Interleukin-6 by X-box binding protein 1. *Journal of Virology*, *90*(1), 368–378. doi:10.1128/JVI.01192-15

Hu, F., Yu, X., Wang, H., Zuo, D., Guo, C., Yi, H., … Wang, X.-Y. (2011). ER stress and its regulator X-box-binding protein-1 enhance polyIC-induced innate immune response in dendritic cells. *European Journal of Immunology*, *41*(4), 1086–1097. doi:10.1002/eji.201040831

Hu, P., Han, Z., Couvillon, A. D., Kaufman, R. J., & Exton, J. H. (2006). Autocrine tumor necrosis factor alpha links endoplasmic reticulum stress to the membrane death receptor pathway through IRE1 -mediated NF- B activation and down-regulation of TRAF2 expression. *Molecular and Cellular Biology*, *26*(8), 3071–3084. doi:10.1128/MCB.26.8.3071-3084.2006

Huang, C., Lin, C., Haataja, L., Gurlo, T., Butler, A. E., Rizza, R. A., & Butler, P. C. (2007). High expression rates of human islet amyloid polypeptide induce endoplasmic reticulum stress–mediated β-Cell Apoptosis, a characteristic of humans with type 2 but not type 1 diabetes. *Diabetes*, *56*(8), 2016–2027. doi:10.2337/db07-0197

Huber, A.-L., Lebeau, J., Guillaumot, P., Pétrilli, V., Malek, M., Chilloux, J., … Manié,

S. N. (2013). p58IPK-mediated attenuation of the proapoptotic PERK-CHOP pathway allows malignant progression upon low glucose. *Molecular Cell*, *49*(6), 1049–1059. doi:10.1016/j.molcel.2013.01.009

Hughes, D., & Mallucci, G. R. (2019). The unfolded protein response in neurodegenerative disorders - therapeutic modulation of the PERK pathway. *The FEBS Journal*, *286*(2), 342–355. doi:10.1111/febs.14422

Hull, R. L., Zraika, S., Udayasankar, J., Aston-Mourney, K., Subramanian, S. L., & Kahn, S. E. (2009). Amyloid formation in human IAPP transgenic mouse islets and pancreas, and human pancreas, is not associated with endoplasmic reticulum stress. *Diabetologia*, *52*(6), 1102–1111. doi:10.1007/s00125-009-1329-4

ikwegbue, p., masamba, p., oyinloye, b., & kappo, a. (2017). roles of heat shock proteins in apoptosis, oxidative stress, human inflammatory diseases, and cancer. *Pharmaceuticals*, *11*(1), 2. doi:10.3390/ph11010002

Ingolia, N. T., Lareau, L. F., & Weissman, J. S. (2011). Ribosome profiling of mouse embryonic stem cells reveals the complexity and dynamics of mammalian proteomes. *Cell*, *147*(4), 789–802. doi:10.1016/j.cell.2011.10.002

Isler, J. A., Skalet, A. H., & Alwine, J. C. (2005). Human cytomegalovirus infection activates and regulates the unfolded protein response. *Journal of Virology*, *79*(11), 6890–6899. doi:10.1128/JVI.79.11.6890-6899.2005

Iwakoshi, N. N., Lee, A.-H., Vallabhajosyula, P., Otipoby, K. L., Rajewsky, K., & Glimcher, L. H. (2003a). Plasma cell differentiation and the unfolded protein response intersect at the transcription factor XBP-1. *Nature Immunology*, *4*(4), 321–329. doi:10.1038/ni907

Iwakoshi, N. N., Lee, A.-H., Vallabhajosyula, P., Otipoby, K. L., Rajewsky, K., & Glimcher, L. H. (2003b). Plasma cell differentiation and the unfolded protein response intersect at the transcription factor XBP-1. *Nature Immunology*, *4*(4), 321–329. doi:10.1038/ni907

Iwawaki, T., Akai, R., Yamanaka, S., & Kohno, K. (2009). Function of IRE1 alpha in the placenta is essential for placental development and embryonic viability. *Proceedings of the National Academy of Sciences of the United States of America*, *106*(39), 16657–16662. doi:10.1073/pnas.0903775106

Iwawaki, T., Hosoda, A., Okuda, T., Kamigori, Y., Nomura-Furuwatari, C., Kimata, Y., … Kohno, K. (2001). Translational control by the ER transmembrane kinase/ribonuclease IRE1 under ER stress. *Nature Cell Biology*, *3*(2), 158–164. doi:10.1038/35055065

Izumiya, Y., Kobayashi, K., Kim, K. Y., Pochampalli, M., Izumiya, C., Shevchenko, B., … Kung, H.-J. (2013). Kaposi's Sarcoma-Associated Herpesvirus K-Rta Exhibits SUMO-Targeting Ubiquitin Ligase (STUbL) Like Activity and Is Essential for Viral Reactivation. *PLoS Pathogens*, *9*(8), e1003506. doi:10.1371/journal.ppat.1003506

Jenner, R. G., Maillard, K., Cattini, N., Weiss, R. A., Boshoff, C., Wooster, R., & Kellam, P. (2003). Kaposi's sarcoma-associated herpesvirus-infected primary effusion lymphoma has a plasma cell gene expression profile. *Proceedings of the National Academy of Sciences of the United States of America*, *100*(18), 10399–

10404. doi:10.1073/pnas.1630810100

Jeong, J., Papin, J., & Dittmer, D. (2001). Differential regulation of the overlapping Kaposi's sarcoma-associated herpesvirus vGCR (orf74) and LANA (orf73) promoters. *Journal of Virology*, *75*(4), 1798–1807. doi:10.1128/JVI.75.4.1798-1807.2001

Jha, H. C., Banerjee, S., & Robertson, E. S. (2016). The role of gammaherpesviruses in cancer pathogenesis. *Pathogens*, *5*(1). doi:10.3390/pathogens5010018

Jheng, J.-R., Lau, K. S., Tang, W.-F., Wu, M., & Horng, J.-T. (2010). Endoplasmic reticulum stress is induced and modulated by enterovirus 71. *Cellular Microbiology*, *12*(6), 796–813. doi:10.1111/j.1462-5822.2010.01434.x

Jiang, H.-Y., Wek, S. A., McGrath, B. C., Lu, D., Hai, T., Harding, H. P., … Wek, R. C. (2004). Activating transcription factor 3 is integral to the eukaryotic initiation factor 2 kinase stress response. *Molecular and Cellular Biology*, *24*(3), 1365–1377. doi:10.1128/MCB.24.3.1365-1377.2004

Jiang, Y., Xu, D., Zhao, Y., & Zhang, L. (2008). Mutual inhibition between Kaposi's Sarcoma-associated herpesvirus and Epstein-Barr virus lytic replication initiators in dually-infected primary effusion lymphoma. *PLoS ONE*, *3*(2), e1569. doi:10.1371/journal.pone.0001569

Joubert, P.-E., Werneke, S. W., de la Calle, C., Guivel-Benhassine, F., Giodini, A., Peduto, L., … Albert, M. L. (2012). Chikungunya virus-induced autophagy delays caspase-dependent cell death. *The Journal of Experimental Medicine*, *209*(5), 1029–1047. doi:10.1084/jem.20110996

Jounai, N., Takeshita, F., Kobiyama, K., Sawano, A., Miyawaki, A., Xin, K.-Q., … Okuda, K. (2007). The Atg5 Atg12 conjugate associates with innate antiviral immune responses. *Proceedings of the National Academy of Sciences*, *104*(35), 14050–14055. doi:10.1073/pnas.0704014104

Jousse, C., Bruhat, A., Carraro, V., Urano, F., Ferrara, M., Ron, D., & Fafournoux, P. (2001). Inhibition of CHOP translation by a peptide encoded by an open reading frame localized in the chop 5'UTR. *Nucleic Acids Research*, *29*(21), 4341–4351. doi:10.1093/nar/29.21.4341

Jurkin, J., Henkel, T., Nielsen, A. F., Minnich, M., Popow, J., Kaufmann, T., … Martinez, J. (2014). The mammalian tRNA ligase complex mediates splicing of *XBP1* mRNA and controls antibody secretion in plasma cells. *The EMBO Journal*, *33*(24), 2922–2936. doi:10.15252/embj.201490332

Kaelin, W. G., & Ratcliffe, P. J. (2008). Oxygen sensing by metazoans: the central role of the HIF hydroxylase pathway. *Molecular Cell*, *30*(4), 393–402. doi:10.1016/j.molcel.2008.04.009

Kamimura, D., & Bevan, M. J. (2008). Endoplasmic reticulum stress regulator XBP-1 contributes to effector CD8+ T cell differentiation during acute infection. *Journal of Immunology (Baltimore, Md. : 1950)*, *181*(8), 5433–5441. doi:10.4049/jimmunol.181.8.5433

Kanda, S., Yanagitani, K., Yokota, Y., Esaki, Y., & Kohno, K. (2016). Autonomous translational pausing is required for XBP1u mRNA recruitment to the ER via the SRP pathway. *Proceedings of the National Academy of Sciences of the United*

States of America, *113*(40), E5886–E5895. doi:10.1073/pnas.1604435113

Kaneko, M., Koike, H., Saito, R., Kitamura, Y., Okuma, Y., & Nomura, Y. (2010). Loss of HRD1-mediated protein degradation causes amyloid precursor protein accumulation and amyloid- generation. *Journal of Neuroscience*, *30*(11), 3924–3932. doi:10.1523/JNEUROSCI.2422-09.2010

Kaposi, M. (1872). Idiopatiches multiples pigment sarcom der Haut. *Archic Fur Dermatologie Syphilis*, (4), 265–272.

Karagöz, G. E., Acosta-Alvear, D., Nguyen, H. T., Lee, C. P., Chu, F., & Walter, P. (2017). An unfolded protein-induced conformational switch activates mammalian IRE1. *ELife*, *6*. doi:10.7554/eLife.30700

Karali, E., Bellou, S., Stellas, D., Klinakis, A., Murphy, C., & Fotsis, T. (2014). VEGF Signals through ATF6 and PERK to Promote Endothelial Cell Survival and Angiogenesis in the Absence of ER Stress. *Molecular Cell*, *54*(4), 559–572. doi:10.1016/j.molcel.2014.03.022

Kaser, A., Lee, A.-H., Franke, A., Glickman, J. N., Zeissig, S., Tilg, H., … Blumberg, R. S. (2008). XBP1 links ER stress to intestinal inflammation and confers genetic risk for human inflammatory bowel disease. *Cell*, *134*(5), 743–756. doi:10.1016/j.cell.2008.07.021

Kashiwagi, K., Takahashi, M., Nishimoto, M., Hiyama, T. B., Higo, T., Umehara, T., … Yokoyama, S. (2016). Crystal structure of eukaryotic translation initiation factor 2B. *Nature*, *531*(7592), 122–125. doi:10.1038/nature16991

Katano, H., Sato, Y., Kurata, T., Mori, S., & Sata, T. (2000). Expression and localization of human herpesvirus 8-encoded proteins in primary effusion lymphoma, Kaposi's sarcoma, and multicentric Castleman's disease. *Virology*, *269*(2), 335–344. doi:10.1006/viro.2000.0196

Kati, S., Tsao, E. H., Günther, T., Weidner-Glunde, M., Rothämel, T., Grundhoff, A., … Schulz, T. F. (2013). Activation of the B-cell antigen receptor triggers reactivation of latent Kaposi's Sarcoma-associated Herpesvirus. *J. Virol*. doi:10.1128/JVI.00506-13

Kaufman, R. J. (2002). Orchestrating the unfolded protein response in health and disease. *Journal of Clinical Investigation*, *110*(10), 1389–1398. doi:10.1172/JCI16886

Kaye, K. M., Izumi, K. M., & Kieff, E. (1993). Epstein-Barr virus latent membrane protein 1 is essential for B-lymphocyte growth transformation. *Proceedings of the National Academy of Sciences of the United States of America*, *90*(19), 9150–9154. doi:10.1073/pnas.90.19.9150

Ke, P.-Y., & Chen, S. S.-L. (2011). Activation of the unfolded protein response and autophagy after hepatitis C virus infection suppresses innate antiviral immunity in vitro. *Journal of Clinical Investigation*, *121*(1), 37–56. doi:10.1172/JCI41474

Kim, H., Tu, H.-C., Ren, D., Takeuchi, O., Jeffers, J. R., Zambetti, G. P., … Cheng, E. H.-Y. (2009). Stepwise activation of BAX and BAK by tBID, BIM, and PUMA initiates mitochondrial apoptosis. *Molecular Cell*, *36*(3), 487–499. doi:10.1016/j.molcel.2009.09.030

Kimmig, P., Diaz, M., Zheng, J., Williams, C. C., Lang, A., Aragón, T., … Walter, P. (2012). The unfolded protein response in fission yeast modulates stability of

select mRNAs to maintain protein homeostasis. *ELife*, *1*, e00048. doi:10.7554/eLife.00048

Klaips, C. L., Jayaraj, G. G., & Hartl, F. U. (2018). Pathways of cellular proteostasis in aging and disease. *The Journal of Cell Biology*, *217*(1), 51–63. doi:10.1083/jcb.201709072

Klein, U., Casola, S., Cattoretti, G., Shen, Q., Lia, M., Mo, T., … Dalla-Favera, R. (2006). Transcription factor IRF4 controls plasma cell differentiation and class-switch recombination. *Nature Immunology*, *7*(7), 773–782. doi:10.1038/ni1357

Kliche, S., Nagel, W., Kremmer, E., Atzler, C., Ege, A., Knorr, T., … Haas, J. (2001). Signaling by human herpesvirus 8 kaposin A through direct membrane recruitment of cytohesin-1. *Molecular Cell*, *7*(4), 833–843. doi:10.1016/S1097-2765(01)00227-1

Ko, Y.-H. (2015). EBV and human cancer. *Experimental & Molecular Medicine*, *47*(1), e130. doi:10.1038/emm.2014.109

Kokame, K., Kato, H., & Miyata, T. (2001). Identification of ERSE-II, a New *cis* -Acting Element Responsible for the ATF6-dependent Mammalian Unfolded Protein Response. *Journal of Biological Chemistry*, *276*(12), 9199–9205. doi:10.1074/jbc.M010486200

Komar, A. A., Gross, S. R., Barth-Baus, D., Strachan, R., Hensold, J. O., Goss Kinzy, T., & Merrick, W. C. (2005). Novel characteristics of the biological properties of the yeast *saccharomyces cerevisiae* eukaryotic initiation factor 2A. *Journal of Biological Chemistry*, *280*(16), 15601–15611. doi:10.1074/jbc.M413728200

Koo, E. H., Lansbury, P. T., & Kelly, J. W. (1999). Amyloid diseases: abnormal protein aggregation in neurodegeneration. *Proceedings of the National Academy of Sciences of the United States of America*, *96*(18), 9989–9990. doi:10.1073/pnas.96.18.9989

Koopal, S., Furuhjelm, J. H., Järviluoma, A., Jäämaa, S., Pyakurel, P., Pussinen, C., … Ojala, P. M. (2007). Viral oncogene–induced DNA damage response is activated in Kaposi sarcoma tumorigenesis. *PLoS Pathogens*, *3*(9), e140. doi:10.1371/journal.ppat.0030140

Koritzinsky, M., Levitin, F., van den Beucken, T., Rumantir, R. A., Harding, N. J., Chu, K. C., … Wouters, B. G. (2013). Two phases of disulfide bond formation have differing requirements for oxygen. *The Journal of Cell Biology*, *203*(4), 615–627. doi:10.1083/jcb.201307185

Kosmaczewski, S. G., Edwards, T. J., Han, S. M., Eckwahl, M. J., Meyer, B. I., Peach, S., … Hammarlund, M. (2014). The RtcB RNA ligase is an essential component of the metazoan unfolded protein response. *EMBO Reports*, *15*(12), 1278–1285. doi:10.15252/embr.201439531

Kozutsumi, Y., Segal, M., Normington, K., Gething, M.-J., & Sambrook, J. (1988). The presence of malfolded proteins in the endoplasmic reticulum signals the induction of glucose-regulated proteins. *Nature*, *332*(6163), 462–464. doi:10.1038/332462a0

Krishnamoorthy, T., Pavitt, G. D., Zhang, F., Dever, T. E., & Hinnebusch, A. G. (2001). Tight binding of the phosphorylated subunit of initiation factor 2 (eIF2) to the

regulatory subunits of guanine nucleotide exchange factor eIF2B is required for inhibition of translation initiation. *Molecular and Cellular Biology*, *21*(15), 5018–5030. doi:10.1128/MCB.21.15.5018-5030.2001

Krishnan, H. H., Naranatt, P. P., Smith, M. S., Zeng, L., Bloomer, C., & Chandran, B. (2004). Concurrent expression of latent and a limited number of lytic genes with immune modulation and antiapoptotic function by Kaposi's sarcoma-associated herpesvirus early during infection of primary endothelial and fibroblast cells and subsequent decline of lytic gene expression. *Journal of Virology*, *78*(7), 3601–3620. doi:10.1128/JVI.78.7.3601-3620.2004

Krock, B. L., Skuli, N., & Simon, M. C. (2011). Hypoxia-induced angiogenesis: good and evil. *Genes & Cancer*, *2*(12), 1117–1133. doi:10.1177/1947601911423654

Kronstad, L. M., Brulois, K. F., Jung, J. U., & Glaunsinger, B. A. (2013). Dual short upstream open reading frames control translation of a herpesviral polycistronic mRNA. *PLoS Pathogens*, *9*(1), e1003156. doi:10.1371/journal.ppat.1003156

Kuang, E., Fu, B., Liang, Q., Myoung, J., & Zhu, F. (2011). Phosphorylation of eukaryotic translation initiation factor 4B (EIF4B) by open reading frame 45/p90 ribosomal S6 kinase (ORF45/RSK) signaling axis facilitates protein translation during Kaposi sarcoma-associated herpesvirus (KSHV) lytic replication. *The Journal of Biological Chemistry*, *286*(48), 41171–41182. doi:10.1074/jbc.M111.280982

Kurtoglu, M., Gao, N., Shang, J., Maher, J. C., Lehrman, M. A., Wangpaichitr, M., … Lampidis, T. J. (2007). Under normoxia, 2-deoxy-D-glucose elicits cell death in select tumor types not by inhibition of glycolysis but by interfering with N-linked glycosylation. *Molecular Cancer Therapeutics*, *6*(11), 3049–3058. doi:10.1158/1535-7163.MCT-07-0310

Lan, K., Kuppers, D. A., & Robertson, E. S. (2005). Kaposi's sarcoma-associated herpesvirus reactivation is regulated by interaction of latency-associated nuclear antigen with recombination signal sequence-binding protein J, the major downstream effector of the notch signaling pathway. *Journal of Virology*, *79*(6), 3468–3478. doi:10.1128/JVI.79.6.3468-3478.2005

Lan, K., Kuppers, D. A., Verma, S. C., Sharma, N., Murakami, M., & Robertson, E. S. (2005). Induction of Kaposi's sarcoma-associated herpesvirus latency-associated nuclear antigen by the lytic transactivator RTA: a novel mechanism for establishment of latency. *Journal of Virology*, *79*(12), 7453–7465. doi:10.1128/JVI.79.12.7453-7465.2005

Lassen, K. G., Kuballa, P., Conway, K. L., Patel, K. K., Becker, C. E., Peloquin, J. M., … Xavier, R. J. (2014). Atg16L1 T300A variant decreases selective autophagy resulting in altered cytokine signaling and decreased antibacterial defense. *Proceedings of the National Academy of Sciences*, *111*(21), 7741–7746. doi:10.1073/pnas.1407001111

Lawless, M. W., Greene, C. M., Mulgrew, A., Taggart, C. C., O'Neill, S. J., & McElvaney, N. G. (2004). Activation of endoplasmic reticulum-specific stress responses associated with the conformational disease Z alpha 1-antitrypsin deficiency. *Journal of Immunology (Baltimore, Md. : 1950)*, *172*(9), 5722–5726. doi:10.4049/jimmunol.172.9.5722

Lebleu, B., Sen, G. C., Shaila, S., Cabrer, B., & Lengyel, P. (1976). Interferon, double-stranded RNA, and protein phosphorylation. *Proceedings of the National Academy of Sciences of the United States of America*, *73*(9), 3107–3111. doi:10.1073/pnas.73.9.3107

Lee, A.-H., Heidtman, K., Hotamisligil, G. S., & Glimcher, L. H. (2011). Dual and opposing roles of the unfolded protein response regulated by IRE1alpha and XBP1 in proinsulin processing and insulin secretion. *Proceedings of the National Academy of Sciences of the United States of America*, *108*(21), 8885–8890. doi:10.1073/pnas.1105564108

Lee, A.-H., Iwakoshi, N. N., & Glimcher, L. H. (2003a). XBP-1 regulates a subset of endoplasmic reticulum resident chaperone genes in the unfolded protein response. *Molecular and Cellular Biology*, *23*(21), 7448–7459. doi:10.1128/MCB.23.21.7448-7459.2003

Lee, A.-H., Iwakoshi, N. N., Anderson, K. C., & Glimcher, L. H. (2003b). Proteasome inhibitors disrupt the unfolded protein response in myeloma cells. *Proceedings of the National Academy of Sciences*, *100*(17), 9946–9951. doi:10.1073/pnas.1334037100

Lee, D. Y., & Sugden, B. (2008). The LMP1 oncogene of EBV activates PERK and the unfolded protein response to drive its own synthesis. *Blood*, *111*(4), 2280–2289. doi:10.1182/blood-2007-07-100032

Lee, J.-S., Li, Q., Lee, J.-Y., Lee, S.-H., Jeong, J. H., Lee, H.-R., … Jung, J. U. (2009). FLIP-mediated autophagy regulation in cell death control. *Nature Cell Biology*, *11*(11), 1355–1362. doi:10.1038/ncb1980

Lee, K. P. K., Dey, M., Neculai, D., Cao, C., Dever, T. E., & Sicheri, F. (2008). Structure of the dual enzyme IRE1 reveals the basis for catalysis and regulation in nonconventional RNA splicing. *Cell*, *132*(1), 89–100. doi:10.1016/J.CELL.2007.10.057

Lee, K., Tirasophon, W., Shen, X., Michalak, M., Prywes, R., Okada, T., … Kaufman, R. J. (2002). IRE1-mediated unconventional mRNA splicing and S2P-mediated ATF6 cleavage merge to regulate XBP1 in signaling the unfolded protein response. *Genes & Development*, *16*(4), 452–466. doi:10.1101/gad.964702

Lee, Y.-R., Kuo, S.-H., Lin, C.-Y., Fu, P.-J., Lin, Y.-S., Yeh, T.-M., & Liu, H.-S. (2018). Dengue virus-induced ER stress is required for autophagy activation, viral replication, and pathogenesis both in vitro and in vivo. *Scientific Reports*, *8*(1), 489. doi:10.1038/s41598-017-18909-3

Lee, Y.-Y., Cevallos, R. C., & Jan, E. (2009). An upstream open reading frame regulates translation of GADD34 during cellular stresses that induce eIF2alpha phosphorylation. *The Journal of Biological Chemistry*, *284*(11), 6661–6673. doi:10.1074/jbc.M806735200

Leidal, A. M., Cyr, D. P., Hill, R. J., Lee, P. W. K., & McCormick, C. (2012). Subversion of autophagy by Kaposi's Sarcoma-associated herpesvirus impairs oncogene-induced senescence. *Cell Host & Microbe*, *11*(2), 167–180. doi:10.1016/j.chom.2012.01.005

Lerner, A. G., Upton, J.-P., Praveen, P. V. K., Ghosh, R., Nakagawa, Y., Igbaria, A., …

Papa, F. R. (2012). IRE1α induces thioredoxin-interacting protein to activate the NLRP3 Inflammasome and promote programmed cell death under irremediable ER stress. *Cell Metabolism*, *16*(2), 250–264. doi:10.1016/J.CMET.2012.07.007

Leung-Hagesteijn, C., Erdmann, N., Cheung, G., Keats, J. J., Stewart, A. K., Reece, D. E., … Tiedemann, R. E. (2013). XBP1s-negative tumor B cells and pre-plasmablasts mediate therapeutic proteasome inhibitor resistance in multiple myeloma. *Cancer Cell*, *24*(3), 289–304. doi:10.1016/j.ccr.2013.08.009

Leung, H. J., Duran, E. M., Kurtoglu, M., Andreansky, S., Lampidis, T. J., & Mesri, E. A. (2012). Activation of the unfolded protein response by 2-deoxy-D-glucose inhibits Kaposi's sarcoma-associated herpesvirus replication and gene expression. *Antimicrobial Agents and Chemotherapy*, *56*(11), 5794–5803. doi:10.1128/AAC.01126-12

Levin, D. H., Petryshyn, R., & London, I. M. (1980). Characterization of double-stranded-RNA-activated kinase that phosphorylates alpha subunit of eukaryotic initiation factor 2 (eIF-2 alpha) in reticulocyte lysates. *Proceedings of the National Academy of Sciences of the United States of America*, *77*(2), 832–836. doi:10.1073/pnas.77.2.832

Li, D., Fu, W., & Swaminathan, S. (2018). Continuous DNA replication is required for late gene transcription and maintenance of replication compartments in gammaherpesviruses. *PLoS Pathogens*, *14*(5), e1007070. doi:10.1371/journal.ppat.1007070

Li, G., Mongillo, M., Chin, K.-T., Harding, H., Ron, D., Marks, A. R., & Tabas, I. (2009). Role of ERO1-α–mediated stimulation of inositol 1,4,5-triphosphate receptor activity in endoplasmic reticulum stress–induced apoptosis. *The Journal of Cell Biology*, *186*(6), 783–792. doi:10.1083/jcb.200904060

Li, H., Komatsu, T., Dezube, B. J., & Kaye, K. M. (2002). The Kaposi's sarcoma-associated herpesvirus K12 transcript from a primary effusion lymphoma contains complex repeat elements, is spliced, and initiates from a novel promoter. *Journal of Virology*, *76*(23), 11880–11888. doi:10.1128/JVI.76.23.11880-11888.2002

Li, H., Zhu, H., Xu, C. J., & Yuan, J. (1998). Cleavage of BID by caspase 8 mediates the mitochondrial damage in the Fas pathway of apoptosis. *Cell*, *94*(4), 491–501. doi:10.1016/S0092-8674(00)81590-1

Li, M., Baumeister, P., Roy, B., Phan, T., Foti, D., Luo, S., & Lee, A. S. (2000). ATF6 as a transcription activator of the endoplasmic reticulum stress element: thapsigargin stress-induced changes and synergistic interactions with NF-Y and YY1. *Molecular and Cellular Biology*, *20*(14), 5096–5106.

Li, M., Lee, H., Yoon, D. W., Albrecht, J. C., Fleckenstein, B., Neipel, F., & Jung, J. U. (1997). Kaposi's sarcoma-associated herpesvirus encodes a functional cyclin. *Journal of Virology*, *71*(3), 1984–1991. doi:10.1097/00042560-199704010-00123

Li, S., Ye, L., Yu, X., Xu, B., Li, K., Zhu, X., … Kong, L. (2009). Hepatitis C virus NS4B induces unfolded protein response and endoplasmic reticulum overload response-dependent NF-kappaB activation. *Virology*, *391*(2), 257–264. doi:10.1016/j.virol.2009.06.039

Li, W., Avey, D., Fu, B., Wu, J., Ma, S., Liu, X., & Zhu, F. (2016). Kaposi's Sarcoma-

Associated Herpesvirus Inhibitor of cGAS (KicGAS), Encoded by ORF52, Is an Abundant Tegument Protein and Is Required for Production of Infectious Progeny Viruses. *Journal of Virology*, *90*(11), 5329–5342. doi:10.1128/JVI.02675-15

Li, W., Okreglak, V., Peschek, J., Kimmig, P., Zubradt, M., Weissman, J. S., & Walter, P. (2018). Engineering ER-stress dependent non-conventional mRNA splicing. *ELife*, *7*. doi:10.7554/eLife.35388

Li, X., Feng, J., & Sun, R. (2011). Oxidative stress induces reactivation of Kaposi's sarcoma-associated herpesvirus and death of primary effusion lymphoma cells. *Journal of Virology*, *85*(2), 715–724. doi:10.1128/JVI.01742-10

Liang, Q., Chang, B., Brulois, K. F., Castro, K., Min, C.-K., Rodgers, M. A., … Jung, J. U. (2013). Kaposi's sarcoma-associated herpesvirus K7 modulates Rubicon-mediated inhibition of autophagosome maturation. *Journal of Virology*, *87*(22), 12499–12503. doi:10.1128/JVI.01898-13

Liang, Y., Chang, J., Lynch, S. J., Lukac, D. M., & Ganem, D. (2002). The lytic switch protein of KSHV activates gene expression via functional interaction with RBP-Jkappa (CSL), the target of the Notch signaling pathway. *Genes & Development*, *16*(15), 1977–1989. doi:10.1101/gad.996502

Liao, W., Tang, Y., Lin, S.-F., Kung, H.-J., & Giam, C.-Z. (2003). K-bZIP of Kaposi's sarcoma-associated herpesvirus/human herpesvirus 8 (KSHV/HHV-8) binds KSHV/HHV-8 Rta and represses Rta-mediated transactivation. *Journal of Virology*, *77*(6), 3809–3815. doi:10.1128/JVI.77.6.3809-3815.2003

Lin, J. H., Li, H., Zhang, Y., Ron, D., & Walter, P. (2009). Divergent effects of PERK and IRE1 signaling on cell viability. *PLoS ONE*, *4*(1), 4170. doi:10.1371/journal.pone.0004170

Lin, K., & Gallay, P. (2013). Curing a viral infection by targeting the host: the example of cyclophilin inhibitors. *Antiviral Research*, *99*(1), 68–77. doi:10.1016/j.antiviral.2013.03.020

Lin, X., Li, X., Liang, D., & Lan, K. (2012). MicroRNAs and unusual small RNAs discovered in Kaposi's sarcoma-associated herpesvirus virions. *Journal of Virology*, *86*(23), 12717–12730. doi:10.1128/JVI.01473-12

Lindquist, S., & Craig, E. A. (1988). The Heat-Shock Proteins. *Annual Review of Genetics*, *22*(1), 631–677. doi:10.1146/annurev.ge.22.120188.003215

Liou, H. C., Boothby, M., & Glimcher, L. (1988). Distinct cloned class II MHC DNA binding proteins recognize the X box transcription element. *Science*, *242*(4875), 69–71. doi:10.1126/science.3140376

Liou, H. C., Boothby, M. R., Finn, P. W., Davidon, R., Nabavi, N., Zeleznik-Le, N. J., … Glimcher, L. H. (1990). A new member of the leucine zipper class of proteins that binds to the HLA DR alpha promoter. *Science*, *247*(4950), 1581–1584. doi:10.1126/science.2321018

Lipson, K. L., Fonseca, S. G., Ishigaki, S., Nguyen, L. X., Foss, E., Bortell, R., … Urano, F. (2006). Regulation of insulin biosynthesis in pancreatic beta cells by an endoplasmic reticulum-resident protein kinase IRE1. *Cell Metabolism*, *4*(3), 245–254. doi:10.1016/j.cmet.2006.07.007

Liu, D., Wang, Y., & Yuan, Y. (2018). Kaposi's sarcoma-associated herpesvirus K8 is an

RNA binding protein that regulates viral DNA replication in coordination with a noncoding RNA. *Journal of Virology*, *92*(7). doi:10.1128/JVI.02177-17

Liu, F., Zhou, F.h. (2007). Comparative virion structures of human herpesviruses. In A. Arvin, B. Roizman, E. Mocarski, G. Campadelli Fiume, K. Yamanishi, P.S. Moore, & R. Whitley. (Eds.), *Human herpesviruses: biology, therapy, and immunoprophylaxis*. Cambridge: Cambridge University Press. Retrieved from https://www.ncbi.nlm.nih.gov/books/NBK47399/

Liu, J., HuangFu, W.-C., Kumar, K. G. S., Qian, J., Casey, J. P., Hamanaka, R. B., … Fuchs, S. Y. (2009). Virus-induced unfolded protein response attenuates antiviral defenses via phosphorylation-dependent degradation of the Type I interferon receptor. *Cell Host & Microbe*, *5*(1), 72–83. doi:10.1016/j.chom.2008.11.008

Lu, M., Lawrence, D. A., Marsters, S., Acosta-Alvear, D., Kimmig, P., Mendez, A. S., … Ashkenazi, A. (2014). Opposing unfolded-protein-response signals converge on death receptor 5 to control apoptosis. *Science*, *345*(6192), 98–101. doi:10.1126/science.1254312

Lu, Y., Liang, F.-X., & Wang, X. (2014a). A synthetic biology approach identifies the mammalian UPR RNA ligase RtcB. *Molecular Cell*, *55*(5), 758–770. doi:10.1016/j.molcel.2014.06.032

Luitweiler, E. M., Henson, B. W., Pryce, E. N., Patel, V., Coombs, G., McCaffery, J. M., & Desai, P. J. (2013). Interactions of the Kaposi's sarcoma-associated herpesvirus nuclear egress complex: ORF69 is a potent factor for remodeling cellular membranes. *Journal of Virology*, *87*(7), 3915–3929. doi:10.1128/JVI.03418-12

Luka, J., Kallin, B., & Klein, G. (1979). Induction of the Epstein-Barr virus (EBV) cycle in latently infected cells by n-butyrate. *Virology*, *94*(1), 228–231. doi:10.1016/0042-6822(79)90455-0

Lukac, D. M., Renne, R., Kirshner, J. R., & Ganem, D. (1998). Reactivation of Kaposi's sarcoma-associated herpesvirus infection from latency by expression of the ORF 50 transactivator, a homolog of the EBV R protein. *Virology*, *252*(2), 304–312. doi:10.1006/VIRO.1998.9486

Luo, S., Baumeister, P., Yang, S., Abcouwer, S. F., & Lee, A. S. (2003). Induction of Grp78/BiP by translational block. *Journal of Biological Chemistry*, *278*(39), 37375–37385. doi:10.1074/jbc.M303619200

Ly, L. D., Xu, S., Choi, S.-K., Ha, C.-M., Thoudam, T., Cha, S.-K., … Park, K.-S. (2017). Oxidative stress and calcium dysregulation by palmitate in type 2 diabetes. *Experimental & Molecular Medicine*, *49*(2), e291. doi:10.1038/emm.2016.157

Ma, K., Vattem, K. M., & Wek, R. C. (2002). Dimerization and Release of Molecular Chaperone Inhibition Facilitate Activation of Eukaryotic Initiation Factor-2 Kinase in Response to Endoplasmic Reticulum Stress. *Journal of Biological Chemistry*, *277*(21), 18728–18735. doi:10.1074/jbc.M200903200

Ma, Q. (2013). Role of nrf2 in oxidative stress and toxicity. *Annual Review of Pharmacology and Toxicology*, *53*, 401–426. doi:10.1146/annurev-pharmtox-011112-140320

Ma, T., Trinh, M. A., Wexler, A. J., Bourbon, C., Gatti, E., Pierre, P., … Klann, E.

(2013). Suppression of eIF2α kinases alleviates Alzheimer's disease–related plasticity and memory deficits. *Nature Neuroscience*, *16*(9), 1299–1305. doi:10.1038/nn.3486

Ma, Y., Brewer, J. W., Alan Diehl, J., & Hendershot, L. M. (2002). Two distinct stress signaling pathways converge upon the CHOP promoter during the mammalian unfolded protein response. *Journal of Molecular Biology*, *318*(5), 1351–1365. doi:10.1016/S0022-2836(02)00234-6

Ma, Y., Shimizu, Y., Mann, M. J., Jin, Y., & Hendershot, L. M. (2010). Plasma cell differentiation initiates a limited ER stress response by specifically suppressing the PERK-dependent branch of the unfolded protein response. *Cell Stress & Chaperones*, *15*(3), 281–293. doi:10.1007/s12192-009-0142-9

Majerciak, V., Kruhlak, M., Dagur, P. K., McCoy, J. P., & Zheng, Z.-M. (2010). Caspase-7 cleavage of Kaposi sarcoma-associated herpesvirus ORF57 confers a cellular function against viral lytic gene expression. *Journal of Biological Chemistry*, *285*(15), 11297–11307. doi:10.1074/jbc.M109.068221

Majumder, M., Huang, C., Snider, M. D., Komar, A. A., Tanaka, J., Kaufman, R. J., … Hatzoglou, M. (2012). A novel feedback loop regulates the response to endoplasmic reticulum stress via the cooperation of cytoplasmic splicing and mRNA translation. *Molecular and Cellular Biology*, *32*(5), 992–1003. doi:10.1128/MCB.06665-11

Marciniak, S. J., Yun, C. Y., Oyadomari, S., Novoa, I., Zhang, Y., Jungreis, R., … Ron, D. (2004). CHOP induces death by promoting protein synthesis and oxidation in the stressed endoplasmic reticulum. *Genes & Development*, *18*(24), 3066–3077. doi:10.1101/gad.1250704

Marcora, M. S., Belfiori-Carrasco, L. F., Bocai, N. I., Morelli, L., & Castaño, E. M. (2017). Amyloid-β42 clearance and neuroprotection mediated by X-box binding protein 1 signaling decline with aging in the Drosophila brain. *Neurobiology of Aging*, *60*, 57–70. doi:10.1016/j.neurobiolaging.2017.08.012

Margariti, A., Li, H., Chen, T., Martin, D., Vizcay-Barrena, G., Alam, S., … Zeng, L. (2013). *XBP1* mRNA splicing triggers an autophagic response in endothelial cells through *BECLIN-1* transcriptional activation. *Journal of Biological Chemistry*, *288*(2), 859–872. doi:10.1074/jbc.M112.412783

Marissen, W. E., Guo, Y., Thomas, A. A., Matts, R. L., & Lloyd, R. E. (2000). Identification of caspase 3-mediated cleavage and functional alteration of eukaryotic initiation factor 2alpha in apoptosis. *The Journal of Biological Chemistry*, *275*(13), 9314–9323. doi:10.1074/JBC.275.13.9314

Martin, D. F., Kuppermann, B. D., Wolitz, R. A., Palestine, A. G., Li, H., & Robinson, C. A. (1999). Oral ganciclovir for patients with cytomegalovirus retinitis treated with a ganciclovir implant. *New England Journal of Medicine*, *340*(14), 1063–1070. doi:10.1056/NEJM199904083401402

Martin, D., Li, Y., Yang, J., Wang, G., Margariti, A., Jiang, Z., … Zeng, L. (2014). Unspliced X-box-binding protein 1 (XBP1) protects endothelial cells from oxidative stress through interaction with histone deacetylase 3. *The Journal of Biological Chemistry*, *289*(44), 30625–30634. doi:10.1074/jbc.M114.571984

Martínez, G., Vidal, R. L., Mardones, P., Inestrosa, N. C., Glimcher, L. H., & Correspondence, C. H. (2016). Regulation of memory formation by the transcription factor XBP1. *Cell Reports*, *14*, 1382–1394. doi:10.1016/j.celrep.2016.01.028

Martinez, S. C., Tanabe, K., Cras-Meneur, C., Abumrad, N. A., Bernal-Mizrachi, E., & Permutt, M. A. (2008). Inhibition of Foxo1 protects pancreatic islet β-cells against fatty acid and endoplasmic reticulum stress-induced apoptosis. *Diabetes*, *57*(4), 846–859. doi:10.2337/db07-0595

Martinon, F., Chen, X., Lee, A.-H., & Glimcher, L. H. (2010). TLR activation of the transcription factor XBP1 regulates innate immune responses in macrophages. *Nature Immunology*, *11*(5), 411–418. doi:10.1038/ni.1857

Massimelli, M. J., Majerciak, V., Kruhlak, M., & Zheng, Z.-M. (2013). Interplay between Polyadenylate-binding protein 1 and Kaposi's sarcoma-associated herpesvirus ORF57 in accumulation of polyadenylated nuclear RNA, a Viral Long Noncoding RNA. *Journal of Virology*, *87*(1), 243–256. doi:10.1128/JVI.01693-12

Matar, C. G., Rangaswamy, U. S., Wakeman, B. S., Iwakoshi, N., & Speck, S. H. (2014). Murine gammaherpesvirus 68 reactivation from B cells requires IRF4 but not XBP-1. *Journal of Virology*, *88*(19), 11600–11610. doi:10.1128/JVI.01876-14

Matolcsy, A., Nádor, R. G., Cesarman, E., & Knowles, D. M. (1998). Immunoglobulin VH gene mutational analysis suggests that primary effusion lymphomas derive from different stages of B cell maturation. *The American Journal of Pathology*, *153*(5), 1609–1614. doi:10.1016/S0002-9440(10)65749-5

Matsuyama, M., Suzuki, T., Tsuboi, H., Ito, S., Mamura, M., Goto, D., … Sumida, T. (2007). Anti-interleukin-6 receptor antibody (tocilizumab) treatment of multicentric Castleman's disease. *Internal Medicine (Tokyo, Japan)*, *46*(11), 771–774. doi:10.2169/internalmedicine.46.6262

Maurel, M., Chevet, E., Tavernier, J., & Gerlo, S. (2014). Getting RIDD of RNA: IRE1 in cell fate regulation. *Trends in Biochemical Sciences*, *39*(5), 245–254. doi:10.1016/j.tibs.2014.02.008

McCormick, C., & Ganem, D. (2005). The Kaposin B protein of KSHV activates the p38/MK2 pathway and stabilizes cytokine mRNAs. *Science*, *307*(5710), 739–741. doi:10.1126/science.1105779

McCullough, K. D., Martindale, J. L., Klotz, L. O., Aw, T. Y., & Holbrook, N. J. (2001). Gadd153 sensitizes cells to endoplasmic reticulum stress by down-regulating Bcl2 and perturbing the cellular redox state. *Molecular and Cellular Biology*, *21*(4), 1249–1259. doi:10.1128/MCB.21.4.1249-1259.2001

McEwen, E., Kedersha, N., Song, B., Scheuner, D., Gilks, N., Han, A., … Kaufman, R. J. (2005). Heme-regulated inhibitor kinase-mediated phosphorylation of eukaryotic translation initiation factor 2 inhibits translation, induces stress granule formation, and mediates survival upon arsenite exposure. *Journal of Biological Chemistry*, *280*(17), 16925–16933. doi:10.1074/jbc.M412882200

McGillivray, P., Ault, R., Pawashe, M., Kitchen, R., Balasubramanian, S., & Gerstein, M. (2018). A comprehensive catalog of predicted functional upstream open reading frames in humans. *Nucleic Acids Research*, *46*(7), 3326–3338.

doi:10.1093/nar/gky188

Mendez, A. S., Vogt, C., Bohne, J., & Glaunsinger, B. A. (2018). Site specific target binding controls RNA cleavage efficiency by the Kaposi's sarcoma-associated herpesvirus endonuclease SOX. *Nucleic Acids Research*, *46*(22), 11968–11979. doi:10.1093/nar/gky932

Mesri, E. A., Cesarman, E., & Boshoff, C. (2010). Kaposi's sarcoma and its associated herpesvirus. *Nature Reviews. Cancer*, *10*(10), 707–719. doi:10.1038/nrc2888

Mettenleiter, T. C. (2002). Herpesvirus assembly and egress. *Journal of Virology*, *76*(4), 1537–1547. doi:10.1128/JVI.76.4.1537-1547.2002

Meurs, E., Chong, K., Galabru, J., Thomas, N. S., Kerr, I. M., Williams, B. R., & Hovanessian, A. G. (1990). Molecular cloning and characterization of the human double-stranded RNA-activated protein kinase induced by interferon. *Cell*, *62*(2), 379–390.

Michalak, M., Robert Parker, J. M., & Opas, M. (2002). Ca2+ signaling and calcium binding chaperones of the endoplasmic reticulum. *Cell Calcium*, *32*(5–6), 269–278. doi:10.1016/S0143416002001884

Miller, M. (2009). The importance of being flexible: the case of basic region leucine zipper transcriptional regulators. *Current Protein & Peptide Science*, *10*(3), 244–269. doi:10.2174/138920309788452164

Mimura, N., Fulciniti, M., Gorgun, G., Tai, Y.-T., Cirstea, D., Santo, L., … Anderson, K. C. (2012). Blockade of XBP1 splicing by inhibition of IRE1α is a promising therapeutic option in multiple myeloma. *Blood*, *119*(24), 5772–5781. doi:10.1182/blood-2011-07-366633

Mogensen, T. H. (2009). Pathogen recognition and inflammatory signaling in innate immune defenses. *Clinical Microbiology Reviews*, *22*(2), 240–273. doi:10.1128/CMR.00046-08

Molden, J., Chang, Y., You, Y., Moore, P. S., & Goldsmith, M. A. (1997). A Kaposi's sarcoma-associated herpesvirus-encoded cytokine homolog (vIL-6) activates signaling through the shared gp130 receptor subunit. *The Journal of Biological Chemistry*, *272*(31), 19625–19631. doi:10.1074/jbc.272.31.19625

Mole, D. R., Blancher, C., Copley, R. R., Pollard, P. J., Gleadle, J. M., Ragoussis, J., & Ratcliffe, P. J. (2009). Genome-wide association of hypoxia-inducible factor (HIF)-1alpha and HIF-2alpha DNA binding with expression profiling of hypoxia-inducible transcripts. *The Journal of Biological Chemistry*, *284*(25), 16767–16775. doi:10.1074/jbc.M901790200

Montaner, S., Sodhi, A., Servitja, J.-M., Ramsdell, A. K., Barac, A., Sawai, E. T., & Gutkind, J. S. (2004). The small GTPase Rac1 links the Kaposi sarcoma-associated herpesvirus vGPCR to cytokine secretion and paracrine neoplasia. *Blood*, *104*(9), 2903–2911. doi:10.1182/blood-2003-12-4436

Montes-Moreno, S., Montalban, C., & Piris, M. A. (2012). Large B-cell lymphomas with plasmablastic differentiation: a biological and therapeutic challenge. *Leukemia & Lymphoma*, *53*(2), 185–194. doi:10.3109/10428194.2011.608447

Moore, P. S. (2007). KSHV manipulation of the cell cycle and apoptosis. In A. Arvin, B. Roizman, E. Mocarski, G. Campadelli Fiume, K. Yamanishi, P.S. Moore, & R.

Whitley. (Eds.), *Human herpesviruses: biology, therapy, and immunoprophylaxis*. Cambridge: Cambridge University Press. Retrieved from https://www.ncbi.nlm.nih.gov/books/NBK47432/

Moore, P. S., Boshoff, C., Weiss, R. A., & Chang, Y. (1996). Molecular mimicry of human cytokine and cytokine response pathway genes by KSHV. *Science*, *274*(5293), 1739–1744. doi:10.1126/science.274.5293.1739

Mori, K., Ma, W., Gething, M. J., & Sambrook, J. (1993). A transmembrane protein with a cdc2+/CDC28-related kinase activity is required for signaling from the ER to the nucleus. *Cell*, *74*(4), 743–756. doi:10.1016/0092-8674(93)90521-Q

Morishima, N., Nakanishi, K., Takenouchi, H., Shibata, T., & Yasuhiko, Y. (2002). An endoplasmic reticulum stress-specific caspase cascade in apoptosis. *Journal of Biological Chemistry*, *277*(37), 34287–34294. doi:10.1074/jbc.M204973200

Morris, D. R., & Geballe, A. P. (2000). Upstream open reading frames as regulators of mRNA translation. *Molecular and Cellular Biology*, *20*(23), 8635–8642. doi:10.1128/MCB.20.23.8635-8642.2000

Mueller, P. P., & Hinnebusch, A. G. (1986). Multiple upstream AUG codons mediate translational control of GCN4. *Cell*, *45*(2), 201–207. 10.1016/0092-8674(86)90384-3

Mukherjee, A., Morales-Scheihing, D., Butler, P. C., & Soto, C. (2015). Type 2 diabetes as a protein misfolding disease. *Trends in Molecular Medicine*, *21*(7), 439–449. doi:10.1016/j.molmed.2015.04.005

Muller, M., & Glaunsinger, B. A. (2017). Nuclease escape elements protect messenger RNA against cleavage by multiple viral endonucleases. *PLOS Pathogens*, *13*(8), e1006593. doi:10.1371/journal.ppat.1006593

Mulvey, M., Arias, C., & Mohr, I. (2006). Resistance of mRNA translation to acute endoplasmic reticulum stress-inducing agents in herpes simplex virus Type 1-infected cells requires multiple virus-encoded functions. *Journal of Virology*, *80*(15), 7354–7363. doi:10.1128/JVI.00479-06

Mulvey, M., Arias, C., & Mohr, I. (2007). Maintenance of endoplasmic reticulum (ER) homeostasis in herpes simplex virus type 1-infected cells through the association of a viral glycoprotein with PERK, a cellular ER stress sensor. *Journal of Virology*, *81*(7), 3377–3390. doi:10.1128/JVI.02191-06

Munro, S., & Pelham, H. R. B. (1986). An hsp70-like protein in the ER: Identity with the 78 kd glucose-regulated protein and immunoglobulin heavy chain binding protein. *Cell*, *46*(2), 291–300. doi:10.1016/0092-8674(86)90746-4

Muralidhar, S., Pumfery, A. M., Hassani, M., Sadaie, M. R., Kishishita, M., Brady, J. N., … Rosenthal, L. J. (1998). Identification of kaposin (open reading frame K12) as a human herpesvirus 8 (Kaposi's sarcoma-associated herpesvirus) transforming gene. *Journal of Virology*, *72*(6), 4980–4988. 10.1128/JVI.76.23.11880-11888.2002

Mutlu, A. D., Cavallin, L. E., Vincent, L., Chiozzini, C., Eroles, P., Duran, E. M., … Mesri, E. A. (2007). In Vivo-restricted and reversible malignancy induced by human herpesvirus-8 KSHV: a cell and animal model of virally induced Kaposi's sarcoma. *Cancer Cell*, *11*(3), 245–258. doi:10.1016/j.ccr.2007.01.015

Myoung, J., & Ganem, D. (2011a). Active lytic infection of human primary tonsillar B cells by KSHV and its noncytolytic control by activated CD4+ T cells. *The Journal of Clinical Investigation*, *121*(3), 1130–1140. doi:10.1172/JCI43755

Myoung, J., & Ganem, D. (2011b). Generation of a doxycycline-inducible KSHV producer cell line of endothelial origin: maintenance of tight latency with efficient reactivation upon induction. *Journal of Virological Methods*, *174*(1–2), 12–21. doi:10.1016/j.jviromet.2011.03.012

Myoung, J., & Ganem, D. (2011c). Infection of lymphoblastoid cell lines by Kaposi's sarcoma-associated herpesvirus: critical role of cell-associated virus. *Journal of Virology*, *85*(19), 9767. doi:10.1128/JVI.05136-11

Nadanaka, S., Okada, T., Yoshida, H., & Mori, K. (2007). Role of disulfide bridges formed in the luminal domain of ATF6 in sensing endoplasmic reticulum stress. *Molecular and Cellular Biology*, *27*(3), 1027–1043. doi:10.1128/MCB.00408-06

Nain, M., Mukherjee, S., Karmakar, S. P., Paton, A. W., Paton, J. C., Abdin, M. Z., … Vrati, S. (2017). GRP78 is an important host factor for japanese encephalitis virus entry and replication in mammalian cells. *Journal of Virology*, *91*(6). doi:10.1128/JVI.02274-16

Nakagawa, T., Zhu, H., Morishima, N., Li, E., Xu, J., Yankner, B. A., & Yuan, J. (2000). Caspase-12 mediates endoplasmic-reticulum-specific apoptosis and cytotoxicity by amyloid-β. *Nature*, *403*(6765), 98–103. doi:10.1038/47513

Nakamura, D., Tsuru, A., Ikegami, K., Imagawa, Y., Fujimoto, N., & Kohno, K. (2011). Mammalian ER stress sensor IRE1β specifically down-regulates the synthesis of secretory pathway proteins. *FEBS Letters*, *585*(1), 133–138. doi:10.1016/j.febslet.2010.12.002

Nakamura, H., Lu, M., Gwack, Y., Souvlis, J., Zeichner, S. L., & Jung, J. U. (2003a). Global changes in Kaposi's sarcoma-associated virus gene expression patterns following expression of a tetracycline-inducible Rta transactivator. *Journal of Virology*, *77*(7), 4205–4220. doi:10.1128/JVI.77.7.4205-4220.2003

Narita, M., Young, A. R. J., Arakawa, S., Samarajiwa, S. A., Nakashima, T., Yoshida, S., … Narita, M. (2011). Spatial coupling of mTOR and autophagy augments secretory phenotypes. *Science (New York, N.Y.)*, *332*(6032), 966–970. doi:10.1126/science.1205407

Nealon, K., Newcomb, W. W., Pray, T. R., Craik, C. S., Brown, J. C., & Kedes, D. H. (2001). Lytic replication of Kaposi's sarcoma-associated herpesvirus results in the formation of multiple capsid species: isolation and molecular characterization of A, B, and C capsids from a gammaherpesvirus. *Journal of Virology*, *75*(6), 2866. doi:10.1128/JVI.75.6.2866-2878.2001

Nikawa, J.-I., & Yamashita, S. (1992). IRE1 encodes a putative protein kinase containing a membrane-spanning domain and is required for inositol phototrophy in Saccharomyces cerevisiae. *Molecular Microbiology*, *6*(11), 1441–1446. doi:10.1111/j.1365-2958.1992.tb00864.x

Nikawa, J., Akiyoshi, M., Hirata, S., & Fukuda, T. (1996). Saccharomyces cerevisiae IRE2/HAC1 is involved in IRE1-mediated KAR2 expression. *Nucleic Acids Research*, *24*(21), 4222–4226. 10.1093/nar/24.21.4222

Nishimura, K., Ueda, K., Sakakibara, S., Do, E., Ohsaki, E., Okuno, T., & Yamanishi, K. (2003). A viral transcriptional activator of Kaposi's sarcoma-associated herpesvirus (KSHV) induces apoptosis, which is blocked in KSHV-infected cells. *Virology*, *316*(1), 64–74.

Nishitoh, H., Matsuzawa, A., Tobiume, K., Saegusa, K., Takeda, K., Inoue, K., … Ichijo, H. (2002). ASK1 is essential for endoplasmic reticulum stress-induced neuronal cell death triggered by expanded polyglutamine repeats. *Genes & Development*, *16*(11), 1345–1355. doi:10.1101/gad.992302

Niwa, M., Patil, C. K., DeRisi, J., & Walter, P. (2005). Genome-scale approaches for discovering novel nonconventional splicing substrates of the IRE1 nuclease. *Genome Biology*, *6*(1), R3. doi:10.1186/gb-2004-6-1-r3

Nojima, H., Leem, S.-H., Araki, H., Sakai, A., Nakashima, N., Kanaoka, Y., & Ono, Y. (1994). Hac1: A novel yeast bZIP protein binding to the CRE motif is a multicopy suppressor for cdcW mutant of Schizosaccharomyces pombe. *Nucleic Acids Research*, *22*(24), 5279–5288. doi:10.1093/nar/22.24.5279

Normington, K., Kohno, K., Kozutsumi, Y., Gething, M. J., & Sambrook, J. (1989). S. cerevisiae encodes an essential protein homologous in sequence and function to mammalian BiP. *Cell*, *57*(7), 1223–1236. doi:10.1016/0092-8674(89)90059-7

Novoa, I., Zeng, H., Harding, H. P., & Ron, D. (2001). Feedback inhibition of the unfolded protein response by GADD34-mediated dephosphorylation of eIF2alpha. *The Journal of Cell Biology*, *153*(5), 1011–1022. doi:10.1083/JCB.153.5.1011

Obeng, E. A., Carlson, L. M., Gutman, D. M., Harrington, W. J., Lee, K. P., Boise, L. H., & Boise, L. H. (2006). Proteasome inhibitors induce a terminal unfolded protein response in multiple myeloma cells. *Blood*, *107*(12), 4907–4916. doi:10.1182/blood-2005-08-3531

Oikawa, D., Tokuda, M., Hosoda, A., & Iwawaki, T. (2010). Identification of a consensus element recognized and cleaved by IRE1 alpha. *Nucleic Acids Research*, *38*(18), 6265–6273. doi:10.1093/nar/gkq452

Okada, T., Yoshida, H., Akazawa, R., Negishi, M., & Mori, K. (2002). Distinct roles of activating transcription factor 6 (ATF6) and double-stranded RNA-activated protein kinase-like endoplasmic reticulum kinase (PERK) in transcription during the mammalian unfolded protein response. *The Biochemical Journal*, *366*(Pt 2), 585–594. doi:10.1042/BJ20020391

Okamura, K., Kimata, Y., Higashio, H., Tsuru, A., & Kohno, K. (2000). Dissociation of Kar2p/BiP from an ER sensory molecule, Ire1p, triggers the unfolded protein response in yeast. *Biochemical and Biophysical Research Communications*, *279*(2), 445–450. doi:10.1006/bbrc.2000.3987

Olden, K., Pratt, R. M., Jaworski, C., & Yamada, K. M. (1979). Evidence for role of glycoprotein carbohydrates in membrane transport: specific inhibition by tunicamycin. *Proceedings of the National Academy of Sciences of the United States of America*, *76*(2), 791–795. doi:10.1073/pnas.76.2.791

Olivares, S., & Henkel, A. S. (2015). Hepatic XBP1 gene deletion promotes endoplasmic reticulum stress-induced liver injury and apoptosis. *The Journal of Biological*

Chemistry, *290*(50), 30142–30151. doi:10.1074/jbc.M115.676239

Ono, S. J., Liou, H. C., Davidon, R., Strominger, J. L., & Glimcher, L. H. (1991). Human X-box-binding protein 1 is required for the transcription of a subset of human class II major histocompatibility genes and forms a heterodimer with c-fos. *Proceedings of the National Academy of Sciences of the United States of America*, *88*(10), 4309–4312. doi:10.1073/PNAS.88.10.4309

Oslowski, C. M., Hara, T., O'Sullivan-Murphy, B., Kanekura, K., Lu, S., Hara, M., … Urano, F. (2012). Thioredoxin-interacting protein mediates ER stress-induced β cell death through initiation of the inflammasome. *Cell Metabolism*, *16*(2), 265–273. doi:10.1016/j.cmet.2012.07.005

Oyadomari, S., & Mori, M. (2004). Roles of CHOP/GADD153 in endoplasmic reticulum stress. *Cell Death and Differentiation*, *11*(4), 381–389. doi:10.1038/sj.cdd.4401373

Oyama, M., Kozuka-Hata, H., Suzuki, Y., Semba, K., Yamamoto, T., & Sugano, S. (2007). Diversity of translation start sites may define increased complexity of the human short ORFeome. *Molecular & Cellular Proteomics : MCP*, *6*(6), 1000–1006. doi:10.1074/mcp.M600297-MCP200

Ozcan, U., Cao, Q., Yilmaz, E., Lee, A.-H., Iwakoshi, N. N., Ozdelen, E., … Hotamisligil, G. S. (2004). Endoplasmic reticulum stress links obesity, insulin action, and type 2 diabetes. *Science (New York, N.Y.)*, *306*(5695), 457–461. doi:10.1126/science.1103160

Pakos-Zebrucka, K., Koryga, I., Mnich, K., Ljujic, M., Samali, A., & Gorman, A. M. (2016). The integrated stress response. *EMBO Reports*, *17*(10), 1374–1395. doi:10.15252/embr.201642195

Palam, L. R., Baird, T. D., & Wek, R. C. (2011). Phosphorylation of eIF2 facilitates ribosomal bypass of an inhibitory upstream ORF to enhance *CHOP* translation. *Journal of Biological Chemistry*, *286*(13), 10939–10949. doi:10.1074/jbc.M110.216093

Papa, F. R., Zhang, C., Shokat, K., & Walter, P. (2003). Bypassing a kinase activity with an ATP-competitive drug. *Science*, *302*(5650), 1533–1537. doi:10.1126/science.1090031

Park, J., Seo, T., Hwang, S., Lee, D., Gwack, Y., & Choe, J. (2000). The K-bZIP protein from Kaposi's sarcoma-associated herpesvirus interacts with p53 and represses its transcriptional activity. *Journal of Virology*, *74*(24), 11977–11982. doi:10.1128/JVI.74.24.11977-11982.2000

Parravicini, C., Chandran, B., Corbellino, M., Berti, E., Paulli, M., Moore, P. S., & Chang, Y. (2000). Differential viral protein expression in Kaposi's sarcoma-associated herpesvirus-infected diseases: Kaposi's sarcoma, primary effusion lymphoma, and multicentric Castleman's disease. *The American Journal of Pathology*, *156*(3), 743–749. doi:10.1016/S0002-9440(10)64940-1

Paton, A. W., Beddoe, T., Thorpe, C. M., Whisstock, J. C., Wilce, M. C. J., Rossjohn, J., … Paton, J. C. (2006). AB5 subtilase cytotoxin inactivates the endoplasmic reticulum chaperone BiP. *Nature*, *443*(7111), 548–552. doi:10.1038/nature05124

Pavio, N., Romano, P. R., Graczyk, T. M., Feinstone, S. M., & Taylor, D. R. (2003).

Protein synthesis and endoplasmic reticulum stress can be modulated by the hepatitis C virus envelope protein E2 through the eukaryotic initiation factor 2alpha kinase PERK. *Journal of Virology*, *77*(6), 3578–3585. doi:10.1128/JVI.77.6.3578-3585.2003

Pavitt, G. D., Ramaiah, K. V, Kimball, S. R., & Hinnebusch, A. G. (1998). eIF2 independently binds two distinct eIF2B subcomplexes that catalyze and regulate guanine-nucleotide exchange. *Genes & Development*, *12*(4), 514–526. doi:0.1101/gad.12.4.514

Pehar, M., Jonas, M. C., Hare, T. M., & Puglielli, L. (2012). SLC33A1/AT-1 Protein Regulates the Induction of Autophagy Downstream of IRE1/XBP1 Pathway. *Journal of Biological Chemistry*, *287*(35), 29921–29930. doi:10.1074/jbc.M112.363911

Peluso, R. W., Lamb, R. A., & Choppin, P. W. (1978). Infection with paramyxoviruses stimulates synthesis of cellular polypeptides that are also stimulated in cells transformed by Rous sarcoma virus or deprived of glucose. *Proceedings of the National Academy of Sciences of the United States of America*, *75*(12), 6120–6124. doi:10.1073/pnas.75.12.6120

Perkins, E. M., Anacker, D., Davis, A., Sankar, V., Ambinder, R. F., & Desai, P. (2008). Small capsid protein pORF65 is essential for assembly of Kaposi's sarcoma-associated herpesvirus capsids. *Journal of Virology*, *82*(14), 7201–7211. doi:10.1128/JVI.00423-08

Pillich, H., Loose, M., Zimmer, K.-P., & Chakraborty, T. (2012). Activation of the unfolded protein response by Listeria monocytogenes. *Cellular Microbiology*, *14*(6), 949–964. doi:10.1111/j.1462-5822.2012.01769.x

Pineau, L., Colas, J., Dupont, S., Beney, L., Fleurat-Lessard, P., Berjeaud, J.-M., … Ferreira, T. (2009). Lipid-Induced ER Stress: Synergistic Effects of Sterols and Saturated Fatty Acids. *Traffic*, *10*(6), 673–690. doi:10.1111/j.1600-0854.2009.00903.x

Plate, L., Cooley, C. B., Chen, J. J., Paxman, R. J., Gallagher, C. M., Madoux, F., … Kelly, J. W. (2016). Small molecule proteostasis regulators that reprogram the ER to reduce extracellular protein aggregation. *ELife*, *5*. doi:10.7554/eLife.15550

Plumb, R., Zhang, Z.-R., Appathurai, S., & Mariappan, M. (2015). A functional link between the co-translational protein translocation pathway and the UPR. *ELife*, *4*. doi:10.7554/eLife.07426

Polizzotto, M. N., Uldrick, T. S., Hu, D., & Yarchoan, R. (2012). Clinical manifestations of Kaposi sarcoma herpesvirus lytic activation: multicentric Castleman disease (KSHV-MCD) and the KSHV inflammatory cytokine syndrome. *Frontiers in Microbiology*, *3*, 73. doi:10.3389/fmicb.2012.00073

Polizzotto, M. N., Uldrick, T. S., Wang, V., Aleman, K., Wyvill, K. M., Marshall, V., … Yarchoan, R. (2013). Human and viral interleukin-6 and other cytokines in Kaposi sarcoma herpesvirus-associated multicentric Castleman disease. *Blood*, *122*(26), 4189–4198. doi:10.1182/blood-2013-08-519959

Polyak, S. J., Tang, N., Wambach, M., Barber, G. N., & Katze, M. G. (1996). The P58 cellular inhibitor complexes with the interferon-induced, double-stranded RNA-

dependent protein kinase, PKR, to regulate its autophosphorylation and activity. *The Journal of Biological Chemistry*, *271*(3), 1702–1707. doi:10.1074/jbc.271.3.1702

Poppers, J., Mulvey, M., Khoo, D., & Mohr, I. (2000). Inhibition of PKR activation by the proline-rich RNA binding domain of the herpes simplex virus type 1 Us11 protein. *Journal of Virology*, *74*(23), 11215–11221. doi:10.1128/JVI.74.23.11215-11221.2000

Pouysségur, J., Shiu, R. P., & Pastan, I. (1977). Induction of two transformation-sensitive membrane polypeptides in normal fibroblasts by a block in glycoprotein synthesis or glucose deprivation. *Cell*, *11*(4), 941–947. doi:10.1016/0092-8674(77)90305-1

Powley, I. R., Kondrashov, A., Young, L. A., Dobbyn, H. C., Hill, K., Cannell, I. G., … Willis, A. E. (2009). Translational reprogramming following UVB irradiation is mediated by DNA-PKcs and allows selective recruitment to the polysomes of mRNAs encoding DNA repair enzymes. *Genes & Development*, *23*(10), 1207–1220. doi:10.1101/gad.516509

Prasanthi, J. R. P., Larson, T., Schommer, J., & Ghribi, O. (2011). Silencing GADD153/CHOP gene expression protects against alzheimer's disease-like pathology induced by 27-hydroxycholesterol in rabbit hippocampus. *PLoS ONE*, *6*(10), e26420. doi:10.1371/journal.pone.0026420

Pria, A. D., Pinato, D., Roe, J., Naresh, K., Nelson, M., & Bower, M. (2017). Relapse of HHV8-positive multicentric Castleman disease following rituximab-based therapy in HIV-positive patients. *Blood*, *129*(15), 2143–2147. doi:10.1182/blood-2016-10-747477

Prischi, F., Nowak, P. R., Carrara, M., & Ali, M. M. U. (2014). Phosphoregulation of IRE1 RNase splicing activity. *Nature Communications*, *5*(1), 3554. doi:10.1038/ncomms4554

Promlek, T., Ishiwata-Kimata, Y., Shido, M., Sakuramoto, M., Kohno, K., & Kimata, Y. (2011). Membrane aberrancy and unfolded proteins activate the endoplasmic reticulum stress sensor IRE1 in different ways. *Molecular Biology of the Cell*, *22*(18), 3520–3532. doi:10.1091/mbc.E11-04-0295

Prostko, C. R., Brostrom, M. A., & Brostrom, C. O. (1993). Reversible phosphorylation of eukaryotic initiation factor 2 alpha in response to endoplasmic reticular signaling. *Molecular and Cellular Biochemistry*, *127–128*, 255–265. doi:10.1007/BF01076776

Purushothaman, P., Uppal, T., Sarkar, R., & Verma, S. C. (2016). KSHV-mediated angiogenesis in tumor progression. *Viruses*, *8*(7). doi:10.3390/v8070198

Puthalakath, H., O'Reilly, L. A., Gunn, P., Lee, L., Kelly, P. N., Huntington, N. D., … Strasser, A. (2007). ER stress triggers apoptosis by activating BH3-only protein bim. *Cell*, *129*(7), 1337–1349. doi:10.1016/j.cell.2007.04.027

Qian, Z., Xuan, B., Chapa, T. J., Gualberto, N., & Yu, D. (2012). Murine cytomegalovirus targets transcription factor ATF4 to exploit the unfolded-protein response. *Journal of Virology*, *86*(12), 6712–6723. doi:10.1128/JVI.00200-12

Qin, J., Li, W., Gao, S.-J., & Lu, C. (2017). KSHV microRNAs: tricks of the devil. *Trends in Microbiology*, *25*(8), 648–661. doi:10.1016/j.tim.2017.02.002

Qin, Q.-M., Pei, J., Ancona, V., Shaw, B. D., Ficht, T. A., & de Figueiredo, P. (2008). RNAi screen of endoplasmic reticulum-associated host factors reveals a role for IRE1alpha in supporting Brucella replication. *PLoS Pathogens*, *4*(7), e1000110. doi:10.1371/journal.ppat.1000110

Qiu, Q., Zheng, Z., Chang, L., Zhao, Y.-S., Tan, C., Dandekar, A., … Fang, D. (2013). Toll-like receptor-mediated IRE1α activation as a therapeutic target for inflammatory arthritis. *The EMBO Journal*, *32*(18), 2477–2490. doi:10.1038/emboj.2013.183

Ramalingam, D., & Ziegelbauer, J. M. (2017). Viral microRNAs target a gene network, inhibit STAT activation and suppress interferon responses. *Scientific Reports*, *7*(1), 40813. doi:10.1038/srep40813

Ramji, D. P., & Foka, P. (2002). CCAAT/enhancer-binding proteins: structure, function and regulation. *The Biochemical Journal*, *365*(Pt 3), 561–575. doi:10.1042/BJ20020508

Rathore, A. P. S., Ng, M.-L., & Vasudevan, S. G. (2013). Differential unfolded protein response during Chikungunya and Sindbis virus infection: CHIKV nsP4 suppresses eIF2α phosphorylation. *Virology Journal*, *10*(1), 36. doi:10.1186/1743-422X-10-36

Ray, P. D., Huang, B.-W., & Tsuji, Y. (2012). Reactive oxygen species (ROS) homeostasis and redox regulation in cellular signaling. *Cellular Signalling*, *24*(5), 981–990. doi:10.1016/j.cellsig.2012.01.008

Reimold, A. M., Etkin, A., Clauss, I., Perkins, A., Friend, D. S., Zhang, J., … Glimcher, L. H. (2000). An essential role in liver development for transcription factor XBP-1. *Genes & Development*, *14*(2), 152–157. doi:10.1101/gad.14.2.152

Reimold, A. M., Iwakoshi, N. N., Manis, J., Vallabhajosyula, P., Szomolanyi-Tsuda, E., Gravallese, E. M., … Glimcher, L. H. (2001). Plasma cell differentiation requires the transcription factor XBP-1. *Nature*, *412*(6844), 300–307. doi:10.1038/35085509

Reimold, A. M., Ponath, P. D., Li, Y. S., Hardy, R. R., David, C. S., Strominger, J. L., & Glimcher, L. H. (1996). Transcription factor B cell lineage-specific activator protein regulates the gene for human X-box binding protein 1. *The Journal of Experimental Medicine*, *183*(2), 393–401. doi:10.1084/jem.183.2.393

Reinke, A. W., Baek, J., Ashenberg, O., & Keating, A. E. (2013). Networks of bZIP protein-protein interactions diversified over a billion years of evolution. *Science (New York, N.Y.)*, *340*(6133), 730–734. doi:10.1126/science.1233465

Reith, W., Satola, S., Sanchez, C. H., Amaldi, I., Lisowska-Grospierre, B., Griscelli, C., … Mach, B. (1988). Congenital immunodeficiency with a regulatory defect in MHC class II gene expression lacks a specific HLA-DR promoter binding protein, RF-X. *Cell*, *53*(6), 897–906. doi:10.1016/S0092-8674(88)90389-3

Riggs, M. G., Whittaker, R. G., Neumann, J. R., & Ingram, V. M. (1977). n-Butyrate causes histone modification in HeLa and Friend erythroleukaemia cells. *Nature*, *268*(5619), 462–464. doi:10.1038/268462a0

Ritossa, F. (1962). A new puffing pattern induced by temperature shock and DNP in drosophila. *Experientia*, *18*(12), 571–573. doi:10.1007/BF02172188

Ron, D., & Habener, J.F. (1992). CHOP, a novel developmentally regulated nuclear protein that dimerizes with transcription factors C/EBP and LAP and functions as a dominant-negative inhibitor of gene transcription. *Genes & Development, 6,* 439-453. doi:10.1101/gad.6.3.439

Ron, D., & Walter, P. (2007). Signal integration in the endoplasmic reticulum unfolded protein response. *Nature Reviews Molecular Cell Biology*, *8*(7), 519–529. doi:10.1038/nrm2199

Rossetto, C. C., & Pari, G. (2012). KSHV PAN RNA Associates with Demethylases UTX and JMJD3 to Activate Lytic Replication through a Physical Interaction with the Virus Genome. *PLoS Pathogens*, *8*(5), e1002680. doi:10.1371/journal.ppat.1002680

Rossetto, C. C., & Pari, G. S. (2014). PAN's Labyrinth: Molecular biology of Kaposi's sarcoma-associated herpesvirus (KSHV) PAN RNA, a multifunctional long noncoding RNA. *Viruses*, *6*(11), 4212–4226. doi:10.3390/v6114212

Rossetto, C. C., Tarrant-Elorza, M., Verma, S., Purushothaman, P., & Pari, G. S. (2013). Regulation of viral and cellular gene expression by Kaposi's sarcoma-associated herpesvirus polyadenylated nuclear RNA. *Journal of Virology*, *87*(10), 5540–5553. doi:10.1128/JVI.03111-12

Roulston, A., Marcellus, R. C., & Branton, P. E. (1999). Viruses and apoptosis. *Annual Review of Microbiology*, *53*(1), 577–628. doi:10.1146/annurev.micro.53.1.577

Roussel, B. D., Kruppa, A. J., Miranda, E., Crowther, D. C., Lomas, D. A., & Marciniak, S. J. (2013). Endoplasmic reticulum dysfunction in neurological disease. *The Lancet Neurology*, *12*(1), 105–118. doi:10.1016/S1474-4422(12)70238-7

Roussou, I., Thireos, G., & Hauge, B. M. (1988). Transcriptional-translational regulatory circuit in Saccharomyces cerevisiae which involves the GCN4 transcriptional activator and the GCN2 protein kinase. *Molecular and Cellular Biology*, *8*(5), 2132–2139. doi:10.1128/MCB.8.5.2132

Roy, B., & Lee, A. S. (1999). The mammalian endoplasmic reticulum stress response element consists of an evolutionarily conserved tripartite structure and interacts with a novel stress-inducible complex. *Nucleic Acids Research*, *27*(6). doi:10.1093/nar/27.6.1437

Roy, C. R. (2005). Bacterial subversion of the host secretory pathway. *Proceedings of the National Academy of Sciences of the United States of America*, *102*(5), 1271–1272. doi:10.1073/pnas.0409531101

Rozen, R., Sathish, N., Li, Y., & Yuan, Y. (2008). Virion-wide protein interactions of Kaposi's sarcoma-associated herpesvirus. *Journal of Virology*, *82*(10), 4742–4750. doi:10.1128/JVI.02745-07

Rüegsegger, U., Leber, J. H., & Walter, P. (2001). Block of HAC1 mRNA translation by long-range base pairing is released by cytoplasmic splicing upon induction of the unfolded protein response. *Cell*, *107*(1), 103–114. doi:10.1016/S0092-8674(01)00505-0

Ruggiano, A., Foresti, O., & Carvalho, P. (2014). ER-associated degradation: Protein quality control and beyond. *The Journal of Cell Biology*, *204*(6), 869–879. doi:10.1083/jcb.201312042

Ruiz, A., Matute, C., & Alberdi, E. (2009). Endoplasmic reticulum Ca2+ release through ryanodine and IP3 receptors contributes to neuronal excitotoxicity. *Cell Calcium*, *46*(4), 273–281. doi:10.1016/j.ceca.2009.08.005

Russo, J. J., Bohenzky, R. A., Chien, M. C., Chen, J., Yan, M., Maddalena, D., … Moore, P. S. (1996). Nucleotide sequence of the Kaposi sarcoma-associated herpesvirus (HHV8). *Proceedings of the National Academy of Sciences of the United States of America*, *93*(25), 14862–14867. doi:10.1073/pnas.93.25.14862

Rutkowski, D. T., Arnold, S. M., Miller, C. N., Wu, J., Li, J., Gunnison, K. M., … Kaufman, R. J. (2006). Adaptation to ER stress is mediated by differential stabilities of pro-survival and pro-apoptotic mRNAs and proteins. *PLoS Biology*, *4*(11), e374. doi:10.1371/journal.pbio.0040374

Rutkowski, D. T., Kang, S.-W., Goodman, A. G., Garrison, J. L., Taunton, J., Katze, M. G., … Hegde, R. S. (2007). The role of p58IPK in protecting the stressed endoplasmic reticulum. *Molecular Biology of the Cell*, *18*(9), 3681–3691. doi:10.1091/mbc.e07-03-0272

Rzymski, T., Milani, M., Pike, L., Buffa, F., Mellor, H. R., Winchester, L., … Harris, A. L. (2010). Regulation of autophagy by ATF4 in response to severe hypoxia. *Oncogene*, *29*(31), 4424–4435. doi:10.1038/onc.2010.191

Sadler, R., Wu, L., Forghani, B., Renne, R., Zhong, W., Herndier, B., & Ganem, D. (1999). A complex translational program generates multiple novel proteins from the latently expressed kaposin (K12) locus of Kaposi's sarcoma-associated herpesvirus. *Journal of Virology*, *73*(7), 5722–5730. Retrieved from https://jvi.asm.org/content/73/7/5722.long

Saeed, M., Suzuki, R., Watanabe, N., Masaki, T., Tomonaga, M., Muhammad, A., … Suzuki, T. (2011). Role of the endoplasmic reticulum-associated degradation (ERAD) pathway in degradation of hepatitis C virus envelope proteins and production of virus particles. *Journal of Biological Chemistry*, *286*(43), 37264–37273. doi:10.1074/jbc.M111.259085

Saji, C., Higashi, C., Niinaka, Y., Yamada, K., Noguchi, K., & Fujimuro, M. (2011). Proteasome inhibitors induce apoptosis and reduce viral replication in primary effusion lymphoma cells. *Biochemical and Biophysical Research Communications*, *415*(4), 573–578. doi:10.1016/j.bbrc.2011.10.107

Sakakibara, S., & Tosato, G. (2011). Viral interleukin-6: role in Kaposi's sarcoma-associated herpesvirus: associated malignancies. *Journal of Interferon & Cytokine Research : The Official Journal of the International Society for Interferon and Cytokine Research*, *31*(11), 791–801. doi:10.1089/jir.2011.0043

Saltini, G., Dominici, R., Lovati, C., Cattaneo, M., Michelini, S., Malferrari, G., … Biunno, I. (2006). A novel polymorphism in SEL1L confers susceptibility to Alzheimer's disease. *Neuroscience Letters*, *398*(1–2), 53–58. doi:10.1016/j.neulet.2005.12.038

Sancak, Y., Bar-Peled, L., Zoncu, R., Markhard, A. L., Nada, S., & Sabatini, D. M. (2010). Ragulator-rag complex targets mTORC1 to the lysosomal surface and is necessary for its activation by amino acids. *Cell*, *141*(2), 290–303. doi:10.1016/j.cell.2010.02.024

Sandow, J. J., Dorstyn, L., O'Reilly, L. A., Tailler, M., Kumar, S., Strasser, A., & Ekert, P. G. (2014). ER stress does not cause upregulation and activation of caspase-2 to initiate apoptosis. *Cell Death & Differentiation*, *21*(3), 475–480. doi:10.1038/cdd.2013.168

Santoro, M. G. (2000). Heat shock factors and the control of the stress response. *Biochemical Pharmacology*, *59*(1), 55–63. doi:10.1016/S0006-2952(99)00299-3

Sathish, N., Wang, X., & Yuan, Y. (2012). Tegument proteins of Kaposi's sarcoma-associated herpesvirus and related gamma-herpesviruses. *Frontiers in Microbiology*, *3*, 98. doi:10.3389/fmicb.2012.00098

Sathish, N., Zhu, F. X., & Yuan, Y. (2009). Kaposi's sarcoma-associated herpesvirus ORF45 interacts with kinesin-2 transporting viral capsid-tegument complexes along microtubules. *PLoS Pathogens*, *5*(3), e1000332. doi:10.1371/journal.ppat.1000332

Sato, Y., Nadanaka, S., Okada, T., Okawa, K., & Mori, K. (2011). Luminal domain of ATF6 alone is sufficient for sensing endoplasmic reticulum stress and subsequent transport to the Golgi apparatus. *Cell Structure and Function*, *36*(1), 35–47. Retrieved from http://www.ncbi.nlm.nih.gov/pubmed/21150130

Sattler, C., Steer, B., & Adler, H. (2016). Multiple lytic origins of replication are required for optimal gammaherpesvirus fitness in vitro and in vivo. *PLOS Pathogens*, *12*(3), e1005510. doi:10.1371/journal.ppat.1005510

Schapansky, J., Olson, K., Van Der Ploeg, R., & Glazner, G. (2007). NF-κB activated by ER calcium release inhibits Aβ-mediated expression of CHOP protein: Enhancement by AD-linked mutant presenilin 1. *Experimental Neurology*, *208*(2), 169–176. doi:10.1016/j.expneurol.2007.04.009

Schindler, A. J., & Schekman, R. (2009). In vitro reconstitution of ER-stress induced ATF6 transport in COPII vesicles. *Proceedings of the National Academy of Sciences*, *106*(42), 17775–17780. doi:10.1073/pnas.0910342106

Sekine, Y., Zyryanova, A., Crespillo-Casado, A., Fischer, P. M., Harding, H. P., & Ron, D. (2015). Mutations in a translation initiation factor identify the target of a memory-enhancing compound. *Science*, *348*(6238), 1027–1030. doi:10.1126/science.aaa6986

Senft, D., & Ronai, Z. A. (2015). UPR, autophagy, and mitochondria crosstalk underlies the ER stress response. *Trends in Biochemical Sciences*, *40*(3), 141–148. doi:10.1016/j.tibs.2015.01.002

Sha, H., He, Y., Chen, H., Wang, C., Zenno, A., Shi, H., … Qi, L. (2009). Cell metabolism the IRE1a-XBP1 pathway of the unfolded protein response is required for adipogenesis. *Cell Metabolism*, *9*. doi:10.1016/j.cmet.2009.04.009

Shaffer, A. L., Lin, K.-I., Kuo, T. C., Yu, X., Hurt, E. M., Rosenwald, A., … Staudt, L. M. (2002). Blimp-1 orchestrates plasma cell differentiation by extinguishing the mature B cell gene expression program. *Immunity*, *17*(1), 51–62. doi:10.1016/S1074-7613(02)00335-7

Shaffer, A. L., Shapiro-Shelef, M., Iwakoshi, N. N., Lee, A.-H., Qian, S.-B., Zhao, H., … Staudt, L. M. (2004). XBP1, downstream of Blimp-1, expands the secretory apparatus and other organelles, and increases protein synthesis in plasma cell

differentiation. *Immunity*, *21*(1), 81–93. doi:10.1016/j.immuni.2004.06.010

Shaffer, A. L., Yu, X., He, Y., Boldrick, J., Chan, E. P., & Staudt, L. M. (2000). BCL-6 represses genes that function in lymphocyte differentiation, inflammation, and cell cycle control. *Immunity*, *13*(2), 199–212. doi:10.1016/S1074-7613(00)00020-0

Shamu, C. E., & Walter, P. (1996). Oligomerization and phosphorylation of the Ire1p kinase during intracellular signaling from the endoplasmic reticulum to the nucleus. *The EMBO Journal*, *15*(12), 3028–3039. doi:10.1002/j.1460-2075.1996.tb00666.x

Shannon-Lowe, C. D., Neuhierl, B., Baldwin, G., Rickinson, A. B., & Delecluse, H.-J. (2006). Resting B cells as a transfer vehicle for Epstein-Barr virus infection of epithelial cells. *Proceedings of the National Academy of Sciences of the United States of America*, *103*(18), 7065–7070. doi:10.1073/pnas.0510512103

Sharma, M., Bhattacharyya, S., Sharma, K. B., Chauhan, S., Asthana, S., Abdin, M. Z., … Kalia, M. (2017). Japanese encephalitis virus activates autophagy through XBP1 and ATF6 ER stress sensors in neuronal cells. *Journal of General Virology*, *98*(5), 1027–1039. doi:10.1099/jgv.0.000792

Sharma, R. B., O'Donnell, A. C., Stamateris, R. E., Ha, B., McCloskey, K. M., Reynolds, P. R., … Alonso, L. C. (2015). Insulin demand regulates β cell number via the unfolded protein response. *Journal of Clinical Investigation*, *125*(10), 3831–3846. doi:10.1172/JCI79264

Shen, J., Snapp, E. L., Lippincott-Schwartz, J., & Prywes, R. (2005). Stable Binding of ATF6 to BiP in the Endoplasmic Reticulum Stress Response. *Molecular and Cellular Biology*, *25*(3), 921–932. doi:10.1128/MCB.25.3.921-932.2005

Shi, Y., Vattem, K. M., Sood, R., An, J., Liang, J., Stramm, L., & Wek, R. C. (1998). Identification and characterization of pancreatic eukaryotic initiation factor 2 α-subunit kinase, PEK, involved in translational control. *Molecular and Cellular Biology*, *18*(12), 7499–7509. doi:10.1128/MCB.18.12.7499

Shin, H. J., DeCotiis, J., Giron, M., Palmeri, D., & Lukac, D. M. (2014). Histone deacetylase classes i and ii regulate Kaposi's sarcoma-associated herpesvirus reactivation. *Journal of Virology*, *88*(2), 1281–1292. doi:10.1128/JVI.02665-13

Shiu, R. P., Pouyssegur, J., Pastan, I. (1977). Glucose depletion accounts for the induction of two transformation-sensitive membrane proteinsin Rous sarcoma virus-transformed chick embryo fibroblasts. *Proceedings of the National Academy of Sciences of the United States of America*, 74(9), 3840-3844. doi:10.1073/pnas.74.9.3840

Shoulders, M. D., Ryno, L. M., Genereux, J. C., Moresco, J. J., Tu, P. G., Wu, C., … Wiseman, R. L. (2013). Stress-independent activation of XBP1s and/or ATF6 reveals three functionally diverse ER proteostasis environments. *Cell Reports*, *3*(4), 1279–1292. doi:10.1016/j.celrep.2013.03.024

Siddiquey, M. N. A., Zhang, H., Nguyen, C. C., Domma, A. J., & Kamil, J. P. (2018). The human cytomegalovirus endoplasmic reticulum-resident glycoprotein UL148 Activates the unfolded protein response. *Journal of Virology*, *92*(20). doi:10.1128/JVI.00896-18

Sidrauski, C., Acosta-Alvear, D., Khoutorsky, A., Vedantham, P., Hearn, B. R., Li, H., … Walter, P. (2013). Pharmacological brake-release of mRNA translation enhances cognitive memory. *ELife*, *2*, e00498. doi:10.7554/eLife.00498

Sidrauski, C., Cox, J. S., & Walter, P. (1996). tRNA ligase is required for regulated mRNA splicing in the unfolded protein response. *Cell*, *87*(3), 405–413. doi:10.1016/S0092-8674(00)81361-6

Sidrauski, C., McGeachy, A. M., Ingolia, N. T., & Walter, P. (2015). The small molecule ISRIB reverses the effects of eIF2α phosphorylation on translation and stress granule assembly. *ELife*, *4*. doi:10.7554/eLife.05033

Sidrauski, C., Tsai, J. C., Kampmann, M., Hearn, B. R., Vedantham, P., Jaishankar, P., … Walter, P. (2015). Pharmacological dimerization and activation of the exchange factor eIF2B antagonizes the integrated stress response. *ELife*, *4*, e07314. doi:10.7554/eLife.07314

Sidrauski, C., & Walter, P. (1997). The transmembrane kinase ire1p is a site-specific endonuclease that initiates mRNA splicing in the unfolded protein response. *Cell*, *90*(6), 1031–1039. doi:10.1016/S0092-8674(00)80369-4

Silva, R. M., Ries, V., Oo, T. F., Yarygina, O., Jackson-Lewis, V., Ryu, E. J., … Burke, R. E. (2005). CHOP/GADD153 is a mediator of apoptotic death in substantia nigra dopamine neurons in an in vivo neurotoxin model of parkinsonism. *Journal of Neurochemistry*, *95*(4), 974–986. doi:10.1111/j.1471-4159.2005.03428.x

Simonelli, C., Spina, M., Cinelli, R., Talamini, R., Tedeschi, R., Gloghini, A., … Tirelli, U. (2003). Clinical features and outcome of primary effusion lymphoma in HIV-infected patients: a single-institution study. *Journal of Clinical Oncology*, *21*(21), 3948–3954. doi:10.1200/JCO.2003.06.013

Sir, D., Chen, W., Choi, J., Wakita, T., Yen, T. S. B., & Ou, J. J. (2008). Induction of incomplete autophagic response by hepatitis C virus via the unfolded protein response. *Hepatology*, *48*(4), 1054–1061. doi:10.1002/hep.22464

Slavoff, S. A., Mitchell, A. J., Schwaid, A. G., Cabili, M. N., Ma, J., Levin, J. Z., … Saghatelian, A. (2013). Peptidomic discovery of short open reading frame–encoded peptides in human cells. *Nature Chemical Biology*, *9*(1), 59–64. doi:10.1038/nchembio.1120

Smith, J. A. (2014). A new paradigm: innate immune sensing of viruses via the unfolded protein response. *Frontiers in Microbiology*, *5*, 222. doi:10.3389/fmicb.2014.00222

Smith, J. A., Khan, M., Magnani, D. D., Harms, J. S., Durward, M., Radhakrishnan, G. K., … Splitter, G. A. (2013). Brucella induces an unfolded protein response via tcpb that supports intracellular replication in macrophages. *PLoS Pathogens*, *9*(12), e1003785. doi:10.1371/journal.ppat.1003785

Smith, J. A., Turner, M. J., DeLay, M. L., Klenk, E. I., Sowders, D. P., & Colbert, R. A. (2008). Endoplasmic reticulum stress and the unfolded protein response are linked to synergistic IFN-beta induction via X-box binding protein 1. *European Journal of Immunology*, *38*(5), 1194–1203. doi:10.1002/eji.200737882

Smith, W. W., Jiang, H., Pei, Z., Tanaka, Y., Morita, H., Sawa, A., … Ross, C. A. (2005). Endoplasmic reticulum stress and mitochondrial cell death pathways mediate

A53T mutant alpha-synuclein-induced toxicity. *Human Molecular Genetics*, *14*(24), 3801–3811. doi:10.1093/hmg/ddi396

So, J.-S., Hur, K. Y., Tarrio, M., Ruda, V., Frank-Kamenetsky, M., Fitzgerald, K., … Lee, A.-H. (2012). Silencing of lipid metabolism genes through IRE1α-mediated mRNA decay lowers plasma lipids in mice. *Cell Metabolism*, *16*(4), 487–499. doi:10.1016/j.cmet.2012.09.004

Sonenberg, N., & Hinnebusch, A. G. (2009). Regulation of translation initiation in eukaryotes: mechanisms and biological targets. *Cell*, *136*(4), 731–745. doi:10.1016/j.cell.2009.01.042

Song, B., Scheuner, D., Ron, D., Pennathur, S., & Kaufman, R. J. (2008). Chop deletion reduces oxidative stress, improves β cell function, and promotes cell survival in multiple mouse models of diabetes. *Journal of Clinical Investigation*, *118*(10), 3378–3389. doi:10.1172/JCI34587

Song, M., Sandoval, T. A., Chae, C.-S., Chopra, S., Tan, C., Rutkowski, M. R., … Cubillos-Ruiz, J. R. (2018). IRE1α–XBP1 controls T cell function in ovarian cancer by regulating mitochondrial activity. *Nature*, *562*(7727), 423–428. doi:10.1038/s41586-018-0597-x

Sood, R., Porter, A. C., Olsen, D. A., Cavener, D. R., & Wek, R. C. (2000). A mammalian homologue of GCN2 protein kinase important for translational control by phosphorylation of eukaryotic initiation factor-2alpha. *Genetics*, *154*(2), 787–801. Retrieved from http://www.ncbi.nlm.nih.gov/pubmed/10655230

Soulier, J., Grollet, L., Oksenhendler, E., Cacoub, P., Cazals-Hatem, D., Babinet, P., … Degos, L. (1995). Kaposi's sarcoma-associated herpesvirus-like DNA sequences in multicentric Castleman's disease. *Blood*, *86*(4), 1276–1280.

Speck, S. H., & Ganem, D. (2010). Viral latency and its regulation: lessons from the γ-herpesviruses. *Cell Host & Microbe*, *8*(1), 100–115. doi:10.1016/j.chom.2010.06.014

Sriburi, R., Jackowski, S., Mori, K., & Brewer, J. W. (2004). XBP1: a link between the unfolded protein response, lipid biosynthesis, and biogenesis of the endoplasmic reticulum. *The Journal of Cell Biology*, *167*(1), 35–41. doi:10.1083/jcb.200406136

Stahl, S., Burkhart, J. M., Hinte, F., Tirosh, B., Mohr, H., Zahedi, R. P., … Brune, W. (2013). Cytomegalovirus downregulates IRE1 to repress the unfolded protein response. *PLoS Pathogens*, *9*(8), e1003544. doi:10.1371/journal.ppat.1003544

Starck, S. R., Tsai, J. C., Chen, K., Shodiya, M., Wang, L., Yahiro, K., … Walter, P. (2016). Translation from the 5' untranslated region shapes the integrated stress response. *Science*, *351*(6272), aad3867-aad3867. doi:10.1126/science.aad3867

Staudt, M. R., & Dittmer, D. P. (2007). The Rta/Orf50 transactivator proteins of the gamma-herpesviridae. *Current Topics in Microbiology and Immunology*, *312*, 71–100. doi:10.1007/978-3-540-34344-8_3

Stürzl, M., Gaus, D., Dirks, W. G., Ganem, D., & Jochmann, R. (2013). Kaposi's sarcoma-derived cell line SLK is not of endothelial origin, but is a contaminant from a known renal carcinoma cell line. International Journal of Cancer, 132(8), 1954-1958. doi: 10.1002/ijc.27849

Su, A., Wang, H., Li, Y., Wang, X., Chen, D., & Wu, Z. (2017). Opposite roles of RNase and kinase activities of inositol-requiring enzyme 1 (IRE1) on HSV-1 replication. *Viruses*, *9*(9), 235. doi:10.3390/v9090235

Sun, R., Lin, S. F., Staskus, K., Gradoville, L., Grogan, E., Haase, A., & Miller, G. (1999). Kinetics of Kaposi's sarcoma-associated herpesvirus gene expression. *Journal of Virology*, *73*(3), 2232–2242. Retrieved from http://www.ncbi.nlm.nih.gov/pubmed/9971806

Sun, R., Lin, S. F., Gradoville, L., Yuan, Y., Zhu, F., & Miller, G. (1998). A viral gene that activates lytic cycle expression of Kaposi's sarcoma-associated herpesvirus. Proceedings of the National Academy of Sciences of the United States of America, 95(18), 10866-10871. doi:10.1073/pnas.95.18.10866

Surma, M. A., Klose, C., Peng, D., Shales, M., Mrejen, C., Stefanko, A., … Ernst, R. (2013). A lipid E-MAP identifies Ubx2 as a critical regulator of lipid saturation and lipid bilayer stress. *Molecular Cell*, *51*(4), 519–530. doi:10.1016/j.molcel.2013.06.014

Suthaus, J., Stuhlmann-Laeisz, C., Tompkins, V. S., Rosean, T. R., Klapper, W., Tosato, G., … Rose-John, S. (2012). HHV-8-encoded viral IL-6 collaborates with mouse IL-6 in the development of multicentric Castleman disease in mice. *Blood*, *119*(22), 5173–5181. doi:10.1182/blood-2011-09-377705

Swanton, C., Mann, D. J., Fleckenstein, B., Neipel, F., Peters, G., & Jones, N. (1997). Herpes viral cyclin/Cdk6 complexes evade inhibition by CDK inhibitor proteins. *Nature*, *390*(6656), 184–187. doi:10.1038/36606

Szabat, M., Page, M. M., Panzhinskiy, E., Skovsø, S., Mojibian, M., Fernandez-Tajes, J., … Johnson, J. D. (2016). reduced insulin production relieves endoplasmic reticulum stress and induces β cell proliferation. *Cell Metabolism*, *23*(1), 179–193. doi:10.1016/j.cmet.2015.10.016

Szegezdi, E., Logue, S. E., Gorman, A. M., & Samali, A. (2006). Mediators of endoplasmic reticulum stress-induced apoptosis. *EMBO Reports*, *7*(9), 880–885. doi:10.1038/sj.embor.7400779

Taguchi, Y., Imaoka, K., Kataoka, M., Uda, A., Nakatsu, D., Horii-Okazaki, S., … Murata, M. (2015). Yip1A, a novel host factor for the activation of the IRE1 pathway of the unfolded protein response during brucella infection. *PLOS Pathogens*, *11*(3), e1004747. doi:10.1371/journal.ppat.1004747

Tam, A. B., Koong, A. C., & Niwa, M. (2014). IRE1 has distinct catalytic mechanisms for XBP1/HAC1 splicing and RIDD. *Cell Reports*, *9*(3), 850–858. doi:10.1016/j.celrep.2014.09.016

Tam, A. B., Mercado, E. L., Hoffmann, A., & Niwa, M. (2012). ER stress activates NF-κB by integrating functions of basal IKK activity, IRE1 and PERK. *PLoS ONE*, *7*(10), e45078. doi:10.1371/journal.pone.0045078

Tam, A. B., Roberts, L. S., Chandra, V., Rivera, I. G., Nomura, D. K., Forbes, D. J., & Niwa, M. (2018). The UPR activator ATF6 responds to proteotoxic and lipotoxic stress by distinct mechanisms. *Developmental Cell*, *46*(3), 327–343.e7. doi:10.1016/j.devcel.2018.04.023

Tandon, R., Mocarski, E., & Conway, J. (2015). The A, B, Cs of herpesvirus capsids.

Viruses, *7*(3), 899–914. doi:10.3390/v7030899

Tang, C.-H. A., Chang, S., Paton, A. W., Paton, J. C., Gabrilovich, D. I., Ploegh, H. L., … Hu, C.-C. A. (2018). Phosphorylation of IRE1 at S729 regulates RIDD in B cells and antibody production after immunization. *The Journal of Cell Biology*, *217*(5), 1739–1755. doi:10.1083/jcb.201709137

Taniuchi, S., Miyake, M., Tsugawa, K., Oyadomari, M., & Oyadomari, S. (2016). Integrated stress response of vertebrates is regulated by four eIF2α kinases. *Scientific Reports*, *6*(1), 32886. doi:10.1038/srep32886

Tardif, K. D., Mori, K., Kaufman, R. J., & Siddiqui, A. (2004). Hepatitis C virus suppresses the IRE1-XBP1 pathway of the unfolded protein response. *The Journal of Biological Chemistry*, *279*(17), 17158–17164. doi:10.1074/jbc.M312144200

Tardif, K. D., Mori, K., & Siddiqui, A. (2002). Hepatitis C virus subgenomic replicons induce endoplasmic reticulum stress activating an intracellular signaling pathway. *Journal of Virology*, *76*(15), 7453–7459. doi:10.1128/JVI.76.15.7453-7459.2002

Tavernier, S. J., Osorio, F., Vandersarren, L., Vetters, J., Vanlangenakker, N., Van Isterdael, G., … Janssens, S. (2017). Regulated IRE1-dependent mRNA decay sets the threshold for dendritic cell survival. *Nature Cell Biology*, *19*(6), 698–710. doi:10.1038/ncb3518

Thakker, S., & Verma, S. C. (2016). Co-infections and pathogenesis of KSHV-associated malignancies. *Frontiers in Microbiology*, *7*, 151. doi:10.3389/fmicb.2016.00151

Thibault, G., Shui, G., Kim, W., McAlister, G. C., Ismail, N., Gygi, S. P., … Ng, D. T. W. (2012). The membrane stress response buffers lethal effects of lipid disequilibrium by reprogramming the protein homeostasis network. *Molecular Cell*, *48*(1), 16–27. doi:10.1016/j.molcel.2012.08.016

Thompson, D. J. (1993). A chemical hypothesis for arsenic methylation in mammals. *Chemico-Biological Interactions*, *88*(2–3), 89–14. doi:10.1016/0009-2797(93)90086-E

Thuerauf, D. J., Morrison, L., & Glembotski, C. C. (2004). Opposing roles for ATF6α and ATF6β in endoplasmic reticulum stress response gene induction. *Journal of Biological Chemistry*, *279*(20), 21078–21084. doi:10.1074/jbc.M400713200

Tirasophon, W., Welihinda, A. A., Kaufman, R. J. (1998). A stress response pathway from the endoplasmic reticulum to the nucleus requires a novel bifunctional protein kinase/endoribonuclease (Ire1p) in mammalian cells. *Genes & Development*, 12(12), 1812-1824. doi:10.1101/gad.12.12.1812

Todd, D. J., McHeyzer-Williams, L. J., Kowal, C., Lee, A.-H., Volpe, B. T., Diamond, B., … Glimcher, L. H. (2009). XBP1 governs late events in plasma cell differentiation and is not required for antigen-specific memory B cell development. *The Journal of Experimental Medicine*, *206*(10), 2151–2159. doi:10.1084/jem.20090738

Toth, Z., Maglinte, D. T., Lee, S. H., Lee, H.-R., Wong, L.-Y., Brulois, K. F., … Jung, J. U. (2010). Epigenetic analysis of KSHV latent and lytic genomes. *PLoS Pathogens*, *6*(7), e1001013. doi:10.1371/journal.ppat.1001013

Totonchy, J., Osborn, J. M., Chadburn, A., Nabiee, R., Argueta, L., Mikita, G., &

Cesarman, E. (2018). KSHV induces immunoglobulin rearrangements in mature B lymphocytes. *PLOS Pathogens*, *14*(4), e1006967. doi:10.1371/journal.ppat.1006967

Treacy-Abarca, S., & Mukherjee, S. (2015). Legionella suppresses the host unfolded protein response via multiple mechanisms. *Nature Communications*, *6*(1), 7887. doi:10.1038/ncomms8887

Trujillo-Alonso, V., Maruri-Avidal, L., Arias, C. F., & Lopez, S. (2011). Rotavirus infection induces the unfolded protein response of the cell and controls it through the nonstructural protein NSP3. *Journal of Virology*, *85*(23), 12594–12604. doi:10.1128/JVI.05620-11

Tsaytler, P., Harding, H. P., Ron, D., & Bertolotti, A. (2011). Selective inhibition of a regulatory subunit of protein phosphatase 1 restores proteostasis. *Science*, *332*(6025), 91–94. doi:10.1126/science.1201396

Tschurtschenthaler, M., Adolph, T. E., Ashcroft, J. W., Niederreiter, L., Bharti, R., Saveljeva, S., … Kaser, A. (2017). Defective ATG16L1-mediated removal of IRE1α drives Crohn's disease–like ileitis. *The Journal of Experimental Medicine*, *214*(2), 401–422. doi:10.1084/jem.20160791

Tsuchiya, Y., Saito, M., Kadokura, H., Miyazaki, J.-I., Tashiro, F., Imagawa, Y., … Kohno, K. (2018). IRE1-XBP1 pathway regulates oxidative proinsulin folding in pancreatic β cells. *The Journal of Cell Biology*, *217*(4), 1287–1301. doi:10.1083/jcb.201707143

Tsuru, A., Imai, Y., Saito, M., & Kohno, K. (2016). Novel mechanism of enhancing IRE1alpha-XBP1 signalling via the PERK-ATF4 pathway. *Scientific Reports*, *6*, 24217. doi:10.1038/srep24217

Tzamarias, D., Alexandraki, D., & Thireos, G. (1986). Multiple cis-acting elements modulate the translational efficiency of GCN4 mRNA in yeast. *Proceedings of the National Academy of Sciences of the United States of America*, *83*(13), 4849–4853. doi:10.1073/pnas.83.13.4849

Ubeda, M., & Habener, J. F. (2000). CHOP gene expression in response to endoplasmic-reticular stress requires NFY interaction with different domains of a conserved DNA-binding element. *Nucleic Acids Research*, *28*(24), 4987–4997. doi:10.1093/nar/28.24. 4987

Uppal, T., Banerjee, S., Sun, Z., Verma, S., & Robertson, E. (2014). KSHV LANA—The Master Regulator of KSHV Latency. *Viruses*, *6*(12), 4961–4998. doi:10.3390/v6124961

Upton, J.-P., Austgen, K., Nishino, M., Coakley, K. M., Hagen, A., Han, D., … Oakes, S. A. (2008). Caspase-2 cleavage of BID is a critical apoptotic signal downstream of endoplasmic reticulum stress. *Molecular and Cellular Biology*, *28*(12), 3943–3951. doi:10.1128/MCB.00013-08

Upton, J.-P., Wang, L., Han, D., Wang, E. S., Huskey, N. E., Lim, L., … Oakes, S. A. (2012). IRE1α cleaves select microRNAs during ER stress to derepress translation of proapoptotic Caspase-2. *Science (New York, N.Y.)*, *338*(6108), 818–822. doi:10.1126/science.1226191

Urano, F., Wang, X., Bertolotti, A., Zhang, Y., Chung, P., Harding, H. P., & Ron, D.

(2000). Coupling of stress in the ER to activation of JNK protein kinases by transmembrane protein kinase IRE1. *Science*, *287*(5453), 664–666. doi:10.1126/science.287.5453.664

van ‘t Wout, E. F. A., van Schadewijk, A., van Boxtel, R., Dalton, L. E., Clarke, H. J., Tommassen, J., … Hiemstra, P. S. (2015). Virulence factors of pseudomonas aeruginosa induce both the unfolded protein and integrated stress responses in airway epithelial cells. *PLOS Pathogens*, *11*(6), e1004946. doi:10.1371/journal.ppat.1004946

Vart, R. J., Nikitenko, L. L., Lagos, D., Trotter, M. W. B., Cannon, M., Bourboulia, D., … Boshoff, C. (2007). Kaposi’s sarcoma-associated herpesvirus-encoded interleukin-6 and G-protein-coupled receptor regulate angiopoietin-2 expression in lymphatic Endothelial cells. *Cancer Research*, *67*(9), 4042–4051. doi:10.1158/0008-5472.CAN-06-3321

Vattem, K. M., & Wek, R. C. (2004). Reinitiation involving upstream ORFs regulates ATF4 mRNA translation in mammalian cells. *Proceedings of the National Academy of Sciences of the United States of America*, *101*(31), 11269–11274. doi:10.1073/pnas.0400541101

Verma, S. C., Lan, K., & Robertson, E. (2007). Structure and function of latency-associated nuclear antigen. *Current Topics in Microbiology and Immunology*, *312*, 101–136. doi:10.1007/978-3-540-34344-8_4

Vidal, R. L., Figueroa, A., Court, F. A., Thielen, P., Molina, C., Wirth, C., … Hetz, C. (2012). Targeting the UPR transcription factor XBP1 protects against Huntington’s disease through the regulation of FoxO1 and autophagy. *Human Molecular Genetics*, *21*(10), 2245–2262. doi:10.1093/hmg/dds040

Vieira, J., & O’Hearn, P. M. (2004). Use of the red fluorescent protein as a marker of Kaposi’s sarcoma-associated herpesvirus lytic gene expression. *Virology*, *325*(2), 225–240. doi:10.1016/j.virol.2004.03.049

Volmer, R., van der Ploeg, K., & Ron, D. (2013). Membrane lipid saturation activates endoplasmic reticulum unfolded protein response transducers through their transmembrane domains. *Proceedings of the National Academy of Sciences*, *110*(12), 4628–4633. doi:10.1073/pnas.1217611110

von dem Bussche, A., Machida, R., Li, K., Loevinsohn, G., Khander, A., Wang, J., … Li, J. (2010). Hepatitis C virus NS2 protein triggers endoplasmic reticulum stress and suppresses its own viral replication. *Journal of Hepatology*, *53*(5), 797–804. doi:10.1016/J.JHEP.2010.05.022

Walter, P., & Ron, D. (2011). The unfolded protein response: from stress pathway to homeostatic regulation. *Science*, *334*(6059), 1081–1086. doi:10.1126/science.1209038

Wan, X., Wang, H., & Nicholas, J. (1999). Human herpesvirus 8 interleukin-6 (vIL-6) signals through gp130 but has structural and receptor-binding properties distinct from those of human IL-6. *Journal of Virology*, *73*(10), 8268–8278. Retrieved from http://www.ncbi.nlm.nih.gov/pubmed/10482577

Wang, F.-M., Chen, Y.-J., & Ouyang, H.-J. (2011). Regulation of unfolded protein response modulator XBP1s by acetylation and deacetylation. *Biochemical*

Journal, *433*(1), 245–252. doi:10.1042/BJ20101293

Wang, P., Li, J., Tao, J., & Sha, B. (2018). The luminal domain of the ER stress sensor protein PERK binds misfolded proteins and thereby triggers PERK oligomerization. *Journal of Biological Chemistry*, *293*(11), 4110–4121. doi:10.1074/jbc.RA117.001294

Wang, S., & Kaufman, R. J. (2012). The impact of the unfolded protein response on human disease. *The Journal of Cell Biology*, *197*(7), 857–867. doi:10.1083/jcb.201110131

Wang, X.-Z., Harding, H. P., Zhang, Y., Jolicoeur, E. M., Kuroda, M., & Ron, D. (1998). Cloning of mammalian IRE1 reveals diversity in the ER stress responses. *The EMBO Journal*, *17*(19), 5708–5717. doi:10.1093/emboj/17.19.5708

Wang, X., Zhu, N., Li, W., Zhu, F., Wang, Y., & Yuan, Y. (2015). Mono-ubiquitylated ORF45 mediates association of KSHV particles with internal lipid rafts for viral assembly and egress. *PLoS Pathogens*, *11*(12), e1005332. doi:10.1371/journal.ppat.1005332

Wang, Y., Alam, G. N., Ning, Y., Visioli, F., Dong, Z., Nör, J. E., & Polverini, P. J. (2012). The unfolded protein response induces the angiogenic switch in human tumor cells through the PERK/ATF4 pathway. *Cancer Research*, *72*(20), 5396–5406. doi:10.1158/0008-5472.CAN-12-0474

Wang, Y., Lu, X., Zhu, L., Shen, Y., Chengedza, S., Feng, H., … Feng, P. (2013). IKK epsilon kinase is crucial for viral G protein-coupled receptor tumorigenesis. *Proceedings of the National Academy of Sciences*, *110*(27), 11139–11144. doi:10.1073/pnas.1219829110

Wang, Y., Shen, J., Arenzana, N., Tirasophon, W., Kaufman, R. J., & Prywes, R. (2000). Activation of ATF6 and an ATF6 DNA binding site by the endoplasmic reticulum stress response. *The Journal of Biological Chemistry*, *275*(35), 27013–27020. doi:10.1074/jbc.M003322200

Wang, Y., Tang, Q., Maul, G. G., & Yuan, Y. (2006). Kaposi's sarcoma-associated herpesvirus ori-Lyt-dependent DNA replication: dual role of replication and transcription activator. *Journal of Virology*, *80*(24), 12171–12186. doi:10.1128/JVI.00990-06

Wang, Z. V., Deng, Y., Gao, N., Pedrozo, Z., Li, D. L., Morales, C. R., … Hill, J. A. (2014). Spliced X-Box binding protein 1 couples the unfolded protein response to hexosamine biosynthetic pathway. *Cell*, *156*(6), 1179–1192. doi:10.1016/J.CELL.2014.01.014

Wang, Z., Zhao, Y., & Zhang, Y. (2017). Viral lncRNA: A regulatory molecule for controlling virus life cycle. *Non-Coding RNA Research*, *2*(1), 38–44. doi:10.1016/j.ncrna.2017.03.002

Wek, R. C., Jackson, B. M., & Hinnebusch, A. G. (1989). Juxtaposition of domains homologous to protein kinases and histidyl-tRNA synthetases in GCN2 protein suggests a mechanism for coupling GCN4 expression to amino acid availability. *Proceedings of the National Academy of Sciences of the United States of America*, *86*(12), 4579–4583. doi:10.1073/pnas.86.12.4579

Welch, W. J. (1992). Mammalian stress response: cell physiology, structure/function of

stress proteins, and implications for medicine and disease. *Physiological Reviews*, *72*(4), 1063–1081. doi:10.1152/physrev.1992.72.4.1063

Welihinda, A. A., Kaufman, R. J. (1996). The unfolded protein response pathway in Saccharomyces cerevisiae. Oligomerization and trans-phosphorylation of Ire1p (Ern1p) are required for kinase activation. *Journal of Biological Chemistry*, 271(30), 18181-18187. doi:10.1074/jbc.271.30.18181

Wen, X. Y., Stewart, A. K., Sooknanan, R. R., Henderson, G., Hawley, T. S., Reimold, A. M., … Hawley, R. G. (1999). Identification of c-myc promoter-binding protein and X-box binding protein 1 as interleukin-6 target genes in human multiple myeloma cells. *International Journal of Oncology*, *15*(1), 173–178. doi:10.3892/ijo.15.1.173

Wies, E., Hahn, A. S., Schmidt, K., Viebahn, C., Rohland, N., Lux, A., … Neipel, F. (2009). The Kaposi's sarcoma-associated herpesvirus-encoded virf-3 inhibits cellular IRF-5. *Journal of Biological Chemistry*, *284*(13), 8525–8538. doi:10.1074/jbc.M809252200

Wilson, S. J., Tsao, E. H., Webb, B. L. J., Ye, H., Dalton-Griffin, L., Tsantoulas, C., … Kellam, P. (2007). X box binding protein XBP-1s transactivates the kaposi's sarcoma-associated herpesvirus (KSHV) ORF50 promoter, linking plasma cell differentiation to KSHV reactivation from latency. *Journal Of Virology*, *81*(24), 13578–13586. doi:10.1128/JVI.01663-07

Withers, J. B., Li, E. S., Vallery, T. K., Yario, T. A., & Steitz, J. A. (2018). Two herpesviral noncoding PAN RNAs are functionally homologous but do not associate with common chromatin loci. *PLOS Pathogens*, *14*(11), e1007389. doi:10.1371/journal.ppat.1007389

Wolfson, J. J., May, K. L., Thorpe, C. M., Jandhyala, D. M., Paton, J. C., & Paton, A. W. (2008). Subtilase cytotoxin activates PERK, IRE1 and ATF6 endoplasmic reticulum stress-signalling pathways. *Cellular Microbiology*, *10*(9), 1775–1786. doi:10.1111/j.1462-5822.2008.01164.x

Woo, C. W., Cui, D., Arellano, J., Dorweiler, B., Harding, H., Fitzgerald, K. A., … Tabas, I. (2009). Adaptive suppression of the ATF4–CHOP branch of the unfolded protein response by toll-like receptor signalling. *Nature Cell Biology*, *11*(12), 1473–1480. doi:10.1038/ncb1996

Woo, C. W., Kutzler, L., Kimball, S. R., & Tabas, I. (2012). Toll-like receptor activation suppresses ER stress factor CHOP and translation inhibition through activation of eIF2B. *Nature Cell Biology*, *14*(2), 192–200. doi:10.1038/ncb2408

Wu, F. Y., Ahn, J. H., Alcendor, D. J., Jang, W. J., Xiao, J., Hayward, S. D., & Hayward, G. S. (2001). Origin-independent assembly of Kaposi's sarcoma-associated herpesvirus DNA replication compartments in transient cotransfection assays and association with the ORF-K8 protein and cellular PML. *Journal of Virology*, *75*(3), 1487–1506. doi:10.1128/JVI.75.3.1487-1506.2001

Wu, J.-J., Avey, D., Li, W., Gillen, J., Fu, B., Miley, W., … Zhu, F. (2016). ORF33 and ORF38 of Kaposi's sarcoma-associated herpesvirus interact and are required for optimal production of infectious progeny viruses. *Journal of Virology*, *90*(4), 1741–1756. doi:10.1128/JVI.02738-15

Wu, J., Rutkowski, D. T., Dubois, M., Swathirajan, J., Saunders, T., Wang, J., … Kaufman, R. J. (2007). ATF6α optimizes long-term endoplasmic reticulum function to protect cells from chronic stress. *Developmental Cell*, *13*(3), 351–364. doi:10.1016/j.devcel.2007.07.005

Wu, Y.-P., Chang, C.-M., Hung, C.-Y., Tsai, M.-C., Schuyler, S. C., & Wang, R. Y.-L. (2011). Japanese encephalitis virus co-opts the ER-stress response protein GRP78 for viral infectivity. *Virology Journal*, *8*(1), 128. doi:10.1186/1743-422X-8-128

Xu, C., Bailly-Maitre, B., & Reed, J. C. (2005). Endoplasmic reticulum stress: cell life and death decisions. *The Journal of Clinical Investigation*, *115*(10), 2656–2664. doi:10.1172/JCI26373

Xu, Y., Rodriguez-Huete, A., & Pari, G. S. (2006). Evaluation of the lytic origins of replication of Kaposi's sarcoma-associated virus/human herpesvirus 8 in the context of the viral genome. *Journal of Virology*, *80*(19), 9905–9909. doi:10.1128/JVI.01004-06

Xuan, B., Qian, Z., Torigoi, E., & Yu, D. (2009). Human cytomegalovirus protein pUL38 induces ATF4 expression, inhibits persistent JNK phosphorylation, and suppresses endoplasmic reticulum stress-induced cell death. *Journal of Virology*, *83*(8), 3463–3474. doi:10.1128/JVI.02307-08

Yadav, R. K., Chae, S.-W., Kim, H.-R., & Chae, H. J. (2014). Endoplasmic reticulum stress and cancer. *Journal of Cancer Prevention*, *19*(2), 75–88. doi:10.15430/JCP.2014.19.2.75

Yamaguchi, H., & Wang, H.-G. (2004). CHOP is involved in endoplasmic reticulum stress-induced apoptosis by enhancing DR5 expression in human carcinoma cells. *The Journal of Biological Chemistry*, *279*(44), 45495–45502. doi:10.1074/jbc.M406933200

Yamamoto, K., Sato, T., Matsui, T., Sato, M., Okada, T., Yoshida, H., … Mori, K. (2007). Transcriptional induction of mammalian er quality control proteins is mediated by single or combined action of ATF6α and XBP1. *Developmental Cell*, *13*(3), 365–376. doi:10.1016/j.devcel.2007.07.018

Yamamoto, K., Yoshida, H., Kokame, K., Kaufman, R. J., & Mori, K. (2004). Differential contributions of ATF6 and XBP1 to the activation of endoplasmic reticulum stress-responsive cis-acting elements ERSE, UPRE and ERSE-II. *Journal of Biochemistry*, *136*(3), 343–350. doi:10.1093/jb/mvh122

Yan, W., Frank, C. L., Korth, M. J., Sopher, B. L., Novoa, I., Ron, D., & Katze, M. G. (2002). Control of PERK eIF2 kinase activity by the endoplasmic reticulum stress-induced molecular chaperone P58IPK. *Proceedings of the National Academy of Sciences*, *99*(25), 15920–15925. doi:10.1073/pnas.252341799

Yanagitani, K., Imagawa, Y., Iwawaki, T., Hosoda, A., Saito, M., Kimata, Y., & Kohno, K. (2009). Cotranslational targeting of XBP1 protein to the membrane promotes cytoplasmic splicing of its own mRNA. *Molecular Cell*, *34*(2), 191–200. doi:10.1016/J.MOLCEL.2009.02.033

Yanagitani, K., Kimata, Y., Kadokura, H., & Kohno, K. (2011). Translational pausing ensures membrane targeting and cytoplasmic splicing of XBP1u mRNA. *Science*, *331*(6017), 586–589. doi:10.1126/SCIENCE.1197142

Yang, L., Calay, E. S., Fan, J., Arduini, A., Kunz, R. C., Gygi, S. P., … Hotamisligil, G. S. (2015). METABOLISM. S-Nitrosylation links obesity-associated inflammation to endoplasmic reticulum dysfunction. *Science*, *349*(6247), 500–506. doi:10.1126/science.aaa0079

Yang, Q., & Sarnow, P. (1997). Location of the internal ribosome entry site in the 5' non-coding region of the immunoglobulin heavy-chain binding protein (BiP) mRNA: evidence for specific RNA-protein interactions. *Nucleic Acids Research*, *25*(14), 2800–2807. doi:10.1093/nar/25.14.2800

Yang, T., Espenshade, P. J., Wright, M. E., Yabe, D., Gong, Y., Aebersold, R., … Brown, M. S. (2002). Crucial step in cholesterol homeostasis: sterols promote binding of SCAP to INSIG-1, a membrane protein that facilitates retention of SREBPs in ER. *Cell*, *110*(4), 489–500. doi:10.1016/S0092-8674(02)00872-3

Yang, W.-S., Hsu, H.-W., Campbell, M., Cheng, C.-Y., & Chang, P.-C. (2015). K-bZIP mediated SUMO-2/3 specific modification on the KSHV genome negatively regulates lytic gene expression and viral reactivation. *PLOS Pathogens*, *11*(7), e1005051. doi:10.1371/journal.ppat.1005051

Yang, Z., Zhang, J., Jiang, D., Khatri, P., Solow-Cordero, D. E., Toesca, D. A. S., … Koong, A. C. (2018). A human genome-wide RNAi screen reveals diverse modulators that mediate IRE1α–XBP1 activation. *Molecular Cancer Research*, *16*(5), 745–753. doi:10.1158/1541-7786.MCR-17-0307

Yarchoan, R., & Davis, D. A. (2002). Development of Kaposi's sarcoma at the site of a biopsy. *New England Journal of Medicine*, *347*(10), 763–764. doi:10.1056/NEJM200209053471015

Ye, F.-C., Zhou, F.-C., Yoo, S. M., Xie, J.-P., Browning, P. J., & Gao, S.-J. (2004). Disruption of Kaposi's sarcoma-associated herpesvirus latent nuclear antigen leads to abortive episome persistence. *Journal of Virology*, *78*(20), 11121–11129. doi:10.1128/JVI.78.20.11121-11129.2004

Ye, F., Chen, E. R., & Nilsen, T. W. (2017). Kaposi's sarcoma-associated herpesvirus utilizes and manipulates RNA N^6-adenosine methylation to promote lytic replication. *Journal of Virology*, *91*(16). doi:10.1128/JVI.00466-17

Ye, F., Zhou, F., Bedolla, R. G., Jones, T., Lei, X., Kang, T., … Gao, S.-J. (2011). Reactive oxygen species hydrogen peroxide mediates Kaposi's sarcoma-associated herpesvirus reactivation from latency. *PLoS Pathogens*, *7*(5), e1002054. doi:10.1371/journal.ppat.1002054

Ye, J., Rawson, R. B., Komuro, R., Chen, X., Davé, U. P., Prywes, R., … Goldstein, J. L. (2000). ER stress induces cleavage of membrane-bound ATF6 by the same proteases that process SREBPs. *Molecular Cell*, *6*(6), 1355–1364. doi:10.1016/S1097-2765(00)00133-7

Yoneda, T., Imaizumi, K., Oono, K., Yui, D., Gomi, F., Katayama, T., & Tohyama, M. (2001). Activation of caspase-12, an endoplastic reticulum (ER) resident caspase, through tumor necrosis factor receptor-associated factor 2-dependent mechanism in response to the ER stress. *The Journal of Biological Chemistry*, *276*(17), 13935–13940. doi:10.1074/jbc.M010677200

Yoshida, H., Haze, K., Yanagi, H., Yura, T., & Mori, K. (1998). Identification of the cis-

acting endoplasmic reticulum stress response element responsible for transcriptional induction of mammalian glucose-regulated proteins. Involvement of basic leucine zipper transcription factors. *Journal of Biological Chemistry*, 273(50), 33741-33749.doi:10.1074/jbc.273.50.33741

Yoshida, H., Matsui, T., Yamamoto, A., Okada, T., & Mori, K. (2001). XBP1 mRNA is induced by ATF6 and spliced by IRE1 in response to ER stress to produce a highly active transcription factor. *Cell*, 107(7), 881-891. doi:doi:10.1016/S0092-8674(01)00611-0

Yoshida, H., Okada, T., Haze, K., Yanagi, H., Yura, T., Negishi, M., & Mori, K. (2000). ATF6 activated by proteolysis binds in the presence of NF-Y (CBF) directly to the cis-acting element responsible for the mammalian unfolded protein response. *Molecular and Cellular Biology*, *20*(18), 6755–6767. doi:10.1128/MCB.20.18.6755-6767.2000

Yoshida, H., Okada, T., Haze, K., Yanagi, H., Yura, T., Negishi, M., & Mori, K. (2001). Endoplasmic reticulum stress-induced formation of transcription factor complex ersf including NF-Y (CBF) and activating transcription factors 6 and 6 that activates the mammalian unfolded protein response. *Molecular and Cellular Biology*, *21*(4), 1239–1248. doi:10.1128/MCB.21.4.1239-1248.2001

Yoshida, H., Oku, M., Suzuki, M., & Mori, K. (2006). pXBP1(U) encoded in XBP1 pre-mRNA negatively regulates unfolded protein response activator pXBP1(S) in mammalian ER stress response. *Journal of Cell Biology*, *172*(4), 565–575. doi:10.1083/JCB.200508145

Young, S. K., & Wek, R. C. (2016). Upstream open reading frames differentially regulate gene-specific translation in the integrated stress response. *Journal of Biological Chemistry*, *291*(33), 16927–16935. doi:10.1074/jbc.R116.733899

Yu, C.-Y., Hsu, Y.-W., Liao, C.-L., & Lin, Y.-L. (2006). Flavivirus infection activates the XBP1 pathway of the unfolded protein response to cope with endoplasmic reticulum stress. *Journal of Virology*, *80*(23), 11868–11880. doi:10.1128/JVI.00879-06

Yu, F., Feng, J., Harada, J. N., Chanda, S. K., Kenney, S. C., & Sun, R. (2007). B cell terminal differentiation factor XBP-1 induces reactivation of Kaposi's sarcoma-associated herpesvirus. *FEBS Letters*, *581*(18), 3485–3488. doi:10.1016/j.febslet.2007.06.056

Yu, Y., Pierciey, F. J., Maguire, T. G., & Alwine, J. C. (2013). PKR-like endoplasmic reticulum kinase is necessary for lipogenic activation during HCMV infection. *PLoS Pathogens*, *9*(4), e1003266. doi:10.1371/journal.ppat.1003266

Yu, Y., Wang, S. E., & Hayward, G. S. (2005). The KSHV immediate-early transcription factor rta encodes ubiquitin E3 ligase activity that targets IRF7 for proteosome-mediated degradation. *Immunity*, *22*(1), 59–70. doi:10.1016/j.immuni.2004.11.011

Zhan, K., Narasimhan, J., & Wek, R. C. (2004). Differential activation of eIF2 kinases in response to cellular stresses in *Schizosaccharomyces pombe*. *Genetics*, *168*(4), 1867–1875. doi:10.1534/genetics.104.031443

Zhan, K., Vattem, K. M., Bauer, B. N., Dever, T. E., Chen, J.-J., & Wek, R. C. (2002).

Phosphorylation of eukaryotic initiation factor 2 by heme-regulated inhibitor kinase-related protein kinases in Schizosaccharomyces pombe is important for resistance to environmental stresses. *Molecular and Cellular Biology*, *22*(20), 7134–7146. doi:10.1128/MCB.22.20.7134-7146.2002

Zhang, G., Chan, B., Samarina, N., Abere, B., Weidner-Glunde, M., Buch, A., … Schulz, T. F. (2016). Cytoplasmic isoforms of Kaposi sarcoma herpesvirus LANA recruit and antagonize the innate immune DNA sensor cGAS. *Proceedings of the National Academy of Sciences*, *113*(8), E1034–E1043. doi:10.1073/pnas.1516812113

Zhang, J., He, S., Wang, Y., Brulois, K., Lan, K., Jung, J. U., & Feng, P. (2015). Herpesviral G protein-coupled receptors activate NFAT to induce tumor formation via inhibiting the SERCA calcium ATPase. *PLoS Pathogens*, *11*(3), e1004768. doi:10.1371/journal.ppat.1004768

Zhang, K., Shen, X., Wu, J., Sakaki, K., Saunders, T., Rutkowski, D. T., … Kaufman, R. J. (2006). endoplasmic reticulum stress activates cleavage of CREBH to induce a systemic inflammatory response. *Cell*, *124*(3), 587–599. doi:10.1016/j.cell.2005.11.040

Zhang, K., Wong, H. N., Song, B., Miller, C. N., Scheuner, D., & Kaufman, R. J. (2005). The unfolded protein response sensor IRE1α is required at 2 distinct steps in B cell lymphopoiesis. *Journal of Clinical Investigation*, *115*(2), 268–281. doi:10.1172/JCI21848

Zhang, P., McGrath, B. C., Reinert, J., Olsen, D. S., Lei, L., Gill, S., … Cavener, D. R. (2002). The GCN2 eIF2alpha kinase is required for adaptation to amino acid deprivation in mice. *Molecular and Cellular Biology*, *22*(19), 6681–6688. doi:10.1128/MCB.22.19.6681-6688.2002

Zhang, Y., Liu, R., Ni, M., Gill, P., & Lee, A. S. (2010). Cell surface relocalization of the endoplasmic reticulum chaperone and unfolded protein response regulator GRP78/BiP. *The Journal of Biological Chemistry*, *285*(20), 15065–15075. doi:10.1074/jbc.M109.087445

Zhao, Y., Li, X., Cai, M.-Y., Ma, K., Yang, J., Zhou, J., … Zhu, W.-G. (2013). XBP-1u suppresses autophagy by promoting the degradation of FoxO1 in cancer cells. *Cell Research*, *23*(4), 491–507. doi:10.1038/cr.2013.2

Zhou, J., Liu, Y., Back, S. H., Clark, R. L., Peisach, D., Xu, Z., & Kaufman, R. J. (2006). The crystal structure of human IRE1 luminal domain reveals a conserved dimerization interface required for activation of the unfolded protein response. *Source*, *103*(39), 14343–14348. doi:10.1073/pnas.0606480103

Zhou, J., Wan, J., Shu, X. E., Mao, Y., Liu, X.-M., Yuan, X., … Qian, S.-B. (2018). N6-Methyladenosine guides mRNA alternative translation during integrated stress response. *Molecular Cell*, *69*(4), 636–647.e7. doi:10.1016/J.MOLCEL.2018.01.019

Zhou, Y., Lee, J., Reno, C. M., Sun, C., Park, S. W., Chung, J., … Ozcan, U. (2011). Regulation of glucose homeostasis through a XBP-1–FoxO1 interaction. *Nature Medicine*, *17*(3), 356–365. doi:10.1038/nm.2293

Zhu, C., Johansen, F. E., & Prywes, R. (1997). Interaction of ATF6 and serum response

factor. *Molecular and Cellular Biology*, *17*(9), 4957–4966. doi:10.1128/MCB.17.9.4957

Zhu, F. X., Cusano, T., & Yuan, Y. (1999). Identification of the immediate-early transcripts of Kaposi's sarcoma-associated herpesvirus. *Journal of Virology*, *73*(7), 5556–5567. Retrieved from http://www.ncbi.nlm.nih.gov/pubmed/10364304

Zhu, F. X., & Yuan, Y. (2003). The ORF45 protein of Kaposi's sarcoma-associated herpesvirus is associated with purified virions. *Journal of Virology*, *77*(7), 4221–4230. doi:10.1128/JVI.77.7.4221-4230.2003

Zyryanova, A. F., Weis, F., Faille, A., Akeel, †, Alard, A., Crespillo-Casado, A., … Ron, D. (2018). Binding of ISRIB reveals a regulatory site in the nucleotide exchange factor eIF2B. *Science*, *359*(6383), 1533-1536. doi:10.1126/science.aar5129

APPENDIX A THE ISR PROMOTES ACTIVATION OF THE IRE1-XBP1 PATHWAY

Introduction

Proteins translated in the ER need to be folded correctly to be functional. The ER proteostasis network is a highly regulated process that aims to prevent protein misfolding by balancing the protein load with the ER folding capacity (Klaips et al., 2018). This is largely achieved through a network of enzymes that promote folding and degrade terminally misfolded or aggregated proteins through ERAD and autophagy. However, severe changes in physiology or exposure to stressful environmental factors, can shift this balance and results in an accumulation of misfolded proteins, which is called ER stress. ER stress sensors become activated and mount the unfolded protein response (UPR) (Walter & Ron, 2011). Central to this response is the highly conserved transmembrane protein IRE1, which undergoes *trans*-autophosphorylation and activation through oligomerization. Activated IRE1 excises an intron of XBP1 mRNA in the cytoplasm. mRNA re-ligation by the tRNA ligase RtcB enables a translational frameshift generating the active transcription factor XBP1s.

The regulation of XBP1/Hac1 splicing is very different in yeast and metazoan cells. In the case of yeast, the Hac1 intron, which is 252-nt long (compared to 26-nt in mammals) can interact with the 5'-UTR and block translation (Rüegsegger, Leber, & Walter, 2001). Inhibition of translation promotes the recruitment of Hac1 mRNA to oligomerized IRE1 through an interaction with a bipartite element in the 3'-UTR (Aragón et al., 2008).

Conversely, in mammalian cells XBP1 splicing dependent on its translation. Translation of unspliced XBP1 (XBP1u) protein causes ribosomal pausing at a domain near the C-terminus (Yanagitani et al., 2011). Upstream of this domain is a hydrophobic region (HR) and translational pausing enables HR binding to the signal recognition particle (SRP) (Kanda et al., 2016; Yanagitani et al., 2009). SRP subsequently translocates the ribosome-bound XBP1u nascent chain to the ER. The HR interacts with the Sec61 translocon as a pseudo-transmembrane domain. IRE1 also binds to the Sec61 translocon, bringing it into close proximity with the translating XBP1 mRNA for intron excision (Plumb et al., 2015). However, when IRE1 is inactive in the absence of ER stress, XBP1u protein is quickly degraded by the proteasome due to the presence of a degradation domain at the C-terminus (Yoshida et al., 2006).

There have been multiple studies showing that XBP1u protein may have functions other than controlling splicing, but this is somewhat unclear due to its short half-like (~ 11 minutes) and low expression (Calfon et al., 2002). Furthermore, the expression levels of XBP1u in the absence of ER stress likely need to be minimal to prevent aberrant mRNA splicing, since multiple groups have observed that overexpression of XBP1u results in splicing and translation of XBP1s (Calfon et al., 2002; K. Lee et al., 2002; Yoshida et al., 2001). Therefore, XBP1 expression needs to be tightly regulated.

The mechanisms that regulate XBP1 expression to prevent spontaneous XBP1 mRNA splicing are not well understood, but it is becoming apparent that the other two arms of the UPR (PERK and ATF6) are likely involved. Yoshida *et al.* (2001) first identified that XBP1 was spliced by IRE1 and they demonstrated that the XBP1 mRNA levels were the rate limiting factor that controls splicing. They showed that ATF6 can transcriptionally upregulate XBP1, which provides more template for translation of XBP1u. Therefore, ATF6 promotes XBP1 splicing through upregulation of XBP1 mRNA.

In another initial study of XBP1 mRNA splicing, David Ron's lab observed that PERK knockout MEFs expressed less XBP1s than wild type MEFs following exposure to ER stress (Calfon et al., 2002). Consistently, Majumder *et al*. (2012) showed that activation of the ISR also promotes XBP1s protein accumulation by stabilizing XBP1s mRNA. They further showed that this was specific to spliced XBP1 mRNA, as they observed no significant changes to XBP1u mRNA half-life following exposure to ER stress. As previously mentioned, XBP1u protein is also highly unstable. Since XBP1u translation is required for its splicing, in the absence of ER stress, the labile XBP1u mRNA and/or protein may reduce the chance of interaction with IRE1, which would prevent spontaneous splicing. Following ER stress, enhanced XBP1u translation or increases in mRNA levels and/or stability may supersede this inhibitory effect of unstable XBP1u to promote robust XBP1 splicing. The ISR has also been shown to influence XBP1 splicing through ATF4 transcriptional upregulation of IRE1 (Tsuru et al., 2016). It is therefore possible that this increase in IRE1 levels promotes IRE1 oligomerization for enhanced recruitment and splicing of XBP1.

In contrast to these studies, others have found that the ISR can attenuate XBP1 splicing. T.-K. Chang *et al.* (2018) reported that inhibition of PERK or treatment with the

small molecule ISRIB (ISR inhibitor) resulted in enhanced XBP1 mRNA splicing and XBP1s protein levels. They demonstrated that PERK-dependent activation of the phosphatase RPAP2 dephosphorylated IRE1, resulting in the attenuation of XBP1 mRNA splicing. It has also been reported that PERK can reduce XBP1 expression through activation of the microRNA mIR-30c-2*, which binds to the 3'UTR of XBP1 mRNA (Byrd et al., 2012). Whereas, these data show that the ISR can inhibit XBP1 activation, still other have reported that inhibiting the ISR had no impact on XBP1 activation (Sidrauski et al., 2013). Clearly, more clarification is needed to explain the conflicting results of the role of the ISR in the IRE1-XBP1 pathway.

This thesis focused on investigating the modulation of the UPR by KSHV during lytic replication. I found that the transcription factors ATF6-N, XBP1s, and ATF4 are inhibited despite activation of the upstream sensors. Due to the increasing evidence that there is crosstalk between these branches, I began investigating how the ISR plays a role in IRE1 activation of XBP1 in uninfected cells. I confirmed previous studies that PERK activation is required for maximum XBP1 splicing following ER stress. I also discovered that activation of the ISR, regardless of the eIF2α kinase involved, resulted in the accumulation of XBP1u protein and this increase in XBP1u may in part be dependent on ATF4, since ATF4 ectopic expression promoted both IRE1 and XBP1u expression. In response to increased eIF2α phosphorylation, mRNAs that encode stress responsive factors, such as ATF4, are preferentially translated due to the presence of uORFs in their 5'UTR. I provide preliminary evidence that the 5'UTR of XBP1 may play a role in regulating XBP1 expression and splicing that may be regulated by the ISR. Therefore, my research provides further support to the model that the ISR promotes IRE1-XBP1 signaling rather than inhibiting it.

Results

A previous study demonstrated that activation of ATF4 increases IRE1 transcription to promote XBP1 splicing (Tsuru et al., 2016). To confirm that ATF4 upregulates IRE1, I ectopically expressed FLAG-tagged ATF4 in 293A cells, which showed a noticeable increase in IRE1 protein levels by immunoblot analysis (Fig A1, lane 2). This increase in IRE1 also corresponded to a slight increase in XBP1u, but XBP1s was too low to be detected. Cells treated with Tg also showed an increase in IRE1 levels and was slightly

more enhanced in ATF4-expressing cells (lanes 5 & 6). This increase in IRE1 also corresponded to a slight increase in XBP1s. IRE1 knockdown abrogated XBP1s accumulation after Tg treatment as expected, but interestingly, XBP1u levels were higher than the untreated samples (lane 7 vs 1). The combined treatment of PERKi and Tg reduced this increase in XBP1u in IRE1-silenced cells (lane 11 vs 7), indicating that activation of the ISR promotes XBP1 expression. Consistently, ectopic ATF4 expression minimized this reduction of XBP1u by PERKi, which was judged based on the slight increase in XBP1s compared to the vector control (lane 12). ATF4 did not activate a global UPR since there was no change in PERK or eIF2α phosphorylation. ATF4 did however, enhance BiP levels, which confirms previous reports that ATF4 can promote BiP transcription. These data show that the ISR plays a role in IRE1 and XBP1 expression and may be partially executed through the transcription factor ATF4.

Since ATF4 is also expressed in response to GCN2, HRI, or PKR phosphorylation of eIF2α, I hypothesized that activation of one of these kinases should also promote IRE1 and XBP1u/s expression. To test this, HeLa cells were treated with either the GCN2 agonist L-histidinol (HisD) or the PKR agonist poly(I:C). Tm, which causes ER stress and activates PERK, was used as a positive control. Both HisD and poly(I:C) increased phospho-eIF2α and ATF4 in a dose-dependent manner, although poly(I:C) had a nominal effect on ATF4 expression and ATF4 expression began to wane following high doses of HisD (Fig A2A). Interestingly, increasing concentrations of HisD and poly(I:C) caused a corresponding increase in XBP1u protein and a slight increase in IRE1 levels but IRE1 was not phosphorylated. There was also a marginal increase in XBP1s, but these levels paled in comparison to Tm treatment. The increase in XBP1 in response to HisD or poly(I:C) was not due to low levels of ER stress since there were no changes in PERK phosphorylation or expression of the ATF6 target gene BiP.

Sodium arsenite (Ars) is an inducer of the ISR but the exact kinase that facilitates eIF2α phosphorylation is unclear; in fact, arsenite may activate multiple eIF2α kinases (Taniuchi et al., 2016). Increasing concentrations of arsenite also increased XBP1u protein levels in A549 cells, which corresponded with increases in phospho-eIF2α, ATF4, and CHOP (Fig A2B). Following 6 h of 250 μM arsenite, there was a robust increase in XBP1u and a nominal amount of XBP1s was detected. Unfortunately, IRE1

levels were not analyzed in this experiment to determine if arsenite also induced IRE1 expression.

To determine if this increase in IRE1 and XBP1 expression was dependent on the ISR, ISR-deficient HeLa eIF2α Ser51Ala CRISPR knock-in cells and their matched wild type control cells were treated with either Tm, HisD, or arsenite. As an additional control, cells were also treated with ISRIB. Wild type HeLa cells treated with either Tm or HisD in the presence of ISRIB resulted in the loss of ATF4 expression (Fig A3, lanes 3 vs 2; and 5 vs 4). eIF2α phosphorylation was also higher in these cells, likely due to the lack of GADD34, which facilitates eIF2α dephosphorylation (Novoa et al., 2001). Curiously, the phospho-eIF2α immunoblot in eIF2α Ser51Ala mutant cells displayed bands that migrate to the same size as in the immunoblots with wild type cells. I believe this is a non-specific band because it did not change with different stress stimuli and I have tried a different phospho-eIF2α antibody, which did not generate this band in these mutant cells.

Exposure to ISRIB reduced XBP1s in Tm-treated cells (lane 3 vs 2) and XBP1u in HisD treated cells (lane 5 vs lane 4). Consistently, treatment of the phospho-eIF2α Ser51Ala HeLa cells with Tm or HisD also resulted in a decrease in XBP1s or XBP1u, respectively (lane 9 vs 2; and 11 vs 4). Compared to wild type HeLa cells, the levels of XBP1 in the eIF2α mutant cells did not change with ISRIB treatment providing further evidence that enhanced XBP1 expression and/or mRNA splicing was dependent on the ISR. Conversely, IRE1 levels did not change significantly with ISRIB treatment suggesting that although XBP1 levels were impacted by the ISR, this may not be dependent on enhanced IRE1 expression.

Unexpectedly, arsenite treatment did not behave the same way as Tm or HisD. In fact, arsenite treatment in the presence of ISRIB actually enhanced XBP1u accumulation concomitant with an observable induction of XBP1s and phosphorylation of IRE1 (lane 7). This also corresponded to an increase in PERK phosphorylation. ISRIB also failed to inhibit arsenite-induced ATF4 expression. This effect is not specific to ISRIB treatment since eIF2α Ser51Ala mutant cells exposed to arsenite also resulted in IRE1 and PERK activation (lane 13). These data suggest that failure to inhibit translation following arsenite treatment disrupts protein homeostasis in the ER, thereby causing ER stress and activation of the UPR. Furthermore, the mechanism of activation of the ISR by arsenite

may not be as straightforward compared to other stresses that induce eIF2α phosphorylation.

How might the ISR be impacting XBP1u expression? Stress-responsive genes, like ATF4, are specifically translated following eif2α phosphorylation due to the presence of uORFs in the 5'UTR of their mRNAs (Pakos-Zebrucka et al., 2016). Human XBP1 mRNA does not contain any potential uORFs with AUG start codons but it is short and highly GC-rich, which may impact translation. The 5'UTR also contains potential near-cognate CUG start codons that if translated could bypass the XBP1 AUG start codon. To test if the 5'UTR is important for regulating splicing, I first performed 5'-RACE (5' rapid amplification of cDNA ends) and cloned and sequenced 24 different RACE fragments (data not shown). Interestingly, some of the sequencing revealed clones that had an extended 5'UTR of 7-nucleotides (nt) compared to the NCBI reference sequence NM_005080.3 (data not shown). This extended 5'UTR was cloned onto a XBP1 lentiviral vector that expresses myc-epitope tags fused to the C-termini of both XBP1u and XBP1s. In addition, the expression vector is controlled by a dox-inducible promoter (Fig A4A).

293A cells were transduced with lentiviral vector expressing rtTA3 to convert the cells to 293A Tet-On. These dox-responsive 293A cells were transduced with the XBP1u/s-myc vectors with or without the presence of the 5'UTR. These cells were also transduced with shRNA lentiviral vectors targeting the 3'UTR of XBP1s as a precaution that endogenous XBP1 may impact splicing of the XBP1 expression vectors. Cells were treated with dox followed by treatment with thapsigargin (Tg) to induce ER stress. In the absence of Tg treatment, XBP1s-myc expression was markedly lower in cells expressing the construct that contains the 5'UTR compared to the cells that do not have the XBP1 5'UTR in the mRNA (Fig A4B). This indicates that the 5'UTR may be important for repressing XBP1 splicing in the absence of ER stress. Tg treatment enhanced XBP1s accumulation in both samples but the levels of XBP1s were consistently lower in the cells that contained the XBP1 5'UTR in the expression vector. This may suggest that the 5'UTR is important for repressing expression of XBP1 but that it may not promote XBP1 expression following activation of the ISR.

These are preliminary studies that require further investigation to identify the full potential of the 5'UTR in regulating XBP1 translation, both in the absence and presence

of ER stress. Collectively, the data presented in Appendix A indicate that the 5'UTR of XBP1 mRNA may be important for regulating splicing, and that the ISR can promote the accumulation of XBP1u, potentially to facilitate robust mRNA splicing in response to ER stress.

Discussion

It is becoming increasingly clear that there is crosstalk between the ISR and IRE1-XBP1 pathway, but this investigation has largely been limited to the context of ER stress. The data presented here expands beyond this scope and confirms that ectopic expression of ATF4 in the absence of stress can upregulate IRE1 and BiP. These data indicate that ATF4 can also enhance XBP1u, and that XBP1u is upregulated by drugs that activate eIF2α kinases other than ER stress-induced PERK. These results are intriguing and suggest that these UPR effectors, namely IRE1, BiP, and XBP1, may have ER stress-independent roles. Alternatively, since many cellular stress responses and signaling pathways are interconnected, this upregulation of the UPR markers may be a priming mechanism for the ER in case of impending changes in protein homeostasis.

XBP1u translation is likely a rate-limiting step to regulate mRNA splicing. Ribosomal stalling of XBP1u nascent peptide facilitates recruitment of translating XBP1u mRNA to the ER, which then facilitates the interaction with IRE1 required for mRNA splicing (Yanagitani et al., 2011). Therefore, activation of the ISR during ER stress may promote translation of XBP1u to enhance ER recruitment. This would explain the reduction in XBP1 splicing in cells co-treated with the PERK inhibitor (Fig A1). The role of increased XBP1u protein through activation of the ISR in the absence of ER stress warrants further exploration.

There are other stresses that may indirectly impact the ER folding potential. ROS and oxidative stress may trigger protein misfolding (Ikwegbue, Masamba, Oyinloye, & Kappo, 2017). Depletion of glucose and ATP can impact glycosylation and ER chaperone activity (Kaufman, 2002; Kurtoglu et al., 2007). ER Ca^{2+} is required for chaperone function, and oxidative stress can trigger the release of ER Ca^{2+} through either the IP3R (inositol trisphosphate receptor) or RyR (ryanodine receptor), which may disrupt protein folding in the ER (Görlach, Bertram, Hudecova, & Krizanova, 2015; Ruiz, Matute, &

Alberdi, 2009). Activation of the ISR by these different stresses could upregulate IRE1 and XBP1u to prime the cell for possible ER stress.

Alternatively, XBP1u has also been shown to bind XBP1s and promote proteasomal degradation (Yoshida et al., 2006). Therefore, increased XBP1u protein in the absence of activated IRE1 could block any sporadic increases in XBP1s that may unnecessarily change the ER gene expression program in the absence of *bona fide* ER stress. XBP1u has also been shown to promote proteasomal degradation of FoxO1, an important regulator of cell growth and autophagy (Zhao et al., 2013). Thus, XBP1u accumulation during the ISR may control FoxO1-dependent cellular events. It is entirely possible that XBP1u may interact with other regulators of stress responses to influence protein stability and/or signaling. Therefore, the role of XBP1u in response to ER stress-independent activation of the ISR demands further investigation.

How exactly the ISR upregulates XBP1u is worth exploring. Ectopic ATF4 expression upregulated XBP1u slightly and therefore there may be ATF4 binding sites in the promoter of XBP1 to facilitate ATF4 transactivation. ATF4 is a member of the ATF/CREB family of transcription factors and can bind to ATF/CRE-like sequences with a consensus sequence of 5'-TGACGTCA-3', and amino acid response elements (AAREs) that have a conserved core sequence 5'-ATTGCATCA-3' (Hai & Hartman, 2001). A quick search of the XBP1 gene for these conserved elements revealed an AARE core sequence in the intron between exon 1 and 2 that is approximately 1200-nt upstream of the transcription start site. Further investigation is required to see if this potential AARE promotes XBP1 expression by ATF4.

ATF4 may not be the only regulator of XBP1 expression since minimal amounts of ATF4 was induced by poly(I:C) treatment, even though XBP1u was upregulated (Fig A2A). Therefore, it is possible that the ISR may also regulate XBP1u expression by an ATF4-independent mechanism. ATF4 and many other stress-related genes contain uORFs in their 5'UTR mRNAs, which enable translation following eIF2α phosphorylation. The murine 5'UTR of XBP1 mRNA (NCBI reference sequence: NM_013842.3) contains one putative uORF with an AUG start site, while the XBP1 mRNA 5'UTR in humans (NM_005080.3) is strikingly different: it is extremely short (~ 50-nt) and does not contain any AUG codons. uORF start codons can also contain near-cognate start codons such as CUG, UUG, and GUG. For example, the 5'UTR of BiP

mRNA has two uORFs initiated with CUG start codons that have been reported to be important for regulating translation during the ISR (Starck et al., 2016). Along these lines, human XBP1 5'UTR contains two CUG codons that if translated would terminate downstream of the XBP1 AUG start codon. As previously described, the 5'UTR of XBP1 is also GC-rich (~ 80% GC content) and possibly a combination of stable secondary structures due to high GC content and the presence of near-cognate start codons may prevent translation of XBP1 in the absence of stress. Phosphorylation of eIF2α could allow more time for the ribosome to melt the 5'UTR and bypass the CUG start codon in order to initiate translation of XBP1u. In support of this, preliminary findings indicated that the attachment of the human 5'UTR to an XBP1 expression vector reduced the amount of spontaneous XBP1 mRNA splicing (Fig A4). Further work is needed to fully characterize the role of the 5'UTR in controlling XBP1u translation and splicing.

The increase in XBP1u following arsenite exposure is intriguing and may be independent of the ISR, since ISRIB or eIF2α Ser51Ala cells did not reduce XBP1u levels following arsenite treatment (Fig A3). Interestingly, ATF4 was also not reduced by ISRIB following arsenite treatment. The precise mechanism of how arsenite induces stress is not known but it is thought that arsenite may induce oxidative stress, as well as oxidize cysteine residues in its substrate to inhibit activity and/or promote protein misfolding (Thompson, 1993). Arsenite has also been reported to inhibit proteasome activity, which may further promote protein misfolding (Brunt, Khan, & Heikkila, 2012). Arsenite-induced eIF2α phosphorylation has been reported to be primarily dependent on HRI (McEwen et al., 2005). There is evidence of redundancy between kinases, since GCN2 can also be activated in response to arsenite (Taniuchi et al., 2016). However, the original study showed that arsenite treatment in eIF2α Ser51Ala cells still resulted in translation attenuation albeit markedly less than in wild type cells (McEwen et al., 2005). Therefore, arsenite can also likely inhibit translation in a phospho-eIF2α-independent manner. Surprisingly, inhibition of the ISR provoked arsenite-induced activation of PERK, as well as IRE1 suggesting the presence of ER stress (Fig A3). Arsenite has been shown to induce cytoplasmic- and ER-localized (Welch, 1992), but there is little evidence that arsenite activates the UPR (Harding et al., 1999). However, my data shows that failure to suppress translation in response to arsenite may overwhelm the folding capacity

of the HSPs and causes misfolded proteins to accumulate in the ER, which activates the UPR.

The findings presented in Appendix A are consistent with previous studies that show that the ISR can promote activation of the IRE1/XBP1 pathway, but there are also studies that demonstrate that PERK and the ISR attenuate IRE1 signaling. These conflicting findings prove that further studies are required to fully understand the crosstalk between these two branches of the UPR.

The bulk of this thesis demonstrated that KSHV lytic replication impairs activation of all three transcription factors of the UPR. I showed that both ATF4 and XBP1s failed to accumulate even though IRE1 was activated and eIF2α was phosphorylated; and that ATF6 was proteolytically cleaved into its active form, ATF6-N, but did upregulate its target genes (Chapter 3). Furthermore, overexpression of XBP1s can potently inhibited KSHV virus production (Chapter 4), thus indicating the importance of inhibiting XBP1s accumulation. Since the signaling of the UPR branches are inter-dependent, one of the main possibilities why XBP1s does not accumulate during lytic replication is due to the suppression of the ISR and/or ATF6 activity. Therefore, reversing this inhibition on the ISR and ATF6 during lytic replication may restore XBP1s expression to enable its anti-viral effects to occur. Furthermore, understanding of how KSHV dismantles the crosstalk among the ER stress sensors may help advance our understanding of its role in normal physiology and disease.

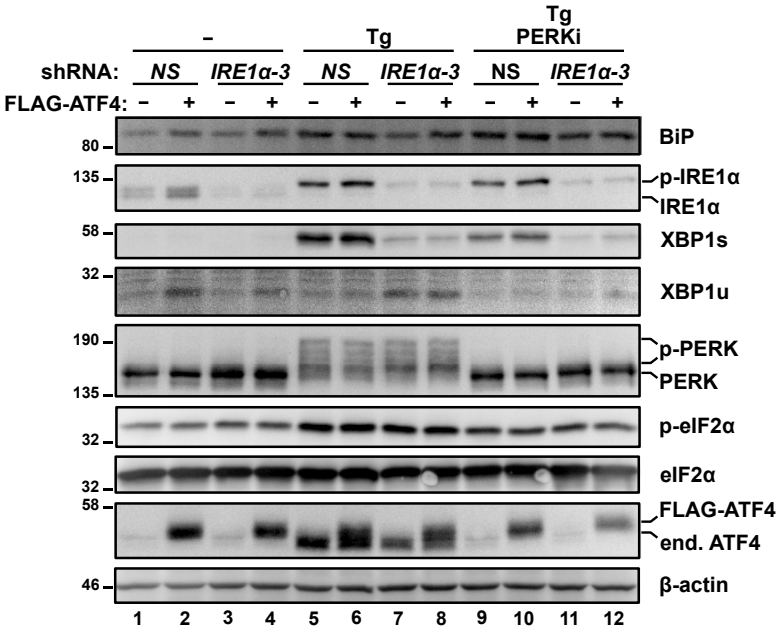

Fig A1 ATF4 upregulates UPR markers IRE1, XBP1, and BiP
293A cells were transduced with lentiviral vectors expressing IRE1α-targeting shRNAs or an shRNA non-targeting control followed by transduction with FLAG-tagged ATF4 or empty vector control lentivirus. Following antibiotic selection, 293A cells were untreated or treated with 150nM Tg with or without 500 nM PERK inhibitor GSK2606414 (PERKi) for 4 h. Cells were harvested for immunoblot analysis of UPR markers. All immunoblots are N=1.

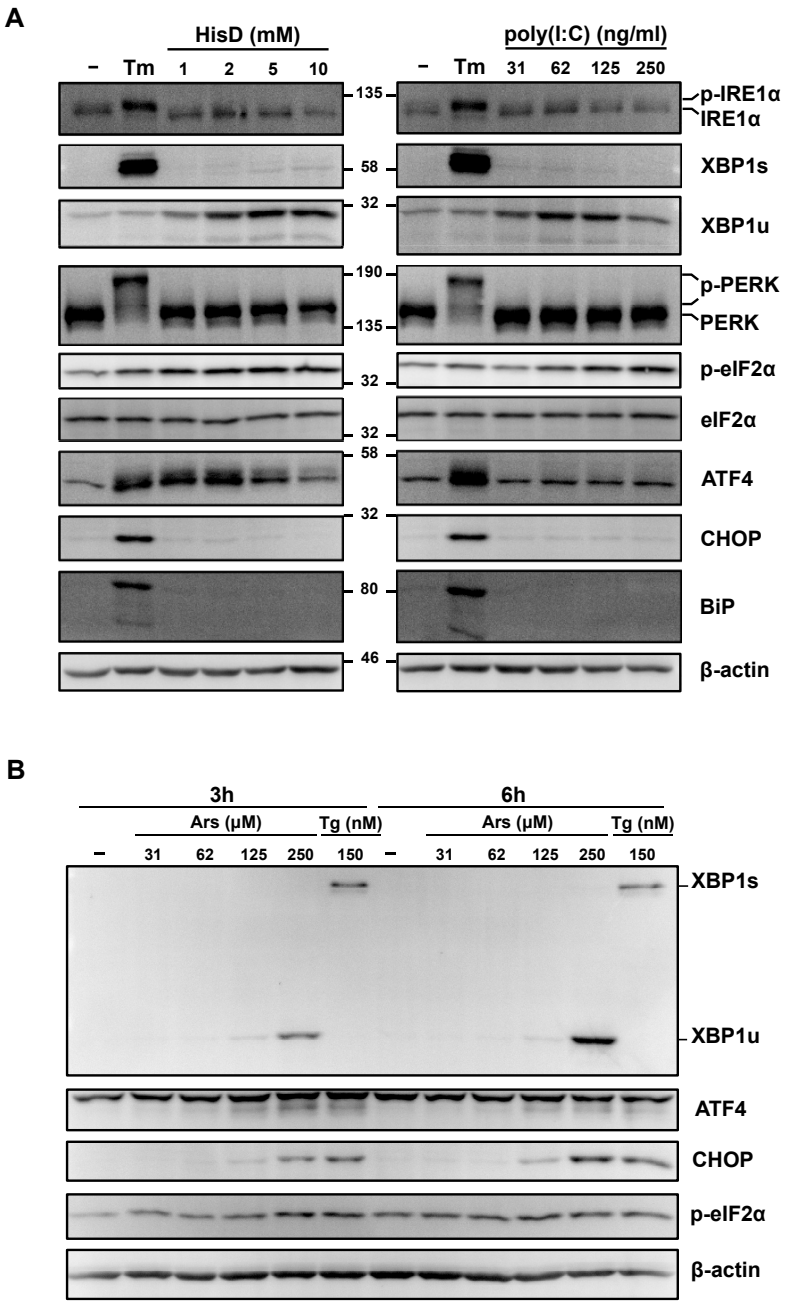

Fig A2 Drugs that induce the ISR also upregulate XBP1
(A) HeLa cells were treated with 5 μg/mL Tm or increasing concentrations of HisD or poly(I:C) for 8 h and whole cell lysates were analyzed by immunoblots. (B) A549 cells were treated with increasing concentrations of sodium arsenite (Ars) or 150 nM Tg for 3 and 6 h followed by immunoblot analysis of whole cell lysates. All immunoblots in panel are N=1.

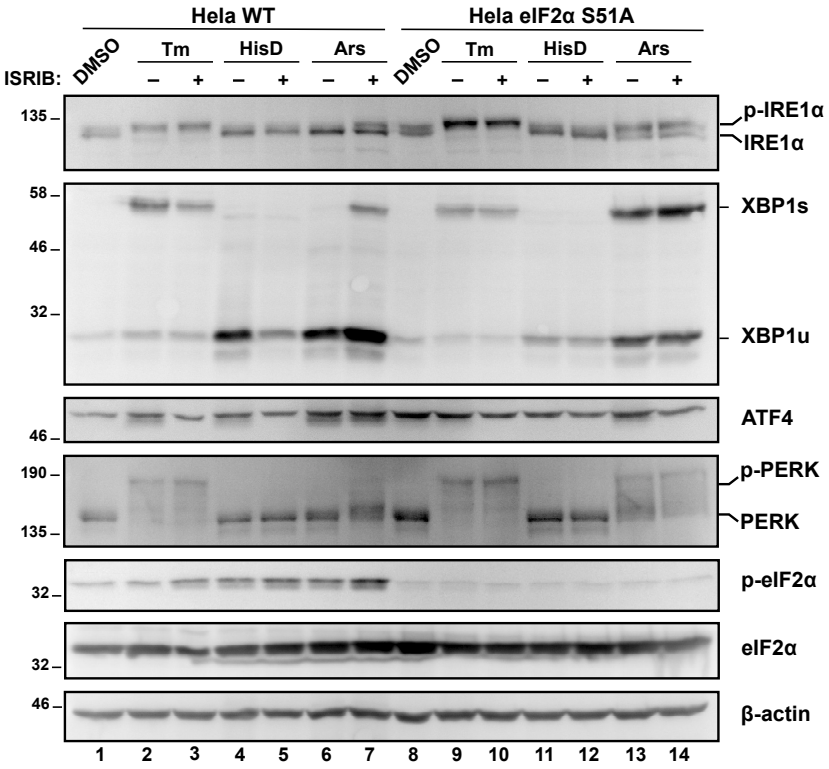

Fig A3 The ISR induces XBP1 accumulation independent of ER stress
HeLa eIF2α Ser51Ala CRISPR knock-in mutants and their matched control were treated with 2.5 µg/mL Tm for 6 h, 5mM L-Histidinol (HisD) for 12 h, or 25 µM sodium arsenite (Ars) for 6 h with or without combined treatment of 200 nM ISRIB. Cells were harvested for immunoblot analysis of UPR markers. All immunoblots in panel are N=1.

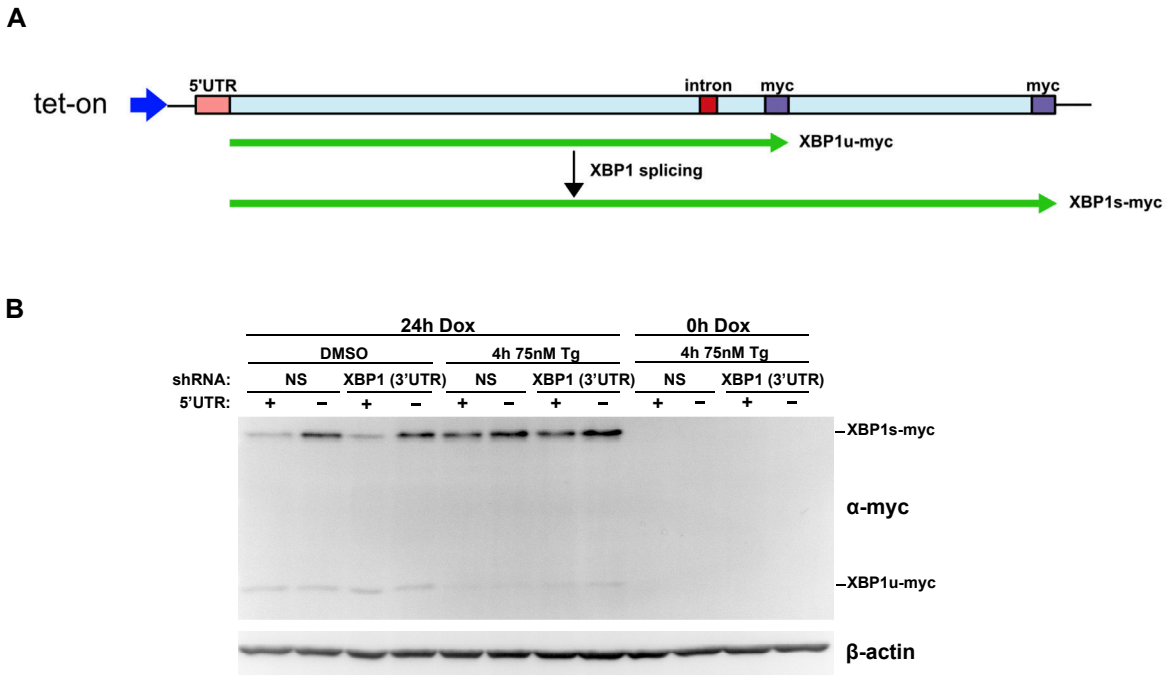

Fig A4 The 5'UTR of XBP1 reduces XBP1 splicing
(A) A cartoon of the XBP1u-myc and XBP1s-myc open reading frames of the pLJM1 7xTetO 5'UTR-XBP1u/s-myc expression vector. The human XBP1 expression vector contains the IRE1 splice site and myc-epitope tags at both the C-termini of XBP1u and XBP1s. The 5'UTR of human XBP1 was also added directly downstream of the AUG start codon. Expression of this construct is responsive to dox due to the presence of tetracycline response element (7xTetO) in the promoter. Theoretically, dox treatment in the absence of stress, will preferentially induce XBP1u-myc expression. Increases in ER stress will induce XBP1 splicing and therefore XBP1s-myc will be expressed. (B) 293A cells were transduced with lentiviral vectors expressing rtTA3 to convert the cells to 293A Tet-On. These cells were then co-transduced with lentiviral vectors expressing shRNAs against the 3'UTR of XBP1s or a non-targeting control, and XBP1u/s-myc expression vector with or without the human XBP1 5'UTR. Transduced cells were treated with or without dox for 24 h to induce XBP1u/s-myc expression. 4 h prior to harvesting lysates, the cells were treated with 75 nM Tg or DMSO control. Myc-epitope tag immunoblots were performed to determine levels of XBP1u-myc and XBP1s-myc. β-actin was used as a loading control. The immunoblot is an N of 1.

APPENDIX B KSHV PROTEIN-CODING ORFS; EXPRESSION AND PRIMARY FUNCTIONS.

Table B. A summary of the key features of the protein coding ORFs and timing of expression

ORF	*Key Features*	*Timing*	*Primary Function*
K1	Glycoprotein; binds AMPKγ1 and activates Akt	Latent	survival
K2 (vIL-6)	IL-6 homolog; requires only gp130 and not IL-6Rα for activity; poorly secreted and activity is mainly in ER	Latent and early lytic	cell growth; survival; inflammation
K3	Membrane-associated RING-CH (MARCH) E3 Ubiquitin ligase	Early lytic	immune evasion
K4 (vCCL-2)	Viral chemokine	Early lytic	immune evasion; survival
K4.1 (vCCL-3)	Viral chemokine	Early lytic	immune evasion; survival
K4.2	Disrupts IgM secretion and calcium homeostasis; increases viral gene expression	Early lytic	immune evasion; virus replication
K5	Membrane-associated RING-CH (MARCH) E3 Ubiquitin ligase	Early lytic	immune evasion
K6 (vCCL-1)	Viral chemokine	Early lytic	immune evasion; survival

ORF	*Key Features*	*Timing*	*Primary Function*
K7	Survivin homolog; inhibits autophagy and apoptosis; bridges Bcl2 and caspases; targets cyclophilin to modulate Ca2+; induces vGPCR degradation	Early lytic	survival
K8 (K-bZIP)	SUMO-2/3 E3 ligase; important for viral gene transactivation	Early lytic	viral replication
K8.1	Envelope glycoprotein; interacts with heparan sulfate	Late lytic	viral replication
K9 (vIRF-1)	Blocks TLR3-mediated IFN-β signaling; blocks STING interaction with TBK1; binds Bim to inhibit apoptosis	Late lytic	cell growth; survival; immune evasion
K10 (vIRF-4)	Suppresses G1-S transition; promotes MDM2 stability to degrade p53	Late lytic	cell growth; survival
K10.5 (vIRF-3/ LANA-2)	Stimulates c-myc; inhibits IRF7	Late lytic	cell growth; immune evasion
K11 (vIRF-2)	Inhibits IRF3	Late lytic	immune evasion
K12 (Kaposin A)	Interacts with cytohesin-1 to activate ARF-GTPase; has transforming properties	Latent and early lytic	cell growth
Kaposin B	Activates MAPK p38-MK2 pathway; stabilizes mRNAs with AREs	Latent and early lytic	inflammation

ORF	*Key Features*	*Timing*	*Primary Function*
Kaposin C	Unknown	Latent and early lytic	unknown
K13 (vFLIP)	Activates NFκB signaling; blocks autophagy; translated via IRES	Latent	survival; inflammation
K14 (vOX-2)	CD200 homolog; induces inflammatory cytokine production; bicistronic mRNA with ORF74	Late lytic	inflammation
K15	EBV LMP1/2 homolog; 12-transmembrane protein; NFκB activation; recruits PLCγ1 to activate Calcineurin/NFAT1-dependent RCAN1 expression	Early lytic	inflammation
ORF2	Dihydrofolate reductase; important for purine and thymidylate synthesis	Early lytic	viral replication
ORF4 (KCP)	Complement binding protein; accelerates C3 convertase decay, and acts as a cofactor for factor I degradation of C4b and C3b	Early lytic	immune evasion
ORF6 (SSB)	ssDNA binding protein; part of the core viral lytic DNA replication machinery	Early lytic	viral replication
ORF7 (TRM1)	Tripartite terminase subunit 1; complex with ORF29 and ORF67A; DNA packaging	Late lytic?	viral replication
ORF8 (gB)	Glycoprotein B; binds αvβ3 integrin and DC-SIGN	Late lytic	viral replication

ORF	*Key Features*	*Timing*	*Primary Function*
ORF9 (POL)	DNA polymerase; imported into nucleus by ORF59	Early Lytic	viral replication
ORF10 (RIF)	Regulator of IFN function; binds IFNAR, Jak1, Tyk2, STAT2; binds RNA export factor Rae1 to inhibit mRNA nuclear export	Early lytic	immune evasion
ORF11	dUTPase-related protein; abundant mRNA and highly translated	Early lytic	viral replication
ORF16 (vBCL-2)	Inhibits autophagy and apoptosis; essential for replication; binds ORF55	Early lytic	viral replication; cell survival
ORF17	Protease; cleaves scaffold protein as DNA enters capsid	Late lytic	viral replication
ORF17.5 (SCAF)	Scaffolding or assembly protein; promotes capsid formation	Early lytic	viral replication
ORF18	Part of late gene transcription pre-initiation complex (vPIC)	Early lytic	viral replication
ORF19	Capsid-associated tegument protein; binds pentons	Late lytic	viral replication
ORF20	Induces G2 cell cycle arrest and apoptosis; binds OASL in response to IFN to enhance KSHV replication	Early lytic	viral replication
ORF21	Thymidine kinase; also has tyrosine kinase activity	Late lytic	viral replication

ORF	*Key Features*	*Timing*	*Primary Function*
ORF22 (gH)	Glycoprotein H; forms heterodimer with gL (ORF47); binds ephrin receptor tyrosine kinase A2 (EphA2); inhibits p53-mediated apoptosis	Late lytic	viral replication; cell survival
ORF23	Unknown; predicted glycoprotein; interacts with ORF34	Late lytic	N/A
ORF24	Part of late gene transcription pre-initiation complex (vPIC)	Late lytic	viral replication
ORF25 (MCP)	Major capsid protein	Late lytic	viral replication
ORF26	Triplex-2 capsid protein; forms heterotrimer with 1 ORF62 and 2 ORF26 proteins	Late lytic	viral replication
ORF27	Unknown; MHV68 ORF27 may be a glycoprotein and is important for virus production	Late lytic	N/A
ORF28	Unknown; EBV BDLF3 homolog	Late lytic	N/A
ORF29 (TRM3)	Tripartite terminase subunit 3; complex with ORF7 and ORF67A; DNA packaging	Late lytic	viral replication
ORF30	Part of late gene transcription pre-initiation complex (vPIC)	Late lytic	viral replication
ORF31	Part of late gene transcription pre-initiation complex (vPIC)	Late lytic	viral replication

ORF	*Key Features*	*Timing*	*Primary Function*
ORF32	Tegument protein; anchors to triplex (ORF26/ORF62) and helps assemble tegument proteins	Late lytic	viral replication
ORF33	Tegument protein; interacts with ORF38; important for obtaining ORF45 in tegument; required for full viral production	Late lytic	viral replication
ORF34	Part of late gene transcription pre-initiation complex (vPIC); directly interacts with ORF24	Early lytic	viral replication
ORF35	Unknown; part of ORF35/ORF36 dicistron; has uORFs in mRNA that regulate expression; Important for efficient viral reactivation	Early lytic	N/A
ORF36 (vPK)	Serine protein kinase; phosphorylates ORF59; mimics S6KB1 to increase protein synthesis; phosphorylates K8 which may reduce SUMOylation	Early lytic	viral replication
ORF37 (SOX)	Shutoff and exonuclease; degrades cellular mRNAs for host shutoff; processing viral DNA for packaging	Early lytic	viral replication; immune evasion?
ORF38	Myristylated tegument protein; interacts with ORF33; required for optimal viral production	Early lytic	viral replication
ORF39 (gM)	Glycoprotein M; forms a complex with gN (ORF53)	Early lytic	viral replication

ORF	*Key Features*	*Timing*	*Primary Function*
ORF40/41 (PAF)	Primase-associated factor; part of trivalent helicase-primase complex (ORF40/41, ORF44, ORF56); DNA replication	Late lytic	viral replication
ORF42	Tegument protein; stimulates global protein production when overexpressed; Important for efficient viral reactivation	Late lytic	viral replication
ORF43	Portal protein; forms channel on one of the pentamers; DNA packaging	Late lytic	viral replication
ORF44 (HEL)	Helicase; part of trivalent helicase-primase complex (ORF40/41, ORF44, ORF56); DNA replication	Late lytic	viral replication
ORF45	Tegument protein; RSK (p90 ribosomal S6 kinase) and ERK activator; enhances translation; capsid egress; important for replication	Early lytic	viral replication; immune evasion
ORF46	Uracil DNA glycosylase; important for replication	Early lytic	viral replication
ORF47 (gL)	Glycoprotein L; forms heterodimer with gH (ORF22); binds ephrin receptor tyrosine kinase A2 (EphA2);	Early lytic	viral replication
ORF48	Unknown	unknown	unknown
ORF49	Activates MAPK JNK and p38	Early lytic	inflammation

ORF	*Key Features*	*Timing*	*Primary Function*
ORF50 (RTA)	Replication and transcription activator; immediate early protein; initiates lytic replication	Early lytic	viral replication
ORF52	Tegument protein; important for recruiting other tegument proteins; inhibits cGAS	Late lytic	viral replication; immune evasion
ORF53 (gN)	Glycoprotein N; Forms a complex with gM (ORF39)	Late lytic	viral replication
ORF54	dUTPase; downregulates NKp44L independent of dUTPase activity	Late lytic	viral replication; immune evasion
ORF55	Tegument protein; is incorporated into virion by interacting with vBCL2	Late lytic	viral replication
ORF56 (PRI)	Primase; part of trivalent helicase-primase complex (ORF40/41, ORF44, ORF56); DNA replication	Late lytic	viral replication
ORF57 (MTA)	mRNA transcript accumulation; mRNA export and splicing; promotes expression of intron containing viral genes	Early lytic	viral replication
ORF58	Unknown; EBV BMRF2 homolog (glycoprotein); important for viral replication	Early lytic	viral replication
ORF59	Processivity factor; recruits ORF9 (DNA polymerase) to nucleus to facilitate ORF9 binding to *ori*Lyt via ORF50	Early lytic	viral replication

ORF	*Key Features*	*Timing*	*Primary Function*
ORF60	Ribonucleoprotein reductase small subunit; forms a heterodimer with ORF61; converts RNA to DNA	Early lytic	viral replication
ORF61	Ribonucleoprotein reductase large subunit; forms a heterodimer with ORF60; converts RNA to DNA	Early lytic	viral replication
ORF62	Triplex-1 capsid protein; forms heterotrimer with 1 ORF62 and 2 ORF26 proteins	Late lytic	viral replication
ORF63	Tegument protein; viral NLRP1 homolog; blocks Caspase-1, IL-1β and IL-18 activation	Early lytic	survival
ORF64	Tegument protein; likely acts as a scaffold; Deubiquitinase (DUB); suppresses RIG-I activation by de-ubiquitination; inhibits p53-mediated apoptosis	Late lytic	viral replication; immune evasion; survival
ORF65 (SCP)	Small capsid protein; essential for virus production	Late lytic	viral replication
ORF66	Part of late gene transcription pre-initiation complex (vPIC)	Late lytic	viral replication
ORF67	Binds ORF69 to form nuclear egress complex (NEC)	Late lytic	viral replication
ORF67A (TRM2)	Tripartite terminase subunit 2; forms complex with ORF7 and ORF29; DNA packaging	Late lytic	viral replication

ORF	*Key Features*	*Timing*	*Primary Function*
ORF68	Viral DNA processing and packaging protein; binds DNA and can promote cleavage	Late lytic	viral replication
ORF69	Binds ORF67 to form nuclear egress complex (NEC)	Late lytic	viral replication
ORF70	Thymidylate synthase; catalyzes the reaction of 5,10-methylenetetrahydrofolate and dUMP to dTMP	Early lytic	viral replication
ORF72 (vCyclin)	Constitutive activator of CDK6 to promote cell cycle; can induce DNA damage, autophagy, and apoptosis or oncogene induced senescence on bicistronic mRNA with vFLIP	Latent	cell growth
ORF73 (LANA)	Tethers genome to host chromatin; enhance IL-6; inhibit cGAS	Latent	viral replication; inflammation; immune evasion
ORF74 (vGPCR)	Constitutively active CXCR1 and CXCR2 homolog; increases growth factors and cytokines; angiogenic and transforming activity	Late lytic	cell growth; inflammation
ORF75 (vFGARAT)	Viral homolog formyl-glycinamide-phosphoribosyl-amidotransferase enzyme; tegument protein; disperses Sp100 and Daxx from ND10	Late lytic	immune evasion

APPENDIX C RELATIVE CHANGES IN MFI OF UPR REPORTERS WITH KSHV ORF EXPRESSION

Table C The relative MFIs of CHOP::GFP and XBP1-mCherry in CHO-7.1 cells expressing KSHV ORFs

ORF	Untreated CHOP::GFP	Untreated XBP1-mCherry	Tg CHOP::GFP	Tg XBP1-mCherry
K1	0.98611111	0.80681818	0.86660263	0.61622465
K10	1.03546099	1.02597403	1.02925107	0.91942735
K10.5	1.05673759	0.905549	0.97541311	0.97503549
K11	1.09219858	0.65997639	0.72821162	0.76822054
K14	0.80193237	0.89460154	1.23389855	1.11582868
K15	0.96453901	1.07378176	0.94922708	1.02910554
K2	0.99295775	1.34375	0.70022414	1.82787311
K3	0.9858156	0.74147727	0.54050592	0.48439938
K4	0.99280576	0.84375	0.76721102	0.55382215
K4.1	0.98550725	0.80965909	0.80064041	0.54056162
K4.2	1.10294118	0.99431818	1.02158181	0.81799272
K5	0.91333333	0.71022727	0.83554275	0.54056162
K6	0.96350365	0.80681818	0.78136407	0.5624025
K7	1.01515152	0.81534091	0.80800512	0.54212168

ORF	Untreated CHOP::GFP	Untreated XBP1-mCherry	Tg CHOP::GFP	Tg XBP1-mCherry
K8	1.10447761	1.00284091	0.95536343	0.78627145
K8.1	1.02702703	0.89488636	0.94377201	0.66692668
K9	1.21764706	0.74293059	1.29552579	0.74636872
KapA	1.11038961	0.91053228	0.91825085	1.03718493
KapB	1.09036145	0.90488432	1.0122542	0.90167598
KapC	0.9558011	0.58611825	0.92106013	0.82048417
ORF10	1.10989011	1.00771208	1.11591622	1.23761639
ORF11	1.15346535	1.03856041	1.376888	1.45884544
ORF16	4.14887218	2.14961832	1.88440152	1.83915985
ORF17	1.16906475	1.15625	0.96478419	0.95952677
ORF17.5	1.17985612	1.15625	1.03905321	1.01681196
ORF18	1.20503597	1.19270833	0.98339389	1.03237858
ORF19	1.22661871	1.171875	0.94427276	1.04607721
ORF2	0.98	0.96454768	0.98793886	0.8745711
ORF20	1.20503597	1.17708333	0.98811424	1.02054795
ORF21	0.95683453	0.91145833	0.87282236	1.0249066
ORF22	1.29136691	1.734375	1.03406119	1.02241594
ORF23	1.54676259	1.23958333	0.97870751	1.25840598

ORF	Untreated CHOP::GFP	Untreated XBP1-mCherry	Tg CHOP::GFP	Tg XBP1-mCherry
ORF24	1.33093525	1.21875	1.06167012	1.11519303
ORF25	0.9929078	1.03305785	0.89412313	0.94474681
ORF26	1.17266187	1.19791667	1	1.13200498
ORF27	1.14634146	1.24032587	1.00608293	0.98474814
ORF28	1	1.16089613	0.98187971	0.78848083
ORF29a	1.03546099	1.06375443	0.92617271	0.89493611
ORF29b	1.02836879	1.05430933	0.96501866	0.99408424
ORF30	0.965	1.00366748	1.00919513	0.90989961
ORF31	1.41463415	1.41344196	1.11249143	1.08569135
ORF32	1.11788618	1.27087576	0.97888108	0.85350191
ORF33	1.10569106	1.21792261	1.01842015	0.86132852
ORF34	1.05691057	1.17718941	1.01842015	0.86132852
ORF35	1.01219512	1.21792261	1.12268677	0.871764
ORF36	1.19105691	1.74541752	1.16805175	1.39795304
ORF37	1.05691057	0.72708758	0.88528101	1.1157937
ORF38	1.04065041	1.28309572	1.05311857	0.80794702
ORF39	1.04878049	1.23014257	1.10910727	0.84065824
ORF4	0.96531792	0.87917738	1.26047307	1.03091248

ORF	Untreated CHOP::GFP	Untreated XBP1-mCherry	Tg CHOP::GFP	Tg XBP1-mCherry
ORF40	1.04878049	1.18940937	1.07912097	0.85871965
ORF41	1.33949192	1.21727019	1.09902185	1.2005523
ORF42	1.015	0.86185819	1.07917363	0.8692337
ORF43	1.41108545	1.26183844	1.09902185	1.17880566
ORF44	1.43187067	1.2729805	1.09569199	1.20434933
ORF45	4.74364896	2.52924791	1.74085328	2.32516396
ORF46	1.44572748	1.28969359	1.1091155	1.27235071
ORF47	1.015	1.1405868	1.04675185	1.12949549
ORF48	1.32332564	1.52089136	1.153923	1.35208837
ORF49	1.36951501	1.23955432	1.09569199	1.14014498
ORF50	1.17207792	0.27293318	0.74192208	0.24032942
ORF52	1.84526559	1.33426184	1.14341311	1.20814636
ORF53	1.34872979	1.22562674	1.12270552	1.24162927
ORF54	1.84988453	1.44846797	1.18237253	1.39834311
ORF55	1.27927928	1.30790191	1.17159586	1.38527828
ORF56	1.24324324	1.20163488	1.1645098	1.26822262
ORF57	1.32732733	1.54223433	1.13646495	1.70915619
ORF58	1.34834835	1.2506812	1.27981636	1.41508079

ORF	Untreated CHOP::GFP	Untreated XBP1-mCherry	Tg CHOP::GFP	Tg XBP1-mCherry
ORF59	1.1981982	1.13623978	1.15742373	1.20035907
ORF6	1.13173653	1.04627249	1.34375891	1.29944134
ORF60	1.31531532	1.25885559	1.1645098	1.1572711
ORF61	1.27327327	1.20980926	1.19322	1.2994614
ORF62	1.26426426	1.16076294	1.20050567	1.19317774
ORF63	1.24924925	1.20980926	1.29944443	1.67324955
ORF64a	1.08510638	1.54191263	1.04104478	1.53466635
ORF64b	1.03546099	1.04250295	0.97834488	1.01041174
ORF64N	0.91489362	1.33412043	0.98101013	1.58944628
ORF65	1.2012012	1.20163488	1.1645098	1.21508079
ORF66	1.26426426	1.16076294	1.2263881	1.27576302
ORF67	1.23723724	1.17166213	1.1895938	1.20394973
ORF67A	1.01	0.9792176	1.08245761	0.95819037
ORF68	1.23701299	1.13703284	1.01535221	1.08235588
ORF69	1.23376623	1.10305776	0.96705093	1.08572498
ORF7	0.97354497	1.0874036	1.4023226	1.48566108
ORF70	1.1038961	1.13363533	1.01227623	1.08235588
ORF71	1.23051948	1.17214043	1.04996397	1.10569004

ORF	Untreated CHOP::GFP	Untreated XBP1-mCherry	Tg CHOP::GFP	Tg XBP1-mCherry
ORF72	9.73684211	1.45038168	1.3643965	0.78615732
ORF73	1.26623377	1.28765572	1.09236269	1.2954829
ORF74	2.045	4.63080685	0.92954383	1.83326979
ORF75	2.99548872	2.11603053	1.63301141	1.47688187
ORF8	0.98913043	1.01028278	1.35195212	1.34376164
ORF9	1.08	1.24205379	1.0595892	1.29940272

APPENDIX D PLASMID MAP AND MCS OF PLJM1 B* PURO

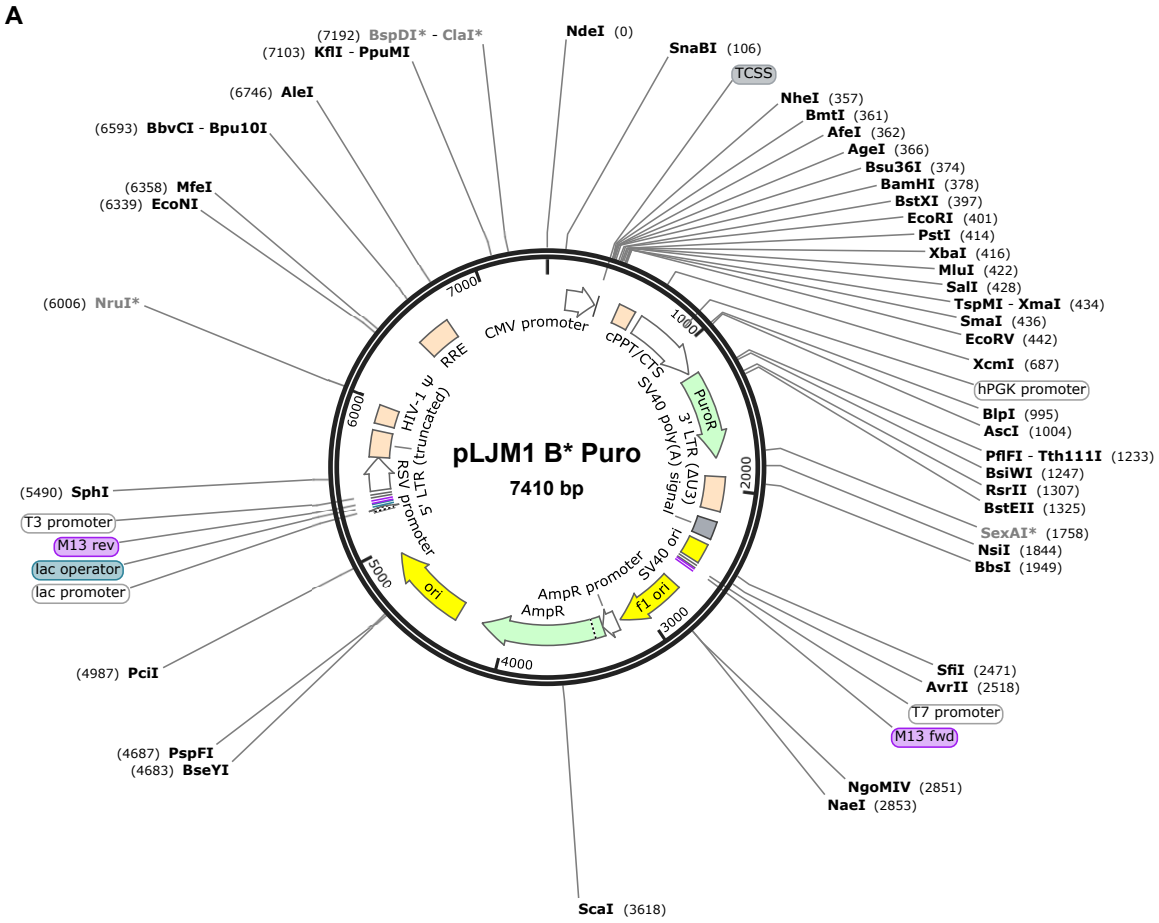

Fig D Plasmid map of pLJM1 B* Puro lentiviral vector

(A) Annotated map of pLJM1 B* Puro lentiviral vector that is derived from pLJM1 plasmid that was originally generated by the Sabatini Lab (MIT). Key plasmid features are shown including unique restriction enzymes (REs) and their location of action. (B) A detailed view of the MCS nucleotide sequence and the unique RE sites.

APPENDIX E SUMMARY OF THE IMPACT THAT XBP1 HAS ON KSHV REPLICATION

Table E A Summary of the data from Chapter 4, which shows the different reactivation and titering methods in two different KSHV cell models, and the differences in replication cycle time and impact of XBP1 on titer

Cell Type	Method of Reactivation	Replication Time	Titer Method	Max Virus Titer	Figure
TREx BCBL1-RTA	Dox-inducible RTA (control)	48 – 72 h post-dox	qPCR of DNase protected genomes	~ 2000-fold increase compared to untreated	Fig 4.6B
TREx BCBL1-RTA	CMV-driven RTA	72 h post-transduction	qPCR of DNase protected genomes	~ 10-fold less than control	Fig 4.6B
TREx BCBL1-RTA	CMV-driven XBP1s	72 h post-transduction	qPCR of DNase protected genomes	~ 4-fold less than control	Fig 4.6B
iSLK.219	Dox-inducible RTA (control)	72 – 96 h post-dox	Flow cytometry of infected 293A cells and calculated IU/ml	~ 5 x 10^6 IU/mL	Figs 4.3A, 4.4B
iSLK.219	CMV-driven RTA	6 d post-transduction	Flow cytometry of infected 293A cells and calculated IU/ml	Same as control	Fig 4.5B
iSLK.219	CMV-driven XBP1s	6 d post-transduction	Flow cytometry of infected 293A cells and calculated IU/ml	~ 100-fold less than control	Fig 4.5B
iSLK.219	Dox-inducible RTA (x2)	24 – 48 h post-dox	Flow cytometry of infected 293A cells and calculated IU/ml	~ 5-fold less than control	Fig 4.4B
iSLK.219	Dox-inducible RTA and XBP1s (1x TetO promoter)	72 – 96 h post-dox	Flow cytometry of infected 293A cells and calculated IU/ml	~ 2-fold less than control	Fig 4.3A
iSLK.219	Dox-inducible RTA and XBP1s (7x TetO promoter)	72 – 96 h post-dox	Flow cytometry of infected 293A cells and calculated IU/ml	~ 40-fold less than control	Fig 4.3A
iSLK.219	Dox-inducible RTA (control)	72 – 96 h post-dox	Flow cytometry of infected 293A cells and calculated % GFP+ve cells	~ 65 % GFP-positive cells	Fig 4.3C
iSLK.219	Dox-inducible RTA and XBP1s (7x TetO promoter)	72 – 96 h post-dox	Flow cytometry of infected 293A cells and calculated % GFP+ve cells	~15-fold less than control	Fig 4.3C

Cell Type	Method of Reactivation	Replication Time	Titer Method	Max Virus Titer	Figure
iSLK.219	Dox-inducible RTA and XBP1u (7x TetO promoter)	72 – 96 h post-dox	Flow cytometry of infected 293A cells and calculated % GFP+ve cells	~ 5-fold less than control	Fig 4.3C
iSLK.219	Dox-inducible RTA and XBP1u*G519A* (7x TetO promoter)	72 – 96 h post-dox	Flow cytometry of infected 293A cells and calculated % GFP+ve cells	Similar to control	Fig 4.3C
iSLK.219	Dox-inducible RTA + NaB	48 – 72 h post-dox/NaB	Flow cytometry of infected 293A cells and calculated % GFP+ve cells	1.4-fold more than control	Fig 4.7A
iSLK.219	Dox-inducible RTA and 7x TetO XBP1s + NaB	48 – 72 h post-dox/NaB	Flow cytometry of infected 293A cells and calculated % GFP+ve cells	1.3-fold more than control	Fig 4.7A

Control samples for each titering method are highlighted in grey.